

Molecular weight control in emulsion polymerization by catalytic chain transfer : aspects of process development

Citation for published version (APA):

Smeets, N. M. B. (2009). *Molecular weight control in emulsion polymerization by catalytic chain transfer : aspects of process development*. [Phd Thesis 1 (Research TU/e / Graduation TU/e), Chemical Engineering and Chemistry]. Technische Universiteit Eindhoven. <https://doi.org/10.6100/IR642709>

DOI:

[10.6100/IR642709](https://doi.org/10.6100/IR642709)

Document status and date:

Published: 01/01/2009

Document Version:

Publisher's PDF, also known as Version of Record (includes final page, issue and volume numbers)

Please check the document version of this publication:

- A submitted manuscript is the version of the article upon submission and before peer-review. There can be important differences between the submitted version and the official published version of record. People interested in the research are advised to contact the author for the final version of the publication, or visit the DOI to the publisher's website.
- The final author version and the galley proof are versions of the publication after peer review.
- The final published version features the final layout of the paper including the volume, issue and page numbers.

[Link to publication](#)

General rights

Copyright and moral rights for the publications made accessible in the public portal are retained by the authors and/or other copyright owners and it is a condition of accessing publications that users recognise and abide by the legal requirements associated with these rights.

- Users may download and print one copy of any publication from the public portal for the purpose of private study or research.
- You may not further distribute the material or use it for any profit-making activity or commercial gain
- You may freely distribute the URL identifying the publication in the public portal.

If the publication is distributed under the terms of Article 25fa of the Dutch Copyright Act, indicated by the "Taverne" license above, please follow below link for the End User Agreement:

www.tue.nl/taverne

Take down policy

If you believe that this document breaches copyright please contact us at:

openaccess@tue.nl

providing details and we will investigate your claim.

**Molecular Weight Control in Emulsion
Polymerization by Catalytic Chain Transfer
Aspects of Process Development**

Niels Mathieu Barbara Smeets

A catalogue record is available from the Eindhoven University of Technology Library
ISBN: 978-90-386-1802-9

© 2009, Niels Mathieu Barbara Smeets

This research was financially supported by the Foundation of Emulsion Polymerization (SEP) and the European Graduate School (EGS).

Cover design: Niels M.B. Smeets and Paul Verspaget

Printed at the Universiteitsdrukkerij , Eindhoven University of Technology

**Molecular Weight Control in Emulsion
Polymerization by Catalytic Chain Transfer
Aspects of Process Development**

PROEFSCHRIFT

ter verkrijging van de graad van doctor aan de
Technische Universiteit Eindhoven, op gezag van de
Rector Magnificus, prof.dr.ir. C.J. van Duijn, voor een
commissie aangewezen door het College voor
Promoties in het openbaar te verdedigen
op vrijdag 3 juli 2009 om 16.00 uur

door

Niels Mathieu Barbara Smeets

geboren te Ermelo

Dit proefschrift is goedgekeurd door de promotoren:

prof.dr. A.M. van Herk

en

prof.dr. J. Meuldijk

Copromotor:

dr.ir. J.P.A. Heuts

“Je moet hoog mikken want de pijl daalt onder het vliegen”

“Shoot for the moon and even if you miss you’ll land amongst the stars”

† Huub Vromans

TABLE OF CONTENTS	i
SUMMARY	iii
SAMENVATTING	v
SAAMEVATTING	vii
CHAPTER 1: Introduction	2
Objective	3
Free radical polymerization	5
Emulsion polymerization	14
Process development in emulsion polymerization	20
Catalytic chain transfer	24
Scope of the thesis	36
References	37
CHAPTER 2: Catalyst partitioning in emulsion polymerization	42
Introduction	43
Results and Discussion	44
Conclusions	55
Experimental	56
Appendix	59
References	62
CHAPTER 3: Mass transport limitations in CCT emulsion polymerization	66
Introduction	67
Results and Discussion	69
Conclusions	81
Experimental	81
References	84
CHAPTER 4: Compartmentalization effects in CCT emulsion polymerization	88
Introduction	89
Results and Discussion	91
Conclusions	109
Experimental	109
References	112

CHAPTER 5: Effect of CCT on the emulsion polymerization kinetics	116
Introduction	117
Results and Discussion	118
Conclusions	137
Experimental	137
References	139
CHAPTER 6: Particle nucleation in batch and continuous CCT emulsion polymerization	144
Introduction	145
Results and discussion	147
Batch experiments	148
Continuous experiments in the PSPC	161
Conclusions	168
Experimental	169
References	173
CHAPTER 7: Process development in CCT emulsion polymerization	178
Introduction	179
Partitioning	182
Catalyst deactivation	185
Application in batch emulsion polymerization	192
Application in continuous emulsion polymerization	194
Concluding remarks	198
References	199
ACKNOWLEDGEMENTS	202
CURRICULUM VITAE	206

SUMMARY

The molecular weight distribution (MWD), amongst others, governs the end use properties of polymeric materials, e.g., coatings. Robust molecular mass control is therefore a key issue in polymer production. Catalytic chain transfer (CCT) has proven to be a robust technique for the control of the MWD. In CCT the radical activity of a propagating polymer chain is transferred via the active cobalt complex to a monomer molecule. The catalytic nature of catalytic chain transfer agents (CCTA), combined with the high activity towards chain transfer allows for the use of very low amounts to achieve proper molecular weight control. This study aims at obtaining a thorough and fundamental understanding of the consequences of the heterogeneity of the emulsion polymerization reaction mixture for the application of CCT in a technical scale.

The average molecular weight of the polymer formed can be predicted fairly accurately by the Mayo equation in bulk and solution polymerization, which relates the catalyst activity and the amount of catalytic chain transfer agent to the instantaneous number-average degree of polymerization. For emulsion polymerization an extended Mayo equation was derived which incorporates the effects of catalytic chain transfer agent partitioning. The lower apparent activity of these cobalt complexes observed in emulsion polymerization, when compared to bulk and solution polymerization, can be explained by the effects of partitioning. CCTA partitioning is a crucial parameter governing the performance of CCT in emulsion polymerization.

The emulsion polymerization reaction system has some important consequences for the application of CCT. The absolute number of polymer particles in an emulsion polymerization very often exceeds the number of CCTA molecules, which implies that fast CCTA transport is required for proper molecular weight control. Partitioning of the CCTA in emulsion polymerization allows for fast transport via the aqueous phase. However, this is not the only transport mechanism in emulsion polymerization. This transport even occurs for a very sparingly water soluble CCTA, which also shows proper molecular weight control, suggesting that a CCTA (or other very hydrophobic species)

can be transported by a shuttle mechanism. CCTA transport can be limited by the increasing viscosity of the polymer particles as the weight fraction of polymer is increasing. The high viscosity of the polymer particles can affect the rate of entry and exit of the CCTA. This results in compartmentalization behavior and a discrete distribution of CCTA molecules over the polymer particles, which is represented by a multimodal molecular weight distribution. The efficiency of chain transfer also severely changes throughout the course of an emulsion polymerization, which is governed by the polymer volume fraction in the polymer particles.

The application of catalytic chain transfer also affects the course of the emulsion polymerization. Aqueous phase chain transfer, as a consequence of partitioning, affects the entry rate of radicals as well as the chemical nature of those radicals. This results in an extended nucleation period and as a consequence a broader particle size distribution, lower rates of polymerization throughout the entire course of the polymerization and possibly a loss of colloidal stability. Monomeric radicals, originating from the CCT process, can readily desorb from the polymer particles to the aqueous phase. This monomeric radical desorption, i.e. exit, results in a decrease in the rate of polymerization, relatively small polymer particles and a narrow particle size distribution. The reduced rate of entry in combination with the increased rate of exit results in a decrease of the average number of radicals per particle and consequently a decrease in the rate of polymerization. CCT mediated emulsion polymerizations obey Smith-Ewart Case 1 kinetics.

Application of CCT in continuous emulsion polymerization was demonstrated in a pulsed sieve plate column (PSPC), which combines low net flow rates with limited axial mixing. For a very sparingly water soluble CCTA batch performance was approximately observed in the PSPC. For more water soluble CCTAs deviation from batch performance were observed. The observed differences could originate from CCTA backmixing.

The results presented in this thesis illustrate the potential of CCT as a powerful technique for molecular weight control in emulsion polymerization. The obtained enhanced fundamental understanding allows for application of CCT on a technical scale.

SAMENVATTING

De eindtoepassing polymere materialen wordt onder andere bepaald door de molecuulgewichtsverdeling. Een geschikte techniek voor het beheersen van de molecuulgewichtsverdeling is katalytische ketenoverdracht (KKO). In een polymerisatie met KKO wordt de het vrije radicaal, via een kobaltekatalysator, overgedragen naar een monomeer molecuul. De hoge katalytische activiteit van deze complexen in combinatie met zeer lage hoeveelheden kobaltekatalysator resulteert in een goede beheersing van de molecuulgewichtsverdeling. Het doel van het in dit proefschrift beschreven onderzoek is om fundamenteel inzicht te verschaffen in de toepassing van KKO in emulsie polymerisatie op technische schaal.

De gemiddelde ketenlengte in KKO bulk en solutie polymerisatie worden voorspeld met de Mayo vergelijking, die het verband tussen de gemiddelde ketenlengte en de katalysator concentratie en de katalytische activiteit beschrijft. In emulsie polymerisatie dient de Mayo vergelijking uitgebreid te worden met het verdelingsevenwicht van de katalysator over de water en organische fase. Dit verdelingsevenwicht ligt ten grondslag aan de lage schijnbare katalysator activiteit, in vergelijking met bulk en solutiepolymerisatie, in emulsie polymerisatie. De verdeling van de kobaltekatalysator blijkt van cruciale belang voor de toepassing van KKO in emulsie polymerisatie.

De heterogeniteit van het reactiemengsel bij emulsie polymerisatie heeft grote gevolgen voor de toepassing van KKO. Het aantal kobaltekatalysator moleculen in een emulsie polymerisatie is meestal lager dan het aantal polymeerdeeltjes, waardoor snel transport van de kobaltekatalysator noodzakelijk is voor effectieve beheersing van de molecuulgewichtsverdeling. Verdelingsevenwichten maken de snelle uitwisseling van de katalysator tussen de polymeerdeeltjes mogelijk. Beheersing van de molecuulgewichtverdeling is zelf mogelijk met een zeer slecht wateroplosbare katalysator. Het transport van een katalytische ketenoverdrachtskatalysator (KKOK) kan worden beperkt door de viscositeit van de polymeerdeeltjes, die toeneemt naarmate de gewichtsfractie polymeer in de polymeerdeeltjes stijgt. Uitwisseling van de KKOK kan

door de hoge viscositeit worden vertraagd. Dit kan leiden tot een vrijwel volledige segregatie van de katalysator met als gevolg een discrete verdeling van de katalysator moleculen over de polymeerdeeltjes. Als gevolg van de stijgende viscositeit in de polymeerdeeltjes neemt ook de katalytische ketenoverdrachtsactiviteit af. De gewichtsfractie van het polymeer in de deeltjes blijkt uitermate belangrijk voor de prestatie van de KKOK.

De aanwezigheid van een katalytische ketenoverdrachtskatalysator beïnvloedt het verloop van een emulsie polymerisatie. Katalytische ketenoverdracht in de waterfase, als een gevolg de verdelingsevenwichten, doet de intreesnelheid van radicalen in de micellen en de deeltjes afnemen. Deze vertraging van de intreesnelheid resulteert in een langere nucleatie periode en daarmee een bredere deeltjesgrootteverdeling, een lagere polymerisatie snelheid en mogelijk een verlies van de colloïdale stabiliteit. KKO resulteert in de vorming van monomeer radicalen, die vanuit de polymeerdeeltje kunnen worden overgedragen naar de waterfase. De polymerisatie snelheid neemt hierdoor af en er worden relatief kleine polymeerdeeltjes gevormd met een relatief nauwe deeltjesgrootteverdeling. Door verlaagde intreesnelheid en de verhoogde desorptie snelheid van monomeerradicalen uit de deeltjes is het gemiddelde aantal radicalen per polymeerdeeltje laag en laten KKO emulsie polymerisaties zich beschrijven met “Smith-Ewart limiet 1” kinetiek.

De toepassing van KKO is gedemonstreerd in continue emulsie polymerisatie in een gepulseerde zeefplaat kolom (PSPC), waar een lage netto vloeistof snelheid wordt gecombineerd met een geringe axiale menging. Voor een niet wateroplosbare KKOK is er nauwelijks verschil tussen de prestaties in de PSPC en in een batch reactor, hetgeen niet is waargenomen voor meer wateroplosbare KKOKen. Dit verschil tussen verschillende KKOKen kan wellicht worden toegeschreven aan KKOK terugmenging in de kolom.

De resultaten beschreven in dit proefschrift illustreren de potentie van KKO voor de beheersing van de molecuulgewichtsverdelings in emulsie polymerisatie.

Saamevatting

't Gebruuk van póliemeere materiale wörd aonger angere bepaald door de molekuulgewichsverdeiling. Katalietiêsjje keëte äöverdrach is ein gooje mènnaer òm de molekuulgewichsverdeiling te sjtuure. In katalietiêsjje keëte äöverdrach wörd ein radikaal van ein greuënde poliemeerkeëte, via de kóbalkkataliesator, äövergedrage op ein monomeer molekuul. De kobaltkomplexe in katalietiêsjje keëte äöverdrach zin jèl aktief mit es gevolg dat de molekuulgewichsverdeiling gesjtuurd kent wàere mit jèl ljège wiewäölheede kataliesator. 't Doel van dit ongerzäök wóar òm mjèr inzicht te kriege in 't gebroêk van katalietiêsjje keëte äöverdrach in emulzie poliemeriezaasie.

't Gemiddelde molekuulgewich in bulk en oplossings polymeriezaasie wurd väärsjpled mit de Mayo vergelieking, dàè 't verbandj tösje 't gemiddelde molecuulgewich en de konsentrasie en aktiviteit van de kóbalkkataliesator besjrijf. In emulzie poliemeriezaasie zin driê fase aanwezig: de waterfase, monomeer dröppels (ongevjèr 5 μm) en klein poliemeer bölkes (ongevjèr 30 tot 100 nm) wóa de polymerisasie plaatsj vungk. Omdat de kataliesator sich äöver de versjillende fase verdeilt, mot in emulzie poliemeriezaasie de Mayo vergelieking wàere oêtgebred mit de kataliesator verdeiling. 't Verdeilingsevenwich van de kataliesator äöver de versjillende fase bliek jèl belangrik te zin vääor katalietiêsjje keëte äöverdrach in emulzie poliemeriezaasie.

In ein emulzie poliemeriezaasie zin d'r vriewaal ömmer mjèr poliemeerdeiltjes dán kóbalkkataliesator molekule, wóadoor sjnelle oêtwisseling van de kataliesator nwóadzakelik òm de molekuulgewichsverdeiling te kenne sjtuure. De verdeiling van de kóbalkkataliesator äöver de versjillende fase maak sjnelle oêtwisseling van de kataliesator tösje de versjillende poliemeerdeiltjes mäögelik. Ein neet wateroplosbare kataliesator kent ouch gebruik wàere vääor kontrole äöver de molekuulgewichsverdeiling. De sjtróperigheid in 't poliemeerdeiltje, dae toenömp gedurende de poliemerizaasie, kent d'r vääor zörge dat de kóbalkkataliesator mäöilik de poliemeerdeiltjes in en oet kent góan. 't In en oet góan van de kóbalkkataliesator kent wàere vertraag door de hwage sjtróperigheid van de poliemeerdeiltjes. Dit kent resöltere in ein isólement van de

katalietsator molekule in de polimeerdeiltjes. Door de hwage sjtróperigheid in de polimeer deiltjes nômpe ouch de katalietiêsje keëte äöverdrachsaktiviteit aaf. De gewichsfraksie polimeer in de polimeerdeiltjes is jël belangrik vâör de prestaasie van de kóbalkataliesator.

Katalietiêsje keëte äöverdrach verângerd 't emulzie poliëmeriezaasie proces. Katalietiêsje keëte äöverdrach in de waterfase, es gevolg van de kataliesator verdeiling, verljêg de sjnelheid wóá mit radikale de polimeerdeiltjes ingóan. Dit hàèt ein langere nukleasie tied, ein breiere deiltjesgrootteverdeiling, ein lègere polymerisasie snelheid en mäögelik ein verrees van de kólowiedaale sjtabiliteit es gevolg. Katalietiêsje keëte äöverdrach in de polimeerdeiltjes göf monomeer radikale die gemèkkelik oet ein polimeerdeiltje kenne goan. De polymerisasie sjnelheid nômpe aaf en d'r wàère relatief kleine polimeerdeiltjes gemaak mit ein sjmaale deiltjesgrootteverdeiling. Door de làègere sjnelheid wóá mit radikale de polimeerdeiltjes ingóan en de hwágere sjnelheid wóá mit radikaale de polimeerdeiltjes oet góan is 't gemiddelde aantal radikaale per polimeerdeiltje ljêg en voldoan katalietiêsje keëte äöverdrach polymerisasies aan "Smith-Ewart limiet 1" kienetiek.

De toepassing van katalietiêsje keëte äöverdrach in kontineuje emulzie poliëmeriezaasie is gedemonstreed in ein gepulzeerde zeefplaat kólom (PSPC), wóá ein ljêge vloeisjtof sjnelheid door de kólom wörd gekombineerd mit ein gooje radiaale menging. Vergeliekbare produk eigesjappe, zwóá es 't verloup van de polymerisasie, de molecuulgewichsverdeiling en de deiltjesgrootteverdeiling, op betsj en kontineuje sjaal woar verwach. Versjille tösje betsj en kontineuje emulzie poliëmeriezaasie is experimenteel vastgesjteld vâör wateroplosbare kataliesators. Vâör neet wateroplosbare kataliesators is dit versjil neet gezeen. Dit kent 't gevolg zin van kataliesator trókmenging in de PSPC.

De resóltate besjrêve in dit prófsjrif loate zeen dat katalietiêsje keëte äöverdrach vóäl pótsie haet vóär 't sjtuure van de molecuulgewichsverdeiling in emulzie poliëmeriezaasie.

1

Molecular Weight Control in Emulsion Polymerization by Catalytic Chain transfer: Introduction

OBJECTIVE

The application of a polymer product is governed by the molecular characteristics of the polymer. Properties such as film formation, rheology and mechanical stability, amongst other things, depend on the molecular weight distribution of the polymer. This makes control of the molecular weight distribution a key issue in polymer production.

Control of the molecular weight distribution can be achieved by the addition of chain transfer agents, such as mercaptanes. Disadvantages of these commonly applied chain transfer agents are that significant amounts are required to obtain polymer of low molecular weight and the colouring the polymer products, both due to the incorporation of the chain transfer agent in the polymer chain. Catalytic chain transfer, using cobalt based complexes as the chain transfer agent, is considered to be a promising alternative for mercaptanes. The cobalt complex is not incorporated in the polymer backbone and due to the catalytic nature of catalytic chain transfer and the high chain transfer activity only low amounts of the cobalt complex are required to obtain a significant reduction in the molecular weight of the polymer.

The application of catalytic chain transfer in bulk and solution polymerization has been thoroughly reported over the past two decades. Control of the molecular weight distribution can be achieved and the average molecular weight of the polymer accurately predicted. Loss of control of the molecular weight distribution was mainly accounted to poisoning of the active catalyst. In emulsion polymerization the application of catalytic chain transfer has proven to be less straightforward and only a small number of preliminary studies have been reported.

In this work we report a thorough investigation of the application of catalytic chain transfer in emulsion polymerization. The heterogeneous nature of the emulsion polymerization system apparently affects the performance of the catalytic chain transfer agent. The presence of a catalytic chain transfer agent in an emulsion polymerization subsequently affects the polymerization kinetics. The objective of the reported work is to

elucidate the effects of catalytic chain transfer on the emulsion polymerization mechanism and kinetics and visa versa to obtain full and reproducible control of the molecular weight distribution in emulsion polymerization. Application of catalytic chain transfer in emulsion polymerization will be illustrated in continuous emulsion polymerization on a technical scale.

FREE RADICAL POLYMERIZATION*Classical free radical polymerization kinetics*

The main process and product parameters controlling a free radical polymerization are the rate of polymerization (R_p) and the molecular weight distribution (MWD). Both are governed by the fundamental reaction steps in free radical polymerization, i.e. (i) initiation, (ii) propagation, (iii) transfer and (iv) termination, of which only initiation and termination directly alter the radical concentration, see Equation 1.

$$\frac{d[\mathbf{R}]}{dt} = 2fk_d[\mathbf{I}] - 2k_t[\mathbf{R}]^2 \quad (1)$$

The steady state radical concentration is given by Equation 2.

$$[\mathbf{R}] = \left(\frac{fk_d[\mathbf{I}]}{k_t} \right)^{0.5} \quad (2)$$

$$R_p = -\frac{d[\mathbf{M}]}{dt} = k_p[\mathbf{M}][\mathbf{R}] = \left(\frac{fk_d k_p^2}{k_t} \right)^{0.5} [\mathbf{I}]^{0.5} [\mathbf{M}] \quad (3)$$

The steady-state rate equation for a monomer M, initiated by the thermal decomposition of an initiator I, with a rate coefficient of decomposition k_d and efficiency factor f , is presented by Equation 3. Where k_p is the rate coefficient of propagation and k_t the rate coefficient of termination. The Mayo equation can be used to predict the average degree of polymerization, see Equation 4.¹

$$DP_n^{-1} = (1 + \lambda) \frac{k_t[\mathbf{R}]}{k_p[\mathbf{M}]} + \sum_x \frac{k_{tr,x}[\mathbf{X}]}{k_p[\mathbf{M}]} \quad (4)$$

In the Mayo equation, λ is the fraction of chains terminated by disproportionation, $[R]$ is the total radical concentration and $k_{tr,X}$ the rate coefficient of chain transfer to any chain transfer agent X (i.e. monomer, solvent, polymer or a chain transfer agent). Both the rate equation and the Mayo equation can readily be used to calculate the change in rate and average molecular weight with changing reaction conditions.

The molecular weight distribution

Free radical polymerization is a statistical process and generates polymer chains of different lengths, which are characterized by the molecular weight distribution (MWD). Typically the MWD is characterized by the average molecular weights and the polydispersity index, the broadness of the distribution.

The number average molecular weight, M_n , where n_i is the number of polymer chains with a molecular weight M_i .

$$M_n = \frac{\sum_i n_i M_i}{\sum_i n_i} \quad (5)$$

The weight average molecular weight, M_w , is given by Equation 6.

$$M_w = \frac{\sum_i n_i M_i^2}{\sum_i n_i M_i} \quad (6)$$

The polydispersity index (PDI) is given by the ratio of the weight average and number average molecular weights ($PDI = M_w / M_n$).

The molecular weight distribution is obtained by size exclusion chromatography (SEC), also referred to as gel permeation chromatography (GPC).² The signal obtained from the

RI detector is proportional to the amount of polymer (dW) that passes in a volume (dV), see Equation 7, where k is a normalization constant.

$$H_i = k \frac{dW}{dV} \quad (7)$$

The detector signal, H_i , can be converted into a differential molecular weight distribution, $w(\log M)$, using the slope of the calibration curve, $\frac{dV_i}{d \log M_i}$.

$$w(\log M) = \frac{dW_i}{d \log M_i} = \frac{dW_i}{dV_i} \times \frac{dV_i}{d \log M_i} \quad (8)$$

The number distribution $P(M)$, and the weight distribution $w(M)$ are related directly to the differential molecular weight distribution, see Equation 9.

$$w(M) = \frac{dW_i}{dM_i} = \frac{w(\log M)}{M} \quad \text{and} \quad P(M) \propto \frac{w(\log M)}{M^2} \quad (9)$$

The average molecular weights follow directly the SEC chromatogram or the molecular weight distribution, see Equation 10.

$$M_n = \frac{\sum_i H_i}{\sum_i (H_i / M_i)} \quad \text{and} \quad M_w = \frac{\sum_i H_i M_i}{\sum_i H_i} \quad (10)$$

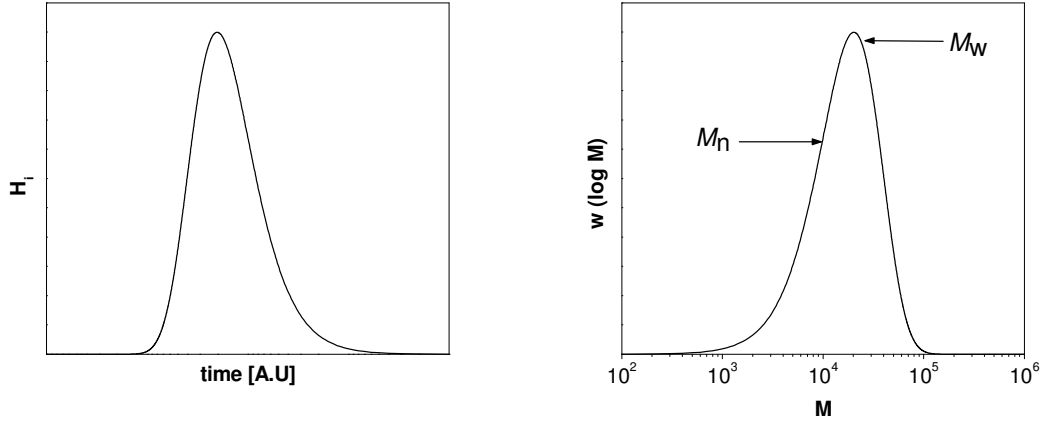


Figure 1. The conversion of a SEC chromatogram to a differential molecular weight distribution and the positions of the number and weight average molecular weight. The molecular weight distribution is generated for MMA using a Flory-Schulz distribution^{4,5} with $M_n = 20199$, $M_w = 30295$ and $PDI = 1.50$.

Kinetic modeling of molecular weight distributions

The two chain stoppage events in free radical polymerization resulting in dead polymer chains with a certain degree of polymerization are termination and chain transfer. The total concentration of dead polymer chains with a chain length i can be denoted as:

$$\frac{d[D_i]}{dt} = 2k_{td}[R_i][R] + k_{tc} \sum_{j=1}^{i-1} [R_j][R_{i-j}] + k_{tr}[R_i][X] \quad (11)$$

In which $[R]$ denotes the total radical concentration, $[R_i]$ the concentration of radicals with chain length i , $[D_i]$ the concentration of polymer chains with a chain length i , $[X]$ the chain transfer agent concentration and k_{td} , k_{tc} and k_{tr} the rate coefficients of termination by disproportionation, termination by combination and chain transfer, respectively. Equation 11 can only be applied if an expression for $[R_i]$ is derived. Using population balance equations for $[R_1]$ and $[R_i]$, and applying the steady-state approximations one obtains:

$$[R_i] = [R_{i-1}]S = [R_1]S^{i-1} = [R](1-S)S^{i-1} \quad (12)$$

Where S is the probability of propagation, see Equation 13, in which k_p is the rate coefficients of propagation.

$$S = \frac{k_p[M]}{k_p[M] + 2k_t[R] + k_{tr}[X]} \quad (13)$$

The probability of propagation can alternatively be written in terms of the kinetic chain length (ν), the number of propagation steps a growing chain can undergo before it undergoes a chain stoppage event (i.e. termination or transfer), see Equation 14.

$$\nu = \frac{k_p[M]}{2k_t[R] + k_{tr}[X]} = \frac{S}{1-S} \text{ or } S = \frac{\nu}{\nu+1} \quad (14)$$

The mass balance of Equation 11 can now be re-written using Equations 12 and 13, see Equation 15.

$$P(i) = \frac{d[D_i]}{dt} \sim F_n(1-S)S^{i-1} + (i-1)(1-F_n)(1-S)^2S^{i-2} \quad (15)$$

Where F_n is the number fraction of chains formed by disproportionation and transfer, see Equation 16.

$$F_n = \frac{k_{tr}[X] + 2k_{td}[R]}{k_{tr}[X] + 2k_{td}[R] + k_{tc}[R]} \quad (16)$$

Equation 15 can be re-arranged to fit the format of a molecular weight distribution obtained by SEC, see Equation 17.³

$$w(\log_{10} i) \propto i^2 n(i) \quad (17)$$

The presented chain length distribution is the Flory-Schulz distribution and is here derived from kinetic principles. For a more in depth derivation of the Flory-Schulz distribution the reader is referred to the original work based on probabilistic principles of Flory and Schulz⁴ or the work based on kinetic principles of Russell.⁵

Chain length dependent kinetics

The rate equation and Mayo equation based on classic free radical kinetics can successfully be used to predict the rate and average degree of polymerization of a free radical polymerization. However, the use of chain-length-averaged rate coefficients, instead of the single chain-length dependent rate coefficient used in the classical free radical polymerization approach, has proven to be a prerequisite and is generally accepted.⁶⁻⁸ The chain-length dependent rate coefficients of propagation (CLDP), termination (CLDT) and transfer (CLDTr) can have major implications for the rate and molecular weight distribution of a free radical polymerization. Chain-length dependent (CLD) kinetics are important in polymerization systems targeting low degrees of polymerization, i.e. high amounts of chain transfer agent and for modeling aqueous phase kinetics in emulsion polymerization.

Rate coefficient of termination (CLDT)

The chain-length dependence of the rate coefficient of termination has long since been recognized and is attributed to diffusion control of the termination reaction.⁶ Besides $\langle k_t \rangle$ being chain-length dependent, $\langle k_t \rangle$ is also known to be highly dependent on conversion, solvent, monomer and so on.^{6,9-11} This results in a situation where a chain-length-averaged $\langle k_t \rangle$ should be used in the rate expression, see Equation 18.

$$\langle k_t \rangle = \sum_{i=1}^{\infty} \sum_{j=1}^{\infty} k_t^{i,j} \frac{[R_i][R_j]}{[R]^2} \quad (18)$$

Where $k_t^{i,j}$ is the termination rate coefficient for the termination reaction between an i -meric radical R_i and a j -meric radical R_j . The total radical concentration is denoted by R . The rate determining step for termination of small radicals is centre-of-mass diffusion which scales with chain length i as $\sim i^{-0.5}$. For long radicals, the rate determining step is segmental diffusion which scales with chain length as i as $\sim i^{-0.16}$. These considerations have been captured in the composite termination model, see Equation 18, where a critical chain-length i_C is assumed to differentiate between centre-of-mass and segmental diffusion.¹⁰

$$k_t^{i,i} = \begin{cases} k_t^{1,1} \times i^{-e_S} & \text{for } i \leq i_C \\ k_t^{1,1} \times i_C^{-e_S+e_L} \times i^{-e_L} & \text{for } i > i_C \end{cases} \quad (19)$$

In Equation 19, $k_t^{i,i}$ is determined by centre-of-mass diffusion for $i \leq i_C$ and by segmental diffusion for $i > i_C$. Where $k_t^{1,1}$ is the “true” termination rate coefficient between two monomeric radicals and e_S and e_L are the scaling exponents for centre-of-mass and segmental diffusion, respectively. Cross-termination between an i -meric radical R_i and a j -meric radical R_j can be described by the geometric mean model, i.e. $k_t^{i,j} = (k_t^{i,i} \times k_t^{j,j})^{1/2}$. The evolution of the CLDT rate coefficient as a function of the chain length i is presented in Figure 2.

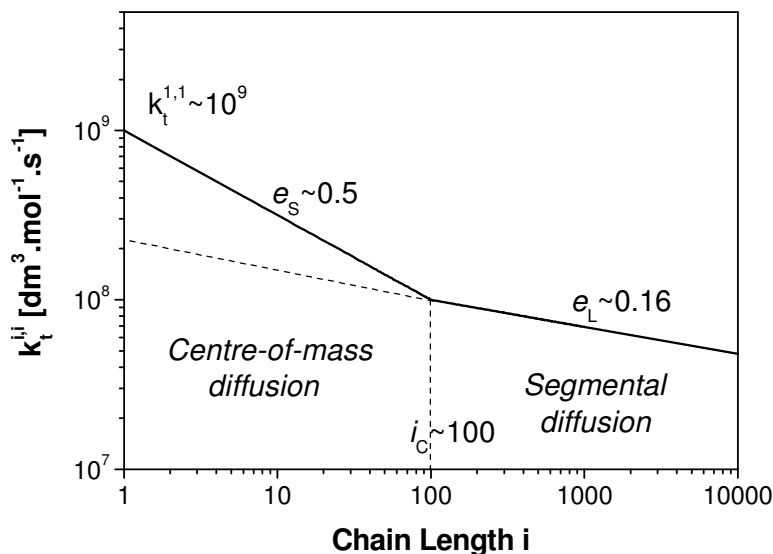


Figure 2. Chain-length dependency of $k_t^{i,i}$ for a methyl methacrylate polymerization as a function of the chain length i . Simulation conditions for $k_t^{i,i}$: $k_t^{1,1} = 10^9 \text{ dm}^3 \cdot \text{mol}^{-1} \cdot \text{s}^{-1}$, $i_c = 100$, $e_s = 0.5$ and $e_L = 0.16$. Indicating the regions of dominant centre-of-mass and segmental diffusion.

Rate coefficients of propagation and chain transfer (CLDP and CLDTr)

Differences in the activation energy and the frequency factor of the addition reaction of different size radicals cause the chain-length dependence of the rate coefficient of propagation.⁹ A chain-length-averaged rate coefficient of propagation is defined by Equation 20, where k_p^i is the rate coefficient of propagation for an i -meric radical with monomer.

$$\langle k_p \rangle = \sum_{i=1}^{\infty} k_p^i \frac{[R_i]}{[R]} \quad (20)$$

The chain-length dependence of the rate coefficient of propagation may be given by an empirical model, see Equation 21, which is able to describe the experimental data available up-to-date.^{9,10}

$$k_p^i = k_p \left\{ 1 + C_1 \exp\left(\frac{-\ln 2}{i_{1/2}}(i-1)\right) \right\} \quad (21)$$

In this equation, k_p denotes the long-chain value rate coefficient of propagation, C_1 is the factor that k_p^1 exceeds the long-chain rate coefficient and $i_{1/2}$ a factor that dictates the chain-length dependence of k_p^i . Even though the chain-length dependence k_p^i quickly converges to the long-chain value, the macroscopic effects of k_p^i on the rate and degree of polymerization may be noticeable in polymerizations with average degrees of polymerization of up to 100.^{9,10} For methyl methacrylate polymerizations it was found that $C_1 = 15.8$ and $i_{1/2} = 1.12$.^{11,12}

Recent modeling studies suggest that the rate coefficient of chain transfer displays comparable chain-length dependence as the rate coefficient of propagation, see Equation 22 and 23.¹³ Where k_{tr}^i is the chain-length dependent rate coefficient for a chain transfer reaction between an i -meric radical with a chain transfer agent.

$$\langle k_{tr} \rangle = \sum_{i=1}^{\infty} k_{tr}^i \frac{[R_i]}{[R]} \quad (22)$$

$$k_{tr}^i = C_T \times k_p^i \quad (23)$$

In Equation 23, C_T is the long-chain value chain transfer constant, which assumed to be chain-length independent. Implementation of chain-length dependent transfer kinetics proved to have no influence on the rate of polymerization but does affect the molecular weight distribution.¹⁰ The evolution of the CLDP rate coefficient as a function of the chain length i is presented in Figure 3.

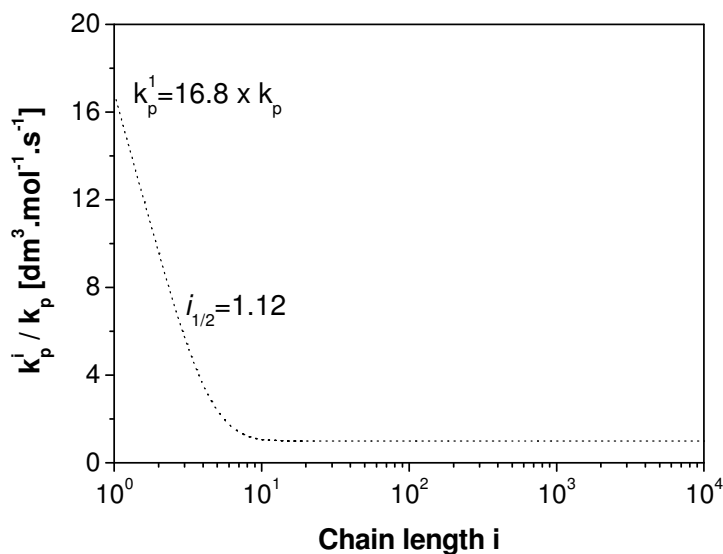


Figure 3. Chain-length dependence of k_p^i and k_{tr}^i for a methyl methacrylate polymerization as a function of the chain length i . Simulation conditions for k_p^i : $C_1 = 15.8$ and $i_{1/2} = 1.12$. Note that the normalized k_{tr}^i results in a similar curve as the one plotted for k_p^i .

EMULSION POLYMERIZATION

Emulsion polymerization is a free radical polymerization in a heterogeneous reaction mixture. In comparison to bulk and solution free radical polymerization, the radicals in an emulsion polymerization are localized within the polymer particles. Emulsion polymerization has some advantages over bulk and solution polymerization, as the overall viscosity remains low, a green solvent (water) is used and due to the compartmentalized nature, high molecular weight polymer can be produced. Products of emulsion polymers are often found in applications as paints and coatings (49%), adhesives (21%) and carpet backing (11%).

The final characteristics of a polymer latex are determined by its micro structural properties, see Figure 4. On a molecular level they include the molecular weight distribution, polymer architecture (branching, crosslinking, grafting), copolymer

composition and the monomer sequence. On a particle level they include the particle size distribution, particle morphology and the surface composition.¹⁴ The molecular properties for instance control the T_g of the (co)polymer, which is an important parameter for the minimum film forming temperature. They also determine the scratch resistance and weatherability of a coating. The molecular weight distribution is a key parameter controlling the final application properties.

The stability of a latex, rheology and the final application properties are determined by the particle size distribution and the surface composition. Rheology of a latex is important as it determines the mixing, heat transfer and the maximum solid content achievable. Particle morphology expands the properties envelope of a latex as it allows for the combination of properties (i.e. hard core and rubbery shell) or the encapsulation of inorganic materials such as silica and clays.

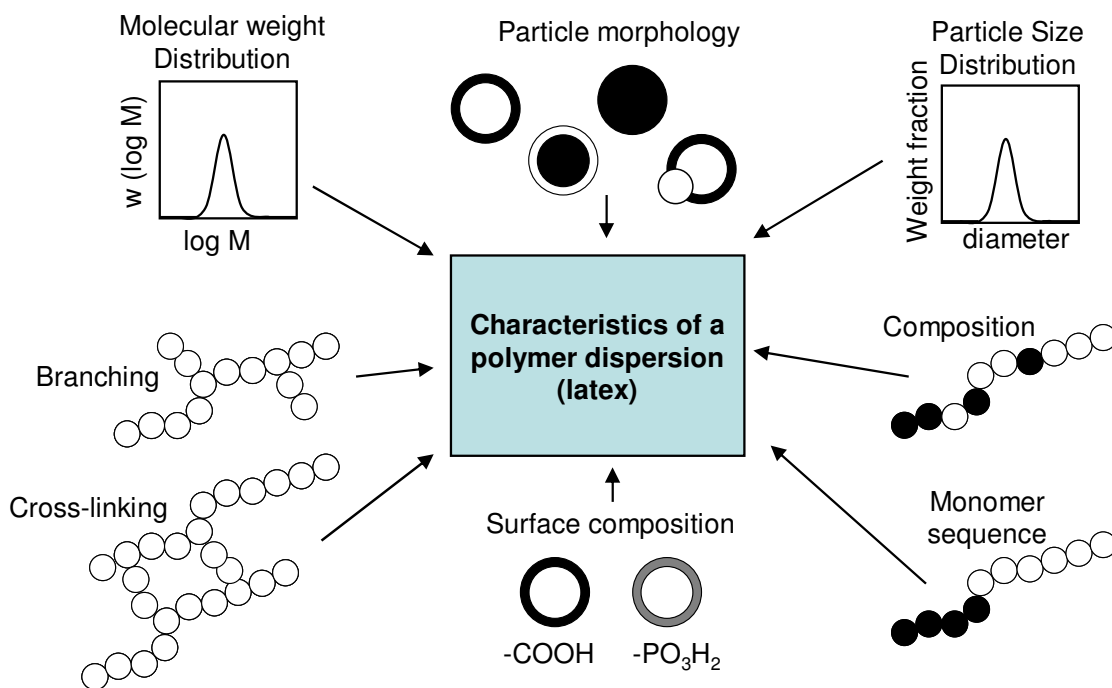


Figure 4. Important micro structural properties determining the characteristics of a polymer latex.

Modified from ref 14

Figure 4 illustrates that the control of the application properties of a latex is complex as many individual micro structural properties can be altered to obtain the desired properties. Moreover, changing the molecular properties of a latex might results in changes of the particle properties. Thorough understanding of the emulsion polymerization kinetics and mechanism is a prerequisite to obtain the desired latex characteristics.

Kinetic considerations

The main loci of polymerization in an emulsion polymerization are the monomer swollen micelles and/or the polymer particles. The radical concentration in an emulsion polymerization can be expressed in terms of an average number of radicals per particle, \bar{n} , see Equation 24, where N_p is the total number of particles per unit volume of water, N_{av} Avogadro's number, n the number of radicals in a particle and N_n the number of particles with n radicals.

$$[R] = \frac{\bar{n}N_p}{N_{av}} \quad \text{where} \quad \bar{n} = \frac{\sum_{n=0}^{n=\infty} nN_n}{\sum_{n=0}^{n=\infty} N_n} \quad (24)$$

$$R_p = -\frac{d[M]}{dt} = k_p[M]_p \frac{\bar{n}N_p}{N_{av}} \quad (25)$$

In emulsion polymerization the radical concentration is expressed in terms of an average number of radicals per particle, \bar{n} . In the expression for the rate of polymerization, $[M]_p$ denotes the monomer concentration inside a polymer particle. The chain-length averaged rate coefficient of propagation is used, however CLDP cannot be ignored. In emulsion polymerization, three distinct intervals can be distinguished: (i) nucleation, (ii) particle growth at the expense of monomer droplets and (iii) complete monomer consumption, see Figure 5.

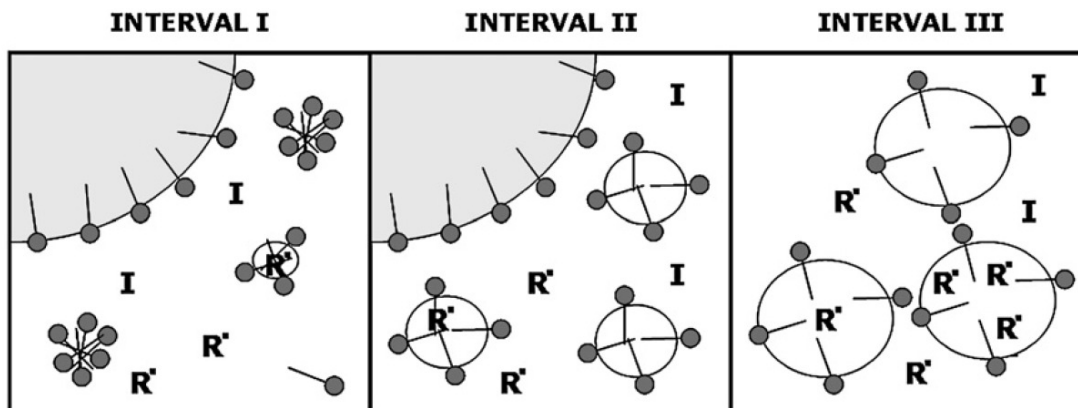


Figure 5. The three intervals of emulsion polymerization, showing surfactant molecules (\bullet —), large monomer droplets, micelles (indicated by clusters of surfactant molecules in interval I), radicals (R^\bullet), initiator (I) and surfactant stabilized latex particles. Reprinted from Ref 15.

An emulsion polymerization typically starts from a monomer-in-water dispersion in the presence of an aqueous surfactant above its critical micelle concentration (CMC). Interval I is that where particle formation takes place by the nucleation of monomer swollen micelles by surface active radicals. A nucleated particle will start growing and consequently absorb surfactant molecules to maintain its colloidal stability. As the particle number N_p continuously increases, the rate of polymerization continuously increases. At a certain point the surfactant concentration in the aqueous phase will drop below the CMC, which marks the end of interval I. In interval II the number of polymer particles remains constant and the monomer concentration inside the polymer particles remains at a saturation level, resulting in a constant rate of polymerization. The large monomer droplets act as monomer reservoirs and continuous monomer transport from the droplets, via the aqueous phase, to the polymer particles maintains the saturation concentration inside the particles; the rate of monomer diffusion is rapid on the time scale of the polymerization. The disappearance of the monomer droplets marks the end of interval II. Interval III commences and the remaining amount of monomer inside the polymer particles is consumed by the propagation reaction. As the monomer concentration inside the polymer particles continuously decreases, the rate of polymerization continuously decreases.

Besides initiation, propagation, termination and chain transfer, the emulsion polymerization kinetics contain the entry and exit of radicals, which in combination with termination govern \bar{n} . Initiation typically occurs in the aqueous phase, however the polymer particles are the predominant locus of polymerization. Hence there has to be a driving force for radicals to enter a polymer particle. The driving force is the water solubility of the radical itself. Propagation of a water soluble radical with a sparsely water soluble monomer results in the formation of surface active radicals that give entry into a polymer particle. Inside the polymer particle, the radical will propagate until a chain stoppage event, i.e. termination or transfer, occurs. Exit of radicals can occur upon formation of small (monomeric) radicals due to the chain transfer reaction. The effect of entry, exit and termination on \bar{n} has been summarized by Smith and Ewart, see Equations 26 and 27.¹⁶

$$\frac{d\bar{n}}{dt} = \text{entry} - \text{exit} - \text{termination} \quad (26)$$

$$\frac{d\bar{n}}{dt} = \left(\frac{\rho}{N} \right) - \left(kA \frac{\bar{n}}{V_p} \right) - \left\{ 2k_t \bar{n} \left(\frac{\bar{n}-1}{V_p} \right) \right\} \quad (27)$$

Where ρ is the pseudo-first-order rate coefficient of entry from the aqueous phase, k the pseudo-first-order rate coefficient of exit from a particle and k_t the rate coefficient of bimolecular termination. A population balance over the number of particles containing n radicals, N_n , at a given instant in time is given by Equation 28.

$$\frac{dN_n}{dt} = \rho [N_{n-1} - N_n] + k [(\bar{n} + 1)N_{n+1} - \bar{n}N_n] + \quad (28)$$

$$k_t [(\bar{n} + 2)(\bar{n} + 1)N_{n+2} - \bar{n}(\bar{n} - 1)N_n], \quad n = 0, 1, 2, 3, \dots$$

Due to the compartmentalized nature of the emulsion polymerization system, bimolecular termination between two radicals in two different particles need not be considered. The rate coefficients of entry, exit and termination depend on a number of different variables

such as the initiator concentration, the number of particles, particle size, presence of a chain transfer agent and so on. The complete steady-state solution of Equation 4 has been reported by Hansen and Ugelstad¹⁷ and Ballard et al.¹⁸ Mechanistic information can be obtained by evaluating the limits of the Smith-Ewart equations:¹⁶

Case 1	$\bar{n} \ll 1$
Case 2	$\bar{n} \sim 0.5$
Case 3	$\bar{n} > 1$

Case 1 is that where the average number of radicals per particle is much lower than unity. If the probability of radicals being transferred out of a particle is high enough, at a given time only a small number of particles will contain a radical (i.e. $\rho \ll k$). Case 1 is typically observed for small particles ($< 100 \text{ nm}$), large particle numbers or a low radical generation rate. The average number of radicals per particle is given by Equation 29, where $[T^*]_{aq}$ is the total radical concentration in the aqueous phase.

$$\bar{n} = \frac{\rho[T^*]_{aq}}{2\rho[T^*]_{aq} + k} \quad (29)$$

Case 2 is that where the average number of radicals per particle is approximately 0.5. The entry of a radical into a polymer particle which already contains a radical results in “instantaneous” termination (i.e. ρ and $k \ll k_t$). As a consequence the number of radicals a particle can contain is restricted to $N_n = 0$ or 1. This limit of the Smith-Ewart kinetics is also referred to as the *zero-one* kinetics and typically holds for relatively small particles ($< 200 \text{ nm}$).

Case 3 is that where the average number of radicals per particle exceeds unity. The compartmentalization effect of radicals has no effect on the kinetics, which are comparable to bulk polymerization kinetics. This limit of the Smith-Ewart kinetics is also referred to as the *pseudo-bulk* kinetics. Case 3 typically holds for relatively large particles ($> 200 \text{ nm}$), high initiator concentration or slow termination rates as for instance occurs

during the gel-effect. The average number of radicals per particle in case 3 is given by Equation 30.

$$\bar{n} = \left(\frac{\rho[T^\bullet]_{aq}}{\frac{2k_t}{V_p N_A}} \right)^{0.5} \quad (30)$$

PROCESS DEVELOPMENT IN EMULSION POLYMERIZATION

Batch emulsion polymerization

Emulsion polymerizations are frequently carried out in (semi-) batch processes. The properties of the latex in terms of e.g. the particle number and the particle size distribution, in a batch reactor strongly depends on the reactor configuration, e.g. impeller type, axial position of the impeller, the number and size of the baffles and the ratio of the impeller diameter and the tank diameter.¹⁹ In addition, a number of operation variables, e.g. the temperature, stirring speed are important.²⁰

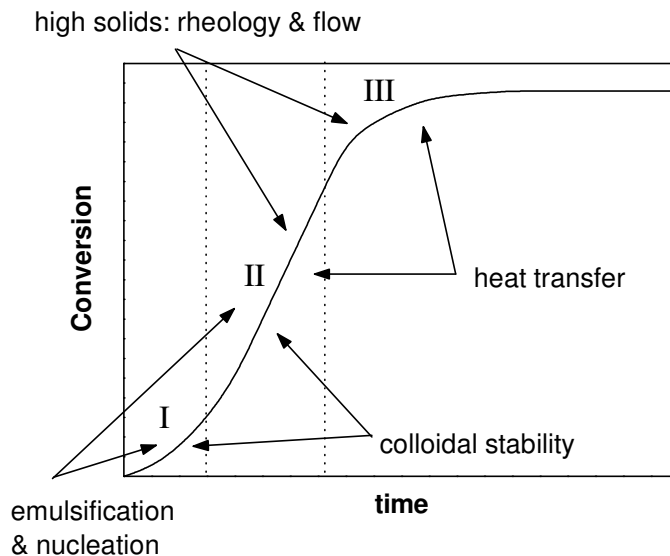


Figure 6. Schematic representation of the various important issues in an *ab-initio* batch emulsion polymerization with sparsely water soluble monomers. Modified from Ref 21.

The course of a typical *ab-initio* batch emulsion polymerization is presented schematically in Figure 6. As the different stages of the emulsion polymerization proceed, different issues need to be addressed to control the product properties of the final product. Proper emulsification of the sparsely water soluble monomer is crucial during the initial stages of the polymerization. The surface area of the monomer-water interphase has to be sufficiently high in order to prevent any mass transport limitations. In the case of negligible resistance to mass transport of monomer from the monomer droplets via the aqueous phase to the growing particles, the polymerization is only determined by its intrinsic rate coefficients of all the fundamental reaction steps involved and by the occurring phase equilibria, i.e. monomer partitioning. Insufficient emulsification has severe implications for the nucleation stage of an emulsion polymerization and consequently for the final product properties in terms of conversion, particle concentration and the particle size distribution. As the nucleation stage is known to be very sensitive to small fluctuations in the recipe, temperature, operation conditions etc. this stage is often circumvented by seeded emulsion polymerization.

The particle concentration is determined by the nucleation stage and remains constant the moment the surfactant concentration drops below the CMC value. During interval II, the polymer particles grow and as a consequence the total surface area of the particles increases. The fractional surface coverage decreases and consequently the repulsive forces between the particles decreases. Particle coagulation can occur^{22,23} if the attractive Van der Waals forces exceed the repulsive forces. If the fractional surface coverage falls below a critical value, particle coagulation occurs until the critical value is reached again. Loss of the colloidal stability results in coagulation, which can result in troublesome operation and the production off-spec product.

In the latter stages of the emulsion polymerization rheology, flow and heat transfer become more important, especially for higher solid content recipes. The apparent viscosity increases significantly during the polymerization resulting in reduced mixing and reduced heat transfer.

Continuous emulsion polymerization

Demands for improved process control and narrow product specifications make that continuous operation may become an interesting alternative to batch polymerization. There are several advantages and disadvantages for continuous emulsion polymerization when compared to batch emulsion polymerization:

Advantages:

- The cost to production volume ratio is decreased.
- Improved product control, i.e. less fluctuation in the product quality.
- Full utilization of the heat transfer capacity.
- Stable operation in terms of fouling due to coagulation.

Disadvantages:

- Less flexibility in terms of operation and product characteristics.
- Formation of off-spec product during the start-up, step-over and shut-down of the process.

For emulsion polymerization in continuously operated reactors, product properties, such as conversion, particle number, particle size distribution and the molecular weight distribution are strongly dependent on the residence time distribution. A single continuously operated stirred tank reactor (CSTR) has a broad residence time distribution. As a consequence intervals I, II and III proceed simultaneously. The conversion and particle number in the product stream of a CSTR are much lower than for a batch process. In a plug flow reactor the three intervals are spatially separated. If the reaction time in an ideally mixed isothermal batch reactor is equal to the residence time in a plug flow reactor, the product properties in terms of the conversion, particle number, particle size distribution and molecular weight distribution are the same for both reactor types. A disadvantage, however, is that plug flow in a tubular reactor demands for turbulent flow and as a consequence for high liquid velocities, leading to impractical reactor dimensions for high monomer conversions. Turbulent flow is also necessary for

proper emulsification and for a low resistance against transfer of the heat of polymerization to the reactor wall. A combination of low net flow rates, limited backmixing, high local flow rates and intensive radial mixing is achieved with the pulsed packed column (PPC),^{24,25} and with the pulsed sieve plate column (PSPC).^{26,27}

Pulsed Sieve Plate Column

Figure 6 shows the Pulsed Sieve Plate Column (PSPC) equipment as used in this study. The PSPC is equipped with a stainless steel packing, consisting of sieve plates which reduce the possibility of fouling. The feed to the column is pulsated and in combination with the sieve plates, this results in high local liquid velocities and consequently proper emulsification inside the reactor. The net-flow through the column is low and this results in practical equipment size.

The residence time distribution in the PSPC is quantified by the plug flow with axial mixing model²⁵ in which axial mixing coefficient E is the key parameter. The dimensionless Peclet number (Pe_L) quantifies the degree of axial mixing, see Equation 31.

$$Pe_L = \frac{u \cdot L}{E} \quad (31)$$

For a column with length L and net liquid velocity u , the Peclet number relates the residence time distribution in the column with that of a series of N equally sized tanks,²⁸ see Equation 32.

$$N_{\text{tanks}} = \frac{Pe_L}{2} \quad (32)$$

The PSPC has proven to be a promising alternative for continuous emulsion polymerization. For ab-initio styrene emulsion polymerization at 90°C a reactor length of 5 m and a mean residence time of about 20 minutes are sufficient for complete conversion

and product properties not significantly different from those of a batch process.²⁶ The PSPC has proven to be a promising reactor for control of the intermolecular chemical composition in seeded emulsion copolymerization.^{27,29}

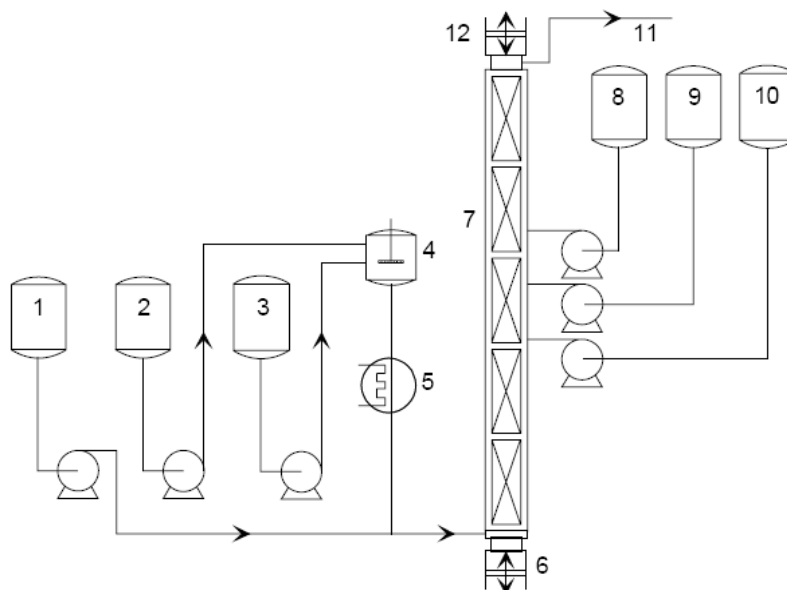
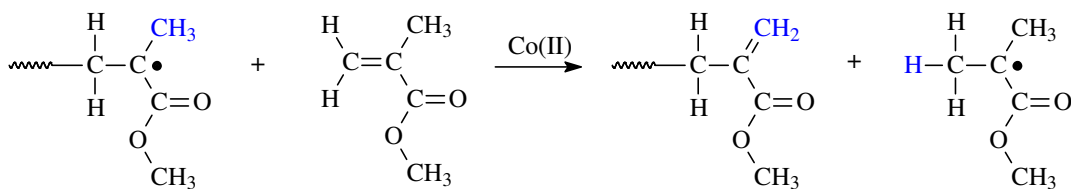


Figure 7. Pulsed Sieve Plate Column (PSPC) flow chart: storage vessels for respectively initiator solution (1), aqueous phase (2) and monomers (3, 8, 9, 10). (4), (5), (6), (7), (11), (12) represent the premixer, the preheater, the pulsation pump, the column packed with sieve plates, the product stream and the pulsation dampener, respectively.²⁹

CATALYTIC CHAIN TRANSFER

Catalytic chain transfer emerged as a new technique for molecular weight control in free radical polymerization in the early 1980's.³⁰⁻³³ Smirnov and co-workers reported that certain low-spin Co(II) complexes are able to catalyze the chain transfer to monomer reaction and hence provide a means for molecular weight control. The most widely accepted mechanism suggests that the radical activity of a propagating polymeric radical is transferred to a monomer molecule, resulting in a dead polymer chain with a vinyl end group functionality and a monomeric radical, see Scheme 1.



Scheme 1. The Co(II) mediated chain transfer to monomer for methyl methacrylate

The catalytic fashion of the Co(II) complex in combination with the high activity in the chain transfer reaction, results in a situation where low molecular weight polymer can be produced with only ppm amounts of the active Co(II) complex. The average degree of polymerization can be predicted by the Mayo Equation.¹ Since catalytic chain transfer is the dominant transfer mechanism, Equation 4 can be re-written, see Equation 33, where $DP_{n,0}$ represents the degree of polymerization obtained in the absence of a chain transfer agent, assuming chain-length independent kinetics.

$$DP_n^{-1} = DP_{n,0}^{-1} + C_T \frac{[Co]}{[M]} \quad (33)$$

The transfer constant measured for the most commonly used catalytic chain transfer agent, bis[(difluoroboryl) dimethylglyoximato]cobalt(II) (COBF), and an overview of different chain transfer agents and their transfer constants, is presented in Table 1.

Table 1. An overview of typical chain transfer constants in bulk methyl methacrylate polymerization at 60°C.

<i>Compound</i>	C_T	<i>Reference</i>
	[-]	
Monomer	$1 \cdot 10^{-5}$	34
n-dodecanethiol	1.2	35
CBr ₄	0.27	34
COBF	$(24 - 40) \cdot 10^3$	36
COPhBF	$(18 - 24) \cdot 10^3$	36

An overview of the most important aspects of catalytic chain transfer are presented below. For more a more extensive overview the reader is referred to some excellent reviews.³⁷⁻⁴¹

Mechanistic Aspects

The most widely accepted mechanism for catalytic chain transfer is a two-step reaction involving a Co(III)-H intermediate.^{33,37,41,42-45} During the catalytic chain transfer process, the Co(II) catalyst abstracts a hydrogen atom from a carbon atom in the α -position relative to the radical centre and subsequently a Co(III)-H and a dead polymer chain are formed. The Co(III)-H is extremely reactive and will react with a monomer molecule by a hydrogen transfer reaction yielding the Co(II) chain transfer catalyst and a propagating monomeric radical. The kinetic equations for the chain transfer and re-initiation step are presented in Equations 34 and 35, expressing the true catalytic nature of the process.



Organocobalt complexes can be formed by the radical-radical combination of a Co(II) with an organic radical. The formed Co-C bonds are known to be reversible and have been observed in the polymerization of monomers forming secondary radicals, such as styrene and acrylates,⁴⁶⁻⁵² see Equation 36.

The formation of Co-C bonds in a catalytic chain transfer mediated polymerization decreases the active Co(II) concentration. As the steady-state radical concentration is in the order of 10^{-7} - 10^{-8} mol.dm⁻³ and the Co(II) concentration comparable or higher, a significant amount of the radicals formed at the initial stages of the polymerization are captured by Co-C bond formation. This results in an inhibition period and the formation of Co(III)-R in the early stages of the polymerization.⁵¹ Co-C bond formation in methyl methacrylate polymerizations is negligible and most of the cobalt complex is in its Co(II)

state⁵³ whereas in styrene polymerization the cobalt complex is predominantly in its Co(III) state,⁵¹ see Equation 36 and 37.



$$K = \frac{[Co(III) - R]}{[Co(II)][R^{\bullet}]} \quad (37)$$

As the steady-state effective Co(II) concentration is lower as a consequence of Co-C bond formation, the measured chain transfer constant is apparently lower, see Equation 38. Where $[Co(II)]$ and $[Co(II)]_0$ are the actual and initial Co(II) concentration respectively and C_T^{app} the apparent chain transfer constant.

$$C_T^{app} = C_T \frac{[Co(II)]}{[Co(II)]_0} \quad (38)$$

This consideration has two important implications for polymerizations with significant Co-C bond formation. First, as the actual Co(II) concentration is decreasing in the initial stages of the polymerization, DP_n is increasing and the apparent chain transfer constant shows a dependency on conversion. Secondly, the apparent chain transfer constant depends on the initiator concentration, see Equation 39.⁵²

$$C_T^{app} = C_T \frac{1}{1 + K \sqrt{\frac{fk_d[I]}{\langle k_t \rangle}}} \quad (39)$$

As mentioned before, the formation of Co-C bonds is reversible and an increase in the Co(II) concentration can be achieved by performing the polymerization under ultraviolet conditions.^{52,54}

Determination of the Chain Transfer Constant

The activity of a transfer agent is expressed in terms of the chain transfer constant, the ratio of the transfer rate coefficient and the propagation rate coefficient, see Equation 40. The transfer constant can be measured experimentally in two ways: (i) by the Mayo method and (ii) by the chain length distribution (CLD) method.

$$C_T = \frac{k_{tr}}{k_p} \quad (40)$$

The Mayo method depends on the measurement of the degree of polymerization as a function of different ratios of the chain transfer agent concentration and the monomer concentration. The degree of polymerization is obtained from the molecular weight distribution at low conversions. Note that the number average molecular weight is known to be prone to uncertainties in the baseline correction, therefore for the determination of the instantaneous degree of polymerization, from an experimentally obtained molecular weight distribution, the use of the weight average molecular weight is preferred, i.e.

$DP_n = \frac{M_w}{2M_0}$.^{55,56} The obtained degrees of polymerization can be plotted against the inverse degree of polymerization and the slope of the best linear fit equals the chain transfer constant, see Figure 8.

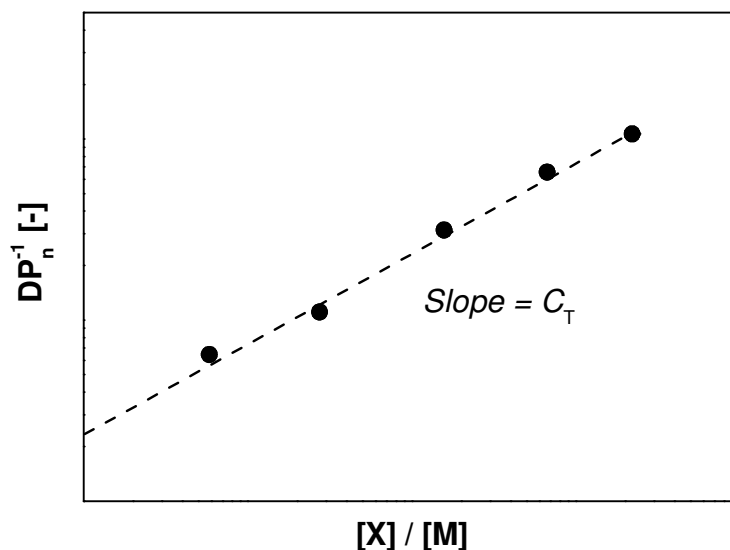


Figure 8. Mayo plot for the determination of the chain transfer constant.

An alternative approach to the Mayo method is the chain length distribution method, which uses the high molecular weight slope, Λ_H , of the chain length distribution $P(M)$, plotted as $\ln(P(M))$ against M , Equation 41.^{3,57-59}

$$\lim_{M \rightarrow \infty} \frac{d \ln P(M)}{dM} = - \left(\frac{\langle k_t \rangle [R]}{k_p [M]} + C_M + C_T \frac{[X]}{[M]} \right) \frac{1}{M_0} = \Lambda_H \quad (41)$$

The slope, Λ_H , can be measured for different chain transfer agent to monomer concentration ratios and a plot of Λ_H against $[X] / [M]$ should yield a straight line of which the slope equals $-C_T / M_0$. To reduce baseline correction errors, it was suggested to use the slope in the peak region, Λ_p , of the molecular weight distribution.^{56,60} When chain transfer is the predominant chain stoppage event, Equation 5 can be simplified to Equation 42.

$$\Lambda_p = \frac{d \ln P(M)}{dM} \approx - \left(C_T \frac{[X]}{[M]} \right) \frac{1}{M_0} \quad (42)$$

The number distribution $P(M)$ is calculated from the molecular weight distribution. The arbitrary constant is irrelevant in this procedure, as only the slope of the $\ln P(M)$ curve is evaluated.

$$P(M) = (\text{arbitrary constant}) \times \frac{w(\log M)}{M^2} \quad (43)$$

The conversion of the SEC chromatogram to the molecular weight distribution, the number distribution is presented and the CLD plot are presented in Figure 9.

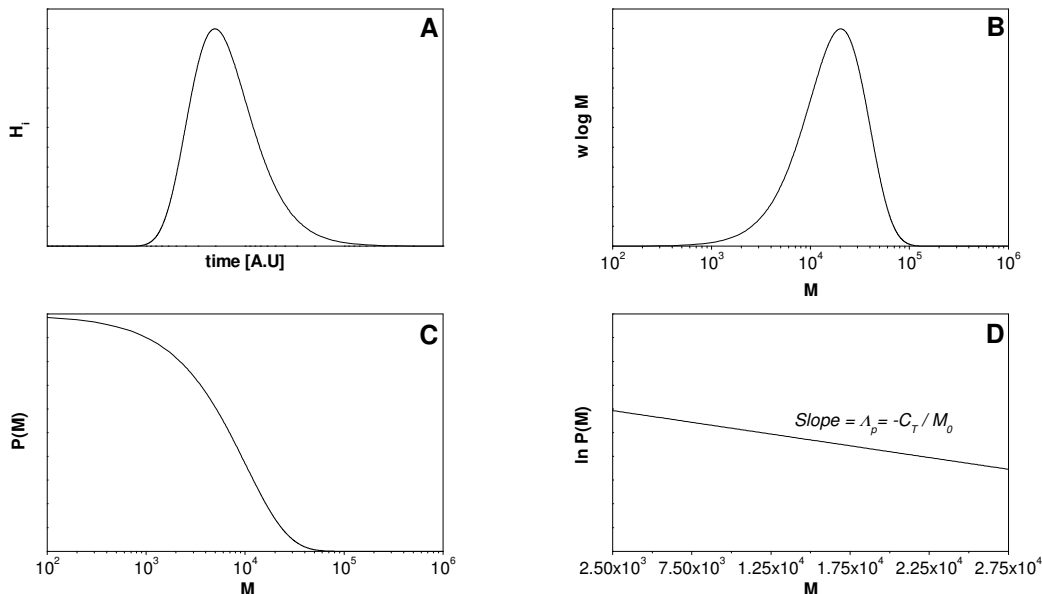


Figure 9. The conversion of an experimental size exclusion chromatogram (A) to a molecular weight distribution (B), the number distribution (C) and the CLD plot (D).

The molecular weight distribution is generated for MMA using a Flory-Schulz distribution⁵ with $F_n = 0.99$ and $S = 0.9905$, resulting in a $M_n = 20.200$ and a PDI = 1.50. The CLD method results in $\Lambda_p = 1 \cdot 10^{-4}$.

The Mayo method and the CLD method are intrinsically identical. However, there are two distinct problems while using the Mayo method. First, the Mayo method encounters

problems when very low molecular weights are considered. Accurate determination of the number average molecular weight (M_n) and the weight average molecular weight (M_w) are difficult at low molecular weights and the rate coefficient for chain transfer becomes chain-length dependent at low degrees of polymerization. The Mayo Equation was derived using the long-chain approximation, which is not valid anymore at these low degrees of polymerization. Gridnev and co-workers have shown that a modified Mayo equation is more appropriate in under these conditions, which has been derived from the notion that chains shorter than 2 units will not be produced, see Equation 44.^{37,42} At the high catalytic chain transfer agent concentrations required for the production of short oligomers, a substantial amount of monomeric radicals will be converted back to monomer before a second monomer addition can occur. Pierik et al estimated that as much as 28% of the monomer consumption is caused by the re-initiation of monomer.⁴⁸

$$DP_n^{-1} = 2 + C_T \frac{[Co]}{[M]} \quad (44)$$

Secondly, accuracy using the Mayo method is lost when a SEC chromatogram consisting of multiple molecular weight distributions is analyzed. Peak selection becomes increasingly difficult when the individual molecular weight distributions overlap. The degree of polymerization of each individual molecular weight distributions can be determined, however multiple manipulations are necessary to extract the required information. The CLD method has proven to be more accurate when dealing with low molecular weight and contaminated samples. First, values for Λ_H can be obtained from the higher molecular weight end of the distribution in case of very low molecular weight samples and secondly, a value for Λ_p can be obtained from the individual molecular weight regions of the P(M) distribution.⁵⁶

Catalytic chain transfer in homogeneous reaction media

In catalytic chain transfer mediated homogeneous polymerization systems, i.e. bulk and solution polymerization, the rate of polymerization and the average degree of

polymerization can be accurately predicted by the rate and Mayo equations. However, as the polymerization proceeds, the Mayo equation predicts a decreasing instantaneous degree of polymerization as the monomer concentration in the reaction mixture keeps decreasing. Most experimental data available up-to-date reveals a constant or slightly increasing instantaneous degree of polymerization.⁴⁵ Only two studies have actually measured a decrease in the instantaneous degree of polymerization.^{61,62}

Catalytic chain transfer in heterogeneous reaction media

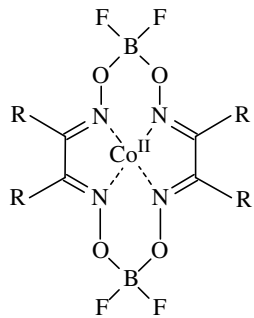
Heterogeneous reaction media, i.e. (mini)emulsion polymerization poses a number of complications for the application of catalytic chain transfer. Straightforward usage of the Mayo and rate equations is no longer possible. A number of observations concerning catalytic chain transfer in (mini)emulsion polymerization have been made:

- The hydrophobicity of the monomer and catalyst are important.⁶³⁻⁶⁵
- Catalytic chain transfer is less effective as in bulk and solution polymerization.^{65,66}
- The rate of polymerization is affected by the presence of a catalytic chain transfer agent.^{64,65,67}
- Feed conditions and the T_g are import for proper molecular weight control.^{64,66,68}

In an emulsion polymerization the polymerization proceeds predominantly in the polymer particles, the loci of polymerization. Therefore, for proper molecular weight control, the catalytic chain transfer agent has to be at the locus of polymerization. Certain aqueous phase solubility is required, to allow transport of the catalytic chain transfer agent between monomer droplets, aqueous phase and polymer particles, i.e. the catalytic chain transfer agent will partition over the different phases present in an (mini)emulsion polymerization.⁶³⁻⁶⁵ The partitioning behavior, expressed as the partition coefficient, m_{Co} , of a catalytic chain transfer agent depends both on the catalyst structure and the monomer used, Table 2. The partitioning coefficient is expressed as the ratio of the cobalt complex concentration in the organic phase and aqueous phase, see Equation 45.

$$m_{\text{Co}} = \frac{[\text{Co}]_{\text{org}}}{[\text{Co}]_{\text{wat}}} \quad (45)$$

Table 2. Relation between the catalyst structure the activity and partitioning behavior.

	<i>Catalyst</i>	<i>R</i>	C_T^a	m_{Co}^b	<i>Ref.</i>
			[x 10 ³]		
	COBF	Me	20-40	0.31 – 0.68	48, 63, 64
	COEtBF	Et	18	19	48, 69
	COPhBF	Ph	14-20	∞	48, 63

^a Determined at 60°C in bulk polymerization. ^b Partition coefficient calculated from reported experimental observations based on MMA / water systems.

An increase in the hydrophobicity of the *R*-group of the ligand results in a drastic change in the partitioning behavior, from COBF which partitions readily between the aqueous phase and monomer phase to COPhBF which partitions exclusively towards the monomer phase. Catalytic chain transfer mediated emulsion polymerizations in the presence of COPhBF are expected to suffer from severe mass transport limitations and therefore poor molecular weight control. However, semi-batch emulsion polymerization of MMA with COPhBF was found to control the molecular weight distribution to some extent, implying (limited) transport of COPhBF.⁶³ The mode of transport of COPhBF was not further investigated.

Catalytic chain transfer agent partitioning in (mini)emulsion polymerization is suggested to have three major implications (i) a decrease in the rate of polymerization,^{64,65,67} (ii) catalytic chain transfer agent deactivation⁶⁴⁻⁶⁶ and (iii) lower chain transfer activity.^{65,66} The presence of COBF in the aqueous phase of an emulsion polymerization is suggested to result in a decrease of the entry rate of surface active oligomers as aqueous phase chain transfer events can result in termination of propagating radicals prior to entry.⁶³ Besides decreasing the rate of entry in an emulsion polymerization, the catalytic chain transfer

process inside the polymer particles also results in the formation of monomeric radicals, which can easily give exit. A combined reduced rate of entry and an increased rate of exit results in a decrease of \bar{n} and consequently a decrease in the rate of polymerization.^{64,65,67}

A cobalt complex in the aqueous phase of an emulsion polymerization is also prone to deactivation.⁶⁴⁻⁶⁶ Despite the introduction of the BF₂ bridges, which significantly improved the cobalt complex stability, the complex is readily oxidized by oxygen,^{37,70} (peroxide) radicals^{37,53,71} or hydrolyzed in acidic media.³⁷ Cobalt complex deactivation results in a lowering of the overall cobalt concentration and consequently an increase in the average degree of polymerization of the polymer formed. Kukulj et al. showed that, a miniemulsion of MMA with a persulfate initiator resulted in severe deactivation in the case of COBF and consequently loss of control of the molecular weight distribution. However, when CPhBF was used, which resides exclusively in the monomer droplet, no deactivation and a constant reduction in the average degree of polymerization was achieved.⁶⁵

Bon et al. determined the chain transfer constant in a MMA/HEMA emulsion copolymerization and observed chain transfer constants roughly one order of magnitude below the corresponding values determined from bulk polymerization.⁶⁶ The lower activity of a cobalt complex in emulsion polymerization when compared to bulk or solution polymerization has been accounted to the effects of deactivation and partitioning.⁶⁶ Where catalytic chain transfer deactivation results in a decrease of the overall amount of cobalt complex, partitioning merely results in a distribution of the cobalt complex over the different phases present. As in emulsion polymerization molecular weight control is achieved inside the polymer particles, both deactivation and partitioning lower the actual concentration at the locus of polymerization. In addition to the effect of partitioning and deactivation, the increasing viscosity inside a polymer particle was also mentioned to restrict the catalyst mobility and hence the activity.⁶⁶

Throughout the course of an emulsion polymerization, the reaction environment inside the polymer particles is changing from a low viscosity monomer swollen system to a high

viscosity system as the weight fraction of polymer is increasing. Although a shift to lower instantaneous degrees of polymerization is expected at high monomer conversion, a clear increase is experimentally observed. Whereas this increasing degree of polymerization is often attributed to catalyst deactivation, this could also be attributed to the increasing viscosity inside the polymer particle. The rate coefficient of chain transfer is of the same order of magnitude as the rate coefficient of termination, which is known to be diffusion limited. In other words, at high conversion the chain transfer reaction might be diffusion controlled.

When low molecular weight polymer is desired, a plasticizing effect of the catalytic chain transfer agent is observed and consequently proper molecular weight control throughout the whole polymerization.⁶⁸ However, when intermediate molecular weights are desired, the plasticizing effect of the catalytic chain transfer agent alone is not sufficient. Initial shots of monomer, ensuring a low instantaneous conversion and hence monomer flooded conditions, proved to be required for proper control of the molecular weight distribution.^{63,64,66,68} Comparable observations were made for a catalytic chain transfer mediated emulsion polymerization of a low T_g monomer, i.e. butyl methacrylate, however the effects are reduced as a consequence of the lower T_g .⁶⁸

SCOPE OF THE THESIS

Catalytic chain transfer has been an established technique for the control of the molecular weight distribution in free radical polymerization. However, most mechanistic studies have focussed on the catalytic chain transfer mediated bulk and solution polymerization. The main objective of this work was to elucidate the effects a catalytic chain transfer agent has on the control of the molecular weight distribution and the emulsion polymerization kinetics and mechanism.

The most important aspect of catalytic chain transfer in emulsion polymerization is the fact that the heterogeneity of the emulsion polymerization system, implies catalytic chain transfer partitioning. The effect of catalytic chain transfer agent partitioning is presented in Chapter 2.

The effect of the emulsion polymerization system on the catalytic chain transfer process is presented in Chapters 2 - 4. The heterogeneity of the emulsion polymerization system implies catalytic chain transfer partitioning, which is discussed in Chapter 2. Transport of the catalytic chain transfer agent towards the loci of polymerization is presented in Chapter 3. Severe reduction in the rate of mass transport of the catalytic chain transfer agent might result in compartmentalization behavior which is discussed in Chapter 4.

The presence of a catalytic chain transfer agent in an emulsion polymerization affects the emulsion polymerization kinetics and mechanism. The effect on the course of the polymerization and kinetic events such as entry and exit is presented in Chapter 5.

Complete mechanistic understanding of a (polymer) process is required before any larger scale operation can be investigated. The control of the molecular weight distribution on a large continuous scale is presented in Chapter 6. The implications the addition a catalytic chain transfer agent has on the latex properties and operation characteristics are illustrated by a number of polymerizations in the pulsed sieve plate column.

REFERENCES

1. Mayo, F.R. *J. Am. Chem. Soc.* 1943, 65, 2324.
2. Shortt, D.W. *J. Liquid. Chrom.* 1993, 16, 3371.
3. Clay, P.A.; Gilbert, R.G. *Macromolecules* 1995, 28, 552.
4. Flory, P.J. *Principles of Polymer Chemistry* 1st Ed. 1953 Cornell university Press, Ithica NY.
5. Russell, G.T. *Aust. J. Chem.* 2002, 55, 399.
6. Buback, M.; Egorov, M.; Gilbert, R.G.; Kaminsky, V.; Olaj, V.F.; Russell, G.T.; Vana, P.; Zifferer, G. *Macromol. Chem. Phys.* 2002, 203, 2570.
7. Barner-Kowollik, C.; Buback, M.; Egorov, M.; Fukuda, T.; Goto, A.; Olaj, O.F.; Russell, G.T.; Vana, P.; Yamada, B.; Zetterlund, P.B. *Prog. Polym. Sci.* 2005, 30, 605.
8. Buback, M.; Gilbert, R.G.; Russell, G.T.; Hill, D.J.T.; Moad, G.; O'Driscoll, K.F.; Shen, J.; Winnik, M.A. *J. Polym. Sci. Part A: Polym. Chem.* 1992, 30, 851.
9. Heuts, J.P.A.; Russell, G.T. *Eur. Polym. J.* 2006, 42, 3.
10. Smith, G.B.; Russell, G.T.; Yin, M.; Heuts, J.P.A. *Eur. Polym. J.* 2005, 41, 225.
11. R.X.E. Willemse; B.B.P. Staal; A.M. van Herk; S.C.J. Pierik; B. Klumperman *Macromolecules* 2003, 36, 9797.
12. Heuts, J.P.A.; Russell, G.T.; van Herk, A.M. *Macromol. Symp.* 2007, 248, 12.
13. Heuts, J.P.A.; Russell, G.T.; Smith, G.B. *Aust. J. Chem.* 2007, 60, 754.
14. Barandiaran, M.J.; de la Cal, J.C.; Asua, J.M. in *Polymer Reaction Engineering*, Ed. Asua, J.M. 2007, Blackwell Publishing Ltd.
15. Thickett, S.C.; Gilbert, R.G. *Polymer*, 2007, 48, 6965.
16. Smith, W.V.; Ewart, R.H. *J. Chem. Phys.* 1948, 16, 592.
17. Ugelstad, J.; Hansen, F.K. *Rubber Chem. Technol.* 1976, 49, 536.
18. Ballard, M.J.; Gilbert, R.G.; Napper, D.H. *J. Polym. Chem. Polym. Lett. Ed.* 1981, 19, 533.
19. Meuldijk, J.; Kemmere, M.F.; de Lima, S.V.W.; Reynhout, X.E.E.; Drinkenburg, A.A.H.; German, A.L. *Polym. React. Eng.* 2003, 11, 259.
20. Poehlein, G.W.; *Reaction engineering for emulsion polymerization, Polymeric Dispersions: Principles and Applications*, Ed. J.M. Asua, Kluwer Academic publishers, pg. 305.
21. Kemmere, M.F., Meuldijk, J., Drinkenburg, A.A.H., German, A.L.; *J. Appl. Polym. Sci.*, 1999, 74, 3225.
22. Hiemenz, P.C., "Principles of colloid and surface chemistry", Marcel Dekker, 1986, New York.

23. Kemmere, M.F., Meuldijk, J., Drinkenburg, A.A.H., German, A.L.; Appl. Polym. Sci., 1998, 69, 2409.
24. Meuldijk, J.; van Strien, C.J.G.; van Doormalen, F.A.H.C.; Thoenes, D. Chem. Eng. Sci. 1992, 47, 2603.
25. Meuldijk, J.; German, A.L. Polym. React. Eng. 1999, 7, 207.
26. Meuldijk, J.; Scholtens, C.A.; Reynhout, X.E.E.; Drinkenburg, A.A.H., DECHEMA Monographien, 2001, 137, 633.
27. Scholtens, C.A.; Meuldijk, J.; Drinkenburg, A.A.H. Chem. Eng. Sci. 2001, 56, 955.
28. Levenspiel, O. "Chemical Reaction Engineering", 1972, Wiley, New York.
29. van den Boomen, F.H.A.M.; Meuldijk, J.; Thoenes, D. Chem. Eng. Sci. 1999, 54, 3283.
30. Smirnov, B.R.; Morozova, I.S.; Pushchaeva, L.M.; Marchenko, A.P.; Enikolopyan, N.S. Dokl. Akad. Nauk. SSSR (Engl. Transl.) 1980, 255, 609.
31. Smirnov, B.R.; Plotnikov, V.D.; Ozerkovskii, B.V.; Roshchupkin, V.P.; Yenikolopyan, N.S. Polym. Sci. USSR 1981, 23, 2807.
32. Smirnov, B.R.; Marchenko, A.P.; Plotnikov, V.D.; Kuzayev, A.I.; Yenikolopyan, N.S. Polym. Sci. USSR 1981, 23, 1169.
33. Enikolopyan, N.S.; Smirnov, B.R.; Ponomarev, G.V.; Belgovskii, I.M. J. Polym. Sci., Polym. Chem. Ed. 1981, 19, 879.
34. Berger, K.C.; Brandrup, G. in Polymer Handbook, 3rd Edition, Eds. Brandrup, J.; Immergut, E.H., Wiley, 1989.
35. Heuts, J.P.A.; Davis, T.P.; Russell, G.T. Macromolecules 1999, 32, 6019.
36. Heuts, J.P.A.; Roberts, G.E.; Biasutti, J.D. Aust. Chem. J. 2002, 55, 381.
37. Gridnev, A. A.; Ittel, S. D. Chem Rev 2001, 101, 3611.
38. Heuts, J. P. A.; Roberts, G. E.; Biasutti, J. D. Aust J Chem 2002, 55, 381.
39. Karmilova, L.V.; Ponomarev, G.V.; Smirnov, B.R.; Belgovskii, I.M. Russ. Chem. Rev. 1984, 53, 132
40. Davis, T.P.; Haddleton, D.M.; Richards, S.N. J. Macromol. Sci., Rev. Macromol. Chem. 1994, C34, 234
41. Davis, T.P.; Kukulj, D.; Haddleton, D.M.; Maloney, D.R. Trends Polym. Sci. 1995, 3, 365
42. Gridnev, A.A.; J. Polym. Sci. Part A: Polym. Chem. 2000, 38, 1753.
43. Kukulj, D.; Davis, T.P. Macromol. Chem. Phys. 1998, 199, 1697.
44. Heuts, J.P.A.; Forster, D.J.; Davis, T.P. Macromol. Rapid Commun. 1999, 20, 299.

45. Heuts, J.P.A.; Forster, D.J.; Davis, T.P. in *Transition Metal Catalysis in Macromolecular Design*, Eds. Boffa, L.S.; Novak, B.M., ACS Symposium Series, 2000, Vol. 760, p. 254, American Chemical Society, Washington.
46. Pierik, S.C.J.; Masclee, D.; van Herk, A.M. *Macromol. Symp.* 2001, 165, 19.
47. Gridnev, A.A.; Ittel, S.D.; Fryd, M.; Wayland, B.B. *J. Chem. Soc., Chem. Commun.* 1993, 1010.
48. Pierik, S.C.J. *Shining a Light on Catalytic Chain Transfer*, Ph.D thesis, Eindhoven University of Technology, Eindhoven, 2002.
49. Roberts, G.E.; Heuts, J.P.A.; Davis, T.P. *Macromolecules* 2000, 33, 7765.
50. Wayland, B.B.; Poszmik, G.; Mukerjee, S.L.; Fryd, M. *J. Am. Chem. Soc.* 1994, 116, 7943.
51. Heuts, J.P.A.; Forster, D.J.; Davis, T.P.; Yamada, B.; Yamazoe, H.; Azukizawa, M. *Macromolecules*, 1999, 32, 2511.
52. Roberts, G.E.; Barner-Kowollik, C.; Davis, T.P.; Heuts, J.P.A. *Macromolecules*, 2003, 36, 1054.
52. Roberts, G.E.; Heuts, J.P.A.; Davis, T.P. *J. Polym. Sci. Part A. Polym. Chem.* 2003, 41, 752.
53. Morrison, D.A.; Davis, T.P.; Heuts, J.P.A.; Messerle, B.; Gridnev, A. A. *J Polym Sci Part A: Polym Chem* 2006, 44, 6171.
54. Pierik, S.C.J.; Vollmerhaus, R.; van Herk, A.M.; German, A.L. *Macromol. Symp.* 2002, 182, 43
55. Heuts, J.P.A. ; Kukulj D. ; Forster, D.J. ; Davis, T.P. *Macromolecules* 1998, 31, 2894
56. Heuts, J.P.A.; Davis, T.P.; Russell, G.T. *Macromolecules* 1999, 32, 6019
57. Whang, B.Y.C.; Ballard, M.J.; Napper, D.H.; Gilbert, R.G. *Aust. J. Chem.* 1991, 44, 1133
58. Christie, D.I.; Gilbert, R.G. *Macromol. Chem. Phys.* 1996, 197, 403.
59. Whang, B.Y.C.; Ballard, M.J.; Napper, D.H.; Gilbert, R.G. *Aust. J. Chem.* 1991, 44, 1133
60. Moad, G.; Moad, C.L. *Macromolecules* 1996, 29, 7727.
61. Kowollik, C. ; Davis, T.P. *J. Polym. Sci. Part A: Polym. Chem.* 2000, 38, 3303.
62. Pierik, S.C.J.; van Herk, A.M. *J. App. Polym. Sci.* 2004, 91, 1375.
63. Kukulj, D.; Davis, T.P.; Suddaby, K.G.; Gilbert, R.G. *J. Polym. Sci. Part A: Polym. Chem.* 1997, 35, 859.
64. Suddaby, K.G.; Haddleton, D.M.; Hastings, J.J.; Richards, S.N.; O'Donnell, J.P. *Macromolecules* 1996, 29, 8083.
65. Kukulj D.; Davis, T.P.; Gilbert R.G. *Macromolecules* 1997, 30, 7661.
66. Bon, S.A.F; Morsely, D.R.; Waterson, J.; Haddleton, D.M. *Macromol. Symp.* 2001, 165, 29.
67. Pierik, S.C.J.; Smeets, B.; van Herk, A.M. *Macromolecules* 2003, 36, 9271.

68. Haddleton, D.M.; Morsely, D.R.; O'Donnell, J.P.; Richards, S.N. *J. Polym. Sci. Part A: Polym. Chem.* 2001, 37, 3549.
69. Waterson, J.L; Haddleton, D.M.; Harrison, R.J.; Richards, S.N. *Pol. Preprints (ACS)* 1998, 39, 457
70. Grindev, A. A. *Polym. Sci. USSR* 1989, 31, 2369.
71. Gridnev, A. A. *Polym. J.* 1992, 7, 613.

Effect of catalyst partitioning in Co(II) mediated catalytic chain transfer miniemulsion polymerization of methyl methacrylate.

ABSTRACT

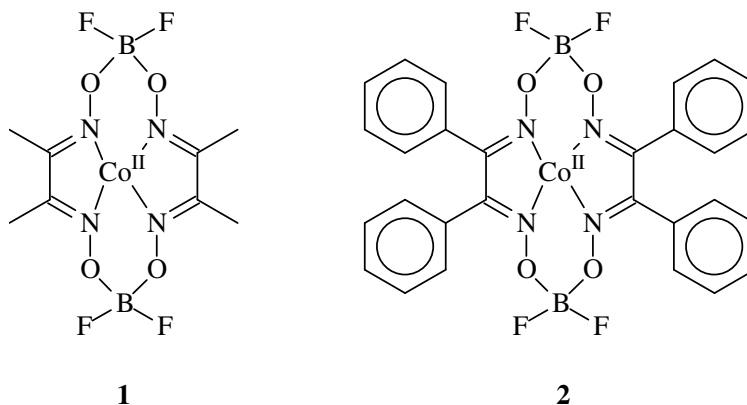
The effect of catalyst partitioning over the organic and water phases in the catalytic chain transfer (CCT) mediated miniemulsion polymerization was investigated and a mathematical model developed to describe the instantaneous degree of polymerization of the formed polymer. Experimental and predicted instantaneous degrees of polymerization prove to be in excellent agreement.

INTRODUCTION

In bulk and solution polymerization the molecular weight of the polymer formed can be predicted accurately by the Mayo equation, which relates the number average degree of polymerization (DP_n) to the catalyst activity and the amount of catalytic chain transfer agent (CCTA)¹, see Equation 1. In this equation, $DP_{n,0}$, $C_{Co,0}$ and C_M are the number average degree of polymerization without CCTA, the concentration of CCTA and monomer, respectively.

$$DP_n^{-1} = DP_{n,0}^{-1} + C_T \frac{C_{Co,0}}{C_M} \quad (1)$$

The CCTA activity is expressed by the chain transfer constant ($C_T = \frac{k_{tr}}{k_p}$), in which k_{tr} is the rate coefficient for the chain transfer reaction and k_p the propagation rate coefficient.



Scheme 1. Catalytic chain transfer agents used in this work, COBF **1** and COPhBF **2**.

Both bulk and solution polymerizations are homogeneous reaction systems, which implies that the concentration of CCTA at the locus of polymerization is equal to the overall (bulk) concentration for a perfectly mixed reactor. For low monomer conversions the molecular weight of the polymer produced can be predicted with Equation 1 as was shown previously.²⁻⁴ In emulsion polymerization⁵⁻¹⁰, however, one cannot simply apply Equation 1 using global concentrations. The reason for this is that the CCTA

concentration at the locus of polymerization, i.e. the polymer particles, differs from the overall CCTA concentration as a result of partitioning^{11,12} of the CCTA over the different phases in the heterogeneous reaction mixture. The range of C_T values reported in literature for the catalysts used in this work, i.e. bis[(difluoroboryl)dimethylglyoximato]cobalt(II) (COBF, **1**) and bis[(difluoroboryl) diphenylglyoximato]cobalt(II) (COPhBF, **2**) in bulk and solution polymerization are $24 - 40 \cdot 10^3$ ⁷ and $14 - 20 \cdot 10^3$ ⁴, respectively. When applied in (mini)emulsion polymerization however, the observed C_T values were significantly lower.⁷ The apparently lower C_T value points to a significantly lower CCTA concentration in the particles than the overall CCTA concentration based on the recipe. Since partition coefficients of the CCTA over the different phases as well as phase ratios govern the actual catalyst concentration in the locus of polymerization, an accurate prediction of the molecular weight distribution in CCT mediated emulsion polymerization requires the partitioning to be taken into account. In the present chapter we evaluate the effect of partitioning of COBF, with limited water solubility ($8 \cdot 10^{-4} \text{ mol} \cdot \text{dm}_w^{-3}$ at 25°C),¹³ and of COPhBF, which is virtually insoluble in water, on the molecular weight distribution. Experimental results are compared with the results of calculations of the instantaneous molecular weight with a global model, based on the Mayo equation and CCTA partitioning.

RESULTS AND DISCUSSION

Global model for the instantaneous degree of polymerization

A mathematical description of the effect of partitioning of catalytic chain transfer agents in miniemulsion polymerization on the number average degree of polymerization was formulated with the following assumptions:

- The Mayo equation, see Equation 1, is the basis of the model.
- The concept of miniemulsion polymerization with an oil-soluble initiator was used.^{17,18} Aqueous phase events, e.g., entry of radicals into the particles, chain transfer in the aqueous phase and termination in the aqueous phase are ignored.

- To exclude the effect of CCTA deactivation,¹⁹⁻²¹ instantaneous degrees of polymerization are determined at low conversion. The saturation concentration of monomer is chosen equal to the bulk concentration ($9.42 \text{ mol}\cdot\text{dm}_M^{-3}$), since the instantaneous degrees of polymerization are determined at low conversion.
- Cobalt-carbon bonding has been neglected.²²
- CCTA partitioning between the continuous aqueous phase and the polymer particles is assumed to be constant at low conversion.
- Calculations are limited to instantaneous degrees of polymerization.
- The overall CCTA to monomer mol-ratio was kept constant throughout the series of experiments.

We believe that this model adequately describes the instantaneous degree of polymerization in CCT miniemulsion polymerization for sparingly water-soluble monomers. Aqueous phase events can probably not be ignored in the cases of very water-soluble polymers, very high amounts of catalytic chain transfer agents and for the description of polymerization rates (e.g., CCT causes an increase in the exit rate)⁸.

Equations 2 and 3 express the CCTA concentration at the locus of polymerization and in the aqueous phase.

$$[Co]_M = [Co]_0 \frac{m_{Co}(\beta + 1)}{m_{Co}\beta + 1} \quad (2)$$

$$[Co]_w = [Co]_0 \frac{\beta + 1}{m_{Co}\beta + 1} \quad (3)$$

In these equations $[Co]_M$ and $[Co]_w$ are the CCTA concentration at the locus of polymerization and in the aqueous phase, respectively. $[Co]_0$ is the overall CCTA concentration in the reaction mixture ($\text{mol}\cdot\text{dm}^{-3}$), m_{Co} ($m_{Co} = \frac{[Co]_M}{[Co]_w}$, i.e. the equilibrium ratio of the concentration CCTA at the locus of polymerization and the concentration of CCTA in the aqueous phase) is the partition coefficient of the CCTA

used ($dm_W^3 \cdot dm_M^{-3}$), β ($\beta = \frac{V_M}{V_W}$, i.e. the ratio of the volume of the monomer phase and the volume of the aqueous phase) is the phase ratio ($dm_M^3 \cdot dm_W^{-3}$).

The expression derived for the CCTA concentration at locus of polymerization can then be substituted into the Mayo equation, linking the number average degree of polymerization directly to the phase ratio and the partition coefficient, see Equation 4 in which $[M]_p$ is the concentration of MMA in the PMMA polymer particles ($mol_M \cdot dm_p^{-3}$).

$$DP_n^{-1} = C_T \frac{[Co]_0}{[M]_p} \left(\frac{m_{Co}(\beta + 1)}{m_{Co}\beta + 1} \right) \quad (4)$$

The instantaneous degree of polymerization can then be calculated by Equation 5, in which $N_{Co,0}$ is the total amount of CCTA in the reaction mixture (mol), see appendix.

$$DP_n = \frac{V_M[M]_p}{C_T} \frac{1}{N_{Co,0}} \left(\frac{m_{Co}\beta + 1}{m_{Co}(\beta + 1)} \right) \left(1 + \frac{1}{\beta} \right) \quad (5)$$

From Equation 5, it can be seen that the instantaneous degree of polymerization depends on (i) the monomer concentration in the PMMA polymer particles ($[M]_p$), (ii) the choice of CCTA (C_T , m_{Co}) and (iii) the emulsion recipe ($N_{Co,0}$, β , V_M).

Since DP_n is governed by the product of C_T and the actual concentration ratio $[Co]_M / [M]_p$, it is convenient to define an apparent chain transfer constant (C_T^{app}) to be used in Equation 1 in combination with the overall CCTA and monomer concentrations, see Equation 6.

$$C_T^{\text{app}} \frac{[Co]_0}{[M]} = C_T \frac{[Co]_M}{[M]_p} \quad (6)$$

Rearrangement of Equation 6, using Equation 2 and 3, yields an expression which directly links the apparent chain transfer coefficient to the phase ratio and the partition coefficient, see Equation 7 and the appendix.

$$C_T^{\text{app}} = \frac{[M]}{[M]_p} \frac{m_{Co}(\beta + 1)}{m_{Co}\beta + 1} \frac{\beta}{\beta + 1} C_T \quad (7)$$

CCTA partitioning

Figure 1 schematically shows the effect of the phase ratio on the partitioning of COBF in a miniemulsion of methyl methacrylate in water. Miniemulsion polymerizations with a very low monomer content, i.e. $\beta \rightarrow 0$, have a large aqueous phase volume and a large total volume of the reaction mixture (a) (note that this situation is not possible in practice; monomer droplets should be present). The overall CCTA concentration is low and so are the equilibrium concentrations in the monomer and the aqueous phase (b). The absolute amounts of CCTA in both phases are also low, but the absolute amount in the aqueous phase is much higher as compared to that in the organic phase (c). Very low monomer to water ratios ($\beta \rightarrow 0$) result in high average molecular weights, since hardly any CCTA will be present at the locus of polymerization, i.e. the monomer phase. The opposite situation occurs when the phase ratio is very high ($\beta \rightarrow \infty$). The total reaction volume is small, resulting in a high overall CCTA concentration (d). The equilibrium CCTA concentrations in the monomer and the aqueous phases are high as compared to the situation characterized by a very low monomer to water ratio (e). However, more importantly, the absolute amount of CCTA in the monomer phase is now much higher than the CCTA concentration in the aqueous phase (f). This situation is comparable to bulk polymerization and yields low average molecular weights. It should be noted that this result is probably counter-intuitive as one would probably assume that with an increasing amount of monomer, a lower effective ratio of CCTA to monomer would

occur and consequently a higher average molecular weight would be obtained. This result is comparable with emulsion copolymerization, where the copolymer composition can also be controlled with the monomer to water ratio, i.e. the phase ratio²³. All these considerations demonstrate that the phase ratio is a key parameter for the control of molecular weight in (mini)emulsion polymerization.

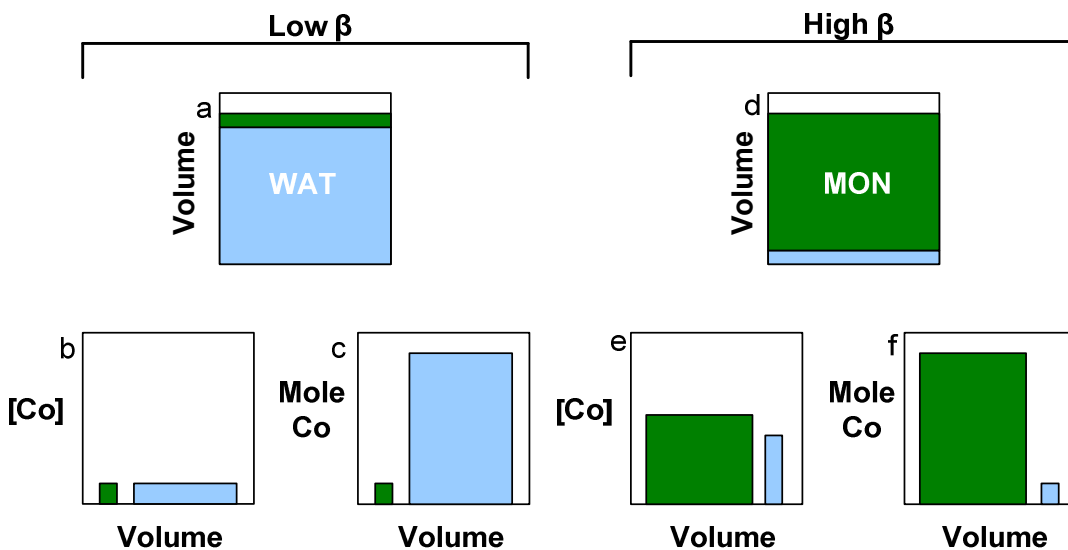


Figure 1. Schematic representation of the effect of the phase ratio on the partitioning of the CCTA in a miniemulsion. The two extremes are shown for a system with a constant monomer phase volume and absolute amount of CCTA: low $\beta \rightarrow 0$, i.e., very low solids content and high β , very high solids content. Shown are the relative amounts of the two phases (a, d), the relative concentrations of CCTA in monomer and aqueous phase (b, e) and the absolute amounts of CCTA (c, f). Partition coefficient: $m_{Co} = 0.72$.

The effect of partitioning on CCTA-mediated miniemulsion polymerization with COBF and COPhBF are used to illustrate the effect of CCTA partitioning on the instantaneous number average degree of polymerization. Various CCTA mediated miniemulsion polymerizations were performed with a varying phase ratio. The experimental results are presented in Table 1.

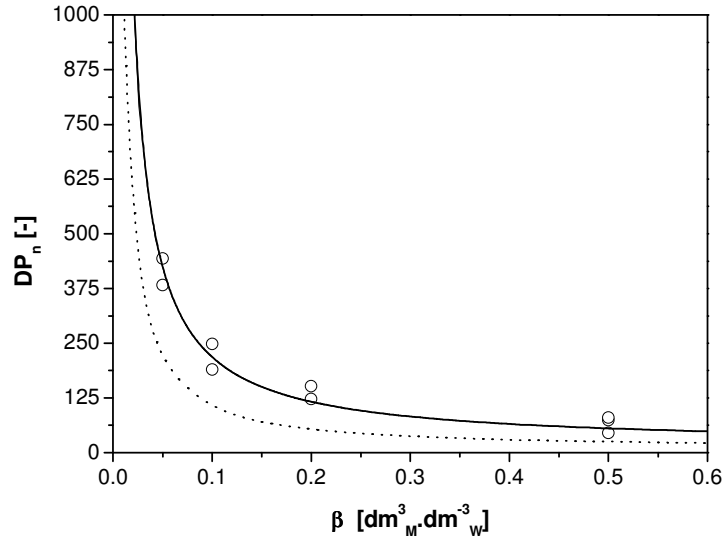


Figure 2. Experimentally observed and calculated values of the instantaneous number-average degree of polymerization as a function of the monomer to water ratio, COBF was used as catalyst (runs 1-8 Table 3). Molecular weight distributions were measured at a monomer conversion below 0.10. (o) number-average degree of polymerization data values (---) Predicted instantaneous number-average degree of polymerization (equation 5), $C_T = 30 \cdot 10^3$, $m_{Co} = 0.72 \text{ dm}_W^3 \cdot \text{dm}_M^{-3}$, $N_{Co,0} = 9.5 \cdot 10^{-7} \text{ mol}$, (—) Predicted instantaneous number-average degree of polymerization (Equation 5), $C_T = 15 \cdot 10^3$

Figure 2 presents the evolution of the instantaneous number average degree of polymerization for COBF, experiments 1 – 8, see Table 1. The phase ratio was varied from 0.050 to 0.50 $\text{dm}_M^3 \cdot \text{dm}_W^{-3}$, corresponding to solid contents increasing from 5 to 32 wt%. The results in Figure 2 demonstrate that the phase ratio has a significant influence on the instantaneous molecular weight and shows that the ratio of COBF to monomer in the particles is not equal to the overall ratio of $5.0 \cdot 10^{-6}$ derived from the recipe. If CCTA partitioning were not considered (i.e. bulk polymerization), the Mayo equation (Equation 1) predicts a number average degree of polymerization of 6.6; this is confirmed experimentally in bulk polymerization, experiment 9, Table 3. Figure 2 also shows that Equation 5 adequately predicts the observed trend of a decrease in instantaneous

molecular weight with increasing phase ratio. The calculations with Equation 5 were performed with a partition coefficient m_{Co} of $0.72 \text{ dm}_W^3 \cdot \text{dm}_M^{-3}$, which was determined experimentally in this work. As the phase ratio increases (i.e. higher solid contents), more COBF will partition towards the particles resulting in a higher COBF concentration at the locus of polymerization and consequently in a lower average molecular weight.

From Figure 2 it is also clear that the use of $C_T = 30 \cdot 10^3$ in Equation 5, as determined by bulk polymerization, underestimates DP_n by roughly a constant factor of approximately 2. A possible explanation for this discrepancy may be found when noting that the axial ligands of the active Co(II) complex in MMA bulk polymerization may differ from those of the active Co(II) complex in miniemulsion polymerization where water is present. Haddleton and co-workers reported that the presence of methanol significantly reduces the chain transfer constant.²⁴ Biasutti *et al* further explored the effects of the presence of hydroxyl groups on the chain transfer coefficient and the catalyst structure.²⁵ A 50% reduction of the chain transfer constant was found when hydroxyl groups were present and observed changes in the UV-Vis spectra were consistent with coordination to the Co(II) centre.²⁵ If we choose a value of $15 \cdot 10^3$ for the chain transfer constant, instead of $30 \cdot 10^3$ (i.e. in accordance with the argument given above), a good agreement between observed instantaneous molecular weights and predicted average molecular weights is obtained, see Figure 2. This agreement between the experimental results and the calculated values of DP_n with $C_T = 15 \cdot 10^3$ points to important influence of water on the catalytic chain activity in miniemulsion polymerization.

Table 1. Miniemulsion polymerization results of MMA with COBF and CPhBF.

Entry	β	CCTA	$\frac{N_{Co,0}}{N_{MMA}} (10^{-6} \frac{mol_{Co}}{mol_{MMA}})$	$DP_n (Calc)^a$	$DP_n (Obsd)^b$
01	0.05	COBF	5.0	400	886
02	0.05	COBF	5.0	400	765
03	0.10	COBF	5.0	200	497
04	0.10	COBF	5.0	200	368
05	0.20	COBF	5.0	100	245
06	0.20	COBF	5.0	100	304
07	0.50	COBF	5.0	50	90
08	0.50	COBF	5.0	50	121
09	∞^c	COBF	5.0	6.6	7.1
10	0.10	CPhBF	5.0	80	82
11	0.10	CPhBF	5.0	80	82
12	0.20	CPhBF	5.0	80	57
13	0.20	CPhBF	5.0	80	82
14	0.50	CPhBF	5.0	80	79
15	0.50	CPhBF	5.0	80	76
16	∞^c	CPhBF	5.0	80	75

Reaction conditions: $T = 75^\circ\text{C}$, $[\text{AIBN}] = 55 \cdot 10^{-3} \text{ mol.dm}_M^{-3}$, $[\text{HD}] = 11 \cdot 10^{-2} \text{ mol.dm}_M^{-3}$, $[\text{SDS}] = 14 \cdot 10^{-2} \text{ mol.dm}_W^{-3}$, miniemulsified for 15 minutes.

^a Predicted instantaneous degree of polymerization using Equation 5 and $C_T = 30 \cdot 10^3$ [-] for COBF and $5 \cdot 10^3$ [-] for CPhBF. ^b Experimentally obtained instantaneous number-average

degree of polymerization $DP_n = \frac{\overline{M}_w}{2M_0}$ ^{17,18}. ^c Bulk polymerization experiments under otherwise

identical experimental conditions.

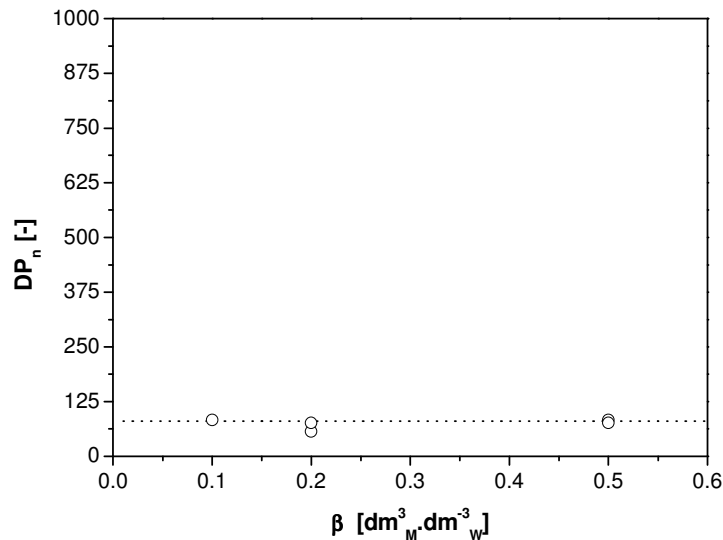


Figure 3. Experimentally observed and calculated values of the instantaneous number-average degree of polymerization as a function of the monomer to water ratio, CPhBF was used as catalyst (runs 10-15 Table 3). Molecular weight distributions were measured at a monomer conversion below 0.10. (\circ) instantaneous number-average degree of polymerization (---) Predicted instantaneous number-average degree of polymerization (Equation 5), $C_T = 5 \cdot 10^3$, $m_{C_0} \rightarrow \infty$, $N_{C_0,0} = 9.4 \cdot 10^{-7}$.

Figure 3 shows the evolution of the instantaneous number-average degree of polymerization as a function of the monomer to water ratio for CPhBF as chain transfer agent, experiments 10 – 15 see Table 3. The results in Figure 3 demonstrate that the instantaneous number-average degree of polymerization does not significantly depend on the monomer to water ratio for the experimental conditions chosen. This observation is completely different from that in the COBF-mediated miniemulsions, where a large influence was found. The difference between both catalysts can be explained by evaluating the partition coefficients of both complexes in water – MMA systems. The partition coefficients in emulsions of MMA and water are $0.72 \text{ dm}^3_{\text{W}} \cdot \text{dm}^{-3}_{\text{M}}$ and approximately infinite for COBF and CPhBF, respectively. The COBF catalyst is moderately water soluble and will partition, whereas the CPhBF catalyst is virtually

insoluble in water and completely resides in the particles. The instantaneous number-average degree of polymerization obtained in COPhBF mediated miniemulsion polymerization is equal to the bulk value of 80, see Table 1.

The derived model was used to predict instantaneous degrees of polymerization reported in literature by Kukulj *et al.*⁶, see Table 2. Both COBF and COPhBF were used as CCTA. Equation 5 and the C_T values for COBF and COPhBF as reported in reference 7 were used to calculate DP_n . The DP_n obtained at low CCTA concentrations shows a discrepancy with the model, probably induced by the susceptibility of the CCTA towards impurities. However, DP_n obtained at higher CCTA concentrations are in good agreement with the model for both COBF and COPhBF.

Table 2. Application of Equation 5 to literature.

Entry	CCTA	$\frac{N_{Co,0}}{N_{MMA}}$ ($10^{-6} \frac{mol_{Co}}{mol_{MMA}}$)	$DP_n (Calc)^a$	$DP_n (Obsd)^b$
01	COBF	3.0	127	450
02	COBF	18.0	21	21
03	COPhBF	2.0	36	80
04	COPhBF	9.3	8	12

Parameters for calculation⁷: $\beta = 0.27$; COBF: $C_T = 24 \cdot 10^3$; COPhBF: $C_T = 14 \cdot 10^3$

^a Predicted instantaneous degree of polymerization using Equation 5 and $C_T = 30 \cdot 10^3$ [-] for COBF and $5 \cdot 10^3$ [-] for COPhBF. ^b Experimentally obtained instantaneous number-average

degree of polymerization $DP_n = \frac{\overline{M_w}}{2M_0}$ ^{17,18}

Apparent Activity in Emulsion Polymerization

In the literature⁵⁻¹⁰, the activity of the CCTA's in emulsion polymerization has been expressed in terms of an apparent chain transfer coefficient (C_T^{app}). Tentative explanations given for the lower C_T^{app} -values are catalyst partitioning, diffusion-controlled chain transfer, and catalyst decomposition by acid hydrolysis.⁹

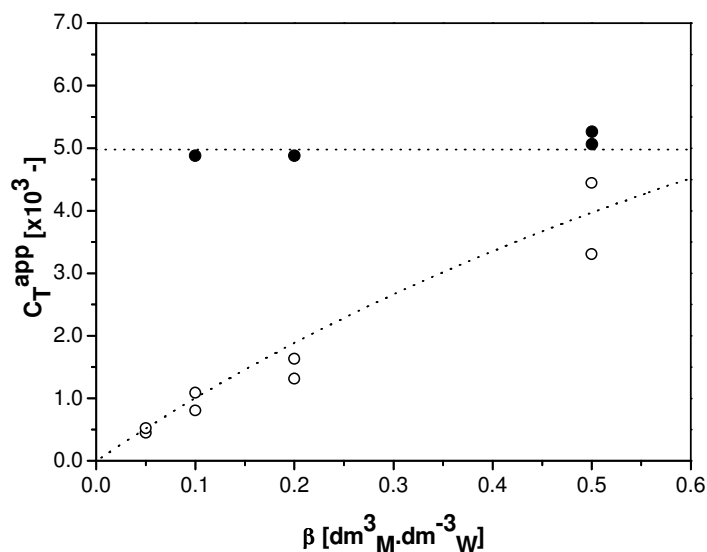


Figure 4. Apparent chain transfer constant (C_T^{app}) as function of the phase ratio. (●) C_T^{app} determined for COPhBF (○) C_T^{app} determined for COBF. (---) Predicted apparent chain transfer constant for COPhBF ($C_T = 5 \cdot 10^3$) and COBF ($C_T = 15 \cdot 10^3$).

Figure 4 clearly demonstrates the different behaviour of COBF and COPhBF. The C_T^{app} -values for COPhBF do not depend on the phase ratio and are within experimental error equal to the value of the chain transfer constant value found for bulk polymerization, i.e. $5 \cdot 10^3$. For COBF the C_T^{app} -values display a strong dependence on the phase ratio and even at high phase ratios do not approach the chain transfer constant value of $30 \cdot 10^3$ as found in bulk polymerization.

The predicted (Equation 7) and experimentally obtained apparent chain transfer constants are collected in Table 3, and it can be seen that they are in good agreement. Since the instantaneous molecular weight was determined at low conversions, catalyst decomposition²⁶ and diffusion limitations^{5,7,8,10} are conceivably not significant and can be neglected. Catalyst partitioning can therefore be identified as the main explanation for the lower C_T^{app} -values in miniemulsion polymerization.

Table 3. Miniemulsion polymerization of MMA with COBF comparison of the measured and the predicted apparent chain transfer constant.

<i>Entry</i> ^a	β	C_T^{app} (<i>Calc</i>) ^b	C_T^{app} (<i>Obsd</i>) ^c
01 - 02	0.05	526	487 ± 50
03 - 04	0.10	1019	946 ± 198
05 - 06	0.20	1909	1474 ± 222
07 - 08	0.50	4004	3875 ± 799

^a Entries correspond to those in Table 3. ^b Average apparent chain transfer coefficient (C_T^{app}) as predicted by equation 7, using $C_T = 15 \cdot 10^3$ [-]. ^c Apparent chain transfer coefficient (C_T^{app}) is

$$\text{defined as } C_T^{\text{app}} = DP_n^{-1} \frac{[M]_p}{[Co]_0}$$

CONCLUSIONS

The results of this work demonstrate that the instantaneous number-average molecular weight in CCT mediated miniemulsion polymerization is not only governed by the catalyst activity but also by catalyst partitioning over the two phases in miniemulsion polymerization. A simple equation based on the Mayo equation and CCTA partitioning accurately describes the instantaneous number-average degree of polymerization at low conversion for miniemulsion polymerization of MMA and is in agreement with earlier results reported in literature.

EXPERIMENTAL

Materials

The bis(methanol) complexes COBF and CPhBF were prepared as described previously^{7,16}. For all experiments, a single batch of catalyst was used. The intrinsic activity of the catalysts was determined by measuring the chain transfer constant in bulk polymerization of methyl methacrylate (MMA) at 60°C (COBF (1): $C_T = 30 \cdot 10^3$; CPhBF (2): $C_T = 5 \cdot 10^3$). MMA (Aldrich, 99%) was purified by passing it over a column of activated basic alumina (Aldrich) in order to remove the methyl hydroquinone (MeHQ) inhibitor. N,N'-azoisobutyronitrile (AIBN) (Fluka, 98%) was recrystallized from methanol twice and used as initiator. Sodium dodecyl sulphate (SDS) (Fluka, 99%) and hexadecane (HD) (Aldrich, 99%) were used as received.

Determination of the chain transfer constant

Two stock solutions were prepared: (i) a catalyst solution, and (ii) an initiator solution. The catalyst solution (i) was prepared by dissolving an accurate amount of COBF (approximately 3 mg, $7 \cdot 10^{-3}$ mmol) or CPhBF (approximately 3 mg, $5 \cdot 10^{-3}$ mmol) in deoxygenated MMA (30.0 mL). The initiator solution (ii) was prepared by dissolving recrystallized AIBN (148 mg; 0.90 mmol) in deoxygenated MMA (40.0 mL). Subsequently aliquots were prepared inside a glove box, containing 0, 0.10, 0.20, 0.30, 0.40, 0.50, 0.60 and 0.70 mL of solution (i) and 4.0 mL of solution (ii). MMA was then added so that all aliquots had a total volume of 5.0 mL. The sealed ampoules were placed in a carousel reactor, thermostated at 60 °C, until an MMA conversion of about 8% of MMA conversion was reached. The polymerization was stopped by respectively cooling, opening the sealed ampoules and adding hydroquinone. The non-polymerized monomer was evaporated rapidly at elevated temperature and ambient pressure.

Determination of the partition coefficient

A 250 mL thermostated glass reactor, equipped with 4 baffles and a 4-bladed pitched blade impeller was connected through a cannula to a thermostated separation funnel. The

reactor and the separation funnel were flushed with argon for 30 minutes prior to each experiment. A catalyst stock solution was prepared by dissolving an accurately amount of COBF (approximately 6 mg, $1.4 \cdot 10^{-2}$ mmol) or CPhBF (approximately 6 mg, $8 \cdot 10^{-3}$ mmol) in deoxygenated MMA (75.0 mL). The required amount of catalyst stock solution and deoxygenated water were then added to the reactor using a gas-tight syringe. The resulting mixture was stirred for 30 minutes at the desired temperature. The reactor content, was then transferred into the separation funnel. After phase separation, samples from both the aqueous and monomer phase were taken and analyzed with UV-Vis spectrometry.

The extinction coefficients were obtained from calibration lines or from literature, see Table 4.

Table 4. Extinction coefficients of COBF and CPhBF in water and MMA

<i>Catalyst</i>	<i>Water</i>	<i>MMA</i>
	$\lambda = 456 \text{ nm}$	$\lambda = 454 \text{ nm}$
COBF	$4060 \text{ dm}^3 \cdot \text{mol}^{-1} \cdot \text{cm}^{-1}$ ^a	$3640 \text{ dm}^3 \cdot \text{mol}^{-1} \cdot \text{cm}^{-1}$ ^b
CPhBF	n / a	$6477 \text{ dm}^3 \cdot \text{mol}^{-1} \cdot \text{cm}^{-1}$ ^b

^a Taken from reference 16 ; ^b Determined experimentally

CCTA mediated miniemulsion polymerization

A typical miniemulsion recipe is presented in Table 5. For each experiment two solutions were prepared: (i) a catalyst stock solution in MMA also containing cosurfactant (hexadecane) and, (ii) an aqueous phase solution containing surfactant (SDS) and initiator (AIBN). The catalyst stock solution (i) was prepared by dissolving an accurate amount of COBF (approximately 2 mg, $5 \cdot 10^{-3}$ mmol) or CPhBF (approximately 3 mg, $5 \cdot 10^{-3}$ mmol) in a mixture of hexadecane (2.2 g, 10 mmol) and MMA (95.0 mL). The same catalyst solution was used for all experiments. SDS and AIBN were placed inside a three-necked round bottom flask and deoxygenated by 3 repeated vacuum – argon cycles. Deoxygenated water was added by means of an gas-tight syringe. An amount of solution (i) was added until a predefined phase ratio was achieved. The organic (MMA) phase was dispersed into the aqueous phase at high stirring speeds for 10 minutes. Subsequently, the

obtained oil-in-water emulsion was transformed into a miniemulsion by ultrasonication. A residence time of 15 minutes in a Vibracell Ultrasonic bath, under an argon atmosphere was sufficient to obtain a droplet size of $100 \leq d_p \leq 200 \text{ nm}$, depending on the phase ratio. Low conversion samples for molecular weight analysis were taken from the reaction mixture ($x < 8\%$).

Table 5. Standard miniemulsion recipe

<i>Compound</i>	<i>Amount</i>	
Water	$\frac{V_M}{\beta}$	$[dm_W^3]$
MMA	V_M	$[dm_M^3]$
HD	$11 \cdot 10^{-2}$	$[mol \cdot dm_M^{-3}]$
SDS	$14 \cdot 10^{-3}$	$[mol \cdot dm_W^{-3}]$
AIBN	$55 \cdot 10^{-3}$	$[mol \cdot dm_M^{-3}]$
CCTA	5.0	$[ppm]^a$

^a ppm's of CCTA defined as 10^{-6} mol CCTA per mol monomer. ^b β is the phase ratio in $(dm_M^3 \cdot dm_W^{-3})$

Size exclusion chromatography

Size exclusion chromatography (SEC) was performed using a Waters GPC equipped with a Waters model 510 pump and a model 410 differential refractometer. A set of two mixed bed columns (Mixed-C, Polymer Laboratories, 30 cm, 40°C) were used. Tetrahydrofuran stabilised with BHT was used as the eluent, and the system was calibrated using narrow molecular weight polystyrene standards ranging from 600 to $7 \times 10^6 \text{ g} \cdot \text{mol}^{-1}$. Mark Houwink parameters used for the polystyrene standards: $K = 1.14 \cdot 10^{-4} \text{ dL} \cdot \text{g}^{-1}$, $a = 0.716$ and for poly(methyl methacrylate): $K = 9.44 \cdot 10^{-5} \text{ dL} \cdot \text{g}^{-1}$, $a = 0.719$.

The number average molecular weight is known to be prone to uncertainties in the baseline correction, therefore for the determination of the instantaneous degree of polymerization, from an experimentally obtained molecular weight distribution, the use

of the weight average molecular weight is preferred, i.e. $DP_n = \frac{\overline{M_w}}{2M_0}$.^{17,18}

APPENDIX**Derivation of Equation 2**

The expression for the CCTA concentration in the organic phase follows from a mass balance for the total amount of CCTA in the reaction system, Equation A1.

$$[Co]_0(V_M + V_W) = [Co]_W V_W + [Co]_M V_M \quad (A1)$$

Using the definitions for the partition coefficient and the phase ratio, substitution in Equation A1 leads to Equation A2.

$$[Co]_0 \left(V_M + \frac{V_M}{\beta} \right) = \frac{[Co]_M V_M}{m_{Co} \beta} + [Co]_M V_M \quad (A2)$$

Re-arranging Equation A2 yields:

$$[Co]_0 \left(1 + \frac{1}{\beta} \right) = [Co]_M \left(1 + \frac{1}{m_{Co} \beta} \right) \quad (A3)$$

Which in turn leads to Equation 2 of the manuscript.

$$[Co]_M = [Co]_0 \frac{m_{Co}(\beta + 1)}{m_{Co} \beta + 1} \quad (A4),(2)$$

Derivation of Equation 5

The simple model for the prediction of the instantaneous molecular weight is based on the Mayo equation, Equation A5, and CCTA partitioning, Equation A4.

$$DP_n^{-1} = DP_{n,0}^{-1} + C_T \frac{[Co]_0}{[M]} \quad (A5),(1)$$

$$[Co]_M = [Co]_0 \frac{m_{Co}(\beta + 1)}{m_{Co}\beta + 1} \quad (A4),(2)$$

Substitution of Equation A4 in Equation A5 yields equation A6, which relates the CCTA partitioning to the instantaneous degree of polymerization.

$$DP_n^{-1} = C_T \frac{[Co]_0}{[M]_p} \left(\frac{m_{Co}(\beta + 1)}{m_{Co}\beta + 1} \right) \quad (A6)$$

Equation A6 can be re-written to relate the CCTA partitioning directly to the instantaneous weight average molecular weight, Equation 4 of the manuscript.

$$DP_n = \frac{[M]_p}{[Co]_0 C_T} \left(\frac{m_{Co}\beta + 1}{m_{Co}(\beta + 1)} \right) \quad (A7),(4)$$

The overall CCTA concentration $[Co]_0$ can be expressed in terms of the amount of moles of CCTA ($N_{Co,0}$) and the total reaction volume, which can be expressed in terms of the volume of the organic phase (V_M) and the phase ratio, Equation 5 of the manuscript.

$$DP_n = \frac{V_M [M]_p}{C_T} \frac{1}{N_{Co,0}} \left(\frac{m_{Co}\beta + 1}{m_{Co}(\beta + 1)} \right) \left(1 + \frac{1}{\beta} \right) \quad (A8),(5)$$

Derivation of equation 7

Ignoring partitioning effects and application of the simple Mayo equation to emulsion polymerization requires the use of an apparent chain transfer constant (C_T^{app}). Realizing that DP_n is controlled by the product of C_T and the concentration ratio of catalyst to monomer in the locus of polymerization, C_T^{app} can be related to true chain transfer constant, see Equation A9.

$$C_T^{\text{app}} \frac{[Co]_0}{[M]} = C_T \frac{[Co]_M}{[Co]_p} \quad (\text{A9}), (6)$$

Substitution of Equation A6 into A9 yields Equation A10.

$$C_T^{\text{app}} \frac{[Co]_0}{[M]} = C_T \frac{[Co]_0}{[M]_p} \frac{m_{Co}(\beta + 1)}{m_{Co}\beta + 1} \quad (\text{A10})$$

Note that for the calculation of the C_T^{app} , the system is considered as being a bulk polymerization, therefore the overall CCTA concentration is related to the *monomer* volume only. The CCTA concentration at the locus of polymerization in emulsion polymerization is related to the *total* reaction volume, see Equation A11.

$$C_T^{\text{app}} \frac{N_{Co,0}}{V_M [M]} = C_T \frac{N_{Co,0}}{(V_M + V_W) [M]_p} \frac{m_{Co}(\beta + 1)}{m_{Co}\beta + 1} \quad (\text{A11})$$

Further re-arranging yields:

$$C_T^{\text{app}} \frac{1}{V_M [M]} = C_T \frac{1}{V_M \left(1 + \frac{1}{\beta}\right) [M]_p} \frac{m_{Co}(\beta + 1)}{m_{Co}\beta + 1} \quad (\text{A12})$$

And subsequently Equation 7 of the manuscript.

$$C_T^{\text{app}} = \frac{[M]}{[M]_p} \frac{m_{Co}(\beta + 1)}{m_{Co}\beta + 1} \frac{\beta}{\beta + 1} C_T \quad (\text{A13}), (7)$$

REFERENCES AND NOTES

1. Mayo, F. R. *J Am Chem Soc* 1943, 65, 2324.
2. Gridnev, A. *J Polym Sci Part A: Polym Chem* 2000, 38, 1753.
3. Gridnev, A. A.; Ittel, S. D. *Chem Rev* 2001, 101, 3611.
4. Heuts, J. P. A.; Roberts, G. E.; Biasutti, J. D. *Aust J Chem* 2002, 55, 381.
5. Suddaby, K.G.; Haddleton, D.M.; Hastings, J.J.; Richards, S.N.; O'Donnell, J.P. *Macromolecules* 1996, 29, 8083.
6. Kukulj, D.; Davis, T. P.; Gilbert, R. G. *Macromolecules* 1997, 30, 7661.
7. Bon, S. A. F.; Morsley, D. R.; Waterson, J.; Haddleton, D. M.; Lees, M. R.; Horne, T. *Macromol Symp* 2001, 165, 29.
8. Kukulj, D.; Davis, T.P.; Suddaby, K.G.; Haddleton, D.M.; Gilbert, R.G. *J Polym Sci Part A: Polym Chem* 1997, 35, 859..
9. Pierik, S.C.J.; Smeets, B.; van Herk, A.M. *Macromolecules* 2003, 36, 9271.
10. Haddleton, D.M.; Morsley, D.R.; O'Donnell, J.P.; Richards, S.N. *J Polym Sci Part A: Polym Chem* 2001, 37, 3549.
11. Nur Alam, M.; Zetterlund, P.B.; Okubo, M. *J Polym Sci Part A: Polym Chem* 2007, 45, 4995.
12. Ma, J.W.; Cunningham, M.F.; McAuley, K.B.; Keoshkerian, B.; Georges, M.K. *J Polym Sci Part A: Polym Chem* 2001, 39, 1081.
13. Measured experimentally by UV-Vis spectroscopy.
14. Bakač, A.; Brynildson, M. E.; Espenson, J. H. *Inorg Chem* 1986, 25, 4108.
15. Heuts, J.P.A. ; Kukulj D. ; Forster, D.J. ; Davis, T.P. *Macromolecules* 1998, 31, 2894.
16. Heuts, J.P.A.; Davis, T.P.; Russell, G.T. *Macromolecules* 1999, 32, 6019.
17. Lin, M.; Hsu, J.C.C.; Cunningham, M.F.; *J Polym Sci Part A: Polym Chem* 2006, 44, 5974.
18. Jeng, J.; Dai, C-A.; Chiu, W-Y.; Chern, C-S.; Lin, K-F.; Young, P-Y. *J Polym Sci Part A: Polym Chem* 2006, 44, 4603.
19. Gridnev, A.A. *Polym Sci USSR* 1989, 31, 2369.
20. Gridnev, A.A. *Polym J* 1992, 24, 613.
21. S. C. J. Pierik, van Herk A.M. *J App Polym Sci* 2004, 91, 1375.
22. Morrison, D.A.; Davis, T.P.; Heuts, J.P.A.; Messerle, B.; Gridnev, A.A. *J Polym Sci Part A: Polym Chem* 2006, 44, 6171.
23. Leiza, J.R.; Meuldijk J. In *Chemistry and Technology of Emulsion Polymerization*; van Herk, A.M., Ed.; Blackwell Publishing; 2005; Oxford ;

24. Haddleton, D.M.; Maloney D.R.; Suddaby, K.G.; Muir, A.V.G.; Richards, S.N. *Macromol Symp* 1996, 111, 37.
25. Biasutti, J.D.; Roberts, G.E.; Lucien, F.P.; Heuts, J.P.A. *Eur Polym J* 2003, 39, 429.
26. Smeets, N.M.B.; Meda, U.S.; Heuts, J.P.A. ; Keurentjes, J.T.F. ; van Herk, A.M. ; Meuldijk, J. *Macromol Symp* 2007, 259, 406.

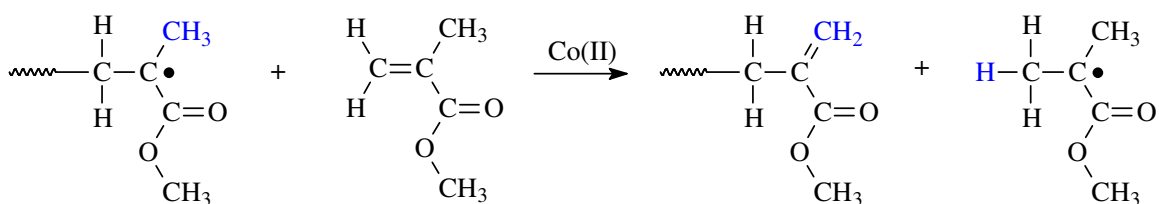
Mass Transport Limitations and their Effect on the Control of the Molecular Weight Distribution in Catalytic Chain Transfer Mediated Emulsion Polymerization.

ABSTRACT

The existence of mass transport limitations in catalytic chain transfer mediated emulsion polymerization using bis[(difluoroboryl) dimethylglyoximato] cobalt(II) (COBF) was investigated. The rate of mass transport of COBF from the aqueous phase towards the polymer particles proved to depend strongly on the viscosity of the polymer particles and consequently on the instantaneous conversion. At high instantaneous conversion the exchange of COBF between the particles and the aqueous phase is severely hindered. As a result the control of the molecular weight distribution is hampered. At low instantaneous conversion COBF is readily transferred between the aqueous phase and polymer particles resulting in immediate molecular weight control. The chain transfer activity of COBF inside the polymer particles during the polymerization was successfully quantified using the chain length distribution method. The results of this work show that the presence of a catalytic chain transfer agent can severely affect the course of the emulsion polymerization. Furthermore it was demonstrated that molecular weight control during the final stages of an emulsion polymerization is affected by the increasing viscosity of the polymer particles.

INTRODUCTION

Robust molecular mass control is a key issue in polymer production. Catalytic chain transfer has proven to be a promising technique to control the molecular weight distribution in free radical polymerization.¹⁻⁷ The most widely accepted mechanism suggests that radical activity of a propagating polymeric radical is transferred to a monomer molecule, resulting in a dead polymer chain with a vinyl end group functionality and a monomeric radical, see Scheme 1.



Scheme 1. The Co(II) mediated chain transfer to monomer for methyl methacrylate

In homogeneous polymerizations, i.e. bulk and solution polymerization, the instantaneous degree of polymerization is directly related to the concentration of the chain transfer agent in the reaction mixture and can be calculated directly with the Mayo equation.⁸ In emulsion polymerization, however, the reaction mixture is heterogeneous by nature, which has important consequences for the application of CCT:⁹⁻¹⁶

- Partition coefficients and phase ratios govern the equilibrium catalyst concentration in the locus of polymerization.
- Transport of the catalytic chain transfer agent (CCTA) from the monomer droplets via the aqueous phase to the particles is a prerequisite for effective molecular weight control.
- CCTA deactivation during polymerization by aqueous phase species lowers the overall amount of CCTA and by that increases the molecular weight.

For effective molecular weight control, it is desired to have a pre-determined catalytic chain transfer agent concentration in the loci of polymerization, i.e., the polymer particles. Furthermore, for successful application of catalytic chain transfer in emulsion polymerization, a finite aqueous phase solubility is required to allow transport of the CCTA from the monomer droplets, through the aqueous phase, to the polymer particles.¹⁰ Aqueous phase solubility of the CCTA results in partitioning of the catalyst complex between the different phases present in the emulsion polymerization reaction mixture.^{9,10,15} Partitioning of the catalytic chain transfer agent results in a lower actual concentration in the loci of polymerization and consequently a lower apparent chain transfer activity.¹⁵ Presence of a CCTA in the aqueous phase might eventually also result in aqueous phase decomposition of the active complex, thereby reducing the absolute amount of active catalytic chain transfer agent in the system.¹⁶ The heterogeneous nature of the emulsion polymerization system has comparable implications for living/controlled radical polymerization techniques.¹⁷⁻²¹

For a typical MMA emulsion polymerization recipe applied in our studies, i.e., 15 w/w% methyl methacrylate (MMA), using a typical amount of catalytic chain transfer agent, i.e., 5.0 ppm COBF and correcting for partitioning, the average number of catalyst molecules per polymer particle can be calculated as a function of the particle diameter, see Figure 1. From Figure 1 it can be concluded that, for the experimental window of typical emulsion polymerizations in our studies, the number of COBF molecules per polymer particle is in the range of roughly 0.1 to 1. Therefore, a single COBF molecule often has to be able to mediate multiple reacting polymer particles to ensure that in all the particles chain-stoppage occurs by COBF catalyzed chain transfer. This can only be achieved if the COBF molecules can efficiently leave and enter the polymer particles. Hence, ideally no mass transport limitations between the different phases in the emulsion polymerization system should be present, i.e. the characteristic time for COBF exchange should be significantly shorter than the characteristic time for chain growth.

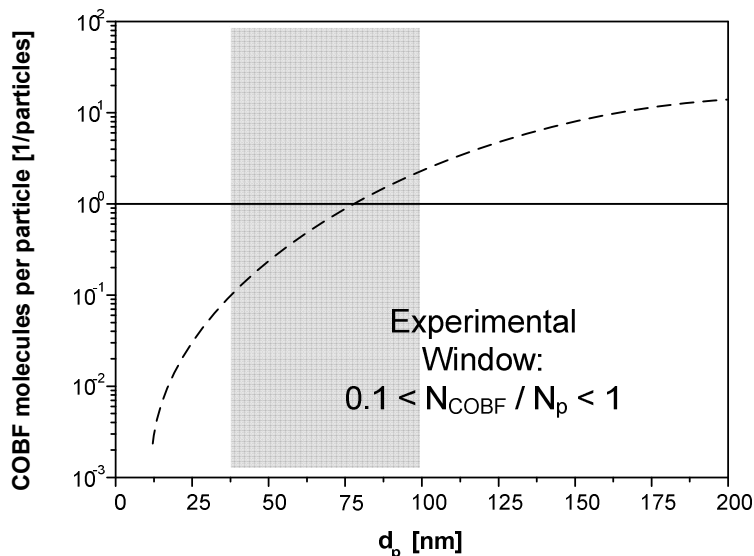


Figure 1. Average number of COBF molecules per polymer particle in a typical methyl methacrylate emulsion polymerization. Conditions for the calculation: 5.0 ppm COBF (mol COBF per mol MMA). The partitioning of COBF is calculated based on a model published previously, using a partition coefficient $m_{Co} = \frac{[Co]_M}{[Co]_W} = 0.72 \text{ dm}_W^3 \cdot \text{dm}_M^{-3}$ and a phase ratio

$$\beta = \frac{V_M}{V_W} = 0.19 \text{ dm}_M^3 \cdot \text{dm}_W^{-3}.^{15}$$

In the present chapter we evaluate the possible existence of mass transport limitations in the COBF mediated *ab initio* and seeded emulsion polymerizations of MMA. First, the impact of the instantaneous addition of a fairly water soluble catalytic chain transfer agent on the course of the emulsion polymerization is demonstrated. Secondly, the rate of COBF exchange and the existence of mass transport limitations are investigated using the chain length distribution (CLD) method.

RESULTS AND DISCUSSION

Determination of the CCTA concentration in the polymer particles.

The effects of COBF partitioning should be evident from examination of the molecular weight distribution, as the presence of COBF inside a polymer particle results in a lowering of the instantaneous degree of polymerization. To determine the amount of the

catalytic chain transfer agent in the locus of polymerization, an approach comparable to that reported by Cunningham et al. was used.^{22,23} The chain length distribution method (CLD method)^{24,25} can be used as a tool to determine the amount of CCTA in the particles from the cumulative molecular weight distribution of the latex product at different conversions.

The concentration of COBF in the polymer particles follows from the high molecular weight slope, Λ_H , of a plot of $\ln(P(M))$ versus M , see Equation 1. Note that an expression for $P(M)$ has been presented by Gilbert and co-workers²⁶ for a zero-one system, i.e., an emulsion polymerization obeying Smith-Ewart case 1 or case 2 kinetics,²⁷ without chain branching. In Equation 1, M and M_0 are the molecular weight of the dead polymer chain and monomer, respectively, $[M]_p$ is the monomer concentration inside the polymer particle and ρ stands for the total rate coefficient for entry of radicals into the polymer particles.^{26,28}

$$\Lambda_H = \lim_{M \rightarrow \infty} \frac{d(\ln P(M))}{dM} = - \left(C_T \frac{[\text{COBF}]_p}{[M]_p} + \frac{\rho}{k_p [M]_p} \right) \frac{1}{M_0} \quad (1)$$

To circumvent effects of baseline correction errors, we used the slope in the peak region, Λ_{peak} , of the molecular weight distribution.^{29,30} When chain transfer is the predominant chain stopping event, Equation 1 can be simplified to determine the amount of catalytic chain transfer agent inside the polymer particles, see Equation 2.

$$\Lambda_{\text{peak}} = \left(\frac{d(\ln P(M))}{dM} \right)_{\text{peak}} \approx - \left(C_T \frac{[\text{COBF}]_p}{[M]_p} \right) \frac{1}{M_0} \quad (2)$$

The CLD method is often used to experimentally determine the chain transfer constant.³⁰⁻³² For the determination of the C_T value a number of samples with different $[\text{COBF}] / [M]$ ratios are prepared. Consequently the value of C_T can be determined from a linear

plot of $[\text{COBF}] / [\text{M}]$ versus Λ_{peak} (in the case of the CLD method) or DP_n^{-1} (in the case of the Mayo method). The reverse is also true: when the activity of the chain transfer agent is known, the value of $[\text{COBF}] / [\text{M}]$ can be determined from experimental values of Λ_{peak} or DP_n^{-1} . It should be noted that Equation 2 is only strictly valid for instantaneous molecular weight distributions (just as the Mayo equation is).

Effect of a pulse-wise CCTA addition on the course of the emulsion polymerization.

To investigate the effect of increasing viscosity of the polymer particles, COBF was added at different instantaneous conversions (i.e. $x \sim 0.10$; 0.20 ; 0.30 ; 0.40 ; 0.70). From the observed conversion time histories, two different regimes can be observed: (i) at low conversion $x \leq 0.30$ and (ii) at higher conversion $x \geq 0.40$. Figure 2 presents the evolution of the conversion time history for the *ab initio* emulsion polymerizations with an instantaneous addition of COBF at a pre-defined conversion level.

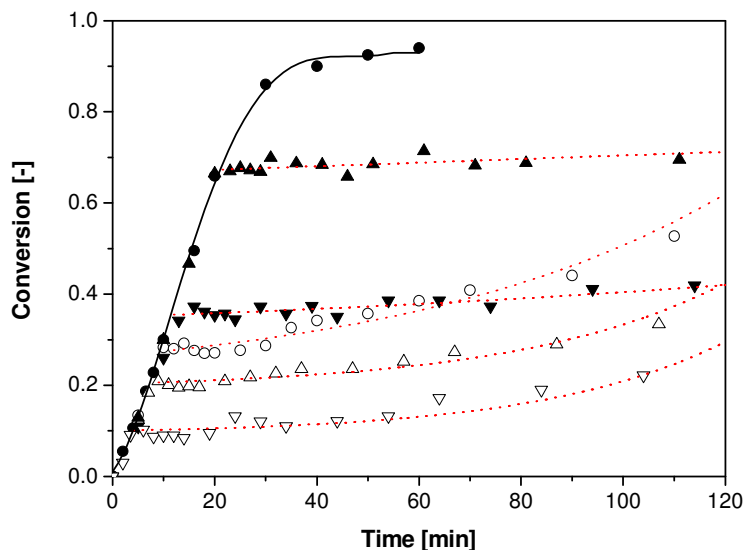


Figure 2. Ab initio emulsion polymerization of methyl methacrylate with instantaneous COBF addition at different instantaneous conversions. Ab initio emulsion polymerization without COBF (●); Ab initio emulsion polymerization with COBF added instantaneously at $x = 0.10$ (▽); $x = 0.20$ (△); $x = 0.30$ (○); $x = 0.40$ (▼) and $x = 0.70$ (▲).

The polymerizations are performed at 50°C to significantly reduce the rate of polymerization of the COBF-free free radical polymerization, allowing accurate and reproducible addition of the catalytic chain transfer agent at a certain conversion level. In the case of the COBF-free emulsion polymerization, approximately complete conversion is obtained within 45 minutes of polymerization. Complete conversion is not reached within the time of the experiment, probably as a result of a gel-effect in the later stages of the polymerization.

The addition of the catalytic chain transfer agent has a severe impact on the rate of polymerization. Since the catalytic chain transfer agent used, COBF, has a fairly high aqueous phase solubility (a partition coefficient $m_{co} = 0.72 \text{ dm}_w^3 \cdot \text{dm}_M^{-3}$),¹⁶ upon the instantaneous addition to the aqueous phase, its aqueous phase concentration is increased momentarily to $9.4 \cdot 10^{-6} \text{ mol} \cdot \text{dm}_w^{-3}$. After partitioning of COBF over the aqueous and polymer particle phases, the equilibrium aqueous phase concentration is $8.2 \cdot 10^{-6} \text{ mol} \cdot \text{dm}_w^{-3}$. This would yield an instantaneous degree of polymerization of 1 of the polymer formed in the aqueous phase, estimated from the Mayo equation⁸ with a C_T of $15 \cdot 10^3$ and an MMA concentration of $0.15 \text{ mol} \cdot \text{dm}_w^{-3}$.³³ The outcome of this calculation illustrates that the presence of COBF, even in very low amounts, may severely affect the course of the polymerization in the aqueous phase. The most generally accepted mechanism for emulsion polymerization^{26,27,34} suggests that oligomeric radicals formed in the aqueous phase will propagate until they become sufficiently surface active, i.e., they reach a length of z , at which instantaneous entry into a micelle or a polymer particle is possible.³⁵ However, in the presence of COBF a propagating oligomeric radical might undergo chain transfer before obtaining the required length for entry. In the latter case, a terminated water soluble oligomer is formed and the radical activity is transferred to a monomer molecule. This aqueous phase chain transfer has two implications for the course of the emulsion polymerization:

- The frequency of entry is lowered, as fewer propagating oligomeric radicals reach the required z-length for entry.
- The rate of short-short termination in the aqueous phase is increased due to an accumulation of short oligomeric radicals.

The result of these two above mentioned effects would be a decreasing rate of polymerization as is confirmed by Figure 3, which shows a decrease of the average number of radicals inside the polymer particles (\bar{n}). The value of \bar{n} follows from the observed rate of polymerization (R_p) and the global rate equation for emulsion polymerization, see Equation 3.

$$R_p = k_p [M]_p \frac{\bar{n} N_p}{N_{av}} \quad (3)$$

where k_p stands for the rate coefficient of propagation, N_p for the particle number based on the number-average particle diameter and N_{av} for Avogadro's number. In the COBF-free *ab initio* emulsion polymerization of MMA \bar{n} values of approximately 0.5 are found. For the experiments where a pulse of COBF is added to the reaction mixture, \bar{n} drops severely, see Figure 3.

At low conversion ($x \leq 0.30$), the polymerization is in interval II of the classic emulsion polymerization mechanism²⁷ and the monomer concentration in the polymer particles is equal to that for the saturation swelling, i.e. $6.6 \text{ mol dm}_p^{-3}$.³³ Hence, a relatively low viscosity of the polymer particles is expected. Upon the addition of COBF, \bar{n} quickly drops from approximately 0.5 to $0.5 \cdot 10^{-3}$, indicating that the system obeys Smith-Ewart case 1 kinetics. This 1000-fold decrease in \bar{n} significantly retards the polymerization, but the polymerization still proceeds.

At higher conversion ($x > 0.30$), the polymerization is in interval III and the polymer particles are partially swollen with monomer. The concentration of monomer inside the polymer particles decreases with conversion and the viscosity keeps increasing depending on the volume fraction of polymer. When COBF is added at higher conversions ($x > 0.30$), again a decrease in \bar{n} is observed, retarding the polymerization. After the initial drop in \bar{n} the polymerization apparently stops.

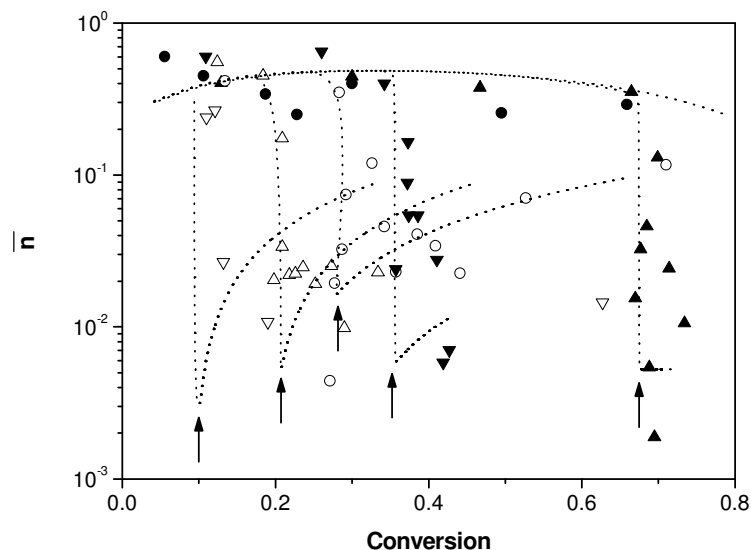


Figure 3. The evolution of \bar{n} as a function of conversion. Ab initio emulsion polymerization without COBF (●); Ab initio emulsion polymerization with COBF added pulse wise at at $x = 0.10$ (▽); $x = 0.20$ (△); $x = 0.30$ (○); $x = 0.40$ (▼) and $x = 0.70$ (▲). Arrows indicate the moment of the COBF addition.

The observed results may conceivably be explained as follows. The instantaneous addition of COBF to the aqueous phase of the emulsion polymerization initially has a severe effect on the entry of surface active oligomers. The rate of entry is lowered and consequently \bar{n} and the rate of polymerization decrease. When the viscosity of the polymer particles is still sufficiently low, the catalytic chain transfer agent will readily partition between the different phases. The partitioning only results in slight decrease in the aqueous phase chain transfer agent concentration thereby hardly changing the probability of entry. However, even when the radical flux from the aqueous phase is constant, \bar{n} is increasing as the polymer particles are slowly growing. The polymerizations obey Smith-Ewart case 1 kinetics, which implies that the value of \bar{n} is governed by the rate of radical desorption from the polymer particles. As the particle size increases, the rate of radical desorption decreases and consequently \bar{n} increases.^{36,37}

Although the rate of polymerization is still significantly lower than in the case for the COBF-free *ab initio* free radical polymerization, the polymerization proceeds.

When COBF is added in interval III, corresponding to high viscosity of the polymer particles, hardly any polymerization is observed after the pulse-wise addition of COBF, i.e., $\bar{n} \rightarrow 0$. There are three explanations for this phenomenon. First, even though the viscosity of the polymer particles is high, equilibrium partitioning will be achieved. As was mentioned before, this hardly affects the aqueous phase COBF concentration. The main difference with the polymerizations at low conversion is that the polymerizations at high conversion proceed in interval III. The polymer particles are only partially swollen with monomer and as a consequence the aqueous phase monomer concentration is also below its saturation concentration, see e.g. Vanzo et al.³⁸ This affects the growth rate of water-soluble oligomers and consequently the rate of radical entry. Secondly, as the aqueous phase monomer concentration is below the saturation concentration, the ratio of the COBF concentration and the monomer concentration in the aqueous phase is higher when COBF is added at higher conversion. According to the Mayo Equation, lower degrees of polymerization are obtained, thereby further affecting the rate of radical entry. Thirdly, the polymerization is in interval III of the classic emulsion polymerization mechanism and consequently particle growth is negligible for MMA emulsion polymerization. So \bar{n} will remain constant at a very low value and the polymerization apparently stops.

Monitoring of CCTA partitioning in seeded emulsion polymerization.

The evolution of the molecular weight distribution can be used as a tool to monitor chain transfer activity at the locus of polymerization.^{22,23} Instantaneous molecular weight distributions can be determined directly after the COBF addition to relate the decrease in the average molecular weight to the amount of COBF mediating the polymerization. The presence of COBF significantly retards the polymerization due to aqueous phase chain transfer effects. Directly after the COBF addition, an inhibition period occurs after which the polymerization eventually continues, see Figure 2. To ensure an acceptable rate of polymerization directly after the addition of COBF, seeded polymerizations are

performed to allow for a higher reaction temperature (70°C) in order to increase the radical flux and consequently increase the rate of entry. The seed latex was swollen with a certain amount of monomer to mimic a conversion of $x = 0.20, 0.40$ or 0.80 . A pulse of the required amount of COBF was added prior to the initiator addition. The overall conversion time histories are presented in Figure 4. The trends observed in the conversion-time histories of the seeded emulsion polymerizations, collected in Figure 4, correspond to those obtained in the *ab initio* polymerization, see Figure 2.

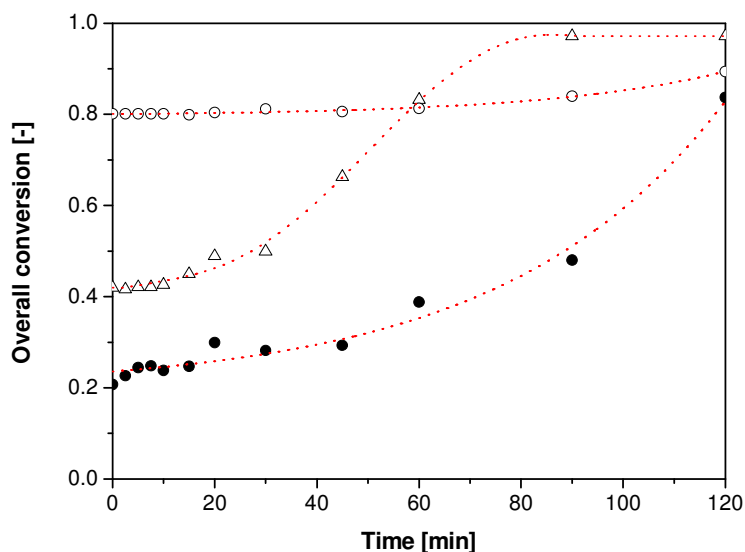


Figure 4. Conversion time history for the seeded emulsion polymerization of methyl methacrylate with an instantaneous COBF addition at different instantaneous conversions. (A): Overall conversion and (B): Instantaneous conversion. Seeded emulsion polymerizations swollen with monomer to mimic a conversion of $x = 0.20$ (●); $x = 0.40$ (△) and $x = 0.80$ (○).

The recipes all have the same phase ratio (β) and the same COBF to monomer ratio (N_{Co} / N_{MMA}). Keeping β and N_{Co} / N_{MMA} constant implies that the partitioning behavior of the catalytic chain transfer agent is comparable for all the experiments shown in Figures 4A and 4B. The same partitioning behavior, in combination with a constant COBF to MMA ratio for all the performed seeded emulsion polymerizations should also result in a comparable average molecular weight of the newly formed polymer if the system reaches equilibrium partitioning. This is confirmed experimentally where the peak

molecular weights of the low molecular weight peak for the final latex coincide around $\log M = 4.9$ ($\sim 80 \cdot 10^3 \text{ g}\cdot\text{mol}^{-1}$), see Figure 5.

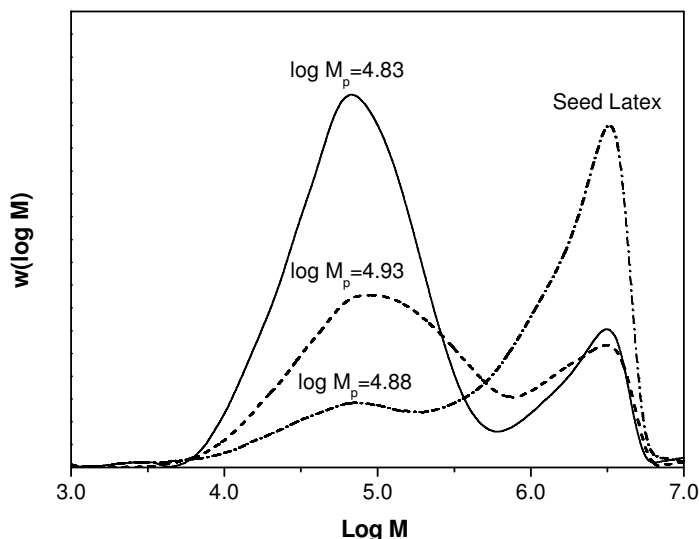


Figure 5. Final molecular weight distributions and $\log M_p$ values of the seeded emulsion polymerizations of MMA. Experimental conditions: $\beta = 0.20$ and $N_{Co} / N_{MMA} = 4.9 \cdot 10^{-6}$. COBF added at 20% conversion (—), COBF added at 40% conversion (---) and COBF added at 80% conversion (- · - · -).

An estimate of the catalytic chain transfer agent concentration inside the polymer particles can be obtained using the CLD method.^{24,25} In principle, (pseudo)-instantaneous molecular weight distributions are required for accurate determination of the instantaneous COBF concentration in the polymer particles. However, the (pseudo)-instantaneous molecular weight distributions are very susceptible to baseline errors, especially for small conversion intervals and could therefore not be determined accurately. Therefore, in this work, we used the cumulative molecular weight distributions in combination with the CLD method. The slope Λ_{peak} is determined at the position of peak molecular weight of the molecular weight distribution of the second-stage polymer, see Figure 6.

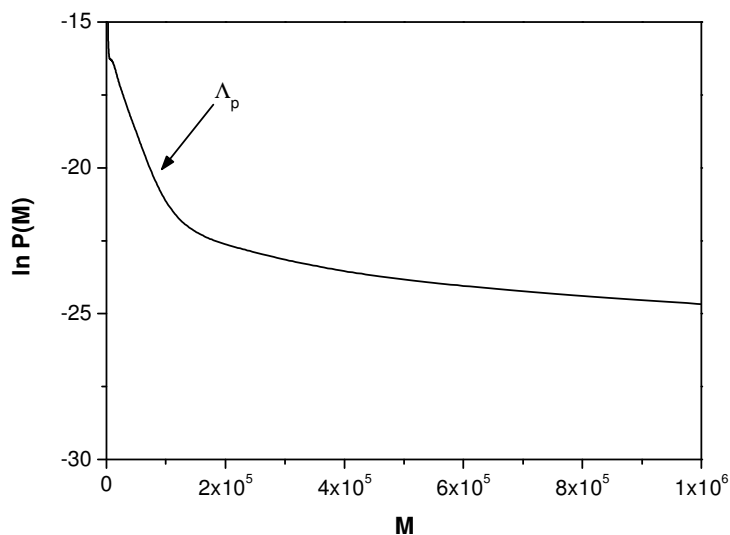


Figure 6. A CLD plot and an indication of the position of the peak molecular weight of the second-stage polymer at which Λ_{peak} is determined from the final molecular weight distribution of the emulsion polymerization initiated at $x = 0.20$, see Figure 5 (—).

The found values for Λ_{peak} directly reflect the value of $C_T \cdot [\text{COBF}]_p / [M]_p$, which is shown as a function of the overall conversion in Figure 7. When the viscosity of the polymer particles is relatively low at the beginning of the polymerization (i.e. the experiments with $x = 0.20$ and $x = 0.40$), the value of $C_T \cdot [\text{COBF}]_p / [M]_p$ rapidly increases to about $8 \cdot 10^{-3}$. After this initial increase the value of $C_T \cdot [\text{COBF}]_p / [M]_p$ gradually decreases to a value of approximately $3 \cdot 10^{-3}$. At high conversion (i.e., the experiment with $x = 0.80$) and consequently at high viscosity of the polymer particles the value of $C_T \cdot [\text{COBF}]_p / [M]_p$ increases and reaches a plateau value of around $3 \cdot 10^{-3}$, see Figure 7. The value of $C_T \cdot [\text{COBF}]_p / [M]_p$ changes during the course of the polymerization, and independent of the initial conversion comparable values are observed at high conversions.

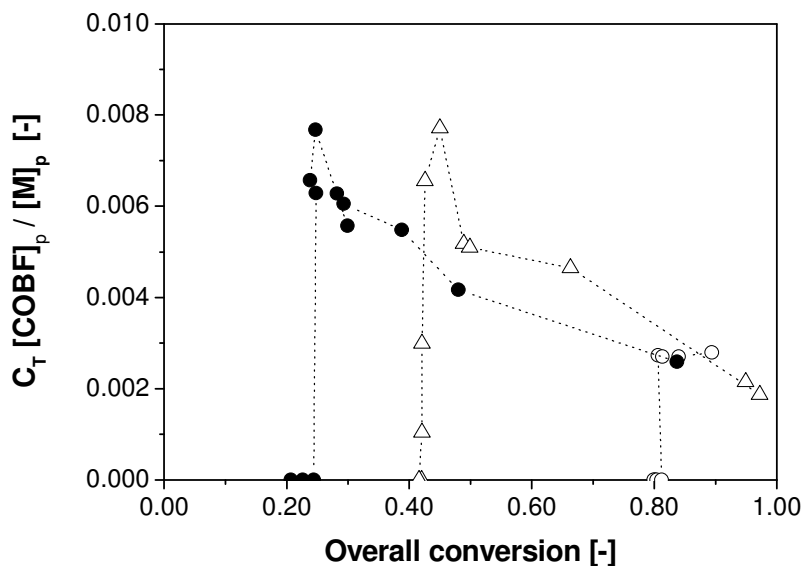


Figure 7. The evolution of $C_T \cdot [\text{COBF}]_p / [M]_p$ as a function of the overall conversion. Seeded emulsion polymerization with a pulse of COBF added at $x = 0.20$ (●); $x = 0.40$ (△) and $x = 0.80$ (○).

The analysis of the obtained molecular weight distributions reveals a decrease in $C_T \cdot [\text{COBF}]_p / [M]_p$ as the reaction progresses. This change is unlikely to be attributed to a changing monomer concentration inside the polymer particles, as this concentration is constant in interval II and continuously decreasing in interval III. Hence, the decrease of $C_T \cdot [\text{COBF}]_p / [M]_p$ can only be attributed to either a change in the COBF concentration inside the polymer particles or a decrease in the chain transfer constant, or a combination of both.

Since no significant changes in partitioning behavior with increasing conversion are expected,^{9,39} a possible decrease in the COBF concentration inside the polymer particles could be caused by aqueous phase decomposition of the catalyst. However, for the applied reaction conditions only a minor effect of decomposition is expected.¹⁶ Hence, both the effect of COBF decomposition and a change in the partition coefficient seem to be insufficient to explain the significant decrease in $C_T \cdot [\text{COBF}]_p / [M]_p$.

Since it does not seem likely that a potential decrease in the COBF concentration inside the polymer particles with increasing conversion is responsible for the observed increase in molecular weight, the only plausible explanation would lie in a decreasing value of C_T . Although there still does not exist any hard evidence for a diffusion-controlled rate determining chain transfer reaction, there are very strong indications that this may be the case. Heuts and co-workers found an inverse relationship between the transfer rate coefficient and the monomer viscosity,^{40,41} suggesting that the reaction rate is governed by the microscopic viscosity (or monomeric friction coefficient).⁴¹ This phenomenon is well-known in the diffusion literature for small-molecule probes (such as monomer and COBF in the present studies) in polymer/solvent systems: although the bulk viscosity may increase over several orders of magnitude with increasing polymer volume fraction, the diffusion coefficients remain approximately constant up to high polymer volume fraction. For higher volume fractions the diffusion coefficient of low molecular species decreases strongly.⁴²⁻⁴⁶ The current situation for catalytic chain transfer is very similar, so it is conceivable that indeed C_T starts decreasing at a certain high polymer content.

The catalytic chain activity over the course of the polymerization can be evaluated from the results collected in Figure 7. High values for $C_T \cdot [\text{COBF}]_p / [\text{M}]_p$ correspond to a situation similar to bulk or solution polymerization. Low values for $C_T \cdot [\text{COBF}]_p / [\text{M}]_p$ indicate that the chain transfer reaction is severely hampered as a result of very slow mass transport. For the polymerization initiated at low viscosity (i.e., $x = 0.20$ and $x = 0.40$) the catalytic chain transfer activity inside the polymer particles rapidly increases, which is an indication for efficient catalytic chain transfer. The COBF complex can readily partition from the aqueous phase towards the polymer particles and the chain transfer reaction is not hindered. As the polymerization proceeds, the chain transfer activity is continuously decreasing indicating that the chain transfer is becoming increasingly difficult. When COBF is added pulse-wise at a conversion of 0.80, a very low chain transfer activity is observed. Moreover, the observed chain transfer activities at high conversion in the individual polymerizations are consistent. The results collected in Figure 7 show that the efficiency of chain transfer severely changes throughout the course of an emulsion

polymerization and that the polymer volume fraction inside the polymer particles is a key parameter governing the chain transfer reaction in emulsion polymerization.

CONCLUSIONS

The results of this work demonstrate that the pulse-wise addition of a fairly water soluble catalytic chain transfer agent, i.e. COBF, severely affects the course of the emulsion polymerization. Aqueous phase chain transfer in combination with increased short-short termination competes with aqueous phase propagation, resulting in a situation where the entry frequency of radicals and consequently \bar{n} decreases. Secondly, the mass transport of COBF from the aqueous phase towards the growing chain in the polymer particles depends strongly on the viscosity (the weight fraction of polymer) inside the polymer particles. The chain length distribution method was used to determine the amount of COBF in the polymer particles from the obtained molecular weight distributions. When the polymer particles are at their saturation concentration, there is hardly any resistance against mass transport and equilibrium partitioning is reached quickly. Below the saturation concentration, partitioning is slower due to mass transport limitations. The observed decrease in $C_T \cdot [\text{COBF}]_p / [\text{M}]_p$ indicates that along the course of the polymerization, i.e., as the weight fraction of polymer is increasing, the chain transfer constant is changing due to changes in the microscopic viscosity.

EXPERIMENTAL SECTION

Materials

The bis(methanol) complex COBF was prepared as described previously.^{12,47} For all experiments, a single batch of catalyst was used. The intrinsic activity of the catalyst was determined by measuring the chain transfer constant in the bulk polymerization of MMA at 60°C: $CT = 30 \cdot 10^3$. Methyl methacrylate (MMA) (Aldrich, 99%) was purified by passing it over a column of activated basic alumina (Aldrich). Sodium bicarbonate (SBC) (Fluka, >99%), sodium dodecyl sulphate (SDS) (Fluka, 99%), potassium persulphate (KPS) (Aldrich >98%) and 2,2'-Azobis[N-(2-carboxylethyl)-2-

methylpropionamide]hydrate (V57) (Wako) were used as received. Distilled deionised water (DDW) was used throughout this work. All experiments were conducted in a 1.2 dm³ Mettler Toledo RC1e reaction calorimeter equipped with an anchor impellor, calibration heater, Tr sensor and sample loop. The reactor was operated in isothermal mode.

Seed latex preparation

The RC1e reactor was charged with MMA (240 g, 2.41 mol), distilled deionized water (DDW) (710 g), SDS (11 g, 3.8·10⁻² mol) and SBC (0.74 g, 7.0·10⁻³ mol). The resulting emulsion was stirred vigorously, purged with nitrogen for 1h and heated to the desired reaction temperature of 70°C. Subsequently, the initiator (KPS) dissolved in 10 g of DDW was added instantaneously. After reacting for 1 h (conversion ~ 0.96), the temperature was raised to 90°C to increase the decomposition rate of the initiator. The final latex was left stirring for 5 h after which less then 0.5 % of the initiator should remain. The latex was then dialyzed against DDW for 7 days, changing the DDW twice a day. The final properties of the seed latex are summarized in Table 1.

Table 1. Properties of the seed latex used for the seeded emulsion polymerization experiments.

<i>Final x</i> ^a	<i>d_p(V)</i> ^b	<i>poly</i> ^c	<i>N_p</i>
[-]	[nm]	[-]	[10 ¹⁸ dm _w ⁻³]
0.98	57.3	0.055	2.0

^a Conversion determined gravimetrically.

^b Volume average particle diameter as determined by dynamic light scattering using a Malvern Nanosizer.

^c poly is the polydispersity of the particle size distribution as calculated by the Malvern® software.

Ab initio catalytic chain transfer mediated emulsion polymerization

SDS (2.75 g, 9.6 mmol) and SBC (0.42 g, 4.0 mmol) were dissolved in DDW (360 g) and added, under continuous stirring, to the reactor. Subsequently MMA (70 g, 0.70 mol) was added and the resulting emulsion was purged with nitrogen for 1 h. The reactor temperature was gradually raised to the final reaction temperature of 50 °C. The polymerization was initiated by the addition of the V57 initiator (0.131 g, 0.38 mmol). A catalyst stock solution was prepared by dissolving an accurate amount of COBF (~10 mg, 24×10^{-3} mmol) in DDW (66.7 g). At different conversion levels ($x = 0.10, 0.20, 0.30, 0.40$ and 0.70) 10 mL of the catalyst stock solution, directly followed by a second addition of V57 (0.536 g, 1.57 mmol) dissolved in 10 g of DDW were added as a pulse injection to the reactor content. Samples were withdrawn periodically to monitor the gravimetric conversion, molecular weight and the particle size distribution.

Seeded catalytic chain transfer mediated emulsion polymerization

SDS (0.25 g, 0.87 mmol) and SBC (0.40 g, 3.8 mmol) were dissolved in DDW and added to the reactor. Subsequently, the reactor was charged with the required amounts of seed latex and MMA. The latex was stirred gently overnight to allow swelling of the polymer particles. The temperature of the latex was set at 10 °C to prevent polymerization. After swelling, the resulting latex was purged with nitrogen for 1 h and the reaction temperature was gradually raised to the reaction temperature of 70 °C. A catalyst stock solution was prepared by dissolving an accurate amount of COBF (~10 mg, 24×10^{-3} mmol) in DDW (61 g). After purging, 10 mL of the catalyst stock solution was added to the reactor, immediately followed by the addition of the V57 initiator (0.15 g, 0.44 mmol). The polymerization conditions are summarized in Table 2. Samples were withdrawn periodically to monitor the gravimetric conversion, molecular weight and particle size distribution.

Table 2. The polymerization conditions for the seeded emulsion polymerization experiments.

x	<i>SEED</i>	<i>DDW</i>	<i>MMA</i>	<i>COBF</i>	$\frac{N_{Co,0}}{N_{MMA}}$	<i>Solid content</i>	β^a
	[g]	[g]	[g]	[mg]	[10 ⁻⁶]	[-]	[-]
20%	70	140	210	280	4.9	0.16	0.20
40%	385	328	277	220	4.9	0.16	0.20
80%	1.65	1.65	1.65	1.65	4.9	0.16	0.20

^a The phase ratio (β) is defined as the ratio of the volume of organic phase and the volume of the aqueous phase.

SEC Analysis.

Size exclusion chromatography was performed using a Waters GPC equipped with a Waters model 510 pump and a Waters model 410 differential refractometer. A set of two mixed bed columns (Mixed-C, Polymer Laboratories, 30 cm, 40 8C) were used. Tetrahydrofuran (Aldrich) was used as the eluent, and the system was calibrated using narrow molecular weight polystyrene standards ranging from 600 to $7 \cdot 10^6$ g.mol⁻¹. Mark-Houwink parameters used for the polystyrene standards: $K = 1.14 \times 10^{-4}$ dL g⁻¹, $a = 0.716$, and for poly(methyl methacrylate): $K = 9.44 \times 10^{-5}$ dL g⁻¹, $a = 0.719$.

REFERENCES AND NOTES

1. Enikolopyan, N. S.; Smirnov, B. R.; Ponomarev, G. V.; Belgovskii, I. M. *J Polym Sci Part A: Polym Chem* 1981, 19, 879.
2. Gridnev, A. *J Polym Sci Part A: Polym Chem* 2000, 38, 1753
3. Gridnev, A. A.; Ittel, S. D. *Chem Rev* 2001, 101, 3611.
4. Heuts, J. P. A.; Roberts, G. E.; Biasutti, J. D. *Aust J Chem* 2002, 55, 381.
5. Karmilova, L.V.; Ponomarev, G.V.; Smirnov, B.R.; Belgovskii, I.M. *Russ. Chem. Rev.* 1984, 53, 132
6. Davis, T.P.; Haddleton, D.M.; Richards, S.N. *J. Macromol. Sci., Rev. Macromol. Chem.* 1994, C34, 234
7. Davis, T.P.; Kukulj, D.; Haddleton, D.M.; Maloney, D.R. *Trends Polym. Sci.* 1995, 3, 365

8. F.R. Mayo J. Am. Chem. Soc. 1943, 65, 2324.
9. Kukulj, D.; Davis, T.P.; Suddaby, K.G.; Haddleton, D.M.; Gilbert, R.G. J Polym Sci Part A: Polym Chem 1997, 35, 859/
10. Pierik, S.C.J.; Smeets, B.; van Herk, A.M. Macromolecules 2003, 36, 9271.
11. Bon, S. A. F.; Morsley, D. R.; Waterson, J.; Haddleton, D. M.; Lees, M. R.; Horne, T. Macromol Symp 2001, 165, 29.
12. Suddaby, K.G.; Haddleton, D.M.; Hastings, J.J.; Richards, S.N.; O'Donnell, J.P. Macromolecules 1996, 29, 8083.
13. Kukulj, D.; Davis, T. P.; Gilbert, R. G. Macromolecules 1997, 30, 7661.
14. Haddleton, D.M.; Morsley, D.R.; O'Donnell, J.P.; Richards, S.N. J Polym Sci Part A: Polym Chem 2001, 37, 3549.
15. Smeets, N.M.B.; Heuts, J.P.A.; Meuldijk, J.; van Herk, A.M. J Polym Sci Part A: Polym Chem 2008, 46, 5839.
16. Smeets, N.M.B.; Meda, U.S.; Heuts, J.P.A.; Keurentjes, J.T.F.; van Herk, A.M.; Meuldijk, J. Macromol Symp 2007, 259, 406.
17. Cunningham, M.F. Prog. Polym. Sci. 2008, 33, 365.
18. Zetterlund, P.B.; Kawaga, Y.; Okubo, M. Chem. Rev. 2008, 108, 3747.
19. McLeary, J.B.; Klumperman, B. Soft Matter 2006, 2, 45.
20. Charleux, B.; Nicolas, J. Polymer, 2007, 48, 5813.
21. Qui, J.; Charleux, B.; Matyjaszewski, K. Prog. Polym. Sci. 2001, 21, 2083.
22. Cunningham, M.F.; Ma, J.W. J. Appl Polym Sci 2000, 78, 217.
23. Ma, J.W.; Cunningham, M.F. Macromol Symp 2000, 150, 85.
24. Whang, B.Y.C.; Ballard, M.J.; Napper, D.H.; Gilbert, R.G. J. Aust Chem 1991, 44, 1133
25. Christie, D.I.; Gilbert, R.G. Macromol Chem Phys 1996, 197, 403
26. Gilbert, R.G. in Emulsion polymerization: A mechanistic approach, ed. Gilbert, R.G., Eds. Academic Press Limited: London, 1995.
27. Smith, W.V.; Ewart, R.H. J Chem Phys 1948, 16, 592
28. Clay, P.A.; Christie, D.I.; Gilbert, R.G. ACS symposium series 685 Ed. Matyjaszewski K., 1998, 104.
29. Heuts, J.P.A. ; Kukulj D. ; Forster, D.J. ; Davis, T.P. Macromolecules 1998, 31, 2894-2905.
30. Moad, G.; Moad, C.L. Macromolecules 1996, 29, 7727.
31. Heuts, J.P.A.; Davis, T.P.; Russell, G.T. Macromolecules 1999, 32, 6019.
32. Hutchinson, R.A.; Paquet Jr., D.A.; McMinn, J.H. Macromolecules 1995, 28, 5655.

33. Ballard, M.J.; Napper, D.H.; Gilbert, R.G. *J. Polym. Sci. Chem. Ed.* 1984, 22, 3225-3253
34. Harkins, W.D. *J Am Chem Soc* 1947, 69, 1428
35. Maxwell, I.A.; Morrison, B.R.; Napper, D.H.; Gilbert, R.G. *Macromolecules* 1991, 24, 1629.
36. Ugelstad, J.; Mork, P.C.; Aasen, J.Q.; *J. Polym. Sci. Part A-1: Polym. Chem.* 1967, 5, 2281.
37. Ugelstad, J. ; Mork, P.C.; Rangnes, P. *J. Polym. Sci. Part C.* 1969, 27,49.
38. Vanzo, E. ; Marchessault, R.H. ; Stannett, V. *J. Colloid. Sci.* 1965, 20, 62.
39. The influence of the presence of polymer on the partitioning of COBF was investigated in a water – MMA – pMMA mixture by Kukulj et al. (Ref 9) These authors reported only a minor effect of the presence of pMMA on the partition coefficient of COBF.
40. Heuts, J.P.A.; Forster, D.J.; Davis, T.P. *Macromolecules*, 1999, 32, 3907.
41. Roberts, G.E.; Davis, T.P.; Heuts, J.P.A.; Russell, G.T. *J. Polym. Chem. Part A: Polym. Chem.* 2002, 40, 782.
42. Wisnudel, M. B.; Torkelson, J. M. *Macromolecules* 1996, 29, 6193.
43. Lodge, T. P.; Lee, J. A.; Frick, T. S. *J Polym Sci Part B: Polym Phys* 1990, 28, 2607.
44. Gisser, D. J.; Johnson, B. S.; Ediger, M. D.; Von Meerwall, E. D. *Macromolecules* 1993, 26, 512.
45. Von Meerwall, E. D.; Amis, A. J.; Ferry, J. D. *Macromolecules* 1985, 18, 260.
46. Landry, M. R.; Gu, Q.-J.; Yu, H. *Macromolecules* 1988, 21, 1158.
47. Bakač, A.; Brynildson, M. E.; Espenson, J. H. *Inorg. Chem.* 1986, 25, 4108.

Evidence of Compartmentalization in Catalytic Chain Transfer Mediated Emulsion Polymerization of Methyl Methacrylate

ABSTRACT

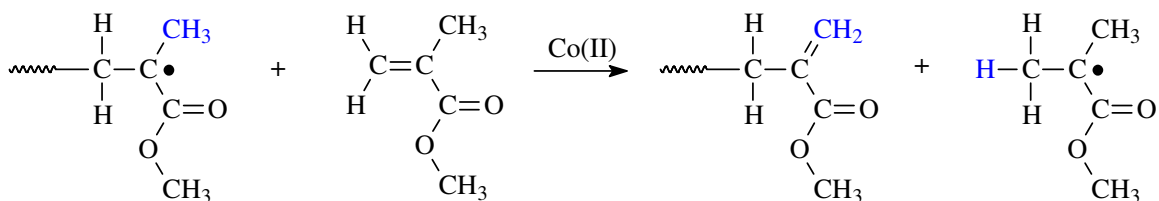
Evidence of compartmentalization of the catalytic chain transfer agent in seeded emulsion polymerization is shown experimentally. The addition of bis[(difluoroboryl)dimethylglyoximato] cobalt(II) (COBF) to seed particles swollen below their maximum saturation concentration, exhibited multimodal molecular weight distributions (MWD) which are contributed to a statistical distribution of COBF molecules over the polymer particles. The experimental observations suggest that there are two limits for catalytic chain transfer in emulsion polymerization: (i) at the earlier stages of the polymerization where a global COBF concentration governs the MWD and (ii) at the latter stages of the polymerization where a statistical distribution of COBF molecules governs the MWD. To the best of our knowledge, these results are the first to suggest evidence of compartmentalization in catalytic chain transfer mediated emulsion polymerization.

INTRODUCTION

Compartmentalization in heterogeneous polymerization systems refers to two distinctive and opposite effects.^{1,2} First, a segregation effect where radicals located in different particles are unable to react with each other. Secondly, a confined space effect where the reaction rate between two radicals in a particle increases with decreasing particle size. When compared to bulk polymerization, the high reaction rates and high average molecular weights in emulsion polymerization are due to the segregation of radicals. Strong compartmentalization behavior in emulsion polymerization can result in a scenario where there are only zero or one radicals in a particle, when bimolecular termination is sufficiently fast. This scenario is also referred to as zero-one kinetics, in which the entry of a radical into a particle already containing one radical results in (pseudo)-instantaneous termination.^{3,4} Both the rate of polymerization per particle and the average molecular weight of the polymer formed depend on the characteristic time of radical entry. In a second scenario, referred to as pseudo-bulk kinetics, the average number of radicals per particle (\bar{n}) is relatively large, radicals move freely between particles and particles can contain more than one radical at a time. In this scenario the effects of compartmentalization are less pronounced.

Compartmentalization in emulsion polymerization is not restricted to radicals only. Over the recent years controlled/living radical polymerization (CLRP) has extended the range of polymer architectures obtainable from classic free radical polymerization.⁵⁻⁸ Controlled/Living radical polymerization techniques such as RAFT, NMP and ATRP include the addition of an agent which controls the molecular weight of the polymer at the loci of polymerization, i.e. the polymer particles. Although compartmentalization in NMP⁹ and ATRP^{1,10} mediated emulsion polymerization depends on the compartmentalization of the controlling agent, and not on the segregation of radicals as in a conventional emulsion polymerization, it does affect the rate of polymerization and livingness of the system^{9,11} (i.e. the average molecular weight obtained and the polydispersity index).

Catalytic chain transfer (CCT) has demonstrated to be a versatile method for robust molecular weight control.¹²⁻¹⁸ In catalytic chain transfer mediated polymerizations, the radical activity is transferred from a propagating radical to a monomer molecule, yielding a dead polymer chain with a vinyl end-group functionality and a monomeric radical, see Scheme 1.



Scheme 1. The overall reaction of catalytic chain transfer to monomer.

In a first step, the active Co(II) complex abstracts a hydrogen atom from the propagating polymer chain, resulting in a dead polymer chain and a Co(III)-H complex. Subsequently, the hydrogen atom is transferred from the Co(III)-H complex to a monomer molecule, regenerating the active Co(II) complex and yielding a monomeric radical capable of propagation.

Bulk and solution polymerizations are homogeneous reactions where the COBF concentration in the locus of polymerization is equal to the overall COBF concentration in the reaction mixture. The degree of polymerization can be predicted accurately by the Mayo equation¹⁹, see Equation 1.

$$\frac{1}{DP_n} = \frac{1}{DP_{n,0}} + C_T \frac{[\text{COBF}]}{[\text{M}]} \quad (1)$$

Due to the compartmentalized nature of the emulsion polymerization, the COBF concentration at the loci of the polymerization, i.e. the polymer particles, differs from the overall COBF concentration. Catalytic chain transfer mediated emulsion polymerizations with COBF often proceed in a regime where the ratio of number of COBF molecules and the number of polymer particles (N_{COBF} / N_p) < 1 , depending on the partition coefficient and the phase ratio. In *ab initio* emulsion polymerization where the viscosity inside the

polymer particles remains relatively low throughout the course of the polymerization, fast COBF mass transport between the polymer particles and the aqueous phase occurs. Monomodal molecular weight distributions are obtained with an instantaneous degree of polymerization that can be predicted by the Mayo equation incorporating COBF partitioning,²⁰ see Equation 2.

$$DP_{n,M} = \frac{V_M[M]_p}{C_T} \frac{1}{N_{Co,0}} \left(\frac{m_{Co}\beta + 1}{m_{Co}(\beta + 1)} \right) \left(1 + \frac{1}{\beta} \right) \quad (2)$$

Fast exchange between the polymer particles results in a situation where a single COBF molecule is able to mediate multiple polymer particles and hence there is an apparent COBF concentration over the entire organic phase. The Mayo equation, incorporating COBF partitioning, is valid in this situation and is able to successfully predict the instantaneous degree of polymerization.²⁰ However, if the mobility of the catalytic chain transfer agent is severely restricted, for instance in interval III of the polymerization when the viscosity of the polymer particles increases tremendously with conversion, compartmentalization of the catalytic chain transfer agent might occur and this could affect the molecular weight distribution.

In the presented chapter we report evidence of compartmentalization effects in the catalytic chain transfer mediated emulsion polymerization of methyl methacrylate with COBF. A catalytic chain transfer agent with considerable water-solubility was used to exclude any transport limitations between the polymer particles and the aqueous phase.

RESULTS AND DISCUSSION

Experimental results.

The number of COBF molecules per particle can be calculated if (i) the number of polymer particles is accurately known and (ii) if there are no monomer droplets present during the polymerization. Seeded emulsion polymerizations where the polymer particles

are swollen below the saturation swelling concentration meet both requirements. The Vanzo equation can be used to estimate the amount of monomer required to swell the polymer particles to 85% of their saturation swelling.²¹

The partitioning behavior of COBF in a methyl methacrylate emulsion polymerization has been described before and the instantaneous number-average degree of polymerization (DP_n) can be predicted accurately with the Mayo equation incorporating COBF partitioning, see Equation 2.^{20,22} In this equation V_M is the total volume of the organic phase, $[M]_p$ the monomer concentration inside the polymer particles, $N_{Co,0}$ the absolute amount of COBF in moles and C_T the intrinsic activity of COBF expressed as the chain transfer constant. The partitioning behavior of COBF is expressed in terms of the partitioning coefficient $m_{Co} = \frac{[COBF]_M}{[COBF]_W}$ and the phase ratio $\beta = \frac{V_M}{V_W}$. The total volume of the organic phase includes the polymer particles and, as the partition coefficient is hardly affected by the presence of polymer in the monomer phase,²³ both monomer and polymer. The phase ratio for a seeded emulsion polymerization is given by Equation 3.

$$\beta = \frac{V_{seed} f_p + V_{seed} f_p \phi_{MMA} + V_{MMA,aq}}{V_{seed} (1 - f_p) + V_W} \quad (3)$$

Calculation of the phase ratio requires of the volume of seed polymer ($=V_{seed} f_p$), the volume of monomer in the polymer particles ($=V_{seed} f_p \phi_{MMA}$), the volume of water ($=V_{seed} (1 - f_p) + V_W$) and the volume of monomer in the aqueous phase, given by Equation 4.

$$V_{MMA,aq} = \frac{C_{MMA,aq}^{sat} M_{MMA} [V_{seed} (1 - f_p) + V_W]}{\rho_{MMA}} \left\{ \frac{\phi_{MMA}}{\phi_{MMA,sat}} \exp(\phi_{MMA,sat} - \phi_{MMA}) \right\} \quad (4)$$

Where V_{seed} and V_{W} are the volume of seed latex and the volume of water respectively, f_{p} the volume fraction of polymer in the seed latex, $C_{\text{MMA,aq}}^{\text{sat}}$ the saturation solubility of MMA in the aqueous phase, M_{MMA} the molecular mass of a monomer molecule, ρ_{MMA} the density of MMA, $\varphi_{\text{MMA,sat}}$ the saturation swelling of MMA in a polymer particle and φ_{MMA} the actual swelling of MMA in a polymer particle. The phase ratio for all reported experiments was taken at 0.25, corresponding to a solid content of 20%. The number of COBF molecules per particle can be calculated by using Equations 3, 4 and a mass balance for COBF and dividing by the absolute number of polymer particles. The number of COBF molecules per polymer particle ($\bar{n}_{\text{COBF}} = N_{\text{COBF}} / N_{\text{p}}$) for different particle diameters are presented in Figure 1.

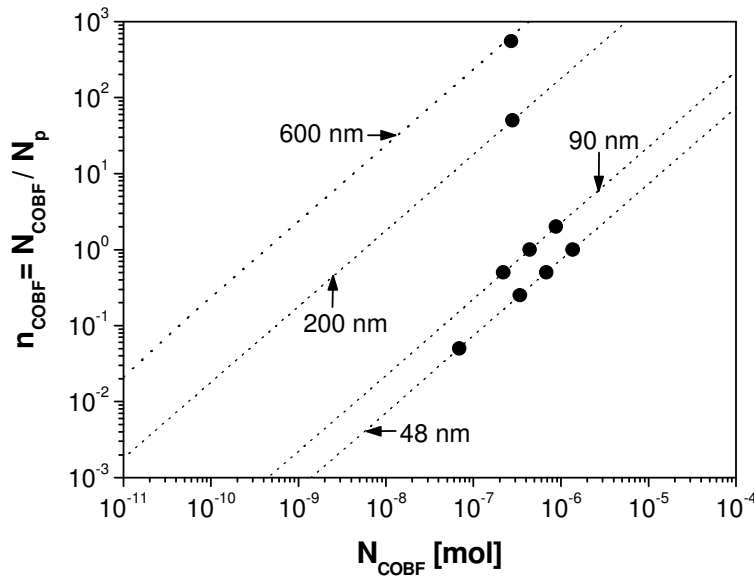


Figure 1. Number of COBF molecules per polymer particle for different particle diameters, i.e. 48, 90, 200 and 600 nm. Calculated \bar{n}_{COBF} based on $m_{\text{Co}} = 0.72 \text{ dm}_W^3 \cdot \text{dm}_M^{-3}$ and β based on Equation 3 (.....). Experiments as reported in this work (●).

Besides the control of the molecular weight distribution, COBF also affects the course of the emulsion polymerization. For small polymer particles, the amount of COBF required to obtain a high \bar{n}_{COBF} is expected to result in low rates of polymerization as the radical

entry rate is severely decreased and the exit and termination rate increased. For large polymer particles, the amount of COBF required to obtain a low n_{COBF} would result in very high degrees of polymerization, most likely hardly indistinguishable from that of the seed latex. As the number of COBF molecules per particle strongly depends on the particle size, seed latexes with different particle sizes are required to cover the full range of $0.05 \leq \bar{n}_{\text{COBF}} \leq 500$. The experimental results of the compartmentalization experiments are summarized in Table 1.

Table 1. Experimental results for the compartmentalization experiments.

<i>Exp.</i>	<i>Seed</i>	$\frac{N_{\text{COBF}}}{N_{\text{MMA}}}$	\bar{n}_{COBF}^a	x^b	N_p	$d_p(V)^c$	<i>Poly</i> ^d
		[ppm]	[-]	[-]	[dm_w^{-3}]	[nm]	[-]
C011	S01	0.0	0.0	1.00	$3.3 \cdot 10^{18}$	68	0.104
C012	S01	1.1	0.05	0.97	$3.3 \cdot 10^{18}$	67	0.086
C013	S01	5.6	0.25	0.61	$3.3 \cdot 10^{18}$	64	0.089
C014	S01	11.2	0.50	0.64	$3.3 \cdot 10^{18}$	71	0.080
C015	S01	22.5	1.00	0.19	$3.3 \cdot 10^{18}$	63	0.076
C021	S02	0.0	0.0	0.92	$7.3 \cdot 10^{17}$	118	0.010
C022	S02	3.5	0.5	0.65	$7.3 \cdot 10^{17}$	105	0.034
C023	S02	7.1	1.0	0.74	$7.3 \cdot 10^{17}$	113	0.031
C024	S02	14.1	2.0	0.46	$7.3 \cdot 10^{17}$	103	0.061
C031	S03	4.0	50	0.90	$1.1 \cdot 10^{16}$	224	0.089
C041	S04	5.4	550	0.86	$6.2 \cdot 10^{14}$	649	0.029

^a The absolute number of COBF molecules was calculated using the phase ratio, which was a constant in all experiments, $\beta = 0.25 \text{ } dm_M^3 \cdot dm_W^{-3}$ and a partition coefficient of $0.72 \text{ } dm_W^3 \cdot dm_M^{-3}$.

^b Final conversion obtained from gravimetric analysis.

^c Particle size analysis performed on a Malvern Zetasizer.

^d poly is the polydispersity of the particle size distribution as calculated by the Malvern® software.

A crucial parameter is the number of polymer particles in the polymerization. The calculations of N_{COBF} / N_p are based on the initial particle number, as obtained from the analysis of the different seed latexes S01 to S04. The poly's of the particle size distributions (PSD) after swelling and polymerization are all below 0.1, which is a good indication for a monomodal latex. The final particle diameters are within experimental error of the calculated swollen particle diameters. Both observations indicate that secondary nucleation, although possible in the case of methyl methacrylate, was negligible. This in turn implies that the pre-determined N_{COBF} / N_p ratio should hold throughout the course of the polymerization and that any possible effects appearing in the molecular weight distribution (MWD) are most likely ascribed to the changes in the partitioning behavior and mass transport of COBF.

The evolution of the MWDs for the experiments with $0.05 \leq \bar{n}_{\text{COBF}} \leq 1$ for the 48 nm seed particles (C012 – C015) are presented in Figure 2, in which the MWDs are normalized with respect to the amount of seed polymer in the polymerization, to clearly visualize the polymer produced in the second stage. The addition of a catalytic chain transfer agent in *ab initio* emulsion polymerization results in a monomodal MWD.²⁰ When added to a seeded polymerization, with polymer particles swollen with monomer below their saturation swelling, independent of the N_{COBF} / N_p ratio, multimodal MWDs are obtained as can be clearly seen from Figure 2. For $\bar{n}_{\text{COBF}} = 0.05$, the multimodality of the MWD is not as apparent as is the case for $\bar{n}_{\text{COBF}} = 0.25, 0.50$ and 1.00 , but still a distinct shoulder at the low molecular weight end of the distribution can be distinguished. The MWD also seems to broaden on its high molecular weight end. For $\bar{n}_{\text{COBF}} = 0.25, 0.50$ and 1.00 the observations are comparable. A distinct set of lower molecular weight peaks are appearing at the lower end of the distribution, whereas hardly any secondary polymer appears at the high molecular weight end. As is clearly seen in Figure 2, the multimodal character of the MWD is already present from the initial stages of the polymerization and becomes more pronounced at higher conversions.

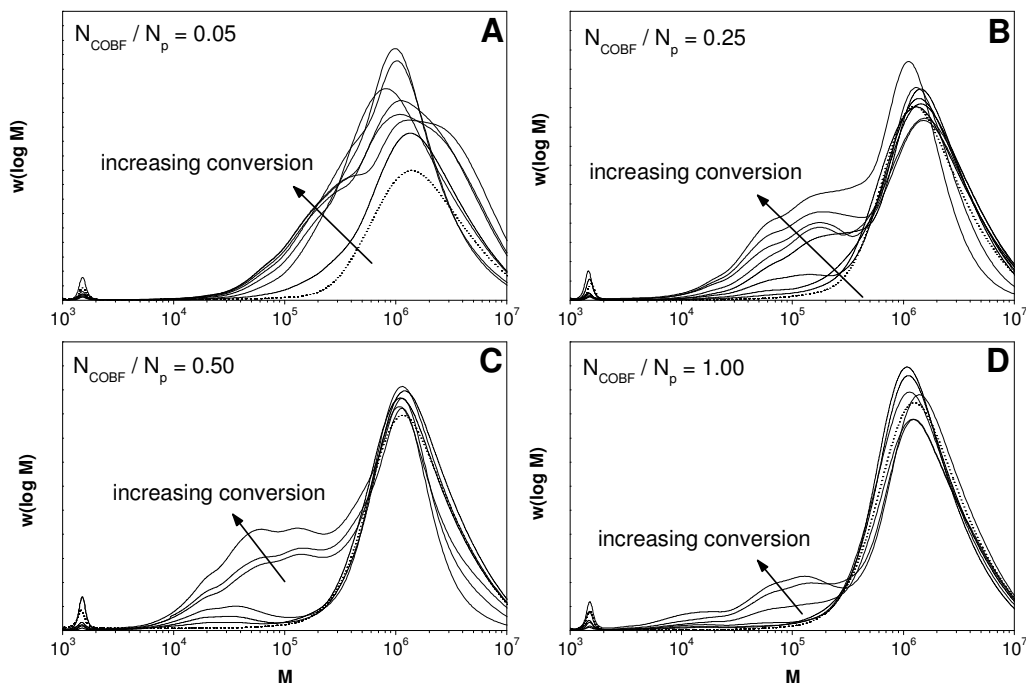


Figure 2. Evolution of the molecular weight distributions for the compartmentalization experiments C012 – C015. Molecular weight distribution of S01 (.....), Molecular weight distributions of C012 – C015 (—). All the distributions have been scaled to the amount of seed polymer.

These multimodal distributions clearly suggest the presence of different polymer populations. It is clear that the results shown in Figure 2 do not correspond to a situation in which an overall COBF concentration is sufficient to describe the produced MWDs. If this were the case, then a monomodal MWD would be expected for the second-stage polymer. For $\bar{n}_{\text{COBF}} = 0.05, 0.25, 0.50$ and 1.00 a DP_n of 404, 81, 40 and 20 was expected based on Equation 2. It is evident that this is not observed experimentally. Moreover, when the obtained MWDs from the experiments with different \bar{n}_{COBF} are compared, it is evident that the location of the peaks observable in the multimodal MWD overlay. In other words, independent of the \bar{n}_{COBF} and thus the total amount of COBF in the polymerization, approximately the same set of polymer populations is formed. This is counter-intuitive as an increase in the amount of COBF is expected to result in a decrease

of the overall average molecular weight obtained. The relative proportions of the individual contributions to the multimodal MWD are changing according to the \bar{n}_{COBF} , see Figure 2. At higher \bar{n}_{COBF} more lower molecular weight polymer is produced. These quantitative observations seem to point in a direction in which there are comparable reaction environments for the polymerizations with various \bar{n}_{COBF} , generating similar polymer populations. Comparable trends are observed for the molecular weight distributions for the experiments with $0.50 \leq \bar{n}_{\text{COBF}} \leq 2$ for the 90 nm seed particles (C022 – C024) which are presented in Figure 3.

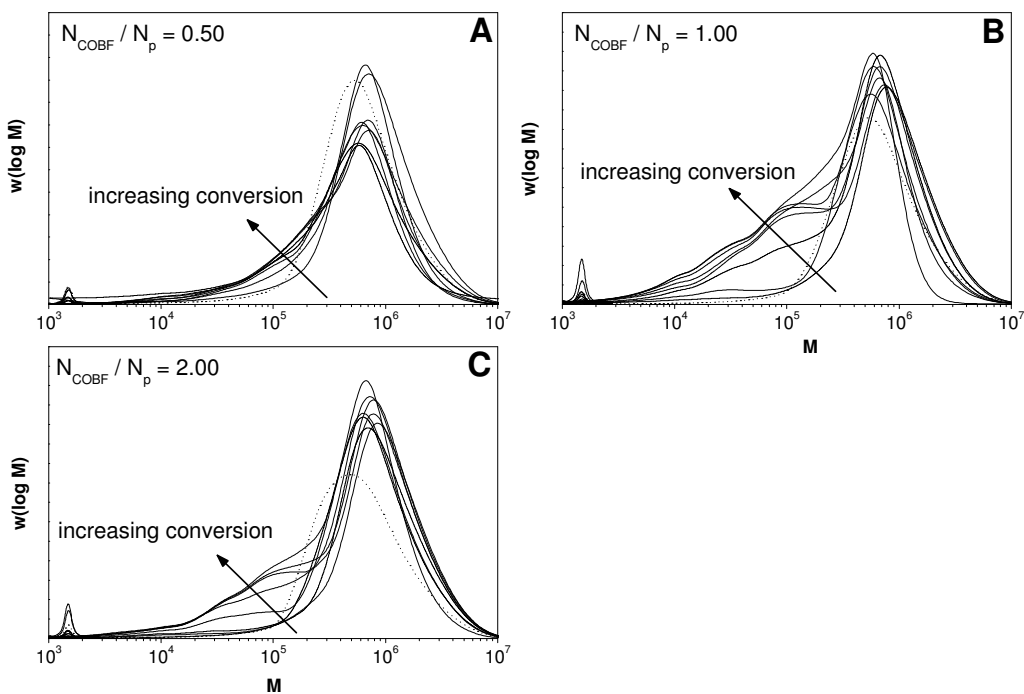


Figure 3. Evolution of the molecular weight distributions for the compartmentalization experiments C022 – C024. Molecular weight distribution of S02 (.....), Molecular weight distributions of C022 – C024 (—). All the distributions have been scaled to the amount of seed polymer.

The average degrees of polymerization of the individual contributions to the multimodal MWD were estimated from the maxima in the first derivative of $w(\log M)$ with respect to $\log M$ (i.e., $d(w(\log M))/d(\log M)$). The derivative plots of the MWDs obtained in the experiments C012 – C015 and C022 – C024 are presented in Figure 4. As expected from the MWDs presented in Figures 2 and 3, the location of the individual peaks of the multimodal MWD do indeed occur at corresponding molecular weight as can be observed in the derivative of the MWD plot, see Figure 4. Moreover, the maxima of the derivative of the MWD of the 48 nm and 90 nm particles overlay. The degrees of polymerization obtained from the derivative MWD plot are presented in Table 2. For the individual MWDs, that make up the multimodal MWDs, the average degrees of polymerization approximately correspond to $DP_n \sim 1200, 400$ and 150.

Table 2. The degrees of polymerization obtained from differentiated MWD plot for the 48 and 90 nm particles.

	$DP_n(0)^a$	$DP_n(1)$	$DP_n(2)$	$DP_n(3)$
C012	7310	1250	497	187
C013	7460	1040	393	167
C014	8240	1030	322	163
C015	7460	1080	454	123
C022	5500	1250	393	145
C023	7310	1120	343	159
C024	8080	1170	473	160

^a $DP_n(0)$ is predominantly the contribution of the seed polymer.

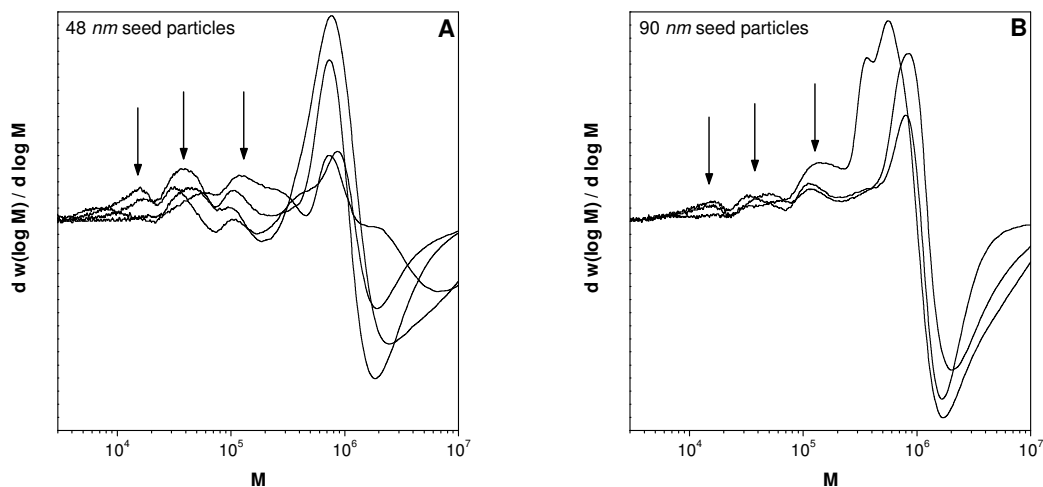


Figure 4. The plot of the differentiated molecular weight distributions ($d(w(\log M))/d(\log M)$). (A) of the molecular weight distributions in Figure 2, 48 nm particles and (B) of the molecular weight distributions in Figure 3, 90 nm particles. The arrows indicate the position of the inflection points of the cumulative MWD.

The fact that the observed degrees of polymerization within the multimodal MWDs of the 48 nm and 90 nm particles are approximately identical, are consistent with the hypothesis that there are identical reaction environments independent of the N_{COBF}/N_p ratio and independent of the particle size. Taking this reasoning one step further, it should than be possible to fit the multimodal MWD with the individual contributions of the individual reaction environments. One possible method to fit free radical MWDs is the Flory-Schulz distribution²⁴ (FSD), see Equation 5.²⁵

$$n(i) = \frac{d[D_i]}{dt} \sim F_n (1-S)S^{i-1} + (i-1)(1-F_n)(1-S)^2 S^{i-2} \quad (5)$$

Where $[D_i]$ is the concentration of dead polymer chains with chain length i , formed either by termination or chain transfer, F_n the number fraction of chains formed by disproportionation and transfer and S the probability of propagation, see Equation 6.

$$DP_n = \frac{1}{1-S} \quad \text{and} \quad F_n = \frac{k_{tr}[X] + 2k_{td}[R]}{k_{tr}[X] + 2k_{td}[R] + k_{tc}[R]} \quad (6)$$

In Equation 6 k_p, k_{td}, k_{tc} and k_{tr} are the rate coefficients of propagation, termination by disproportionation, termination by combination and transfer respectively, $[M]$ and $[R]$ are the monomer and radical concentration, respectively. The FSD can be converted into a MWD, where f is a scaling factor which is proportionated to the amount of polymer, see Equation 7.

$$w(\log_{10} i) = f \times i^2 n(i) \quad (7)$$

For COBF mediated polymerizations, bimolecular termination is negligible when compared to chain transfer and consequently F_n is approximately 1. The value of S is determined based on the DP_n as obtained from the differentiated MWD plots, see Table 2. The FSD fits of the final MWDs of C014 and C023 are presented in Figures 5 and 6, respectively. Three parameters can be adjusted to fit the multimodal MWD with the FSD: (i) F_n , (ii) the average degree of polymerization of the MWD and (iii) a scaling factor to scale for the amount of polymer. As can be seen in Figures 5 and 6, a good fit of the multimodal MWD can be achieved with the contribution of 4 individual distributions as determined from the derivative of the MWD plot. The used average degrees of polymerization are reported in Table 2.

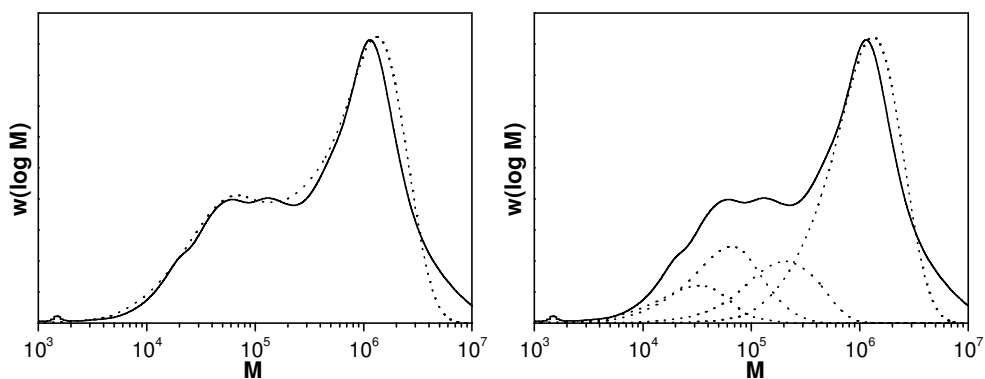


Figure 5. Final molecular weight distributions for the compartmentalization experiment C014, $d_p = 48$ nm, $\bar{n}_{\text{COBF}} = 0.50$ ($x = 0.79$). Molecular weight distribution of C014 (—). Flory fit of the experimentally obtained molecular weight distribution (·····). Used parameters: $F_n = 1$; $DP_n(0) = 6500$, $DP_n(1) = 1030$, $DP_n(2) = 322$ and $DP_n(3) = 163$; $f_0 = 1.3 \cdot 10^{-6}$, $f_1 = 1.9 \cdot 10^{-6}$, $f_2 = 7 \cdot 10^{-6}$ and $f_3 = 7 \cdot 10^{-6}$.

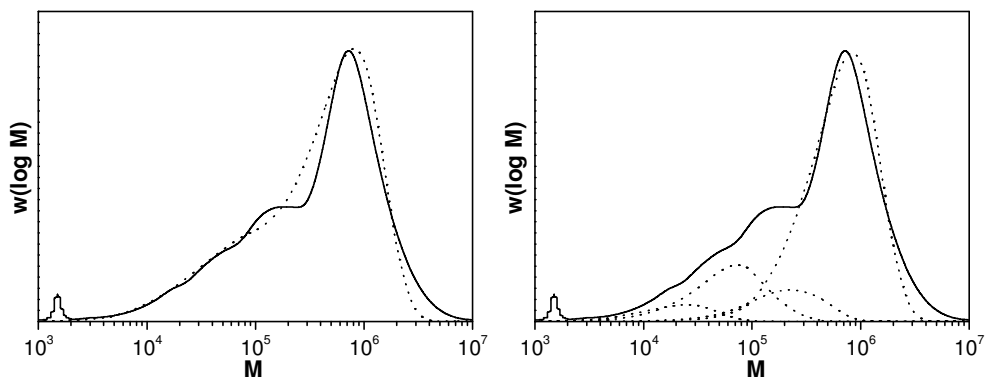


Figure 6. Final molecular weight distributions for the compartmentalization experiment C023, $d_p = 90$ nm, $\bar{n}_{\text{COBF}} = 1.00$ ($x = 0.84$). Molecular weight distribution of C023 (—). Flory fit of the experimentally obtained molecular weight distribution (·····). Used parameters: $F_n = 1$; $DP_n(0) = 3200$, $DP_n(1) = 1120$, $DP_n(2) = 343$ and $DP_n(3) = 159$; $f_0 = 0.5 \cdot 10^{-6}$, $f_1 = 0.25 \cdot 10^{-6}$, $f_2 = 1.3 \cdot 10^{-6}$ and $f_3 = 1.2 \cdot 10^{-6}$.

The evolution of the MWDs for the experiments with $N_{\text{COBF}}/N_p = 50$ and $N_{\text{COBF}}/N_p = 550$ for the 200 nm and 600 nm particles, respectively (C031 and C041) are presented in Figure 7. The 200 nm seed latex has been prepared in a two-step process, where in semi-batch emulsion polymerization a seed latex was grown to the desired particle size of 200 nm. This two-step process is represented in the bimodality of the MWD of S03. The 600 nm seed latex has been prepared in emulsifier-free emulsion polymerization, which resulted in a very broad MWD for this seed latex.

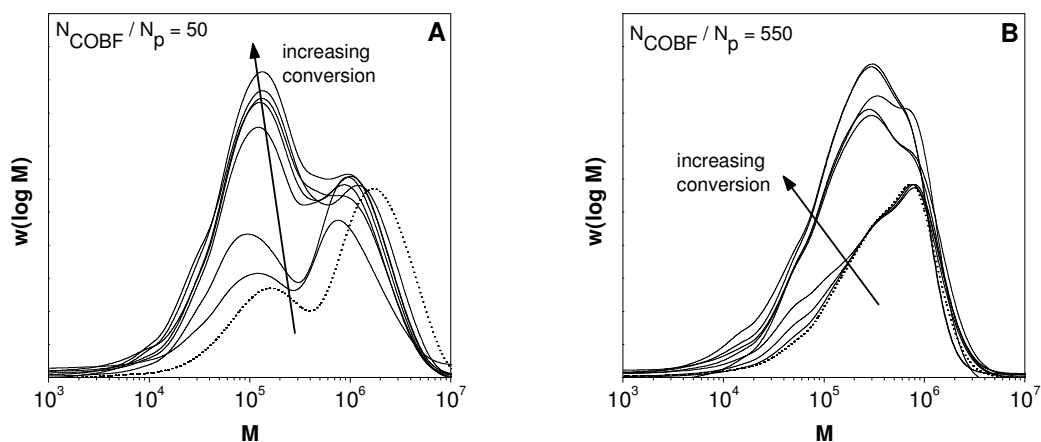


Figure 7. Evolution of the molecular weight distributions for the compartmentalization experiments C031 and C041. Molecular weight distribution of S03 and S04 (.....), Molecular weight distributions of C031 and C041 (—). All the distributions have been scaled to the amount of seed polymer.

As can be seen from Figure 7, in the evolution of the MWD of the experiment with $\bar{n}_{\text{COBF}} = 50$ a large lower molecular weight peak is appearing. However, on closer inspection, two distinct shoulders on the low molecular weight end of this secondary peak can be observed, see Figure 8A. In the evolution of the MWD with $\bar{n}_{\text{COBF}} = 550$ from the initial stages of the polymerization a number of distinct peaks are observed, which is illustrated in Figure 8B. Apparently even at these high numbers of COBF molecules per polymer

particle, still different reaction environments are present within the polymerization system resulting in multimodal molecular weight distributions.

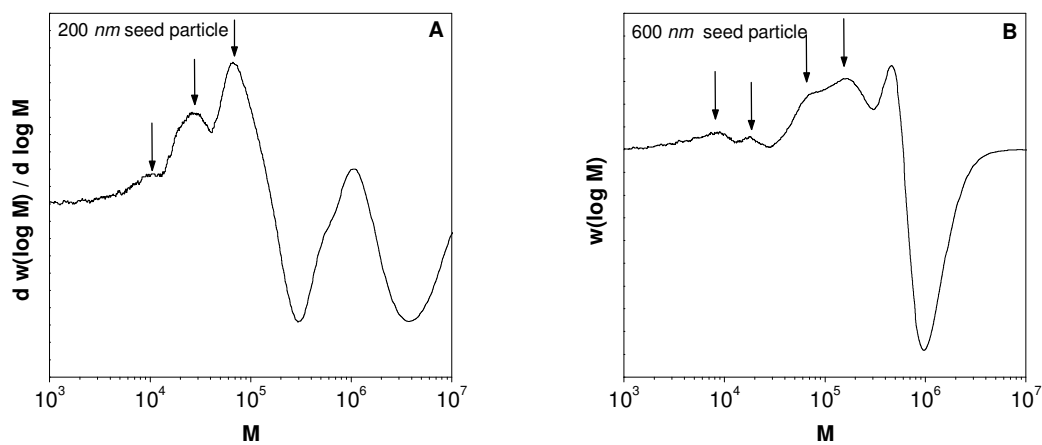


Figure 8. The plot of the differentiated molecular weight distributions ($d(w(\log M))/d(\log M)$). (A) of the molecular weight distributions in Figure 7, 200 nm particles and (B) of the molecular weight distributions in Figure 7, 600 nm particles. The arrows indicate the position of the inflection points of the cumulative MWD.

Since we can determine the position of the different MWDs within the multimodal MWD by means of the differentiated plot of the MWD, we can apply the FSD to fit the experimental MWDs, see Figures 9 and 10. Comparable to the experiments with the 48 and 90 nm seed particles a good fit of the experimental MWDs can be obtained from the FSD. In the case of the 200 nm particles (C031, Figure 7A), the MWD of the seed latex was bimodal. This is represented in the FSD fit with two distributions at $DP_n = 5500$ and 692. The lower molecular weight part of the MWD of the seed latex is not represented in the differentiated MWD plot as it is completely covered by the MWD of the secondary formed polymer. The secondary MWDs are dominated by the distribution at $DP_n = 1500$. The remaining two distributions are represented as shoulders in the multimodal MWD and found at $DP_n = 275$ and 98. Comparable trends are observed for the 600 nm particles (C041, Figure 7B). The secondary MWDs are dominated by the distribution at $DP_n = 1120$, although the remaining distributions are more distinct than is the case in the 200 nm distribution, see Figure 8.

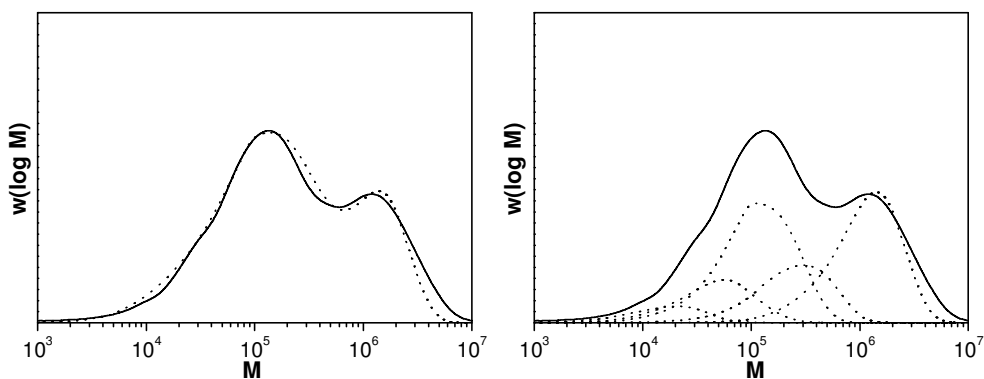


Figure 9. Final molecular weight distributions for the compartmentalization experiment C031, $d_p = 200$ nm, $\bar{n}_{\text{COBF}} = 50$ ($x = 0.90$). Molecular weight distribution of C031 (—). Flory fit of the experimentally obtained molecular weight distribution (·····). Used parameters: $F_n = 1$; $DP_n(0) = 5500$, $DP_n(0) = 1500$, $DP_n(1) = 692$, $DP_n(2) = 275$ and $DP_n(3) = 98$; $f_0 = 0.14 \cdot 10^{-6}$, $f_0 = 0.36 \cdot 10^{-6}$, $f_1 = 1.6 \cdot 10^{-6}$, $f_2 = 1.3 \cdot 10^{-6}$ and $f_3 = 1.5 \cdot 10^{-6}$.

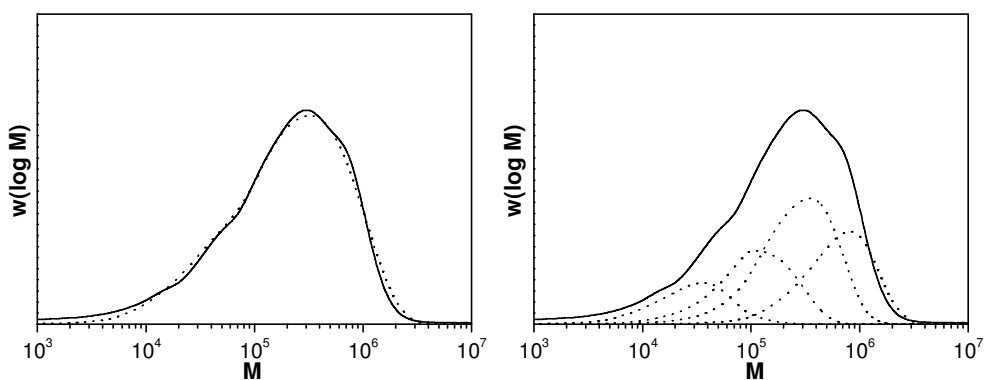


Figure 10. Final molecular weight distributions for the compartmentalization experiment C041, $d_p = 600$ nm, $\bar{n}_{\text{COBF}} = 550$ ($x = 0.87$). Molecular weight distribution of C041 (—). Flory fit of the experimentally obtained molecular weight distribution (·····). Used parameters: $F_n = 1$; $DP_n(0) = 3200$, $DP_n(1) = 1120$, $DP_n(2) = 343$ and $DP_n(3) = 159$; $f_0 = 0.18 \cdot 10^{-6}$, $f_1 = 0.7 \cdot 10^{-6}$, $f_2 = 1 \cdot 10^{-6}$ and $f_3 = 2 \cdot 10^{-6}$.

Evaluation of the experimental results

As is clear from the results presented in the previous section, the MWDs in seeded emulsion polymerization experiments cannot be described adequately by using a global COBF concentration. For proper molecular weight control a COBF molecule has to be able to enter and exit a polymer particle fast enough to prevent the formation of high molecular weight polymer. This implies that a COBF molecule has to enter a polymer particle at a time scale which has to be smaller than that of two consecutive radical entry events. In other words, in a COBF mediated emulsion polymerization it is the entry frequency of COBF molecules that governs the MWD. If the entry frequency of a COBF molecule becomes lower than that of a radical, the MWD is governed by the entry of radicals. If the mobility of COBF is strongly reduced, as might happen for high viscosities of the polymer particles, exchange of COBF between the particles might occur very slowly or even not at all. In the latter scenario the catalytic chain transfer agent might become compartmentalized as entry and exit events are sparsely occurring. The average number of COBF molecules per particle ($= N_{\text{COBF}} / N_p$), which is governed by the polymerization recipe, can be considered as a \bar{n}_{COBF} in these compartmentalized systems. At a certain moment in time a polymer particle can experience an absolute number of COBF molecules, i.e. $n_{\text{COBF}} = 0, 1, 2, 3$ etc. This also implies that at a certain instant in time there are polymer particles present with different numbers of COBF molecules. This results in the formation of a multimodal MWD where each set of polymer particles polymerizing under identical conditions (i.e. $n_{\text{COBF}} = 0, 1, 2, 3\dots$) has an individual contribution to the cumulative MWD. Note that even though the COBF molecules are compartmentalized, entry and exit events of COBF molecules can occur. This implies that multimodal MWDs can be found in every single polymer particle as the number of COBF molecules in a single particle could be changing, however slowly, during the course of the polymerization.

The DP_n of a polymer particle with n COBF molecules can be calculated since a number of compartmentalized COBF molecules can be considered as a concentration within the volume of the polymer particle. This COBF concentration can subsequently be related to

a DP_n using the Mayo equation. Based on the experimentally obtained degrees of polymerization from the FSD fits presented in Figures 5, 6, 9 and 10 a number of COBF molecules per particle can be calculated. The results of these calculations are collected in Figure 11.

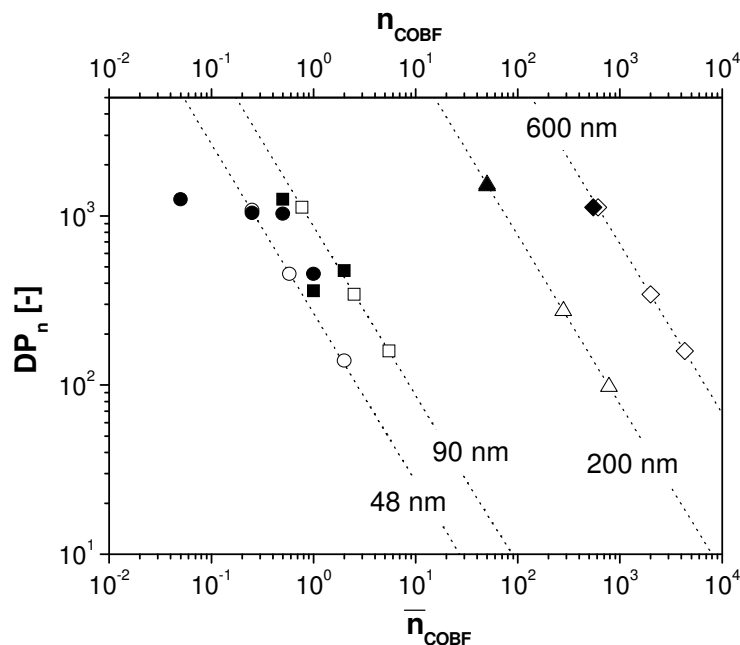


Figure 11. The average degree of polymerization as predicted by the Mayo equation as a function of the absolute number of COBF molecules per particle. Calculated DP_n for n COBF molecules in particles with a radius of 48, 90, 200 and 600 nm (.....). Open symbols: $DP_{n, \text{exp}}$ (Table 4) and the corresponding number of COBF molecules (n_{COBF}) Closed symbols: $DP_{n, \text{exp}}$ of the dominant MWD (Tables 4 and 5) and the average number of COBF molecules per particle (\bar{n}_{COBF}). Experimental observations as reported in Table 4 (○) C012-C015; (□) C022-C024; (△) C031 and (◇) C041.

The area underneath a MWD measured by size exclusion chromatography (SEC) corresponds to a certain mass of polymer. The modelled FSD can be used to determine an equivalent for the amount of polymer corresponding to each individual MWD. The experimentally obtained DP_n of the dominant MWD (i.e. the MWD containing most polymer) can be plotted as a function of \bar{n}_{COBF} , see the closed symbols in Figure 11. The

experimentally obtained DP_n of each individual MWD represented in the derivative of the multimodal MWDs can be related to a concentration of COBF in a particle and consequently in a number of COBF molecules per particle, see the open symbols in Figure 11.

If we accept the notion of a statistical distribution of COBF molecules over the polymer particles, the dominant MWD should originate from the most frequently occurring n_{COBF} . Deviation from the statistical average n_{COBF} results in the formation of secondary MWDs which are lower in intensity. For $\bar{n}_{\text{COBF}} \leq 0.5$ the DP_n of the dominant MWD proves to correspond to the MWD with the highest DP_n in the multimodal MWD. If we assume that the MWD with the highest DP_n in the FSD corresponds to $n_{\text{COBF}} = 1$, then independent of the \bar{n}_{COBF} the majority of the polymer particles will experience 1 COBF molecule over the whole course of the polymerization. The other MWDs in the FSD consequently correspond to $n_{\text{COBF}} = 2, 3, \dots$ which are less likely to occur at such low \bar{n}_{COBF} . No experimental evidence of $n_{\text{COBF}} = 0$ could be obtained as this MWD would be overlapping with the MWD of the seed polymer and therefore could not be distinguished. An attempt was made to determine the pseudo-instantaneous MWDs, however no accurate information could be obtained. For $\bar{n}_{\text{COBF}} \geq 1.0$ the dominant MWD could correspond to $n_{\text{COBF}} = 2$, where the remaining MWDs correspond to $n_{\text{COBF}} = 0, 1, 3, \dots$ which are lower in intensity.

For higher \bar{n}_{COBF} the conditions inside the polymer particles approach pseudo-bulk conditions. At $\bar{n}_{\text{COBF}} = 50$ and 550 the DP_n of the dominant MWD corresponds to the calculated DP_n based on a $n_{\text{COBF}} = 50$ and 550 . Entry and exit of a single COBF molecule will hardly affect the total COBF concentration inside a polymer particle and will consequently hardly affect the DP_n . The DP_n of the remaining MWDs would originate from particles containing significantly higher n_{COBF} .

The multimodal MWDs could not be explained by either the Mayo or a modified Mayo equation for emulsion polymerization, which assume a global concentration of COBF molecules over all the polymer particles (\bar{n}_{COBF}), i.e. negligible resistance to mass transport of COBF. It was postulated that these multimodal MWDs might originate from a statistical distribution of COBF molecules over the particles (n_{COBF}). Polymer particles growing in the presence of 0, 1, 2, ..., n COBF molecules will exhibit MWDs of different average molecular weights, depending on the absolute number of COBF molecules inside the particle. At high instantaneous conversion inside the polymer particles, resistance against COBF exchange could be sufficiently high to result in compartmentalization of the catalytic chain transfer agent.

These observations point in the direction of two limits for catalytic chain transfer in emulsion polymerization. First, at relatively low viscosity of the particles, the particle phase can be regarded as a continuous phase with respect to catalytic chain transfer. Monomodal MWDs are produced with a DP_n which can be predicted by the modified Mayo equation, see Equation 8.

$$DP_n \propto [\text{COBF}]_p \propto \bar{n}_{\text{COBF}} \quad (8)$$

Secondly, at relatively high viscosity of the particles, where a statistical distribution of COBF molecules over the polymer particles is present. The catalytic chain transfer agent becomes compartmentalized, see Equation 9.

$$DP_n \propto [\text{COBF}]_p \propto n_{\text{COBF}} = 0, 1, 2, 3, \dots \quad (9)$$

To the best of the authors knowledge, these results are the first to suggest evidence of compartmentalization in catalytic chain transfer mediated emulsion polymerization.

CONCLUSIONS

The results of this work show that in catalytic chain transfer mediated emulsion polymerization a discrete distribution of COBF molecules over the polymer particles can exist. This is evidence for compartmentalization behaviour of the catalytic chain transfer agent. Catalytic chain transfer seeded emulsion polymerization, with the seed particles swollen to 85% of their maximum saturation swelling, resulted in the formation of multimodal MWDs. The number-average degree of polymerization of the individual MWD of the second-stage polymer, as determined from the differentiated MWDs, proved to be qualitatively identical for different \bar{n}_{COBF} for a certain seed particle size. The amount of polymer contributing to each individual MWD proved to vary with \bar{n}_{COBF} . For large seed particles (i.e. 200 and 600 nm) comparable observations were made. These experimental observations suggest that there are comparable reaction environments within the polymerization systems, independent of \bar{n}_{COBF} , that result in the formation of the multimodal MWDs. The obtained multimodal MWDs could be modelled successfully using a Flory-Schulz approach. In catalytic chain transfer mediated emulsion polymerization two limits seem to exist. One at relatively low particle viscosity where the MWD is governed by a global COBF concentration (\bar{n}_{COBF}) and one at relatively high particle viscosity where the MWD is governed by a discrete COBF distribution over the polymer particles (n_{COBF}).

EXPERIMENTAL SECTION

Materials

The bis(methanol) complex of COBF was prepared as described previously.^{26,27} For all experiments, a single batch of catalyst was used. The intrinsic activity of the catalyst was determined by measuring the chain transfer constant in bulk polymerization of methyl methacrylate (MMA) at 60°C: $C_T = 30 \cdot 10^3$. Methyl methacrylate (MMA) (Aldrich, 99%) was purified by passing it over a column of activated basic alumina (Aldrich). Sodium bicarbonate (SBC) (Fluka, >99%), sodium dodecyl sulphate (SDS) (Fluka, 99%),

potassium persulphate (KPS) (Aldrich >98%) and 2,2'-azobis[N-(2-carboxylethyl)-2-methylpropionamide]hydrate (VA-057, Wako) were used as received. Distilled deionised water was used throughout this work. Seed latexes were prepared in a 1.2 dm³ Mettler Toledo RC1e reaction calorimeter equipped with an anchor impellor, calibration heater, T_r sensor and sample loop. The reactor was operated in isothermal mode.

Seed latex preparation

SDS (if required) and SBC were dissolved in distilled deionized water and charged into the reactor. The monomer, MMA, was added subsequently and the resulting emulsion was purged with nitrogen for an hour while the reactor was heated to the reaction temperature of 70°C. Subsequently, KPS dissolved in a minimal amount of water, was purged with nitrogen and added pseudo-instantaneously to the reactor. After one hour of polymerization the reactor temperature was raised to 90°C to enhance the initiator decomposition. The final emulsion was left stirring for another 5 hours, after which less than 0.5% of the initiator should remain. Finally the seed latex was dialyzed against distilled deionized water for two weeks, changing the water twice a day. The exact recipes for the different seed latexes are reported in Table 3.

Table 3. Experimental conditions for the preparation of the seed latexes.

	<i>MMA</i>	<i>Water</i>	<i>SDS</i>	<i>SBC</i>	<i>KPS</i>
	[g]	[g]	[g]	[g]	[g]
S01	240	720	11.0	0.74	0.58
S02	84.5	520	0.62	0.52	0.44
S03 a	188	541	0.64	0.53	0.38
S04	65.0	600	-	-	0.33

^a The recipe shown in this table corresponds to the initial seed latex which was subsequently grown to the desired size of 200 nm.

In the case of seed latex S03, the seed latex from the general procedure using the recipe as shown in Table 3 was further grown by the following procedure. In a consecutive step the seed latex (100 g), distilled deionized water (500 g), SDS (1.24 g; 4.3·10⁻³ mol) and

MMA (42.6 g; 0.42 mol) were charged into the reactor. After swelling and purging for one hour, KPS (0.25 g; $9.2 \cdot 10^{-4}$ mol), dissolved in a minimal amount of water, was purged with nitrogen was added instantaneously to the reactor. A monomer side feed of $0.278 \text{ g} \cdot \text{min}^{-1}$ was used to reach a final particle size of 200 nm. The properties of the dialyzed latex are reported in Table 4.

Table 4. Properties of the pMMA seed latexes

	PSD			MWD		
	x	$d_p(V)$	N_p	$poly$	M_n	PDI
	[-]	[nm]	[dm_w^{-3}]	[-]	[$g \cdot mol^{-1}$]	[-]
S01	0.96	48	$3.3 \cdot 10^{18}$	0.069	$7.7 \cdot 10^5$	2.8
S02	0.92	90	$7.3 \cdot 10^{17}$	0.002	$3.0 \cdot 10^5$	2.3
S03 ^a	0.98	204	$1.1 \cdot 10^{16}$	0.029	$2.8 \cdot 10^5$	3.7
S04 ^b	0.82	619	$6.2 \cdot 10^{14}$	0.093	$6.0 \cdot 10^4$	6.9

^a Bimodal molecular weight distribution with a main distribution at $1.7 \cdot 10^6 \text{ g} \cdot \text{mol}^{-1}$ and a secondary distribution at $1.5 \cdot 10^5 \text{ g} \cdot \text{mol}^{-1}$

^b Strong tail towards the low molecular weight end of the distribution

Seeded emulsion polymerization

SDS and SBC were dissolved in distilled deionized water and charged into a three-necked round bottom flask. Seed latex and MMA were added subsequently and the latex was left stirring overnight to allow sufficient swelling of the polymer particles with monomer. After swelling, the latex was purged with nitrogen for an hour and heated to the reaction temperature of 70°C. A stock solution of COBF in MMA was prepared prior to the experiments. An accurate amount of COBF was placed inside a schlenk tube and deoxygenated by a repeated vacuum-nitrogen cycle. MMA was deoxygenated by purging with nitrogen prior to use and subsequently added to the COBF catalyst. The required amount of the stock solution was added to the swollen seed latex. The same stock solution was used throughout a series of experiments (C01, C02, C03 and C04). The initiator, VA-057 (0.030 g ; $9.3 \cdot 10^{-2} \text{ mmol}$), was dissolved in a minimal amount of distilled deionized water (typically 1 mL), purged with nitrogen and added pseudo-

instantaneously to the round bottom flask. Samples were withdrawn periodically for further analysis. The recipes for the seeded emulsion polymerizations are collected in Table 5.

Table 5. Experimental conditions for the compartmentalization experiments.

	<i>Seed</i> [#]	<i>Seed</i> [g]	<i>MMA</i> [g]	<i>Water</i> [g]	<i>SDS</i> [g]	<i>SBC</i> [g]	<i>COBF</i> [mg]
C011	S01	24.0	6.0	20.0	0.086	0.020	0.0
C012	S01	24.0	6.0	20.0	0.086	0.020	0.029
C013	S01	24.0	6.0	20.0	0.086	0.020	0.143
C014	S01	24.0	6.0	20.0	0.086	0.020	0.286
C015	S01	24.0	6.0	20.0	0.086	0.020	0.572
C021	S02	35.4	6.2	11.0	0.090	0.010	0.0
C022	S02	35.4	6.2	11.0	0.090	0.010	0.093
C023	S02	35.4	6.2	11.0	0.090	0.010	0.185
C024	S02	35.4	6.2	11.0	0.090	0.010	0.370
C031	S03	29.0	6.9	23.0	0.10	0.020	0.118
C041	S04	40.0	4.8	0.0	0.080	0.020	0.114

REFERENCES AND NOTES

1. Zetterlund, P.B. Okubo, M. *Macromolecules* 2006, 39, 8959.
2. Kagawa, Y.; Zetterlund, P.G.; Minami, H.; Okubo, M. *Macromol. Theory Simul.* 2006, 15, 608.
3. Chern, C-S. in *Principles and applications of emulsion polymerization*. Ed. Chern, C-S., Wiley, 2008.
4. Gilbert, R.G. in *Emulsion polymerization: A mechanistic approach*. Ed. Gilbert, R.G., Academic Press, 1995.
5. Cunningham, M.F. *Prog. Polym. Sci.* 2008, 33, 365.
6. Moad, G.; Rizzardo, E.; Thang, S.H. *Acc. Chem. Res.* 2008, 41, 1133.
7. Zetterlund, P.B.; Kagawa, Y.; Okubo, Y. *Chem. Rev.* 2008, 108, 3747.
8. Braunecker, W.A.; Matyjaszewski, K. *Prog. Polym. Sci.* 2007, 32, 93.

9. Maehata, H.; Liu, X.; Cunningham, M.F. *Macromol. Rapid Comm.* 2008, 29, 479.
10. Zetterlund, P.B.; Okubo, M. *Macromol Theory Sim.* 2008, 16, 221.
11. Simms, R.W.; Cunningham, M.F. *Macromolecules* 2008, 41, 5148.
12. Enikolopyan, N. S.; Smirnov, B. R.; Ponomarev, G. V.; Belgovskii, I. M. *J. Polym. Sci. Part A: Polym. Chem.* 1981, 19, 879.
13. Gridnev, A. *J Polym. Sci. Part A: Polym. Chem.* 2000, 38, 1753.
14. Gridnev, A. A.; Ittel, S. D. *Chem. Rev.* 2001, 101, 3611.
15. Heuts, J. P. A.; Roberts, G. E.; Biasutti, J. D. *Aust. J. Chem.* 2002, 55, 381.
16. Karmilova, L.V.; Ponomarev, G.V.; Smirnov, B.R.; Belgovskii, I.M. *Russ. Chem. Rev.* 1984, 53, 132.
17. Davis, T.P.; Haddleton, D.M.; Richards, S.N. *J. Macromol. Sci., Rev. Macromol. Chem.* 1994, C34, 234.
18. Davis, T.P.; Kukulj, D.; Haddleton, D.M.; Maloney, D.R. *Trends Polym. Sci.* 1995, 3, 365.
19. Mayo, F.R. *J. Am. Chem. Soc.* 1943, 65, 2324.
20. Smeets, N.M.B.; Heuts, J.P.A.; Meuldijk, J.; van Herk, A.M. *J. Polym. Sci. Part A: Polym. Chem.* 2008, 46, 5839.
21. Vanzo, E. ; Marchessault, R.H. ; Stannett, V. J. *Colloid. Sci.* 1965, 20, 62.
22. Smeets, N.M.B. ; Meda, U.S. ; Heuts, J.P.A.; Keurentjes, J.T.F.; van Herk, A.M. ; Meuldijk, J. *Macromol. Symp.* 2007, 259, 406.
23. Kukulj, D.; Davis, T.P.; Suddaby, K.G.; Haddleton, D.M.; Gilbert, R.G. *J Polym Sci Part A: Polym Chem* 1997, 35, 859.
24. Flory, P.J. *Principles of Polymer Chemistry* 1st Ed, 1953 Cornell University Press, Ithica NY
25. Russell, G.T. *Aust. J. Chem.* 2002, 55, 399.
26. Bakač, A.; Brynildson, M. E.; Espenson, J. H. *Inorg Chem* 1986, 25, 4108.
27. Suddaby, K.G.; Haddleton, D.M.; Hastings, J.J.; Richards, S.N.; O'Donnell, J.P. *Macromolecules* 1996, 29, 8083.

The Effect of Co(II) Mediated Catalytic Chain Transfer on the Emulsion Polymerization Kinetics of Methyl Methacrylate.

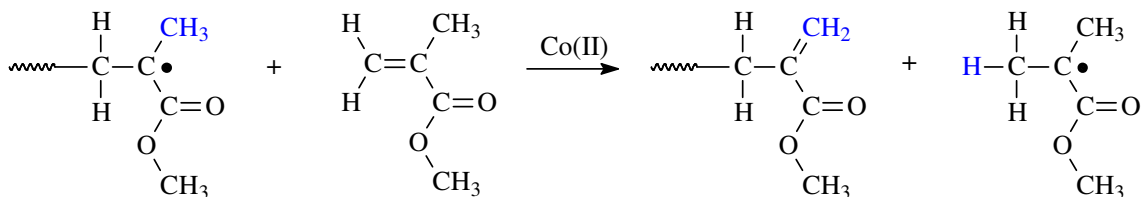
ABSTRACT

The effect the catalytic chain transfer agent, bis[(difluoroboryl) dimethylglyoximato] cobalt(II) (COBF), on the course of the *ab initio* emulsion polymerization of methyl methacrylate and the product properties in terms of the molecular weight distribution were investigated. The emulsion polymerization kinetics have been studied with varying surfactant, initiator and COBF concentrations. The experimentally determined average number of radicals per particle strongly depends on the concentration of COBF and proves to be in good agreement with the results of model calculations. The apparent chain transfer constant, determined up to high conversion, is in excellent agreement with the predicted value based on a mathematical model based on COBF partitioning and the Mayo equation.

The results of this work enhance the fundamental understanding of the influence a catalytic chain transfer agent has on the course of the emulsion polymerization and the control of the molecular weight distribution.

INTRODUCTION

The molecular weight distribution is one of the key properties of a polymer latex governing the final application of the polymer product.¹ Since its discovery in the early 1980's, catalytic chain transfer (CCT) has demonstrated to be a versatile method for efficient molecular weight control.²⁻⁸ In catalytic chain transfer mediated polymerizations, the radical activity is transferred from a propagating radical to a monomer molecule, yielding a dead polymer chain with a vinyl end-group functionality and a monomeric radical, see Scheme 1. In the first step, the active Co(II) complex abstracts a hydrogen atom from the propagating polymer chain, resulting in a dead polymer chain and a Co(III)-H complex. Subsequently, the hydrogen atom is transferred from the Co(III)-H complex to a monomer molecule, regenerating the active Co(II) complex and yielding a monomeric radical capable of propagation.



Scheme 1. The overall reaction of catalytic chain transfer to monomer.

Comparable to the situation where conventional chain transfer agents are used in bulk and solution polymerization, in catalytic chain transfer no net loss of radicals and consequently no decrease in the rate of polymerization are expected. However, in catalytic chain transfer mediated emulsion polymerizations, the rate of polymerization is affected by the presence of a catalytic chain transfer agent (CCTA).⁹⁻¹⁴ Previously it was found that the presence of a catalytic chain transfer agent affects the course of the emulsion polymerization.^{11,14} In conventional chain transfer the rate of polymerization may decrease, due to desorption of chain transfer agent derived radicals from the particles.¹⁵⁻¹⁷ In catalytic chain transfer the catalytic chain transfer agent partitions between the aqueous phase, monomer droplets and polymer particles.¹⁸ This partitioning was suggested to result in a decrease in the rate of entry of oligomeric radicals from the aqueous phase, whereas presence of the CCTA in the polymer particles was suggested to

result in an increase in the rate of exit of monomeric radicals arising from transfer. Both effects would contribute to a significantly lower average number of radicals per particle (\bar{n}) and this should have a strong effect on the rate of polymerization. To the best of our knowledge, the influence of various parameters on the emulsion polymerization kinetics has not been studied in detail.

In the present chapter we will present a detailed study of the effect of a commonly used and fairly water soluble ($m_{Co} = \frac{[Co]_M}{[Co]_W} = 0.72 \text{ dm}_W^3 \cdot \text{dm}_M^{-3}$)¹⁹ CCTA, bis[(difluoroboryl)dimethylglyoximato]cobalt(II) (COBF) on the *ab initio* emulsion polymerization of methyl methacrylate. A fairly water soluble catalyst was selected to clearly and explicitly study both the aqueous phase as well as polymer particle phase effects on the course of the emulsion polymerization. The influence of the catalytic chain transfer agent, surfactant and initiator concentration on the rate of polymerization, the particle concentration and the number-average degree of polymerization have been investigated.

RESULTS AND DISCUSSION

Theoretical evaluation of the emulsion polymerization kinetics

The effect of COBF on the course of the emulsion polymerization should be evident from an evaluation of the number of particles (N_p) and the average number of radicals per particle (\bar{n}). The effect of a CCTA on N_p can be obtained directly from particle size analysis, whereas the effect of a CCTA on \bar{n} can be evaluated from an experimental analysis as well as a the solution of the radical population balance over the polymer particles.²⁰⁻²³ Experimentally observed values of R_p and N_p allow the calculation of the average number of radicals per particle (\bar{n}_{obsd}), see Equation 1.

$$\bar{n}_{\text{obsd}} = \frac{R_p N_A}{k_p [M]_p N_p} \quad (1)$$

where k_p is the long chain propagation rate coefficient, $[M]_p$ the monomer concentration inside the polymer particles and N_A Avogadro's number. The rate of polymerization can be determined from the slope of the conversion-time curve for a batch emulsion polymerization in interval II (dx/dt) and the initial monomer concentration per unit volume of water ($[M]_0$), see Equation 2.

$$R_p = [M]_0 \frac{dx}{dt} = k_p [M]_p \frac{\bar{n} N_p}{N_A} \quad (2)$$

The average number of radicals per particle (\bar{n}_{theo}) can also be calculated from the solution a radical population balance over the polymer particles. The general solution for \bar{n} , as reported by Stockmayer²⁰ and O'Toole,²¹ has to be solved simultaneously with the steady state radical balance in the aqueous phase.^{22,23} When aqueous phase termination is not significant, the desorption of chain-transferred radicals from a polymer particle and the entry of radicals into the polymer particles are balanced.²⁴⁻²⁶ The measure of the degree of aqueous phase termination is captured in a dimensionless parameter Y , which in the case of no aqueous phase termination gives $Y = 0$, see Equation 3.

$$Y = \frac{2N_p k_{t,w} k_{t,p}}{k_c^2 V_p N_A^2} \quad (3)$$

In this equation $k_{t,w}$, $k_{t,p}$ and k_c are the rate coefficients of bimolecular termination in the aqueous phase, bimolecular termination in the polymer particle phase and of capture of free radicals by the polymer particles, respectively. V_p is the volume of a polymer particle. A semi-empirical expression for the steady state \bar{n}_{theo} was proposed is given by Equation 4¹⁷ and provides an approximate relation between \bar{n}_{theo} and the rate constant of radical desorption (k_{dM}).

$$\bar{n}_{theo} = \frac{1}{2} \left\{ \left[\left(\alpha'_w + \frac{\alpha'_w}{m} \right)^2 + \left(\alpha'_w + \frac{\alpha'_w}{m} \right) \right]^{1/2} - \left(\alpha'_w + \frac{\alpha'_w}{m} \right) \right\} + \left(\frac{1}{4} + \frac{\alpha'_w}{2} \right)^{1/2} - \frac{1}{2} \quad (4)$$

In this equation α'_w is the ratio of radical production and bimolecular termination in the polymer particles and m the ratio of radical desorption and radical termination, see Equation 5.

$$\alpha'_w = \frac{\rho_i V_p}{\left(\frac{k_{t,p}}{N_A} \right) N_p} \quad \text{and} \quad m = \frac{k_{dM} V_p}{\left(\frac{k_{t,p}}{N_A} \right)} \quad (5)$$

In this equation ρ_i is the rate of radical production in the aqueous phase ($= 2fk_d[I]N_A$) and k_{dM} is the rate constant for radical desorption from the polymer particles given by Equation 6.

$$k_{dM} = \frac{12D_w \delta}{m_d d_p^2} C_T \quad (6)$$

where C_T is the chain transfer constant (i.e. $C_T = \frac{k_{tr}}{k_p}$, where k_{tr} is the rate coefficient of chain transfer), m_d the partition coefficient of a methyl methacrylate radical ($= [M]_p / [M]_{aq}$), D_w is the diffusion coefficient of a MMA radical in the aqueous phase, d_p the diameter of a polymer particle and δ the ratio of the water-side mass transfer resistance and the overall mass transfer resistance for a radical desorbed from the polymer particles, see Equation 7. In the presence of COBF the value for C_T is $15 \cdot 10^3$,¹⁸ without COBF C_T is 10^{-5} .²⁷

$$\delta = \left(1 + \frac{D_w}{m_d D_p} \right)^{-1} \quad \text{with} \quad D_p = \frac{k_B T}{3\pi\eta_0 d_p} \quad (7)$$

where k_B , T , η_0 and D_p are the Boltzmann constant, the reaction temperature, the viscosity inside a polymer particle and the diffusion coefficient of a monomeric radical in a polymer particle, respectively. The numerical values of the used constants are collected in Table 1.

Table 1. Numerical values of constants used in the calculation of \bar{n}_{theo} .

<i>Constant</i>	<i>Unit</i>	<i>Value</i>	<i>Ref</i>
k_p	$dm^3 mol^{-1} s^{-1}$	$1.0 \cdot 10^3$	28
k_t	$dm^3 mol^{-1} s^{-1}$	$1.0 \cdot 10^7$	-
k_d	s^{-1}	$1.22 \cdot 10^{-4}$	29
k_{tr} (MMA)	$dm^3 mol^{-1} s^{-1}$	10^{-2}	18
k_{tr} (COBF)	$dm^3 mol^{-1} s^{-1}$	$1.5 \cdot 10^7$	27
$[M]_p$ ^a	$mol dm_p^{-3}$	6.6	31
$[M]_{aq}$ ^a	$mol dm_w^{-3}$	0.15	31
m_d	$dm_w^3 dm_p^{-3}$	44	-
D_w	$dm^2 s^{-1}$	$1.5 \cdot 10^{-7}$	17
η_0	$kg m s^{-1}$	$1.58 \cdot 10^{-2}$	32

^a The reported values of $[M]_p$ and $[M]_{aq}$ are only valid at saturation swelling of the polymer particles.

Effect of the surfactant and initiator concentration with and without COBF

In conventional emulsion polymerization with full colloidal stability, the effect of the surfactant and initiator concentration on the rate of polymerization and the particle number are given by a simple scaling law, i.e. $R_p \sim N_p \propto [S]^\alpha \cdot [I]^{1-\alpha}$.³⁴ The addition of a CCTA affects the rate of polymerization⁹⁻¹⁴ and might affect the scaling laws applicable for conventional emulsion polymerization.

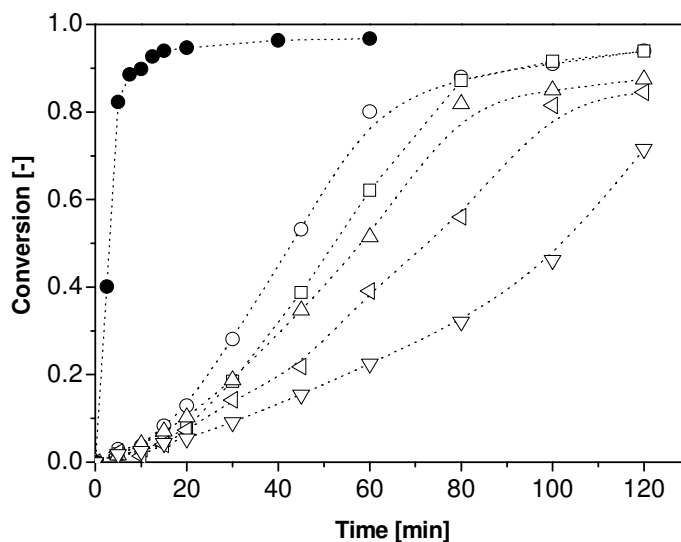


Figure 1. Conversion time histories for the *ab initio* batch emulsion polymerizations with a varying amount of surfactant (run 01 and 06-10, Table 3). ● [SDS] = 10^{-1} M, no COBF; ○ [SDS] = 10^{-1} M, COBF; □ [SDS] = $5 \cdot 10^{-2}$ M; COBF △ [SDS] = $2.5 \cdot 10^{-2}$ M; COBF ▽ [SDS] = 10^{-2} , COBF ▽ [SDS] = $5 \cdot 10^{-3}$ M, COBF. Reaction conditions: T = 70°C, [V50] = 10^{-3} M and [COBF] = 5.0 ppm (5.0 mol of COBF per 10^6 mol of MMA).

The effect of COBF on the course of the emulsion polymerization is presented in Figure 1. There are two observations that can be made from Figure 1. First that the polymerization without COBF reaches nearly complete conversion within 20 minutes, whereas in the presence of 5.0 ppm COBF, and the same surfactant concentration, significantly longer polymerization times are required. Secondly that a higher surfactant concentration increases the rate of polymerization. First the difference in the rate of

polymerization will be addressed. The nucleation stage of the emulsion polymerization in the presence of COBF is prolonged and the rate of polymerization in interval II is significantly reduced as compared with the COBF free experiment. The prolonged nucleation stage and the reduced rate of polymerization can be assigned to the presence of COBF in the aqueous phase and in the polymer particles. The presence of COBF in the aqueous phase can affect the rate of entry whereas presence in the polymer particles can affect the rate of radical desorption. To summarize, the effect a catalytic chain transfer agent has on the course of the emulsion polymerization depends on the partitioning behavior. In the case of COBF in MMA emulsion polymerization the partitioning was determined at $0.72 \text{ dm}_w^3 \cdot \text{dm}_M^{-3}$,¹⁹ which is in good agreement with previously reported values for this system.^{11,14} For the emulsion polymerization recipe used throughout this work ($\beta = \frac{V_M}{V_W} = 0.185$; solids content is 15 w%) this results in a situation where 88% of the total absolute amount of COBF is present in the aqueous phase, independent of the amount of catalytic chain transfer agent added. The absolute amount of COBF in the aqueous phase can be controlled to some extent by changing the phase ratio (β).¹⁸ However, even when a high solids content emulsion recipe is considered (e.g. $\beta = 1.0$; solids content is 50 w%) 58% of the absolute amount of COBF is present in the aqueous phase.

The activity of a (catalytic) chain transfer agent is typically expressed as the chain transfer constant (C_T). The C_T constant for COBF in MMA polymerizations in aqueous environment has not been determined. However, the presence of hydroxyl groups in solution polymerization proved to have a significant influence on the chain transfer constant and the structure of the cobalt complex.³⁵ When compared to the value determined in bulk polymerization, the chain transfer constant was found to be reduced by 50% when hydroxyl groups are present in the reaction medium.¹⁸ Assuming an aqueous phase chain transfer constant of $15 \cdot 10^3$ for further calculations, it is possible to estimate the instantaneous degree of polymerization in the aqueous phase ($DP_{n,w}$) as well as the polymer particle phase ($DP_{n,p}$), see Table 2. Equations 8 and 9 are used to estimate

the instantaneous degree of polymerization in the aqueous and polymer particle phase respectively. Equation 8 is derived from the Mayo equation incorporating catalytic chain transfer agent partitioning.¹⁸ The polymer chains formed in the aqueous phase are very short, which violates the long-chain approximation used to derive the Mayo equation. Gridnev and co-workers have shown that a modified Mayo equation, assuming that chains shorter than 2 units will not be produced, is more appropriate under these conditions.^{4,36} At the high catalytic chain transfer agent concentrations required for the production of short oligomers, a substantial amount of monomeric radicals will be converted back to monomer before a second monomer addition can occur. Pierik et al estimated that as much as 28% of the monomer consumption is caused by the re-initiation of monomer.³⁷ In the current definition of $DP_{n,w}$ we define a polymer chain as a molecule containing at least two monomer units. Equation 9 is derived from the relation reported by Gridnev and co-workers, incorporating catalytic chain transfer agent partitioning. The derivation is similar to that reported elsewhere.¹⁸

$$DP_{n,p} = \frac{V_M[M]_p}{C_T} \frac{1}{N_{Co,0}} \left(\frac{m_{Co}\beta + 1}{m_{Co}(\beta + 1)} \right) \left(1 + \frac{1}{\beta} \right) \quad (8)$$

$$DP_{n,w} = 2 + \frac{V_M[M]_w}{C_T} \frac{1}{N_{Co,0}} \left(\frac{\beta + 1}{m_{Co}\beta + 1} \right) \left(1 + \frac{1}{\beta} \right) \quad (9)$$

where $[M]_w$ and $[M]_p$ are the concentration of monomer in the aqueous and particle phase, respectively.

Both the instantaneous degree of polymerization in the aqueous phase and in the polymer particle phase are only marginally affected by the increase in solids content. An increase of 60% in $DP_{n,p}$ and 22% in $DP_{n,w}$ are calculated for a 10-fold increase of the solids content. In conclusion it is evident that, independent of the choice of solids content, a significant amount of COBF will be present in the aqueous phase and this may affect the aqueous phase kinetics.

Table 2. The instantaneous degree of polymerization in the aqueous and polymer particle phase at low conversion.

β [$dm_M^3 \cdot dm_W^{-3}$]	Solids content [w%]	Aq. phase [%]	Particle phase [%]	$DP_{n,w}$ [-]	$DP_{n,p}$ [-]
0.10	9.1	93	7	3.2	105
0.15	18.5	88	12	3.3	111
0.50	33.3	74	26	3.5	133
1.00	50.0	58	42	3.9	168

Calculations with Equations 8 and 9 are based on a water volume of $0.40 dm^3$, $5.0 ppm$ COBF, $m_{Co} = 0.72 dm_W^3 \cdot dm_M^{-3}$, $C_T = 15 \cdot 10^3$ and $[M]_p = 9.4 mol dm_p^{-3}$.

The increase in the solids content results in an increase in $DP_{n,p}$, which is counter-intuitive. This is a consequence of the fact that for the illustrative calculations a constant aqueous phase volume was assumed. The volume of the monomer phase was adjusted to obtain the desired phase ratios. Even though more COBF is partitioning towards the polymer particles, the ratio of COBF to monomer is continuously increasing, which consequently increases $DP_{n,p}$. The Mayo equation predicts that the presence of COBF inside the polymer particles results in lower values of DP_n as compared to COBF free emulsion polymerization.¹⁸ For all the *ab initio* experiments performed with $5.0 ppm$ of COBF described in this work a number-average degree of polymerization of 200 was obtained from the final molecular weight distribution. The reduction in the number-average degree of polymerization has a plasticizing effect and reduces the increase in the viscosity inside the polymer particles during the polymerization compared to the experiment without COBF. The gel effect which, depending on the solids content, typically occurs at higher conversions in emulsion polymerization, is expected to be suppressed in the presence of a catalytic chain transfer agent. The reduction in the degree of polymerization was only found to be sufficient to suppress the gel effect for low degrees of polymerization.¹³ For intermediate degrees of polymerization a gel effect is often still present. The gel effect has two implications for the polymerization. First, the

increasing viscosity limits the mobility of the catalytic chain transfer agent inside the polymer particles and results in an increase in the instantaneous degree of polymerization. Secondly, the increasing viscosity can also limit the entry and exit of COBF molecules into the polymer particles, resulting in poor control of the molecular weight distribution. Figure 1 shows the effect of the surfactant concentration on the course of the polymerization in the presence of COBF. As the surfactant concentration increases, more polymer particles are formed, resulting in higher rates of polymerization, see Equation 2. This can also be observed from Figure 2, where the heat production rate histories, for the conversion time profiles reported in Figure 1, are collected. The heat rate production time histories in the presence of COBF display a higher heat production rate (Q_r) at higher surfactant concentrations and a sharp increase towards the end of the polymerization independent of the surfactant concentration, see Figure 2.

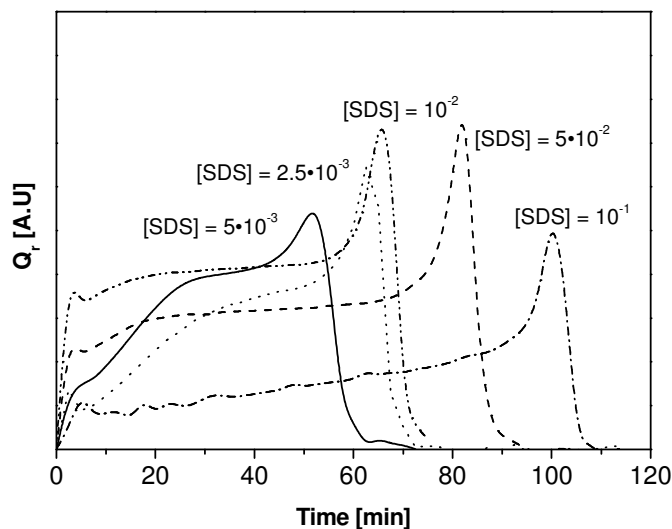


Figure 2. The heat production rate time histories in the presence of COBF obtained from *ab-initio* emulsion polymerization with various surfactant concentrations (run 06-10, Table 2). (— · — · —) [SDS] = 10^{-1} M; (— · · — · ·) [SDS] = $5 \cdot 10^{-2}$ M; (·····) [SDS] = 10^{-2} M; (— — —) [SDS] = $2.5 \cdot 10^{-3}$ M; (—) [SDS] = $5 \cdot 10^{-3}$ M. Conversion-time histories presented in Figure 1.

Further insight in the effect of the surfactant and initiator concentration on the rate of polymerization (R_p) and final particle number (N_p) for an *ab initio* emulsion polymerization with and without COBF is obtained by constructing a log-log plots of either R_p or N_p and [SDS] or [V50], see Figures 3 and 4. In the case of the methyl methacrylate emulsion polymerization with SDS as surfactant and V50 as initiator the relationship of R_p was estimated to be $R_p \propto [\text{SDS}]^{0.8}$ and $R_p \propto [\text{V50}]^{0.6}$. With COBF is the absolute value of R_p changes, but the general trend is apparently not affected, $R_p \propto [\text{SDS}]^{0.5}$ and $R_p \propto [\text{V50}]^{0.6}$. For N_p the dependency of the surfactant and initiator concentration in the presence and absence of COBF was found to be $N_p \propto [\text{SDS}]^{1.3}$ and $N_p \propto [\text{V50}]^{0.3}$. The dependencies found here illustrate that the influence of the surfactant and initiator concentration on the R_p and N_p and that the general trends in the presence and absence of COBF are comparable.

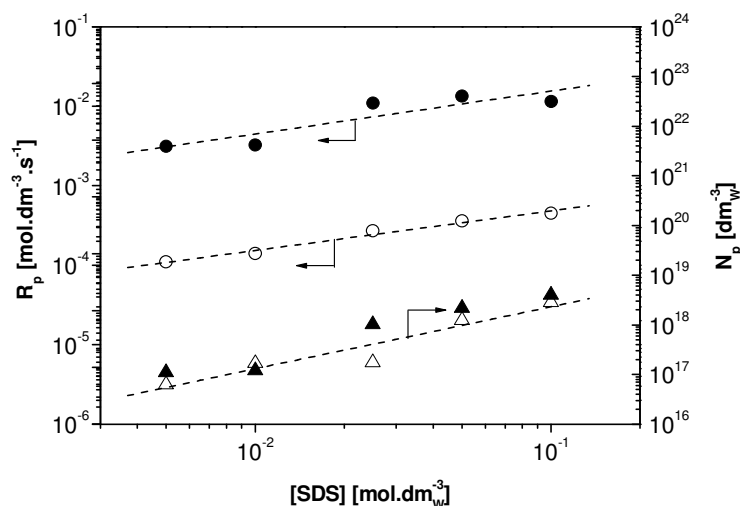


Figure 3. Rate of polymerization and final particle number as a function of the surfactant concentration (runs 01-10, Table 3). [V50] = 10^{-3} M; [COBF] = 5.0 ppm ● Rate of polymerization without COBF, slope = 0.8; ○ Rate of polymerization with COBF, slope = 0.5; ▲ Particle number without COBF, slope = 1.3; △ Particle number with COBF, slope = 1.3.

The results in Figure 3 demonstrate that when the surfactant concentration in the aqueous phase is varied over a range $5 \cdot 10^{-3} \leq [\text{SDS}] \leq 10^{-1}$ M for [V50] = 10^{-3} M, no significant

change in the absolute value of the particle number is observed in whether COBF is present or not. The results collected in Figure 4 show that when the amount of initiator is varied over a range $10^{-4} \leq [V50] \leq 10^{-2} M$ at an $[SDS] = 5 \cdot 10^{-2} M$, the particle number in the presence of COBF are generally lower than in the absence of COBF. The presence of COBF affects the aqueous phase kinetics and consequently the nucleation phase of an emulsion polymerization. The smaller rate of entry results in a longer nucleation period and consequently a shift to larger polymer particles and a broader distribution. The presence of COBF inside the polymer particles also affects the rate of polymerization due to the loss of monomeric radicals to the aqueous phase.

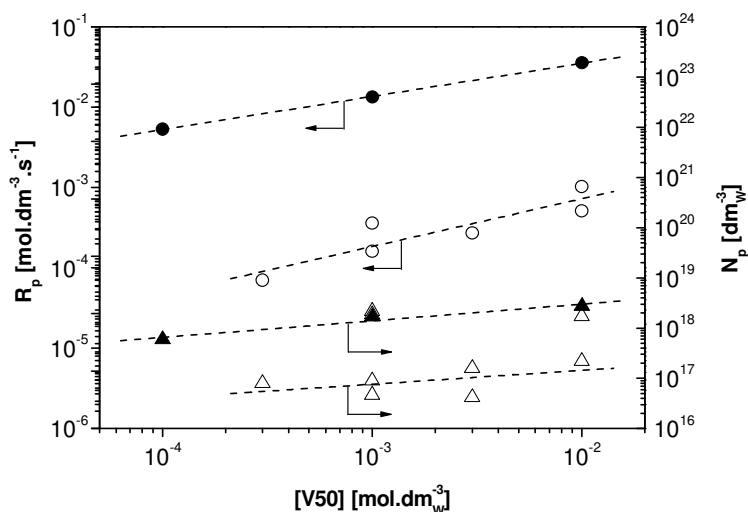
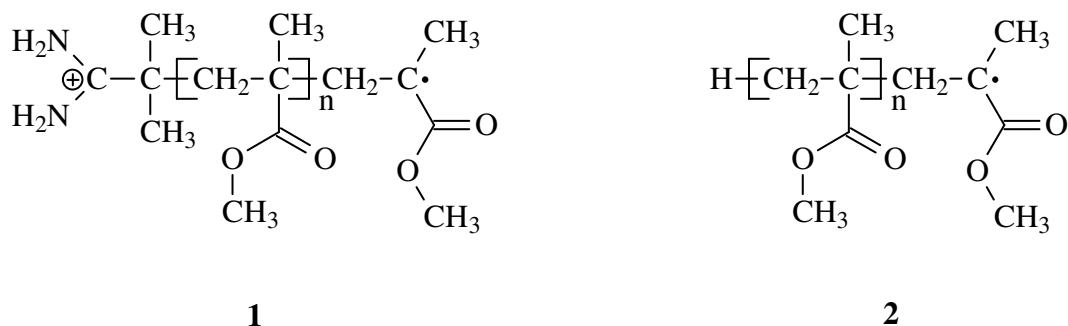


Figure 4. Rate of polymerization and final particle number above CMC as a function of the initiator concentration (run 11-19, Table 3). $[SDS] = 5 \cdot 10^{-2} M$; $[COBF] = 5.0$ ppm ● Rate of polymerization without COBF, slope = 0.6; ○ Rate of polymerization with COBF, slope = 0.6; ▲ Particle number without COBF, slope = 0.3; △ Particle number with COBF, slope = 0.3.

Particle nucleation in an emulsion polymerization suffers in many cases from issues with reproducibility. Apparently, for the investigated range of surfactant concentrations, i.e. $5 \cdot 10^{-3} \leq [SDS] \leq 10^{-1} M$, in combination with the initiator concentration of $10^{-3} M$ hardly any scatter in N_p was observed. When the initiator concentration is varied in the range of $3 \cdot 10^{-4} \leq [V50] \leq 10^{-2} M$ in combination with a surfactant concentration of $5 \cdot 10^{-2} M$ a large scatter in N_p was observed. The scatter in the particle size of the obtained latex is

even more pronounced when the emulsion polymerizations are performed below the critical micelle concentration (CMC). Colloidal stability is then severely affected and coagulation and fouling can occur. The loss of colloidal stability and the scatter in the particle size data could be due to the chemical nature of the radicals giving entry into the polymer particles, see Scheme 2.



Scheme 2. The chemical structures of the radicals in a catalytic chain transfer mediated emulsion polymerization giving entry. 1. Initiator derived radical containing a V50 fragment; 2. Catalytic chain transfer derived radical.

In the COBF-free emulsion polymerization, the polymer chains are predominantly initiated by a V50 fragments, see Scheme 2 structure 1. These radicals carry a cationic charge which, upon entry, anchors at the particle surface and contribute to the colloidal stability. Catalytic chain transfer derived radicals carry a hydrogen atom as the initiating group, see Scheme 2 structure 2. Upon entry these radicals will be buried inside the hydrophobic core of the particle, not contributing the colloidal stability. COBF partitions predominantly towards the aqueous phase and consequently alters the aqueous phase kinetics. Due to the presence of COBF, a significant amount of initiator derived radicals will not be able to propagate to required z-meric or j-crit length. This results in a situation where less surface active radicals are able to give entry into a polymer particle and consequently there is a loss of initiator derived stabilizing groups on the surface. This ultimately affects the colloidal stability and this can result in coagulation, i.e. the formation of larger particles or fouling in the reactor.

Analysis of the emulsion polymerization rates

From the above presented results it is evident that the presence of COBF affects the course of the emulsion polymerization, see Figure 1. The rates of polymerization in the presence of COBF are significantly lower than is the case without COBF, see Figures 3 and 4. Also, the particle number can be affected by a reduced rate of entry and some loss of colloidal stability in the presence of COBF. The rate of polymerization and the particle number are directly related to the average number of radicals per particle. The above discussed experimental results and the average number of radicals per particle, experimentally (\bar{n}_{obsd}) calculated from Equation 1 as well as theoretically (\bar{n}_{theo}) calculated from Equation 4 are presented in Table 3.

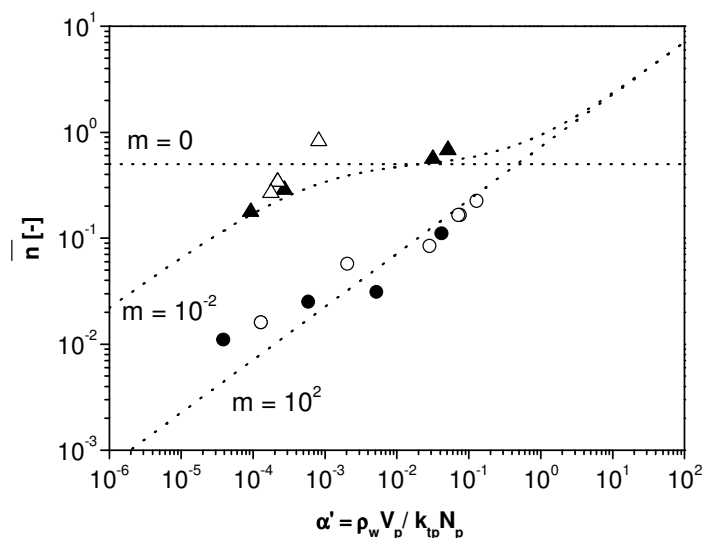


Figure 5. Relationship between the average number of radicals per particle as a function of α'_w . (run 01-19, Table 3) \blacktriangle varying surfactant concentration, no COBF; \triangle varying initiator concentration, no COBF; \bullet varying surfactant concentration, 5.0 ppm COBF and \circ varying initiator concentration, 5.0 ppm COBF. (....) Simulated lines for $m = 0$, $m = 10^{-2}$ and $m = 10^2$.

Figure 5 shows the average number of radicals per particle as calculated from the theory reported by Ugelstad and co-workers^{22,23} for the experimental data collected in Table 3.. Methyl methacrylate is classified as a Smith-Ewart Case 1 monomer. Case 1 occurs when

$\bar{n} \ll 0.5$ and only a small fraction of polymer particles will contain a radical as the probability of radical desorption is higher than radical entry ($\rho \ll k$). Typically case 1 behavior is observed for small particles and it is evident from Figure 5 that as the particle size increases (α'_w correlates to d_p) \bar{n} approaches case 2 behavior, i.e. $\bar{n} = 0.5$. The values of \bar{n}_{obsd} are in good agreement with a simulated theoretical result for $m = 10^{-2}$, which implies a small contribution of radical desorption.

Table 3. Experimental data of emulsion polymerizations with and without COBF at various surfactant and initiator concentrations.

Entry	[SDS] [$\text{mol} \cdot \text{dm}_w^{-3}$]	[V50] [$\text{mol} \cdot \text{dm}_w^{-3}$]	[COBF] [$\text{mol} \cdot \text{dm}_M^{-3}$]	R_p [$10^{-3} \text{ mol} \cdot \text{dm}^{-3} \text{ s}^{-1}$]	N_p [$10^{18} \text{ dm}_w^{-3}$]	\bar{n}_{obsd} [-]	\bar{n}_{theo} [-]
01	$1.0 \cdot 10^{-1}$	$1.0 \cdot 10^{-3}$	-	4.78	2.57	0.177	0.087
02	$5.0 \cdot 10^{-2}$	$1.0 \cdot 10^{-3}$	-	5.95	1.67	0.339	0.410
03	$2.5 \cdot 10^{-2}$	$1.0 \cdot 10^{-3}$	-	4.49	1.50	0.286	0.423
04	$5.0 \cdot 10^{-3}$	$1.0 \cdot 10^{-3}$	-	0.78	0.11	0.560	0.515
05	$1.0 \cdot 10^{-3}$	$1.0 \cdot 10^{-3}$	-	0.82	0.14	0.679	0.524
06	$1.0 \cdot 10^{-1}$	$1.0 \cdot 10^{-3}$	$4.8 \cdot 10^{-5}$	0.45	3.98	0.011	0.004
07	$5.0 \cdot 10^{-2}$	$1.0 \cdot 10^{-3}$	$4.8 \cdot 10^{-5}$	0.36	2.18	0.016	0.008
08	$2.5 \cdot 10^{-2}$	$1.0 \cdot 10^{-3}$	$4.8 \cdot 10^{-5}$	0.27	1.02	0.025	0.017
09	$1.0 \cdot 10^{-2}$	$1.0 \cdot 10^{-3}$	$4.8 \cdot 10^{-5}$	0.14	0.12	0.111	0.146
10	$5.0 \cdot 10^{-3}$	$1.0 \cdot 10^{-3}$	$4.8 \cdot 10^{-5}$	0.11	0.34	0.031	0.051
11	$5.0 \cdot 10^{-2}$	$1.0 \cdot 10^{-2}$	-	23.7	2.73	0.827	0.469
12	$5.0 \cdot 10^{-2}$	$1.0 \cdot 10^{-3}$	-	5.95	1.67	0.340	0.410
13	$5.0 \cdot 10^{-2}$	$1.0 \cdot 10^{-4}$	-	1.64	0.59	0.267	0.396
14	$5.0 \cdot 10^{-2}$	$1.0 \cdot 10^{-2}$	$4.8 \cdot 10^{-5}$	0.51	0.22	0.224	0.258
15	$5.0 \cdot 10^{-2}$	$1.0 \cdot 10^{-2}$	$4.8 \cdot 10^{-5}$	1.03	1.73	0.057	0.032
16	$5.0 \cdot 10^{-2}$	$3.0 \cdot 10^{-3}$	$4.8 \cdot 10^{-5}$	0.27	0.16	0.165	0.196
17	$5.0 \cdot 10^{-2}$	$1.0 \cdot 10^{-3}$	$4.8 \cdot 10^{-5}$	0.16	0.09	0.165	0.192
18	$5.0 \cdot 10^{-2}$	$1.0 \cdot 10^{-3}$	$4.8 \cdot 10^{-5}$	0.36	2.18	0.016	0.008

When 5.0 ppm COBF is present in the reaction mixture of the polymerization, \bar{n}_{obsd} drops one to two orders of magnitude. This results in a situation where the polymerization displays a very pronounced case 1 behavior and consequently \bar{n} displays a strong dependency on the particle size. The \bar{n}_{obsd} values are in good agreement with a simulated theoretical result for $m = 10^2$. This implies that radical desorption from the polymer particles dominates bimolecular termination. These low values for \bar{n} in the presence of COBF explain the large difference between the rates of polymerization with and without COBF.

In emulsion polymerization without COBF, \bar{n} is governed by the surfactant and initiator concentration. However, in COBF mediated emulsion polymerization the effect of the surfactant and initiator concentration on \bar{n} proved to be dominated by the presence of COBF. Although the scaling rules still apply for the surfactant and initiator concentration, it is worthwhile to investigate the effect of the COBF concentration on the emulsion polymerization kinetics.

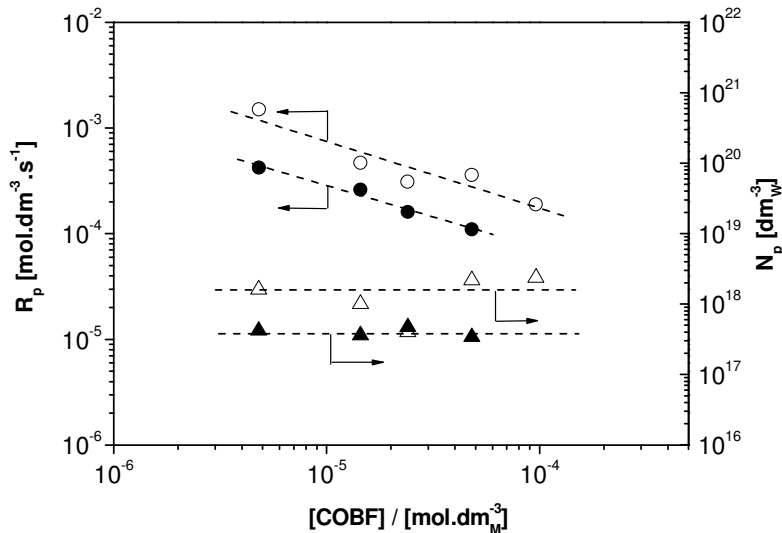


Figure 6. Rate of polymerization and final particle number above as a function of the COBF concentration inside the polymer particles. (run 20-30, Table 4) [SDS] = $5 \cdot 10^{-2}$ M or $5 \cdot 10^{-3}$ M; [V50] = $1 \cdot 10^{-3}$ M. ● Rate of polymerization below CMC, slope = -0.59; ○ Rate of polymerization above CMC, slope = -0.63; ▲ Particle number below CMC; △ Particle number above CMC. CMC = $6 \cdot 10^{-3}$ M³⁸

Figure 6 presents the effect of changing the catalytic chain transfer agent concentration on the rate of polymerization and final particle number. The concentration of COBF can only be varied over a limited concentration interval, i.e. $5 \cdot 10^{-6} \leq [\text{COBF}] \leq 10^{-4}$ M, as higher concentrations than 10^{-4} M will result in a extremely low rates of polymerization. Upon increasing the COBF concentration the rate of polymerization decreases. The influence of the COBF concentration on R_p was estimated to be $R_p \propto [\text{COBF}]^{-0.60}$ and hardly any effect on N_p was observed both for experiments with the surfactant concentration above and below the CMC, see Figure 6. The rates of polymerization and particle numbers as presented in Figure 6 are collected in Table 4.

Table 4. Experimental data of emulsion polymerizations in the presence of COBF above and below CMC.^a

Entry	[SDS] [$\text{mol} \cdot \text{dm}_w^{-3}$]	[V50] [$\text{mol} \cdot \text{dm}_w^{-3}$]	[COBF] [$\text{mol} \cdot \text{dm}_M^{-3}$]	R_p [$10^{-3} \text{ dm}^3 \cdot \text{mol}^{-1} \cdot \text{s}^{-1}$]	N_p [$10^{17} \text{ dm}_w^{-3}$]	\bar{n}_{exp} [-]	\bar{n}_{the} [-]
20	$5.0 \cdot 10^{-2}$	$1.0 \cdot 10^{-3}$	-	5.95	1.67	0.340	0.410
21	$5.0 \cdot 10^{-2}$	$1.0 \cdot 10^{-3}$	$4.8 \cdot 10^{-6}$	1.50	1.60	0.090	0.011
22	$5.0 \cdot 10^{-2}$	$1.0 \cdot 10^{-3}$	$1.4 \cdot 10^{-5}$	0.47	1.00	0.045	0.017
23	$5.0 \cdot 10^{-2}$	$1.0 \cdot 10^{-3}$	$2.4 \cdot 10^{-5}$	0.31	0.40	0.074	0.044
24	$5.0 \cdot 10^{-2}$	$1.0 \cdot 10^{-3}$	$4.8 \cdot 10^{-5}$	0.36	2.18	0.016	0.008
25	$5.0 \cdot 10^{-2}$	$1.0 \cdot 10^{-3}$	$9.6 \cdot 10^{-5}$	0.19	2.36	0.007	0.007
26	$5.0 \cdot 10^{-3}$	$1.0 \cdot 10^{-3}$	-	0.82	0.14	0.564	0.515
27	$5.0 \cdot 10^{-3}$	$1.0 \cdot 10^{-3}$	$4.8 \cdot 10^{-6}$	0.42	0.42	0.096	0.042
28	$5.0 \cdot 10^{-3}$	$1.0 \cdot 10^{-3}$	$1.4 \cdot 10^{-5}$	0.26	0.36	0.071	0.049
29	$5.0 \cdot 10^{-3}$	$1.0 \cdot 10^{-3}$	$2.4 \cdot 10^{-5}$	0.16	0.47	0.034	0.039
30	$5.0 \cdot 10^{-3}$	$1.0 \cdot 10^{-3}$	$4.8 \cdot 10^{-5}$	0.11	0.34	0.031	0.051

^a CMC = $6 \cdot 10^{-3}$ M³⁸

The rates of polymerization and particle sizes presented in Figure 6 allow for the determination of \bar{n}_{obsd} . Figure 7 presents \bar{n}_{obsd} for the experiments listed in Table 4. The higher the COBF concentration, the lower \bar{n} which implies that the rates of entry and

exit are increasingly affected for larger amounts of COBF. The \bar{n}_{obsd} values cover a wide range of m values (i.e. $5 \cdot 10^{-2} \leq m \leq 10^2$) indicating that depending on the amount of COBF in the system, desorption becomes increasingly important.

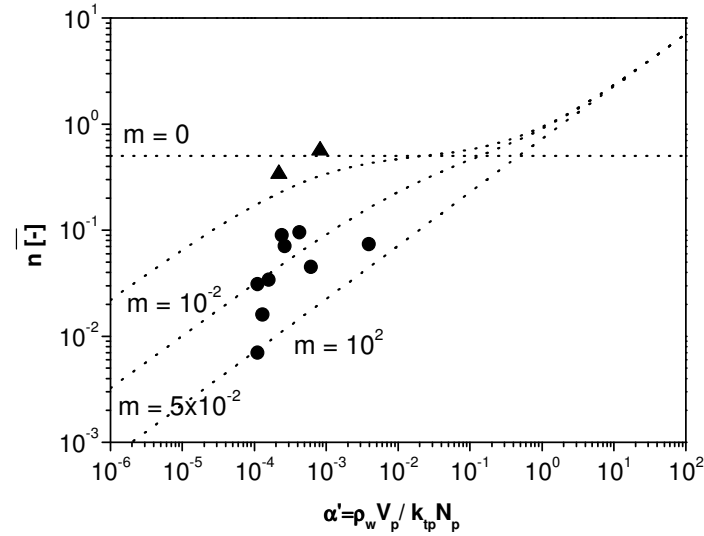


Figure 7. Relationship between the average number of radicals per particle as a function of α'_w . (runs 20-30, Table 4) ▲ Experiments in the absence of COBF; ● Experiments with a varying COBF concentration from 0.0 to 10 ppm COBF. (....) Simulated lines for $m = 0$, $m = 10^{-2}$, $m = 5 \cdot 10^{-2}$ and $m = 10^2$.

The rate of exit of monomeric radicals (Φ_{exit}) is expressed as,

$$\Phi_{\text{exit}} = k_{\text{dM}} [M_1^\bullet]_p \quad (10)$$

where $[M_1^\bullet]_p$ is the monomeric radical concentration inside the polymer particles. Monomeric radicals are produced by the catalytic chain transfer process and the concentration is governed by the chain transfer frequency (f_{tr}), see Equation 11.

$$f_{\text{tr}} = k_{\text{tr}} [\text{COBF}]_p \quad (11)$$

In this equation k_{tr} is the rate coefficient of chain transfer and $[COBF]_p$ the concentration of COBF inside the polymer particles. As the COBF concentration increases, the frequency of chain transfer increases and the monomeric radical concentration inside the particles increases. Consequently the rate of exit is increases as the COBF concentration is increases.

Chain transfer activity

The activity of catalytic chain transfer agents in emulsion polymerization are often expressed in terms of an apparent chain transfer constant (C_T^{app}). In earlier work we reported that the observed C_T^{app} -values in emulsion polymerization can be explained by catalyst partitioning between the different phases.¹⁸ These results were obtained in miniemulsion polymerization for conversions smaller than 0.10 and were found to obey a simple mathematical model, see Equation 11. For the conditions of the current investigation ($m_{Co} = 0.72 \text{ dm}_w^3 \cdot \text{dm}_M^{-3}$, $\beta = 0.185 \text{ dm}_M^3 \cdot \text{dm}_w^{-3}$ and $C_T = 15 \cdot 10^3$), using Equation 12 yields a C_T^{app} value of $1.8 \cdot 10^3$.

$$C_T^{app} = \frac{C_M}{C_{M,p}} \frac{m_{Co}(\beta+1)}{m_{Co}\beta+1} \frac{\beta}{\beta+1} C_T \quad (12)$$

The obtained degrees of polymerization from the final molecular weight distributions and the calculated results for a C_T^{app} of $1.8 \cdot 10^3$ are presented in Figure 8. It is evident that the experimentally obtained degrees of polymerization and theoretical calculations are in good agreement. From the experimental results and using Equation 12 a C_T^{app} of $1.3 \cdot 10^3$ is determined. This result is in close agreement with the predicted value of $1.8 \cdot 10^3$. The discrepancy may be attributed to either COBF decomposition in the aqueous phase or the increasing viscosity inside the polymer particles. First, even under optimal conditions, some COBF decomposition can occur,¹⁹ shifting the instantaneous degrees of

polymerization to the higher end of the molecular weight distribution. Secondly, towards higher conversions, the viscosity inside the polymer particles is increasing which limits the mobility of COBF. The reduced mobility of COBF results in a reduction of the chain transfer frequency which in turn results in slightly higher degrees of polymerization. Chain transfer is the dominant chain-stoppage mechanism and a decrease in the chain transfer frequency results in an increase in the rate of propagation which is observed as a gel effect and an increase in DP_n . Note that the gel effects observed in CCT mediated emulsion polymerization occur due to a different phenomenon when compared to conventional emulsion polymerizations. The observed gel effect also restricts the entry of COBF molecules into the polymer particles.

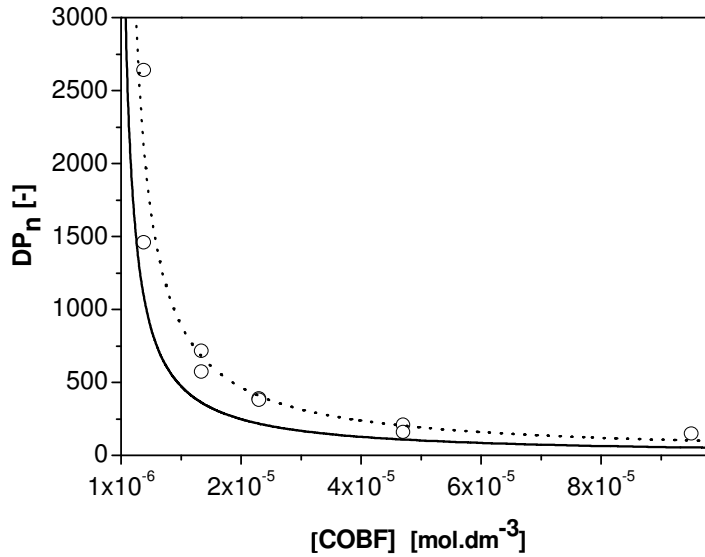


Figure 8. Experimentally observed and calculated values of the number-average degree of polymerization as a function of the COBF concentration. Molecular weight distributions were measured for the final conversion sample. (○) number-average degree of polymerization data values (---) Fitted number-average degree of polymerization, $m_{Co} = 0.72 \text{ dm}_W^3 \cdot \text{dm}_M^{-3}$, $\beta = 0.185 \text{ dm}_M^3 \cdot \text{dm}_W^{-3}$, (—) Predicted instantaneous number-average degree of polymerization, Equation 9, $C_T^{\text{app}} = 1.8 \cdot 10^3$

The good agreement between the theoretical value for C_T^{app} and the experimentally obtained values at high conversion indicates the versatility of the mathematical model to predict the degree of polymerization in *ab initio* catalytic chain transfer mediated emulsion polymerization.

CONCLUSIONS

The results of this work illustrate that the presence of COBF in the *ab initio* emulsion polymerization of methyl methacrylate severely affects the course of the polymerization. Partitioning of COBF between the aqueous phase and the polymer particle phase affects the rate of polymerization and the particle size distribution.

Presence of COBF in the aqueous phase reduces the rate of entry which prolongs the nucleation stage. The catalytic chain transfer process inside the polymer particles results in an enhanced exit rate as compared with the COBF free emulsion polymerization. Both effects contribute to a decrease in \bar{n} and COBF mediated emulsion polymerizations display a pronounced Smith-Ewart case 1 behavior, i.e. $k \gg \rho$. The experimental values for \bar{n} were in good agreement with the theoretical values obtained from the solution of the radical population balance over the particles as given by Ugelstad.

The degree of polymerization obtained from the final, high conversion, molecular weight distributions resulted in an apparent chain transfer constant of $1.3 \cdot 10^3$, which is in agreement with the theoretical predicted value of $1.8 \cdot 10^3$. This result indicates the versatility of the previously derived mathematical model based on partitioning and the Mayo equation¹⁸ for predicting the degree of polymerization throughout the course of the polymerization.

EXPERIMENTAL

Materials

The bis[(difluoroboryl) dimethylglyoximato]cobalt(II) complex (COBF) was prepared as described previously.^{14,39} For all experiments, a single batch of COBF was used. The

intrinsic activity of the catalyst was determined by measuring the chain transfer constant in bulk polymerization of methyl methacrylate (MMA) at 60°C: $C_T = 30 \cdot 10^3$. MMA (Aldrich, 99%) was purified by passing it over a column of activated basic alumina (Aldrich) in order to remove the methyl hydroquinone (MeHQ) inhibitor. Sodium dodecyl sulphate (SDS) (Fluka, 99%), sodium carbonate (SC) (Aldrich, 99%) and 2,2'-azobis(2-methylpropionamide)dihydrochloride (V50) (Aldrich, 97%) were used as received.

COBF mediated ab-initio emulsion polymerization

All reactions are performed in a glass 1.2 dm³ Mettler Toledo RC1 reactor equipped with an anchor impeller, temperature sensor, calibration heater and sample loop. The RC1 program operated in isothermal mode and all additions and sampling were performed manually.

A catalyst stock solution (i) was prepared by dissolving an accurate amount of COBF (approximately 6 mg, $1.4 \cdot 10^{-2}$ mmol) in MMA (40.0 mL). An initiator solution (ii) was prepared by dissolving an accurate amount of V50 in 10.0 mL water. SDS and SC were weighted accurately and dissolved in water (390 mL) and subsequently added to the reactor. MMA (64 mL) was added and the resulting emulsion was purged with N₂ whilst the impeller speed and reactor temperature were gradually raised to 175 rpm and 70°C. After 1 hr of purging, an amount of solution (i) (10.0 mL) was added instantaneously to the reactor and stirred for 20 min to allow COBF to partition between the respective phases. Subsequently, the initiator solution (ii) (10.0 mL) was added instantaneously to the reactor to initiate the polymerization. The reactor was pressurized to 2 bar absolute pressure. Samples were withdrawn periodically for analysis (gravimetry, size exclusion chromatography and dynamic light scattering).

Size exclusion chromatography

Size exclusion chromatography (SEC) was performed using a Waters 2690 separation module and a model 410 differential refractometer. A set of five Waters Styragel HR columns (HR5.0, HR4.0, HR3.0; HR1.0; HR0.5) were used in series at 40°C.

Tetrahydrofuran (THF) (Aldrich, 99%) was used as the eluent at a flow rate of $1 \text{ mL}\cdot\text{min}^{-1}$, and the system was calibrated using narrow molecular weight polystyrene standards ranging from 374 to $1.1\cdot 10^6 \text{ g}\cdot\text{mol}^{-1}$. Mark Houwink parameters used for the polystyrene standards: $K = 1.14\cdot 10^{-4} \text{ dL}\cdot\text{g}^{-1}$, $a = 0.716$ and for poly(methyl methacrylate):

$$K = 9.44\cdot 10^{-5} \text{ dL}\cdot\text{g}^{-1}, a = 0.719.$$

Dynamic light scattering

Particle size distributions were measured on a Malvern Zetasizer Nano. All latexes were diluted with distilled deionized water prior to the measurement. For each measurement the obtained particle size distribution data was averaged over 3 individual runs.

REFERENCES

1. Barandiaran, M.J.; de la Cal, J.C.; Asua, J.M. in Polymer Reaction Engineering, Ed. J.M. Asua., Blackwell Publishing Inc. Oxford 2007, Chapter 6, pp 234.
2. Enikolopyan, N. S.; Smirnov, B. R.; Ponomarev, G. V.; Belgovskii, I. M. J. Polym. Sci. Part A: Polym. Chem. 1981, 19, 879.
3. Heuts, J.P.A.; Roberts, G.E. ; Biasutti, J.D. Aust. Chem. J. 2002, 55, 381.
4. Gridnev, A. A.; Ittel, S. D. Chem Rev 2001, 101, 3611.
5. Karmilova, L.V.; Ponomarev, G.V.; Smirnov, B.R.; Belgovskii, I.M. Russ. Chem. Rev. 1984, 53, 223.
6. Davis, T.P.; Haddleton, D.M.; Richards, S.N. J. Macromol. Sci., Rev. Macromol. Chem. 1994, C34, 234.
7. Davis, T.P.; Kukulj, D.; Haddleton, D.M.; Maloney, D.R. Trends Polym. Sci. 1995, 3, 365.
8. Gridnev, A.A.; J. Polym. Sci. Part A: Polym. Chem. 2000, 38, 1753.
9. Pierik, S.C.J.; Smeets, B.; van Herk, A.M. Macromolecules 2003, 36, 9271.
10. Kukulj, D.; Davis, T. P.; Gilbert, R. G. Macromolecules 1997, 30, 7661.
11. Kukulj, D.; Davis, T.P.; Suddaby, K.G.; Haddleton, D.M.; Gilbert, R.G. J. Polym. Sci. Part A: Polym. Chem. 1997, 35, 859.
12. Bon, S. A. F.; Morsley, D. R.; Waterson, J.; Haddleton, D. M.; Lees, M. R.; Horne, T. Macromol. Symp. 2001, 165, 29.

13. Haddleton, D.M.; Morsley, D.R.; O'Donnell, J.P.; Richards, S.N. *J. Polym. Sci. Part A: Polym. Chem.* 2001, 37, 3549.
14. Suddaby, K.G.; Haddleton, D.M.; Hastings, J.J.; Richards, S.N.; O'Donnell, J.P. *Macromolecules* 1996, 29, 8083.
15. Smith, W.V.; *J. Am. Chem. Soc.* 1946, 68, 2064.
16. Kolthoff, I.M.; Harris, W.E. *J Polym Sci* 1947, 2, 41.
17. Suzuki, S.; Kikuchi, K.; Suzuki, A.; Okaya, T.; Nomura, M. *Colloid Polym. Sci.* 2007, 285, 523.
18. Smeets, N.M.B.; Heuts, J.P.A.; Meuldijk, J.; van Herk, A.M.; *J. Polym. Sci. Part A: Polym. Chem.* 2008, 46, 5839.
19. Smeets, N.M.B.; Meda, U.S.; Heuts, J.P.A.; Keurentjes, J.T.F.; van Herk, A.M.; Meuldijk, J. *Macromol. Symp.* 2007, 259, 406.
20. Stockmayer, W.H. *J. Polym. Sci.* 1957, 24, 313.
21. O'Toole, J.T. *J. App. Polym. Sci.* 1965, 9, 1291.
22. Ugelstad, J.; Mork, P.C.; Aasen, J.Q.; *J. Polym. Sci. Part. A-1: Polym. Chem.* 1967, 5, 2281.
23. Ugelstad, J. ; Mork, P.C.; Rangnes, P. *J. Polym. Sci. Part C.* 1969, 27, 49.
24. Nomura, M.; Harada, M.; Eguchi, W.; Nagata, S. In *Emulsion Polymerization*, Piirma, I.; Gardon, J.L., Eds.; Am. Chem. Soc. Symp. Ser. 1976, 24, 102.
25. Nomura, M.; Fujita, K. *Makromol. Chem. Suppl.* 1985, 10, 25.
26. Nomura, M.; Kubo, M.; Fujita, K. *J. Appl. Polym. Sci.* 1983, 28, 2767.
27. Berger, K.C.; Brandrup, G. In *Polymer Handbook*, Brandrup, J.; Immergut, Eds., Wiley: New York, 1989; 3rd Ed pp.II/109.
28. M. Buback, L. H. Garcia-Rubio, R. G. Gilbert, D. H. Napper, J. Guillot, A. E. Hamielec, D. Hill, K. F. O'Driscoll, K. F. Olaj, J. Shen, D. Solomon, G. Moad, M. Stickler, M. Tirrell, M. A. Winnik, *J. Polym. Sci.. Polym. Letters Ed*, 1988, 26, 293.
29. Arrhenius parameters are obtained from Wako Specialty Chemicals
30. M.J. Ballard, D.H. Napper, R.G. Gilbert, *J. Polym. Sci. Polym. Chem. Ed.* 1984, 22, 3325.
31. The value for the viscosity inside the polymer particle was approximated using an empirical correlation by Stickler et al.³² The intrinsic viscosity of the polymer is

calculated using a M_n of the obtained polymer of $20 \cdot 10^3$ and the Mark-Houwink parameters as reported in the experimental section. The viscosity of the solvent (MMA) was taken from Sastry et al.³³

32. Stickler, M. ; Panke, D. ; Wunderlich, W. Makromol. Chem. 1987, 188, 2651.
33. Sastry, N.V.; Patel, S.R. Int. J. Thermophysics 2000, 21, 1153.
34. Smith, W.V.; Ewart, R.H. J Chem. Phys. 1948, 16, 592.
35. Biasutti, J.D.; Roberts, G.E.; Lucien, F.P.; Heuts, J.P.A. Eur Polym J 2003, 39, 429.
36. Gridnev, A.A. J. Polym. Sci. Part A. Polym. Chem. 2000, 38, 1753.
37. Pierik, S.C.J. Shining a light on catalytic chain transfer, 2002, Ph.D Thesis Eindhoven University of Technology, Eindhoven, 2002.
38. Chen, L-J.; Lin, S-Y.; Chern, C-S.; Wu, S-C. Colloid. Surf. A 1997, 122, 161.
39. Bakač, A.; Brynildson, M. E.; Espenson, J. H. Inorg. Chem. 1986, 25, 4108.

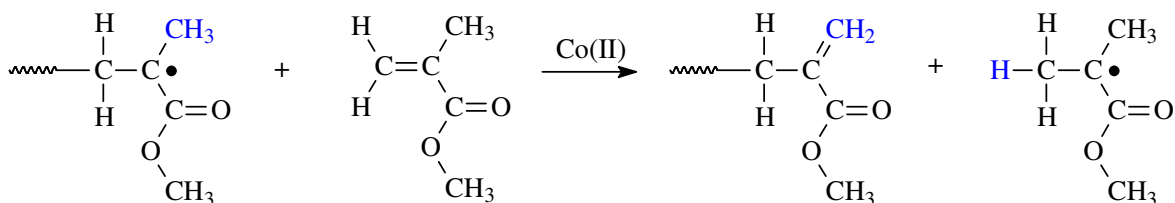
The Effect of Different Catalytic Chain Transfer Agents on Particle Nucleation and the Course of the Polymerization in the *Ab initio* Batch and Continuous Emulsion Polymerization of Methyl Methacrylate

ABSTRACT

The effect the addition of a catalytic chain transfer agent (CCTA) has on the course of the polymerization and the product properties of an emulsion polymerization is governed by the intrinsic activity and the partitioning behavior of the catalyst. The effect on the course of the polymerization, molecular weight distribution and particle size distribution is evaluated for three different CCTAs, which display a range of intrinsic activities and partitioning behaviors. The performance of the different CCTAs will be evaluated in batch and in continuous emulsion polymerization. Radical exit has proven to be the main kinetic event controlling the course of the polymerization and the product properties in terms of the particle size distribution on batch scale. Continuous emulsion polymerization experiments, performed in the pulsed sieve plate column, showed that the aqueous phase solubility of the CCTA is the key parameter controlling the course of the polymerization and the particle size distribution.

INTRODUCTION

For the application in e.g. waterborne coatings, the molecular weight distribution (MWD) and the particle size distribution (PSD) of a latex are key properties. Catalytic chain transfer (CCT) is an established technique for control of the MWD in bulk and solution polymerization.¹⁻⁶ The most widely accepted mechanism for catalytic chain transfer involves a Co(II) complex that abstracts a hydrogen atom from the propagating polymeric radical, yielding a dead polymer chain with a vinyl end-group functionality and a Co(III)-H complex. The Co(III)-H intermediate can subsequently react with a monomer molecule, resulting in the regeneration of the active Co(II) species and the formation of a propagating monomeric radical. The hydrogen abstraction is assumed to be the rate determining step in this mechanism.^{1,2} The overall reaction of catalytic chain transfer to monomer in the case of methyl methacrylate (MMA) is schematically presented in Scheme 1.

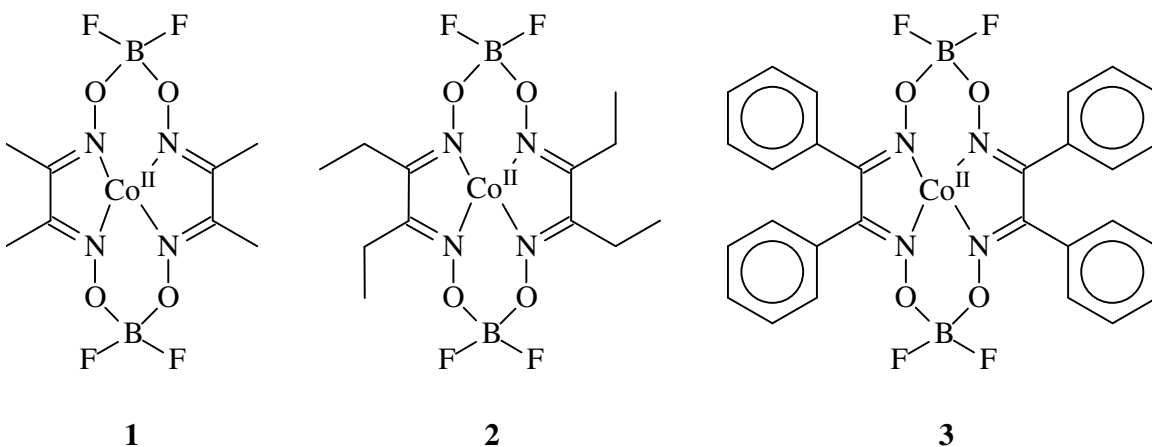


Scheme 1. The overall reaction of catalytic chain transfer to monomer

Recently, there is a growing interest for the application of controlled and living radical polymerization techniques in emulsion polymerization.⁷ The emulsion polymerization system is heterogeneous by nature. This heterogeneity has major implications for the application of CCT and the control of the molecular weight distribution.⁸⁻¹⁴ Partitioning of the catalytic chain transfer agent (CCTA) results in chain transfer events inside the polymer particle phase as well as in the aqueous phase. In CCT, monomeric radicals are formed as a consequence of the catalytic chain transfer process. These monomeric radicals can readily desorb towards the aqueous phase, increasing the rate of exit when compared to a conventional emulsion polymerization. The presence of a CCTA in the aqueous phase affects the rate of radical entry and the chemical nature of those radicals,

see Chapter 5. This results in an extended nucleation stage of the polymerization and a (partial) loss of colloidal stability. The increased rate of exit and decreased rate of entry contribute to a low average number of radicals per particle (\bar{n}) and CCT mediated emulsion polymerizations obey Smith Ewart Case 1 kinetics.^{15,16}

Emulsion polymerizations are frequently carried out in (semi-) batch processes. Demands for improved process control and narrow product specifications make continuous operation may become an interesting alternative. The pulsed packed column (PPC)^{17,18} and the pulsed sieve plate column (PSPC)^{19,20} have demonstrated to be promising continuous alternatives for batch emulsion polymerization.



In the presented work we report the effect of different CCTA's, i.e. [(difluoroboryl)dimethylglyoximato]cobalt(II) (COBF, **1**), [(difluoroboryl)diethylglyoximato]cobalt(II) (COEtBF, **2**) and [(difluoroboryl)diphenylglyoximato]cobalt(II) (COPhBF, **3**), on particle nucleation and the course of the polymerization in *ab initio* batch and continuous emulsion polymerization of methyl methacrylate.

RESULTS AND DISCUSSION

To compare the influence of different CCTA's on the nucleation stage of an emulsion polymerization, an approach was chosen where the catalytic chain transfer activity inside the polymer particles, expressed in the chain transfer frequency (f_{tr}), was approximately constant, see Equation 1.

$$f_{tr} = k_{tr}[\text{CCTA}]_p \quad (1)$$

where k_{tr} is the chain transfer rate coefficient and $[\text{CCTA}]_p$ the concentration of CCTA at the locus of polymerization. The presence of a CCTA in an emulsion polymerization affects the rate of entry as well as the rate of exit of radicals. The catalytic chain transfer process generates monomeric radicals which can desorb from the polymer particles to the aqueous phase. The rate of radical desorption is a first-order process with respect to the monomeric radical concentration with a desorption rate coefficient (k). The desorption rate coefficient is correlated to the partitioning of a monomeric radical and the particle diameter, see Equation 2.²¹

$$k = \frac{12D_w}{m_{M_1}d_p^2} \quad (2)$$

where D_w is the diffusion coefficient of a monomer molecule in water, d_p the radius of the polymer particle and m_{M_1} the partition coefficient for the distribution of a monomer molecule between the polymer particles and the aqueous phase. The overall rate of radical desorption is the product of the desorption rate coefficient and the monomeric radical concentration. The monomeric radical concentration is governed by the concentration and the activity of the CCTA. An approximately equal chain transfer frequency in the polymer particles, for different CCTA's, implies a comparable concentration of monomeric radicals and consequently a comparable rate of radical desorption. Note that this assumption is only valid if the particle sizes are comparable. An

approximately constant chain transfer frequency should result in comparable molecular weight distributions for the different CCTA's. The investigated CCTA's, i.e. COBF, COEtBF and COPhBF, have different partitioning behavior and poses different intrinsic activities. For approximately equal chain transfer activities inside the polymer particles, the differences in the conversion-time history, rate of polymerization and particle size distribution can be attributed to the difference in aqueous phase chain transfer events.

BATCH EXPERIMENTS

Course of the Polymerization

The conversion-time histories for the CCT mediated emulsion polymerization with comparable chain transfer frequencies in the polymer particles are presented in Figure 1. The final latex properties are collected in Table 1.

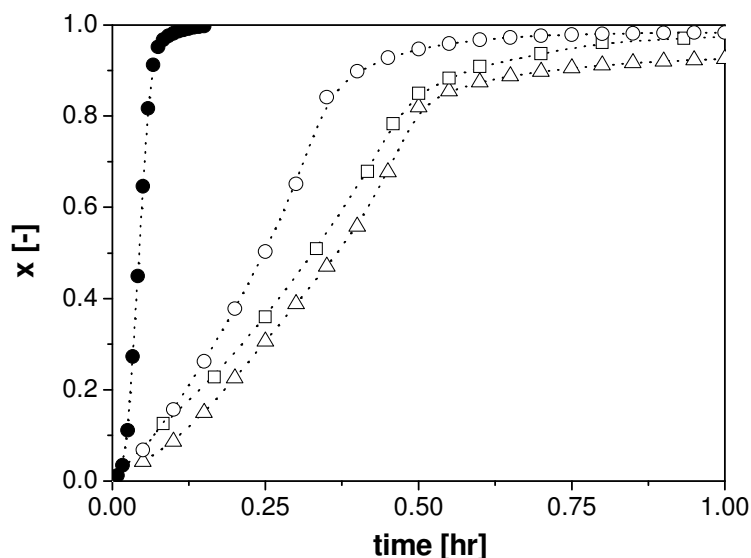


Figure 1. Conversion-time histories for the catalytic chain transfer mediated emulsion polymerization with comparable chain transfer activity inside the polymer particles. Reaction conditions: $T = 343 \text{ K}$, $[\text{SDS}] = 5.0 \cdot 10^{-2} \text{ mol} \cdot \text{dm}_w^{-3}$, $[\text{V50}] = 5.0 \cdot 10^{-3} \text{ mol} \cdot \text{dm}_w^{-3}$, $\beta = 0.19$, $V_r = 1 \text{ dm}^3$. (●) no CCTA; (○) 0.22 ppm COEtBF; (□) 2 ppm COBF and (△) 2 ppm COPhBF. 1 ppm is defined as 1 mol CCTA per 10^6 moles of monomer.

Table 1. Final latex properties of the experimentally obtained latexes in the presence of COBF, COEtBF and CPhBF.

$[CCTA]$	x	DP_n	R_p	\bar{n}_{SS}	$d_p(V)$	$poly$	N_p	$\bar{n}_{SS} N_p$
		[-]	$[mol \cdot dm_w^{-3} s^{-1}]$	[-]	$[nm]$	[-]	$[10^{18} dm_w^{-3}]$	$[10^{16} dm_w^{-3}]$
-	1.00	8857	$1.0 \cdot 10^{-2}$	0.292	49.2	0.057	3.10	90.7
COBF	0.97	375	$6.7 \cdot 10^{-4}$	0.028	58.5	0.127	2.27	6.10
	0.96	325	$9.4 \cdot 10^{-4}$	0.049	55.1	0.086	1.73	8.53
COEtBF	0.98	325	$1.0 \cdot 10^{-3}$	0.007	30.7	0.203	13.6	9.07
	1.00	387	$1.1 \cdot 10^{-3}$	0.005	52.6	0.156	2.62	9.98
CPhBF	1.00	417	$7.7 \cdot 10^{-4}$	0.002	22.2	0.102	34.9	6.98
	0.99	411	$7.3 \cdot 10^{-4}$	0.002	23.9	0.164	28.1	6.60

Reaction conditions: $T = 343$ K, $[SDS] = 5.0 \cdot 10^{-2} mol \cdot dm_w^{-3}$, $[V50] = 5.0 \cdot 10^{-3} mol \cdot dm_w^{-3}$, $\beta = 0.19$, $V = 1 dm^3$ and 2.0 ppm COBF, 0.22 ppm COEtBF or 2.0 ppm CPhBF. 1 ppm is defined as 1 mol CCTA per 10^6 moles of monomer.

The influence of a CCTA on the course of the emulsion polymerization is governed by the intrinsic activity as well as the partitioning behaviour of that CCTA. The intrinsic activity is expressed as the chain transfer constant (C_T), the ratio of the chain transfer and propagation rate coefficient. The partitioning behaviour determines the actual concentration of CCTA at the locus of polymerization and is determined by the partition coefficient ($m_{Co} = \frac{[Co]_M}{[Co]_W}$) of the CCTA and the phase ratio ($\beta = \frac{V_M}{V_W}$) of the emulsion.

The partitioning behaviour and the activity of the used CCTA's in this work are summarized in Table 2. The chain transfer frequency, as calculated from the number-average degree of polymerization (DP_n) and the partition coefficient, is approximately equal for all investigated CCTA's, see Chapter 2 Equation 5.

Table 2. The partitioning behavior and intrinsic activity of the CCTA's used in this work.

$[CCTA]$	DP_n^a	m_{Co}	$[Co]_0$	$[Co]_p$	F_p^b	$C_T^{app\ c}$	$C_T^{emul\ d}$	f_{tr}^e
	[-]	[-]	$[mol \cdot dm^{-3}]$	$[mol \cdot dm_p^{-3}]$	[-]	$[10^3 -]$	$[10^3 -]$	$[10^1 s^{-1}]$
-	8857	-	-	-	-	-	-	-
COBF	350	0.72 ^f	$3.74 \cdot 10^{-6}$	$2.86 \cdot 10^{-6}$	0.153	7.1	31.3	9.4
COEtBF	325	19 ^g	$4.61 \cdot 10^{-7}$	$1.90 \cdot 10^{-6}$	0.826	62.0	50.3	10.1
COPhBF	410	∞^f	$3.74 \cdot 10^{-6}$	$18.7 \cdot 10^{-6}$	1.000	6.0	6.0	8.0

^a Experimentally obtained number-average degree of polymerization $DP_n = M_w / 2M_0$ ^{22,23} ^b The mol fraction of CCTA at the locus of polymerization ^c The experimentally determined apparent chain transfer constant ^d The calculated intrinsic chain transfer constant in emulsion polymerization based on C_T^{app} and the partitioning data ^e The chain transfer frequency, see Equation 1 ^f experimentally determined partitioning coefficient^{14,24} and ^g taken from Waterson et al.²⁵

There is a distinct difference between the partitioning behaviours of the three CCTA's used in this work. COBF is fairly water-soluble and has a relatively low partitioning coefficient. For a given phase ratio of 0.19, merely 15% of the total absolute amount of COBF partitions towards the locus of polymerization. COEtBF and COPhBF are more hydrophobic and COEtBF partitions predominantly (83%) and COPhBF exclusively (100%) towards the polymer particles. The activity, as determined in bulk polymerization, ranges from $(24 - 40) \cdot 10^3 \cdot 6$ for COBF and COEtBF and $(14 - 20) \cdot 10^3$ for COPhBF.⁶ The values as determined experimentally in emulsion polymerization (C_T^{emul}) for COBF and COEtBF are in good agreement with the values reported in literature.⁶ The experimentally obtained C_T^{emul} value for COPhBF is lower than was expected. The value of $6 \cdot 10^3$ was confirmed in bulk polymerization. This discrepancy is most likely due to the moderate purity of the catalyst.

The presence of a CCTA in the aqueous phase of an emulsion polymerization is suggested to result in a decrease of the entry rate of surface active oligomers as aqueous phase chain transfer events can result in termination of propagating radicals prior to reaching sufficient surface activity to allow entry.¹¹ The number-average degree of polymerization is inversely proportional to the CCTA concentration, see Chapter 1 Equation 4. The more CCTA partitions towards the aqueous phase the higher the probability for chain transfer in the aqueous phase becomes and consequently the lower the rate of entry. For CCTA's with a low partition coefficient (m_{C_0}), a significant amount of CCTA will be present in the aqueous phase and a significant decrease in the entry rate can be expected. For CCTA's with high partition coefficients, the effect of aqueous phase chain transfer on the entry rate is negligible. Using the modified Mayo equations (Chapter 5 Equations 1 and 2) and the intrinsic activities and partitioning behavior as reported in Table 2, the aqueous phase number-average degrees of polymerization ($DP_{n,w}$) for the various CCTA's can be estimated. For COBF and COEtBF, which partition towards the aqueous phase, $DP_{n,w}$ of 3 and 122 are calculated. In the case of COBF, $DP_{n,w}$ approaches the predicted required length for entry ($z = 4$ for methyl methacrylate and V50)²⁶ and a severe retardation of the rate of entry can be expected. Note that the so-called z -value is calculated for a radical carrying an initiator fragment. In COBF mediated emulsion polymerization, initiation proceeds predominantly through monomeric radicals. These radicals have poor aqueous phase solubility and will most likely partition between the aqueous phase and the polymer particles ($m_{M_1} = \frac{[M]_p}{[M]_{aq}} = 44$ for MMA).²⁷ The number of propagation steps required in the aqueous phase before chain transfer derived radicals partition completely towards the polymer particle phase are probably less than calculated based on the Maxwell-Morrison model. For COEtBF a small effect on the rate of entry is expected as the $DP_{n,w}$ amply exceeds the required length for entry. CPhBF displays no partitioning towards the aqueous phase and consequently no direct effect on the entry rate is expected. However, desorption of radicals from the particle phase towards the aqueous phase might result in a slight increase in the rate of termination in the aqueous phase. The rate of entry in the

COPhBF mediated emulsion polymerization is expected to be comparable to the rate of entry in the absence of CCTA. The average number of radicals per particle (\bar{n}) depends both on entry and exit events. As the rates of exit, based on the transfer frequency, should be comparable for all CCTA's under investigation, the difference in \bar{n} and consequently the rate of polymerization are directly related to differences in the entry rate. The higher observed rate of polymerization for COEtBF when compared to COBF, see Figure 1, is a result of the difference in partitioning. The highest rate of polymerization was expected for COPhBF, however, this was not observed experimentally, see Figure 1. This could be due to the small particle sizes obtained in the COPhBF mediated polymerizations. The exit rate coefficient depends on the particle size, see Equation 2. Consequently, the small particles obtained in the COPhBF mediated polymerizations could display an enhanced rate of exit when compared to COBF and, in a lesser extent, to COEtBF.

The semi-empirical approach to approximate \bar{n} , as presented in Chapter 5, can be applied to give an estimate of m , the ratio of radical desorption and radical termination, see Equation 3.²⁸⁻³⁰ The results of the calculations are presented in Table 3.

$$m = \frac{k_f V_p}{k_{tp}} \quad \text{with} \quad k_{dM} = \frac{12D_w}{m_{M_1} d_p^2} C_T \quad (3)$$

For the polymerization without a CCTA, a rather low value for m is estimated. Radical termination is dominant for CCTA free recipes. However, the addition of a CCTA results in a large increase in m . It is noteworthy to mention that the value of m for COPhBF (13.5) is approximately one order of magnitude lower than those for COBF and COEtBF (131). The values of m for the various CCTA's indicate that the chain transfer activity in the COEtBF and COBF mediated polymerizations is slightly higher than that in COPhBF. This is in line with the experimentally obtained DP_n , which is slightly higher in the case of COPhBF. A diffusion coefficient for a radical inside a polymer particle can be estimated and consequently a time of escaping of a monomeric radical by exit (θ) calculated, see Equation 4. The time required for one propagation step (t_p), and thus rendering the radical unable to exit the polymer particle, is given in Equation 5.

$$\theta = \frac{d_p^2}{2D_p} \quad \text{where} \quad D_p = \frac{k_B T}{3\pi\eta_0 d_p} \quad (4)$$

$$t_p = \frac{1}{k_p^1 [M]_p} \quad \text{where} \quad k_p^1 = 15.8k_p \quad {}^{31,32} \quad (5)$$

Two limiting situations exist:

$\theta \gg t_p$ radical exit is dominant over propagation.

$\theta \ll t_p$ propagation is dominant over radical exit.

where k_p^1 is the propagation rate coefficient of a monomeric radical and $[M]_p$ the concentration of monomer inside the polymer particle.

Table 3. The results of the semi-empirical calculation of \bar{n} .

$[CCTA]$	α^a	k_{dM}^a	m	\bar{n}_{SS}	\bar{n}	θ	t_p	k^b
	[-]	$[s^{-1}]$	[-]	[-]	[-]	$[10^{-5} s]$	$[10^{-5} s]$	$[10^4 s^{-1}]$
-	$5.3 \cdot 10^{-4}$	$1.0 \cdot 10^{-5}$	$2.0 \cdot 10^{-3}$	0.292	0.250	2.40	0.94	4.73
COBF	$1.0 \cdot 10^{-3}$	$2.4 \cdot 10^4$	$1.3 \cdot 10^2$	0.028	0.016	3.33	0.94	3.35
	$1.7 \cdot 10^{-3}$	$1.9 \cdot 10^4$	$1.3 \cdot 10^2$	0.049	0.021	4.32	0.94	3.77
COEtBF	$2.8 \cdot 10^{-5}$	$1.6 \cdot 10^5$	$1.4 \cdot 10^2$	0.007	0.003	0.55	0.94	12.2
	$7.7 \cdot 10^{-4}$	$4.3 \cdot 10^4$	$2.0 \cdot 10^2$	0.005	0.014	0.29	0.94	4.14
COPhBF	$4.4 \cdot 10^{-6}$	$3.8 \cdot 10^4$	$1.3 \cdot 10^1$	0.002	0.0011	0.22	0.94	23.2
	$6.7 \cdot 10^{-6}$	$3.3 \cdot 10^4$	$1.4 \cdot 10^1$	0.002	0.0013	0.27	0.94	20.1

^a See Chapter 5 for a definition of these parameters. ^b Calculated using Equation 2 with a $D_w = 1.68 \cdot 10^{-9} \text{ m}^2 \text{ s}^{-1}$. ³³ $k_p(343 \text{ K}) = 1053 \text{ dm}^3 \text{ mol}^{-1} \text{ s}^{-1}$. α'_w is the ratio of radical production and radical termination and k_f the rate constant for radical desorption from the polymer particles.

The average time required for a monomeric radical to leave the polymer particle decreases with particle size, see Equation 4. For COEtBF and CPhBF the characteristic time for exit is smaller than the time for the first propagation step, implying that a significant amount of monomeric radicals will exit the polymer particle. Note that the values for m , see Equation 3 and Table 3, reveal that chain stoppage is by far dominated by chain transfer. Bimolecular termination hardly contributes to the total rate of chain stoppage. The exit rate coefficient increases with decreasing particle size, see Equation 2. These global calculations demonstrate that observed differences in the rate of polymerization might be explained by the difference in the average particle size. The small particles obtained in the case of COEtBF and CPhBF result in low time constants for radical exit and consequently in a low value for \bar{n} . A comparison of the performance in terms of the polymerization rate in the presence of the three different CCTA's is not straightforward as partitioning, chain transfer activity and particle size effects are not mutually exclusive. Seeded emulsion polymerization may shine more light on the performance of different CCTA's as the particle number and the particle size can be controlled.

Particle Nucleation

Ab initio emulsion polymerizations of MMA, for recipes without a CCTA result in a monomodal latex with a narrow particle size distribution with an average particle size in the range of 50 to 100 nm. In the presence of a CCTA, the particle size distribution is affected in two ways. First, the presence of a CCTA inside the polymer particles results in radical desorption. Radical desorption shortens the average residence time of radicals inside the polymer particles and consequently lowers the volume growth rate of a particle. Secondly, the presence of a CCTA in the aqueous phase affects the rate of

radical entry and retards particle nucleation. Radical desorption and retarded nucleation have counter-acting effects on the particle size distribution. Per unit of time, fewer particles are nucleated which, under conventional emulsion polymerization conditions, would result in a lower particle number, larger particles and a broader particle size distribution. However, radical desorption restricts the volume growth rate, which under conventional emulsion polymerization conditions, would result in a higher particle number and smaller particles. Transmission electron microscopy (TEM) micrographs and the derived particle size distribution of the final latexes produced with the various CCTA's are presented in Figure 2. The number average and volume average particle diameters as determined by dynamic light scattering (DLS) and transmission electron microscopy (TEM) are collected in Table 4.

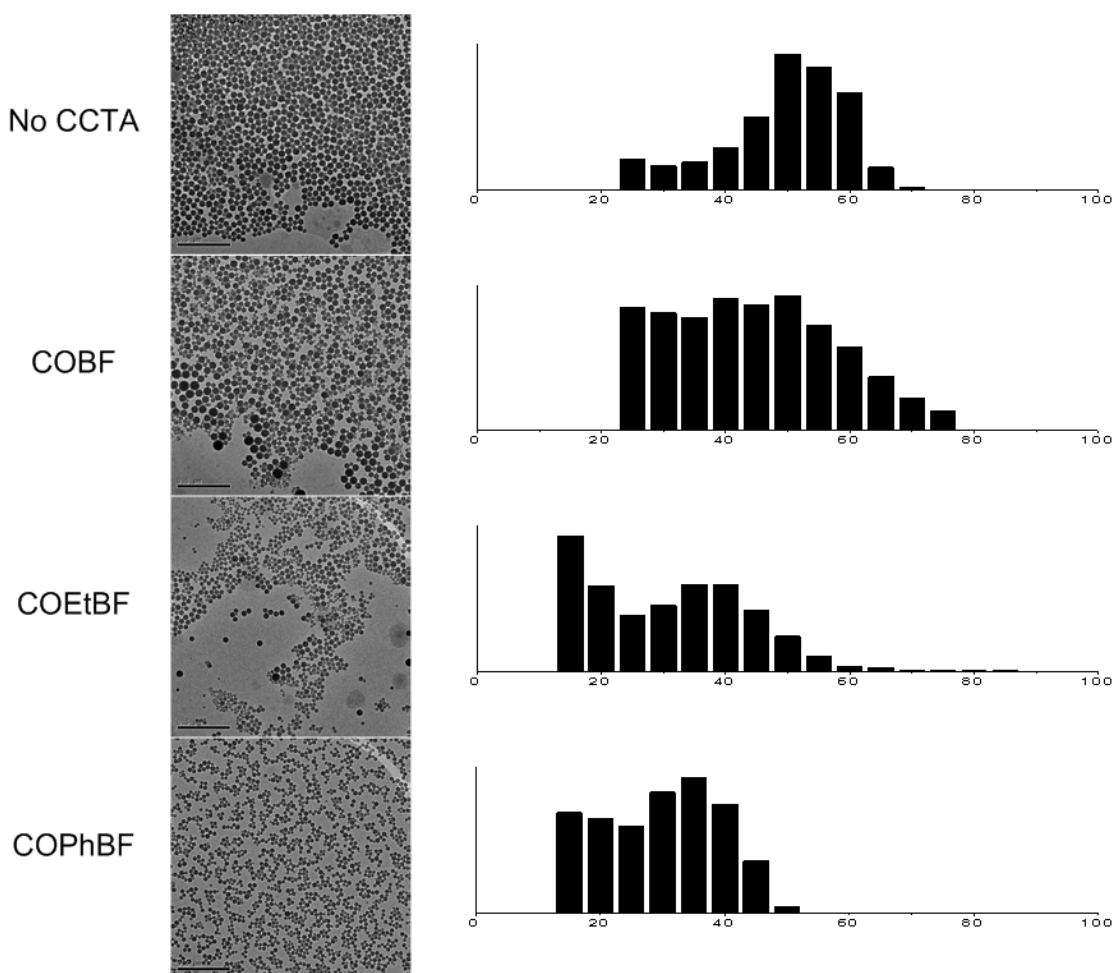


Figure 2. Particle size distributions for the polymerizations with different catalytic chain transfer agents.

The particle size distributions (PSD) as derived from TEM pictures clearly illustrate the effect of different CCTA's on the PSD. The unmediated emulsion polymerization results in a rather narrow PSD with an average particle size of 50 nm. CPhBF partitions exclusively towards the polymer particles. As a consequence, the entry rate of radicals is hardly affected and fast nucleation of polymer particles will occur. However, due to the presence of CPhBF inside the polymer particles, radical desorption occurs, thereby reducing the volume growth rate. The overall result is small particles and a high particle number. When the CCTA is present in the aqueous phase, particle nucleation is affected and this results in a broader PSD. In a batch reactor, the different stages of emulsion polymerization are separated in time. However, when nucleation is retarded, some overlap in particle nucleation and growth can occur. Particle nucleation is retarded and this results in growing particles competing for the available surfactant with the monomer swollen micelles. For COBF the chain transfer activity inside the polymer particle is comparable to the case of COEtBF and CPhBF, see Table 2. However, there is a significant amount of COBF present in the aqueous phase. Besides the reduction in the volume growth rate, particle nucleation is retarded. This apparently results in a situation where the average particle size remains comparable to the case where no CCTA is used, but the obtained distribution has a different shape. For COEtBF only a marginal amount of the CCTA is present in the aqueous phase. Particle nucleation will be reduced, however not to the same extent as is the case for COBF. This results in a PSD which appears as an intermediate between COBF and CPhBF.

Table 4. The number average and volume average particle diameters as determined by DLS and TEM.

	DLS				TEM		
	d_p (N)	d_p (V)	PDI ^a	Poly ^b	d_p (N)	d_p (V)	PDI ^a
	[nm]	[nm]	[-]	[-]	[nm]	[nm]	[-]
-	-	49.2	-	0.057	36.3	51.3	1.41
COBF	47.4	58.5	1.23	0.127	29.7	54.5	1.83
	43.1	55.1	1.28	0.086			
COEtBF	21.9	30.7	1.41	0.203	24.5	41.0	1.67
COPhBF	17.0	22.2	1.30	0.102	24.5	33.9	1.38
	18.4	23.9	1.30	0.164			

^a The polydispersity index of the distribution is defined as: $PDI = d_p(V) / d_p(N)$.

^b poly is the polydispersity of the particle size distribution as calculated by the Malvern® software.

Control of the Molecular Weight Distribution

Figure 3 shows the evolution of the number-average degree of polymerization (DP_n) during the course of the polymerization for the various CCTA's. The absolute DP_n as a function of the conversion is presented in Figure 3A and the normalized DP_n (i.e. $DP_n(x) / DP_n(x \rightarrow 0)$) in Figure 3B. The constant chain transfer frequency was calculated based on the final DP_n as obtained in the polymerizations mediated with COBF, COEtBF and COPhBF. From Figure 3A it is evident that the final values of the cumulative number-average degree of polymerization are comparable, however, a significant difference in DP_n and consequently the chain transfer frequency is obtained during the course of the polymerization, see Figure 3B.

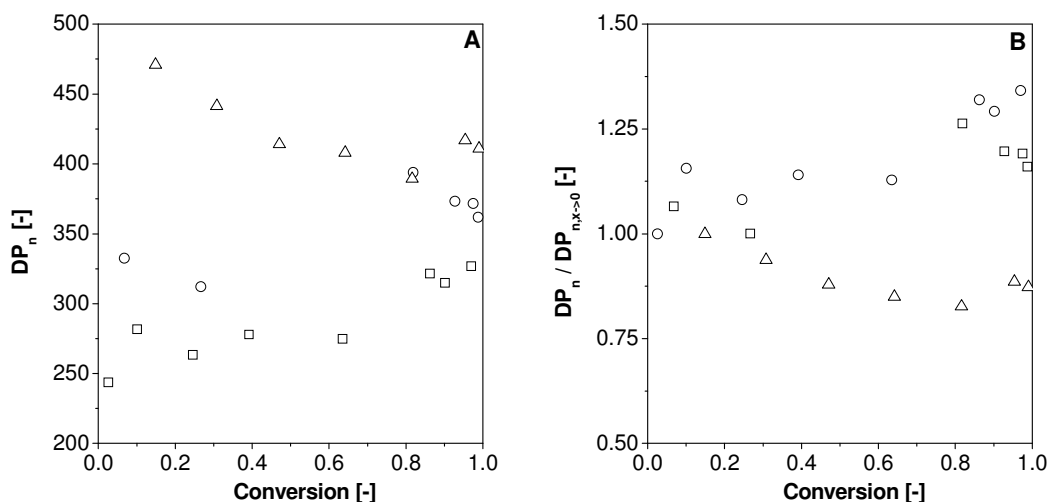


Figure 3. Cumulative number-average degree of polymerization as a function of the conversion for the catalytic chain transfer mediated emulsion polymerization with comparable chain transfer activity inside the polymer particles. A. Absolute DP_n and B. Normalized DP_n , defined as $DP_n(x) / DP_n(x \rightarrow 0)$; (O) 0.22 ppm COEtBF; (□) 2 ppm COBF and (Δ) 2 ppm CPhBF. 1 ppm is defined as 1 mol CCTA per 10^6 moles of monomer.

Both for COBF and COEtBF the DP_n is increasing slowly over the first 60% of the polymerization, followed by a significant increase towards the end of the polymerization. The gradual increase of DP_n over the first 60% of the course of the polymerization can be accounted to CCTA deactivation in the aqueous phase. The strong increase towards the end of the polymerization coincides with the gel-effect. In the case of CPhBF, initially, a relatively strong decrease in DP_n occurs after which DP_n remains approximately constant around $DP_n = 400$. Two major differences between the behavior of CPhBF and the behavior of COBF and COEtBF can be noted. For CPhBF, DP_n decreases in the initial stage of the polymerization and for COBF and COEtBF at conversions above 80% DP_n increases strongly as a result of the gel-effect. The origin of these differences follows from the partitioning behavior of the CCTA's. Both COBF and COEtBF partition towards the aqueous phase. This renders these complexes susceptible towards deactivation in the aqueous phase but it also allows for rapid exchange of the CCTA between the polymer particles. CPhBF has no aqueous phase solubility and

consequently aqueous phase CCTA deactivation is minimized.⁹ Exchange of COPhBF between the particles can only occur by the so-called shuttle-effect.^{34,35} Transport of COPhBF molecules could occur via the collision of two entities, i.e. micelle, droplet or polymer particle. The COPhBF catalyst, initially, resides inside the monomer droplets and monomer swollen micelles. The fact that a decrease in DP_n with conversion is observed experimentally indicates that initially a certain amount of CCTA is not active in the control of the molecular weight of the polymer. The end of interval II marks the disappearance of the monomer droplets. For a MMA emulsion polymerization this occurs at approximately 30% conversion. After the disappearance of the monomer droplets, the CCTA can only reside inside the polymer particles. This is in agreement with the experimental observations, where after approximately 30% conversion DP_n remains constant within experimental error. The observed course of DP_n during the polymerization is a strong indication for the existence of different mass transport mechanisms in emulsion polymerization, i.e. COPhBF by the shuttle-effect and COBF and COEtBF via the aqueous phase.

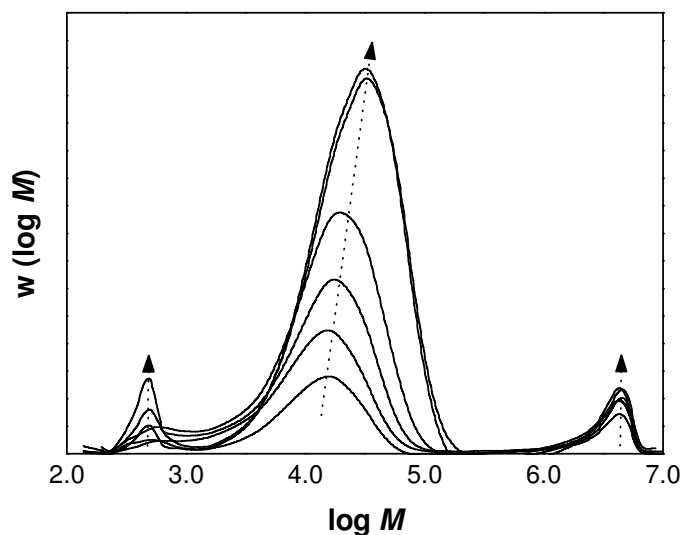


Figure 4. Typical evolution of the molecular weight distribution for an *ab initio* CCTA mediated emulsion polymerization. CCTA: 5.0 ppm COBF. Arrows indicate the increase in conversion.

Figure 4 presents a typical molecular weight distribution for the *ab initio* emulsion polymerizations in the presence of a CCTA. For a CCT mediated free radical polymerization, a monomodal molecular weight distribution, with a polydispersity of 2, is expected.⁶ However, *ab initio* CCT mediated emulsion polymerizations very often display 2 additional molecular weight distributions. The low molecular weight polymer ($\log M < 3.0$) originates from aqueous phase chain transfer events. Oligomers propagating in the aqueous phase can undergo chain transfer before becoming sufficiently surface active to give entry into a polymer particle. The intensity of this molecular weight distribution proved to depend on the type of CCTA (i.e. the partitioning behavior towards the aqueous phase) and the concentration of the CCTA in the aqueous phase. Note that the low molecular weight polymer is being produced throughout the course of the polymerization. The high molecular weight polymer ($\log M > 6.0$) is formed in the initial stages of the polymerization. CCT mediated emulsion polymerizations often proceed in a regime where there are less CCTA molecules than polymer particles. For proper molecular weight control, the CCTA has to be able to mediate multiple polymer particles. This implies that the time constant of CCTA entry has to be larger than the time constant for radical entry. Based on the partitioning data (Table 2) and the final particle number of the polymerizations (Table 1), the number of CCTA molecules per polymer particle can be calculated: $N_{\text{CCTA}} / N_p = 0.17$ for COBF, 0.015 for COEtBF and 0.071 for CPhBF. Although these values are far from unity, control of the molecular weight distribution can be achieved (see Chapter 3 of this thesis). However, in the beginning of the polymerization, the CCTA may be present in the monomer swollen micelles, monomer droplets and freshly nucleated polymer particles. The number of monomer swollen micelles in an emulsion polymerization is typically around 10^{21} dm^{-3} . This results in a situation where the ratio of CCTA molecules to monomer swollen micelles is much smaller than in interval II. As both radical and CCTA entry are statistical processes, it is not unlikely that a freshly nucleated particle experiences no CCTA entry event during the lifetime of a radical inside that particle. This would result in a classic free radical polymerization within that polymer particle and consequently high molecular weight polymer. Note that the high molecular weight polymer is formed mainly during the initial

stages of the polymerization, which coincides with the particle nucleation stage, see Figure 4. As the monomer swollen micelles are consumed by the growing particles the ratio of CCTA molecules to monomer swollen micelles / polymer particles increases and the probability of two consecutive radical entries is reduced. As it is a statistical process, the possibility of the formation of high molecular weight polymer remains throughout the course of the polymerization, as can be observed from Figure 4. Note that the obtained molecular weight distributions from the CPhBF mediated polymerizations also display a very small high molecular weight peak. This implies that the CPhBF mass transport via the shuttle-mechanism is sufficiently fast to ensure proper control of the molecular weight distribution.

CONTINUOUS EXPERIMENTS IN THE PSPC

The continuous emulsion polymerization experiments are performed in the Pulsed Sieve Plate Column (PSPC). In the PSPC the combination of low net flow rates, limited backmixing and intensive radial mixing is achieved.^{20,36} For conventional emulsion polymerization recipes, the properties of the latex produced are not significantly different from those of a batch process, provided that the backmixing is limited.³⁷ The experimental results obtained in the previous section with batch operation are compared with the results in the PSPC. Comparison of the results of batch wise operation and of the continuous operation in the PSPC allows for an evaluation of the performance and scalability of CCT in the PSPC. The axial mixing in the PSPC can be quantified by the dimensionless Peclet number (Pe), see Chapter 1 Equation 31. To ensure proper axial mixing in the column a $Pe \geq 100$ is required. The net liquid velocity in the column is determined by the residence time of the polymerization. Previous results have shown that the colloidal stability of the final dispersion can be affected by the presence of a CCTA. Coagulation, which was incidentally observed for batch experiments, occurred predominantly in the final stages of the polymerization. Coagulation in the PSPC was circumvented, by limiting the conversion in the PSPC to approximately 0.5-0.7. The residence times for the various CCTA's were derived from the corresponding conversion-time profiles of the batch experiments. For COBF, COEtBF and CPhBF

residence times of 1500, 1200 and 2060 s were chosen. The other key parameter defining the axial mixing in the column is the axial mixing coefficient (E), which is related to the pulsation stroke length (s) and the pulsation frequency (f). The reported experiments were performed at a $Pe = 166$, which is sufficient to have the same performance as for an *ab initio* batch emulsion polymerization. A summary of all the operational conditions is presented in Table 9 (Experimental section). The conversion-axial position profiles for the experiments with comparable chain transfer activity inside the polymer particles are presented in Figure 5. The polymerization rate data and final latex properties are collected in Table 5.

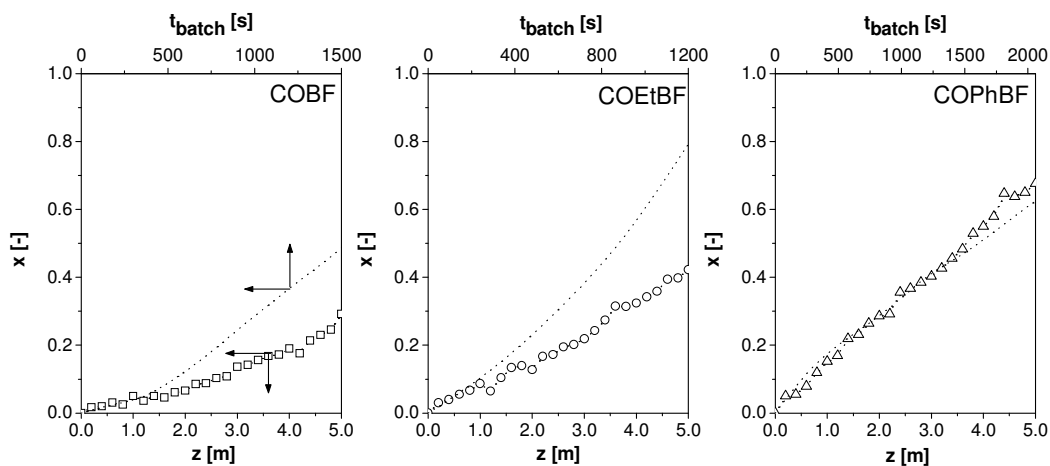


Figure 5. Conversion-axial position profiles for the polymerizations for the *ab initio* emulsion polymerization of MMA in a batch reactor and the PSC. (○) 0.22 ppm COEtBF, $E = 1.25 \cdot 10^{-3} m^2 s^{-1}$, $\tau = 1200 s$; (□) 2 ppm COBF, $E = 0.73 \cdot 10^{-3} m^2 s^{-1}$, $\tau = 1500 s$ and (△) 2 ppm COPhBF, $E = 0.73 \cdot 10^{-3} m^2 s^{-1}$, $\tau = 2060 s$. The dotted lines are the conversion-time profiles of the batch experiments.

Table 5. Final latex properties of the experimentally obtained latexes in the presence of COBF, COEtBF and COPhBF in the PSPC.

[CCTA]	x	DP_n	R_p	\bar{n}_{SS}	d_p	N_p	$\bar{n}_{SS} N_p$
	[-]	[-]	$[mol \cdot dm_w^{-3} s^{-1}]$	[-]	[nm]	$[10^{18} dm_w^{-3}]$	$[10^{16} dm_w^{-3}]$
COBF	0.29	172	$4.1 \cdot 10^{-4}$	0.021	58.7	1.70	3.71
	0.29		$3.6 \cdot 10^{-4}$	0.019	58.1	1.76	3.26
COEtBF	0.45	230	$6.9 \cdot 10^{-4}$	0.028	53.6	2.24	6.30
	0.42		$7.9 \cdot 10^{-4}$	0.029	-	-	-
COPhBF	0.68	380	$7.8 \cdot 10^{-4}$	0.008	33.5	9.15	7.08
	0.67		$8.4 \cdot 10^{-4}$	0.009	34.0	8.77	7.65

The results in Table 5 demonstrate that there is a distinct difference in the behavior of the various CCTA's: if the CCTA partitions towards the aqueous phase, a discrepancy between the rates of polymerization in batch and in the PSPC is obtained. However, when the CCTA displays no partitioning towards the aqueous phase, the conversion-residence time profiles for batch and continuous operation are identical. The polymerizations with COBF and COEtBF in the PSPC display a rate of polymerization which is approximately half of that obtained for batch operation. The differences between batch wise and continuous operation for COBF and COEtBF could arise from differences in the nucleation in both reactor types. The conversion at which the nucleation stage of an emulsion polymerization ends (x_{nuc}) can be calculated according to Equation 6.³⁸

$$x_{nuc} = \frac{\varphi_{pol}}{\varphi_{mon} / \rho_{mon} + \varphi_{pol} \rho_{pol}} V_p \frac{1}{[M]_0} \quad (6)$$

where φ_{pol} is the weight fraction of polymer in the polymer particles, φ_{mon} the weight fraction of monomer in the polymer particles, ρ_{pol} and ρ_{mon} the densities of polymer and monomer respectively, V_p the volume of the polymer particles per unit volume of water and $[M]_0$ the overall concentration of monomer at the start of the polymerization per unit volume of water. For an MMA emulsion polymerization with the recipe used in this

work, the conversion corresponding with the end of the nucleation stage is calculated to be 0.18. For COBF and COEtBF this implies that particle nucleation proceeds throughout a large part of the column, i.e. $z = 3.8$ and 2.5 m respectively. For COPhBF particle nucleation proceeds almost exclusively in the first segment, i.e. $z = 1.1$ m. Nucleation in continuous emulsion polymerization is sensitive towards backmixing. In the nucleation zone of the PSPC, backmixing brings growing polymer particles in a region with a lot of surfactant. As the growing particles adsorb surfactant molecules to maintain their colloidal stability, monomer swollen micelles are consumed. This ultimately results in less nucleation and less particles as compared with batch operation so there is a discrepancy to be expected between batch and PSPC operation with respect to the course of the polymerization and the final latex properties. Due to the residence time distribution in the PSPC the nucleation zone is longer than for a plug flow reactor. Even though proper pulsation conditions have been applied ($Pe \geq 100$), effects of backmixing inside the PSPC cannot be excluded, especially since the presence of a CCTA prolongs the nucleation stage in the PSPC. A comparison between the particle size distributions as obtained in batch polymerization and in the PSPC is presented in Figure 6. The average particle sizes as determined from the TEM micrographs are collected in Table 6.

Table 6. The number average and volume average particle diameters as determined by TEM.

	TEM BATCH				TEM PSPC			
	d_p (N)	d_p (V)	PDI ^a	N_p	d_p (N)	d_p (V)	PDI ^a	N_p
	[nm]	[nm]	[-]	[$10^{18} dm_w^{-3}$]	[nm]	[nm]	[-]	[$10^{18} dm_w^{-3}$]
COBF	29.7	54.5	1.83	2.00	34.9	55.4	1.59	1.73
COEtBF	24.5	41.0	1.67	13.6	26.9	45.5	1.69	2.24
COPhBF	24.5	33.9	1.38	31.6	21.4	38.6	1.80	33.8

^a The polydispersity index of the distribution is defined as: $PDI = d_p(V) / d_p(N)$.

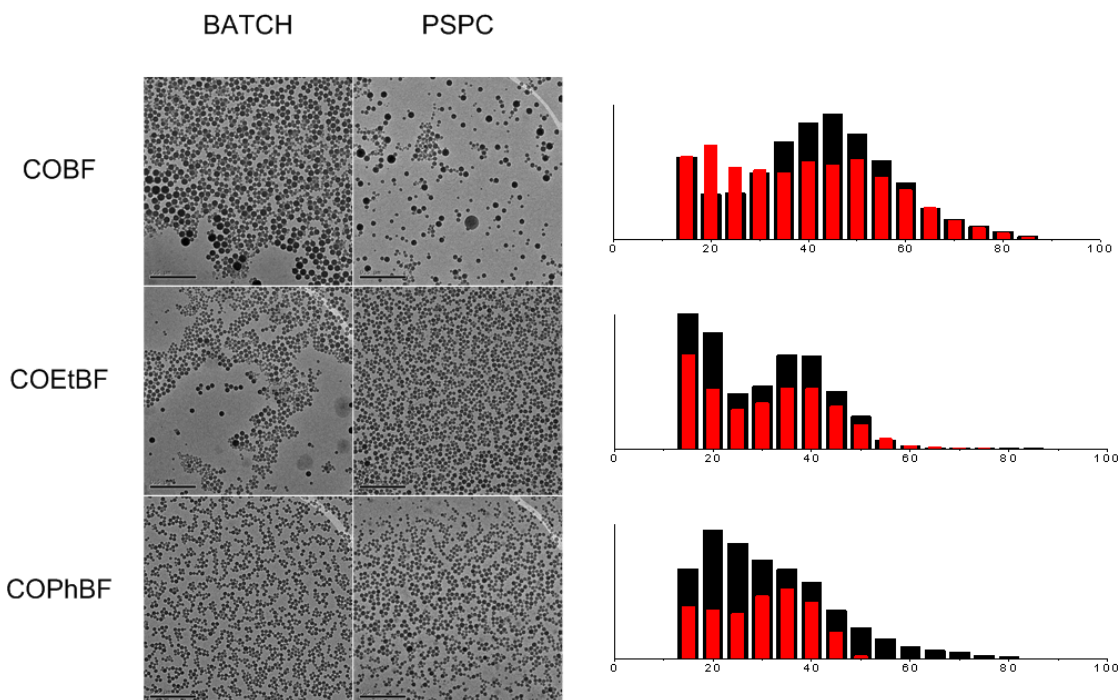


Figure 6. Particle size distributions as obtained in batch (red bars) and PSPC (black bars) as determined from TEM analysis.

From Figure 6 it can be concluded that there is hardly a difference between the PSD as obtained in batch and the PSPC for COBF and COEtBF. The PSD obtained for COPhBF in the PSPC appears to be broader than in batch, see Figure 6. This is a clear effect of backmixing in the PSPC. The average particle sizes for batch and PSPC products are comparable within experimental error. Since the PSDs of the batch and continuous polymerization overlap for COBF and COEtBF, indicates that the effects of backmixing in the PSPC are almost completely overshadowed by the effects of the CCTA on nucleation. For COPhBF the effect on nucleation are less pronounced and as a consequence the effects of backmixing on the PSD are observed, see Figure 6.

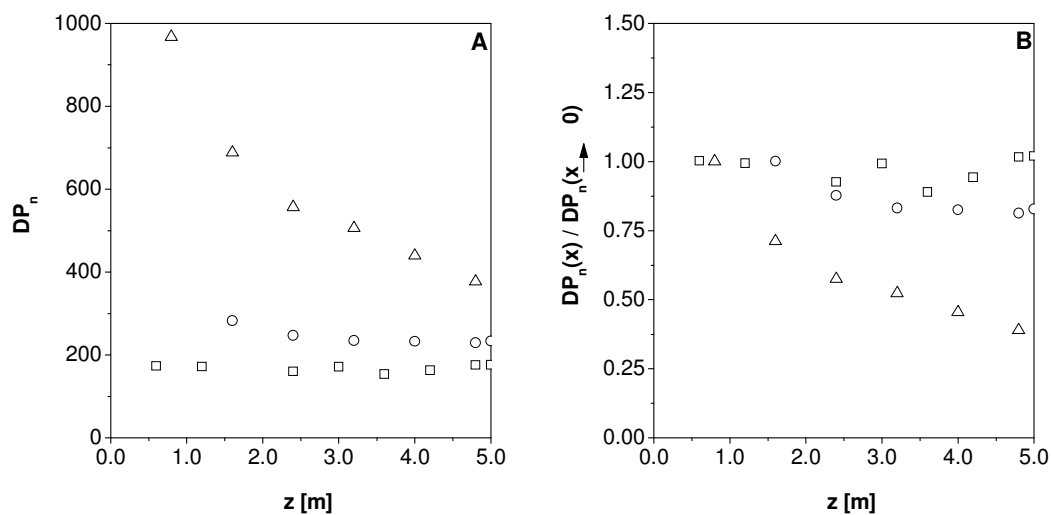


Figure 7. Cumulative number-average degree of polymerization as a function of the conversion for the catalytic chain transfer mediated emulsion polymerization with comparable chain transfer activity inside the polymer particles in the PSPC. A. Absolute DP_n and B. Normalized DP_n , defined as $DP_n(x) / DP_n(x \rightarrow 0)$. (○) 0.22 ppm COEtBF; (□) 2 ppm COBF and (△) 2 ppm COPhBF.

Figure 7 shows the cumulative and normalized DP_n over the course of the polymerization. The observed trends in the DP_n in the PSPC are comparable to those observed in the batch polymerizations, see Figure 3. An increase in DP_n as a consequence of the gel-effect was not observed in the PSPC as the conversion for the experiments was always lower than 0.70. Also, for COBF and COEtBF hardly any increase in DP_n due to CCTA decomposition was observed. The decrease in the DP_n in the COPhBF mediated polymerization is stronger than observed for batch operation. A comparison between batch and continuous operation on the absolute DP_n is presented in Figure 8. For COBF as well as for COEtBF, which both display partitioning towards the aqueous phase, a lower value of DP_n is obtained when compared to the batch experiments. The final DP_n for the COPhBF in the PSPC is comparable to that obtained for batch operation. However, the decrease in the DP_n over the course of the polymerization is more severe in the PSPC than in batch.

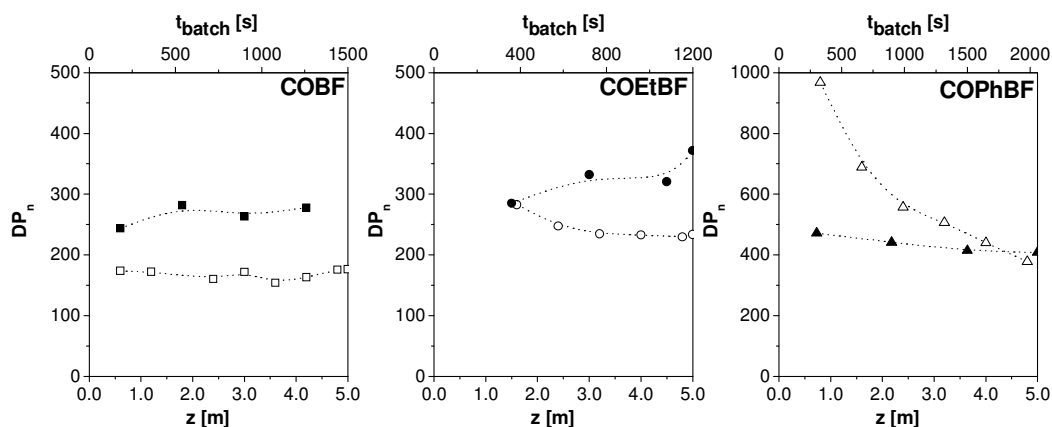


Figure 8. A comparison of the absolute degree of polymerization on batch and continuous scale. Solid symbols = batch and open symbols = PSPC. (\square) COBF; (\circ) COEtBF and (\triangle) CPhBF.

The fact that in the PSPC a lower DP_n is observed than in batch for both COBF and COEtBF implies that the particles experience an apparently higher CCT activity. For COBF and COEtBF chain transfer frequencies of 19.0 s^{-1} and 14.2 s^{-1} are calculated based on the experimentally obtained DP_n . The chain transfer frequency of CPhBF hardly changed, see Table 7.

Table 7. The partitioning behavior and intrinsic activity in the PSPC.

$[CCTA]$	DP_n^a	m_{Co}	$[Co]_0$	$[Co]_p$	F_p^b	$C_T^{app}^c$	f_{tr}^d
	[-]	[-]	$[mol \cdot dm^{-3}]$	$[mol \cdot dm_p^{-3}]$	[-]	$[10^3 \text{ -}]$	$[10^1 \text{ s}^{-1}]$
COBF	172	0.72^e	$3.74 \cdot 10^{-6}$	$2.86 \cdot 10^{-6}$	0.153	14.4	19.0
COEtBF	230	19^f	$4.61 \cdot 10^{-7}$	$1.90 \cdot 10^{-6}$	0.826	99.7	14.2
CPhBF	380	∞^e	$3.74 \cdot 10^{-6}$	$18.7 \cdot 10^{-6}$	1.000	6.5	8.6

^a Experimentally obtained number-average degree of polymerization $DP_n = M_w / 2M_0$ ^{22,23} ^b The mol fraction of CCTA at the locus of polymerization ^c The experimentally determined apparent chain transfer constant ^d The chain transfer frequency, see Equation 1 ^e experimentally determined partitioning coefficient^{14,24} and ^f taken from ref. 25.

This increased chain transfer activity can only originate from a higher CCTA concentration at the locus of polymerization. An increase in the CCTA concentration has detrimental effects on the course of the polymerization. An enhanced aqueous phase CCTA concentration will further restrict the radical growth in the aqueous phase and reduce the rate of entry. The increased chain transfer activity inside the polymer particles will increase the rate of radical exit. The net result is a decrease in \bar{n} and the rate of polymerization. For CPhBF this effect is not observed, indicating that the aqueous phase solubility of the CCTA is crucial in the performance in the PSPC. An obvious explanation for this observation could be backmixing in the bottom section of the column. In the bottom section of the column, the aqueous phase CCTA concentration could experience some backmixing, thereby increasing actual concentration. As the aqueous phase CCTA concentration is increasing, due to the thermodynamic equilibrium, so will the particle phase CCTA concentration. This results in an overall decrease of the DP_n and a retardation of the polymerization rate. CPhBF does not partition towards to aqueous phase and does not suffer from this phenomenon.

CONCLUSIONS

The results of this work demonstrate that the partitioning behavior of a CCTA is crucial for its performance in *ab initio* emulsion polymerization.

- The course of the polymerization depends on the aqueous CCTA concentration.
- Radical exit is significant in CCT mediated emulsion polymerizations. So these emulsion polymerizations obey Smith-Ewart Case 1 kinetics.
- The average particle size is governed by both the aqueous phase and particle phase CCTA concentration. The width of the particle size distribution is governed by the aqueous phase CCTA concentration.
- Especially in the initial stages of the polymerization, some free-radical polymerization without catalytic chain transfer can occur due to the large ratio of entities (i.e. monomer swollen micelles and polymer particles) to CCTA molecules.
- CPhBF mass transport seems to proceed via a shuttle-effect.

- *Ab initio* CCT mediated emulsion polymerization is possible in continuous emulsion polymerization in a PSPC.
- The operation characteristics of the PSPC were close to plug flow. For COBF and COEtBF the PSD in the PSPC proved to be dominated by the presence of the CCTA in the aqueous phase. For COPhBF the PSD proved to be dominated by the effects of backmixing inside the column.
- The presence of a CCTA in the aqueous phase of an emulsion polymerization in the PSPC proves to result in discrepancies between batch and PSPC polymerization with respect to the course of the polymerization and the molecular weight distribution.

These results contribute to a fundamental understanding of particle nucleation in emulsion polymerization in the presence of a catalytic chain transfer agent. The intrinsic activity and the partitioning behavior are key parameters that determine the final latex properties.

EXPERIMENTAL

Materials

The catalytic chain transfer agents, COBF, COEtBF and COPhBF were prepared according to the method of Bakač and Espenson.³⁹ For all experiments, a single batch of catalyst was used. Distilled deionized water (DDW) was used throughout all experiments. The monomer, methyl methacrylate (MMA, Aldrich, 99%) was distilled at reduced pressure to remove the inhibitor and stored at -24°C prior to usage. The initiator, 2,2'-azobis(2-methylpropionamide) dihydrochloride (V50, Aldrich, 97%), the surfactant, sodium dodecyl sulphate (SDS, Aldrich) and the buffer, sodium carbonate (SC, VWR, analysis grade), were used without any further purification.

Equipment

The batch experiments were performed in a 1.6 L Mettler Toledo RC1 reactor, equipped with a pitch blade impeller, calibration heater and temperature sensor. The RC1 program operated in isothermal mode.

The continuous experiments were performed in the Pulsed Packed Sieve Column (PSPC). The PSPC is a tubular reactor with a length (L) of 5 m and an internal diameter of 49.5 mm. Five stainless-steel jacketed segments, which can be thermostated separately, are placed on top of each other. The column contains a stacked stainless-steel sieve plate packing. The plates have a permeability of 34%. The distance between the sieve plates is 9 mm. A modified membrane pump is used for pulsation of the liquid in the column. Stroke length (s) and frequency (f) can be varied between 0 and 35 mm and 1 and 3.5 Hz, respectively. A schematic representation of the PSPC equipment is given in Figure 9.

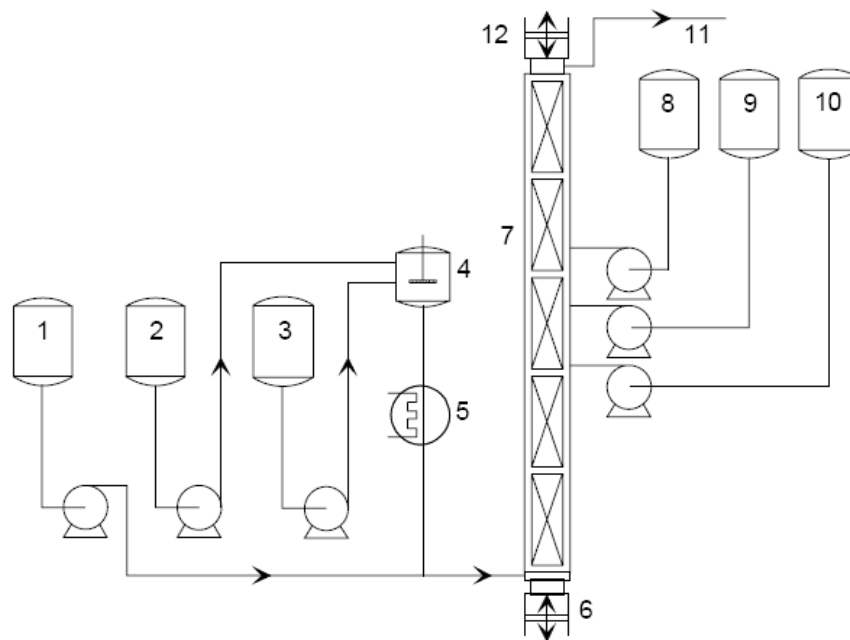


Figure 9. Pulsed Sieve Plate Column (PSPC) flow chart: storage vessels for respectively initiator solution (1), aqueous phase (2) and monomers (3, 8, 9, 10). (4), (5), (6), (7), (11), (12) represent the premixer, the preheater, the pulsator pump, the column packed with sieve plates, the product stream and the pulsation dampener, respectively.⁴⁰

Batch experiments

A catalyst stock solution (*i*) was prepared by dissolving an accurate amount of catalytic chain transfer agent in MMA. An initiator solution (*ii*) was prepared by dissolving an accurate amount of V50 (1.085 g, $4.0 \cdot 10^{-3}$ mol) in DDW (30 g). SDS (11.54 g, $4.0 \cdot 10^{-2}$ mol) and SC (0.848 g, $8.0 \cdot 10^{-3}$ mol) were weighted accurately and dissolved in DDW (770 g) and consequently added to the reactor. MMA (172 g, 1.72 mol) was added and the resulting emulsion was purged with argon whilst the impeller speed and reactor temperature were gradually raised to 250 rpm and 70°C. After 1 hr of purging the calibration was started. Subsequently, an amount of solution (*i*) (14 g) was added instantaneously to the reactor and stirred for 20 min to allow the reactor temperature to stabilize at the desired temperature of 70°C. The initiator solution (*ii*) (30 g) was added to the reactor using an accurate feeding pump to initiate the polymerization. The reactor was pressurized to 2 bars absolute pressure. Samples were withdrawn periodically to monitor the conversion, particle and molecular weight distribution. If the polymerization was performed in calorimetric mode, the final latex was analyzed to obtain the particle and molecular weight distribution and the conversion was obtained from the heat production profile.

PSPC experiments

Methyl methacrylate was charged in the monomer storage vessel (3). A catalyst stock solution was prepared by dissolving an accurate amount of catalytic chain transfer agent in MMA and added to the monomer storage vessel immediately prior to the polymerization. The surfactant (SDS) and buffer (SC) were dissolved in water and stored in the aqueous phase storage vessel (2). An aqueous initiator (SPS) solution was prepared in the initiator solution vessel (1). All vessels were purged with argon prior to the polymerization. Before the start-up, the premixer and the column were filled with water. First, the continuous phase feed was started followed by the monomer and finally initiator feed. The complete recipe and operational conditions are presented in Tables 8 and 9.

Table 8. The recipes for the catalytic chain transfer mediated emulsion polymerizations in the PSPC reactor.

Component	Mass [10^{-3} kg]	Feed rate [10^{-3} kg. s^{-1}]		
		COBF	COEtBF	COPhBF
Methyl methacrylate	1614	1.08	1.35	0.78
Distilled deionized water	6943	4.63	5.79	3.37
Sodium dodecyl sulphate	0.100	0.0667	0.0834	0.0486
Sodium carbonate	0.0074	0.0049	0.0061	0.0036
V50	0.0094	0.0062	0.0079	0.0046
CCTA	-	$9.65 \cdot 10^{-3}$	$1.59 \cdot 10^{-3}$	$1.05 \cdot 10^{-5}$

Table 9. The operational conditions for the catalytic chain transfer mediated emulsion polymerizations in the PSPC reactor.

Operational variables	COBF	COEtBF	COPhBF
Reactor volume [dm^3]	8.7	8.7	8.7
Residence time (τ) [s]	1500	1200	2060
u [10^{-3} m. s^{-1}]	3.33	4.17	2.43
Temperature [$^{\circ}C$]	70	70	70
Absolute pressure [bar]	2.7	2.7	2.7
Column Length (L) [m]	5.0	5.0	5.0
Stroke length (s) [10^{-3} m]	10	10	10
Frequency (f) [Hz]	1.6	2.5	1.5
E [10^{-5} m 2 . s^{-1}]	7.30	12.5	7.30
Peclet number [-]	166	166	166

Size exclusion chromatography

Size exclusion chromatography (SEC) was performed using a Waters 2690 separation module and a model 410 differential refractometer. A set of five Waters Styragel HR columns (HR5.0, HR4.0, HR3.0; HR1.0; HR0.5) were used in series at 40°C. THF was used as the eluent at a flow rate of 1 mL.min⁻¹, and the system was calibrated using

narrow molecular weight polystyrene standards ranging from 374 to $1.1 \cdot 10^6 \text{ g.mol}^{-1}$. Mark Houwink parameters used for the polystyrene standards: $K = 1.14 \cdot 10^{-4} \text{ dL.g}^{-1}$, $a = 0.716$ and for poly(methyl methacrylate): $K = 9.44 \cdot 10^{-5} \text{ dL.g}^{-1}$, $a = 0.719$.

Static light scattering

Particle size distributions were measured on a Malvern Zetasizer Nano. All latex dispersions were diluted with distilled deionized water prior to the measurement. For each measurement the obtained particle size distribution data was averaged over 3 individual runs.

ACKNOWLEDGEMENT

The authors would like to acknowledge Timo J.J Sciarone for the synthesis of the used complexes, Rinske M.J.W. Knoop for the TEM measurements and Jo M.M. Simons for the particle size analysis of the TEM pictures.

REFERENCES AND NOTES

1. Enikolopyan, N.S.; Smirnov, B.R.; Ponomarev, G.V.; Belgovskii, I.M. *J. Polym. Sci., Polym. Chem. Ed.* 1981, 19, 879.
2. Smirnov, B.R.; Morozova, I.S.; Pushchaeva, L.M.; Marchenko, A.P.; Enikolopyan, N.S. *Dokl. Akad. Nauk. SSSR (Engl. Transl.)* 1980, 255, 609
3. Smirnov, B.R.; Morozova, I.S.; Marchenko, A.P.; Markevich, M.A.; Pushchaeva, L.M.; Enikolopyan, N.S. *Dokl. Akad. Nauk. SSSR (Engl. Transl.)* 1980, 253, 891
4. Gridnev, A.A., *J. Polym. Sci. Part A. Polym. Chem* 2000, 38, 1753
5. Gridnev, A.A.; Ittel, S.D. *Chemical Reviews* 2001, 101, 3611.
6. Heuts, J.P.A.; Roberts, G.E.; Biasutti, J.D., *Australian Journal of Chemistry* 2002, 55, 381.
7. Cunningham, M.F. *Prog. Polym. Sci.* 2008, 33, 365.
8. Suddaby, K.G.; Haddleton, D.M.; Hastings, J.J.; Richards, S.N.; O'Donnell, J.P. *Macromolecules* 1996, 29, 8083.
9. Kukulj, D.; Davis, T. P.; Gilbert, R. G. *Macromolecules* 1997, 30, 7661.

10. Bon, S. A. F.; Morsley, D. R.; Waterson, J.; Haddleton, D. M.; Lees, M. R.; Horne, T. *Macromol. Symp.* 2001, 165, 29.
11. Kukulj, D.; Davis, T.P.; Suddaby, K.G.; Haddleton, D.M.; Gilbert, R.G. *J Polym. Sci. Part A: Polym. Chem.* 1997, 35, 859
12. Pierik, S.C.J.; Smeets, B.; van Herk, A.M. *Macromolecules* 2003, 36, 9271
13. Haddleton, D.M.; Morsley, D.R.; O'Donnell, J.P.; Richards, S.N. *J Polym. Sci. Part A: Polym. Chem.* 2001, 37, 3549.
14. Smeets, N.M.B; Heuts, J.P.A.; Meuldijk, J.; van Herk, A.M.; *J. Polym. Sci. Part A: Polym. Chem.* 2008, 46, 5839.
15. Chern, C-S. in *Principles and applications of emulsion polymerization*. Ed. Chern, C-S., Wiley, 2008.
16. Gilbert, R.G. in *Emulsion polymerization: A mechanistic approach*. Ed. Gilbert, R.G., Academic Press, 1995.
17. Meuldijk, J.; van Strien, C.J.G.; van Doormalen, F.A.H.C.; Thoenes, D., *Chem. Eng. Sci.* 1992, 47, 2603.
18. Meuldijk, J.; German, A.L., *Polym. React. Eng.* 1999, 7, 207.
19. Meuldijk, J.; Scholtens, C.A.; Reynhout, X.E.E.; Drinkenburg, A.A.H. *DECHEMA Monographien*, 2001, 137, 633.
20. Scholtens, C.A.; Meuldijk, J.; Drinkenburg, A.A.H. *Chem. Eng. Sci.* 2001, 56, 955.
21. Ugelstad, J.; Hansen, F.K. *Rubber Chem. Tech.* 1976, 49, 53
22. Heuts, J. P. A.; Kukulj, D.; Forster, D. J.; Davis, T. P. *Macromolecules* 1998, 31, 2894–2905.
23. Heuts, J. P. A.; Davis, T. P.; Russell, G. T. *Macromolecules* 1999, 32, 6019–6030.
24. Smeets, N.M.B.; Meda, U.S.; Heuts, J.P.A.; Keurentjes, J.T.F.; van Herk, A.M.; Meuldijk, J. *Macromol. Symp.* 2007, 259, 406.
25. Waterson, J.L.; Haddleton, D.M.; Harrison, R.J. Richards, S.N. *Pol. Preprints (ACS)* 1998, 39, 457.
26. van Berkel, K.Y.; Russell, G.T.; Gilbert, R.G. *Macromolecules* 2003, 36, 3921.
27. Ballard, M.J.; Napper, D.H.; Gilbert, R.G. *J. Polym. Sci. Polym. Chem. Ed.* 1993, 22, 3325.
28. Ugelstad, J.; Mork, P.C.; Dahl, P.; Rangnes, J. J. *Polym. Sci. Part C.* 1969, 27, 49.
29. Harada, M.; Nomura, M.; Eguchi, W.; Nagata, S. *J. Chem. Eng. Jpn.* 1971, 54, 4.
30. Friis, N.; Nyhagen, L. J.. *Appl. Polym. Sci.* 1973, 17, 2311.
31. Willemse, R.X.E.; Staal, B.B.P.; van Herk, A.M.; Pierik, S.C.J.; Klumperman, B. *Macromolecules* 2003, 36, 9797-9803.
32. Heuts, J.P.A.; Russell, G.T.; van Herk, A.M. *Macromol. Symp.* 2007, 248, 12-22.

33. Wilke, C.R.; Chang, P. A. I. Ch. E. J. 1955, 1, 264.
34. Beenackers, A.A.C.M.; van Swaaij, W.P.M.; Chem. Eng. Sci. 1993, 48, 3109
35. Quadri, G.P. Ind. Eng. Chem. Res. 1998, 37, 2850
36. van den Boomen, F.H.A.M.; Meuldijk, J.; Thoenes, D. Chem. Eng. Sci. 1999, 54, 3283.
37. Meuldijk, J.; Scholtens, C.A.; Reynhout, X.E.E.; Drinkenburg, A.A.H. DECHEMA Monographien, 2001, 137, 633.
38. Hoedemakers, G.F.M. Continuous emulsion polymerization in a pulsed packed column, Ph.D. thesis, Eindhoven University of Technology, 1990.
39. Bakac, A.; Brynildson, M.E.; Espenson, J.H. Inorganic Chemistry 1986, 25, 4108.
40. Scholtens, C.A. Process development for continuous emulsion polymerization, Ph.D thesis, Eindhoven University of Technology, 2002

Process Development in Catalytic Chain Transfer Mediated Emulsion Polymerization.

ABSTRACT

In the preceding chapters various key issues of catalytic chain transfer in emulsion polymerization have been addressed. This chapter will expand on some of the topics and combine the obtained results to obtain an overview of catalytic chain transfer in (continuous) heterogeneous systems.

INTRODUCTION

Roughly 30 years after the initial discovery, the mechanistic aspects of catalytic chain transfer (CCT) in bulk/solution and emulsion polymerization have been elucidated to an extent allowing application on a technical scale. Especially the application of CCT in emulsion polymerization seems promising as it combines the control of the molecular weight distribution with very low amounts of chain transfer agent and thus a negligible environmental impact. Furthermore, possible applications in the coating area have already been reported.¹ Most of the mechanistic aspects of CCT in emulsion polymerization have been addressed in detail in the preceding chapters. The presented results can be combined to obtain a schematic overview of catalytic chain transfer in emulsion polymerization, see Figure 1.

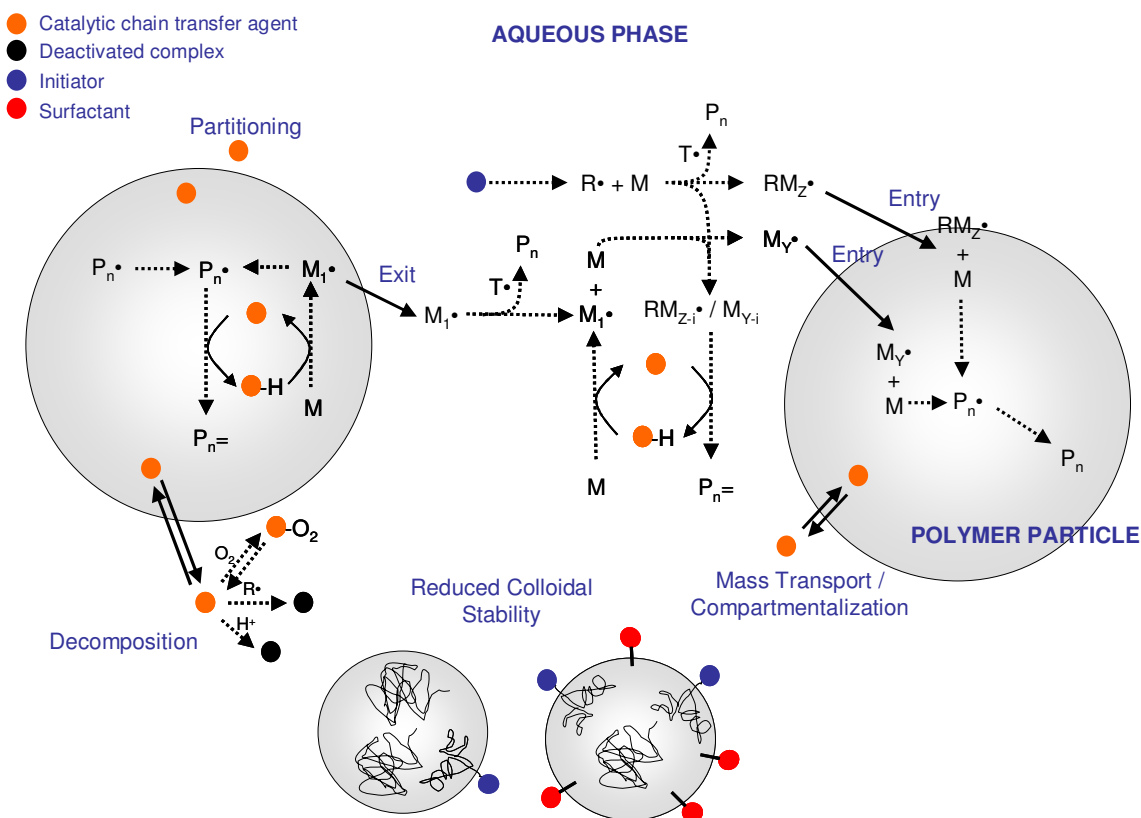


Figure 1. Schematic representation of the kinetic events in a catalytic chain transfer mediated emulsion polymerization and the impact for the colloidal stability.

In Chapters 2, 3, and 4 some consequences of the heterogeneous nature of the emulsion polymerization system for the effectiveness of CCT in emulsion polymerization have been addressed. The heterogeneous nature of the emulsion polymerization system leads to:

- Partitioning of the CCTA over the respective phases.
- Deactivation of the active complex in the aqueous phase.
- Mass transport of the CCTA from the aqueous phase towards the locus of polymerization, i.e. the polymer particles.
- Compartmentalization of the CCTA.

Control of the molecular weight distribution (MWD) is achieved by the presence of a CCTA at the loci of polymerization, i.e. the polymer particles. As only low amounts of CCTA are required to achieve significant reductions in the average molecular weight of the formed polymer, CCT mediated emulsion polymerizations often proceed in a regime where there are more polymer particles than CCTA molecules. This implies that for proper control of the molecular weight distribution rapid exchange of the CCTA molecule between the polymer particles has to occur. Some aqueous phase solubility of the CCTA is therefore required to enhance mass transport, but this solubility also implies CCTA partitioning. Partitioning lowers the effective concentration of the CCTA at the loci of polymerization. The impact of CCTA partitioning on the MWD depends on the phase ratio of the polymerization, as was presented in Chapter 2, but also on the type of CCTA, monomer and the recipe as is illustrated in this Chapter. However, as long as the viscosity inside the polymer particles remains relatively low, CCTA molecules can move freely and a global concentration governs the MWD. As the viscosity increases the resistance against mass transport of the CCTA increases and can become restricted. In an extreme situation this can result in compartmentalization behavior and multimodal MWDs. Presence in the aqueous phase renders the active complex susceptible towards deactivation and affects the emulsion polymerization kinetics, which will be addressed in more detail in this chapter.

In Chapters 5 and 6 an overview of the effects of the presence of a CCTA on the course of the emulsion polymerization and final latex properties was presented. The presence of a CCTA affects:

- The rate of exit of primary radicals from the polymer particles towards the aqueous phase.
- The rate of entry of initiator and chain transfer derived radicals.
- The nucleation period of the emulsion polymerization.
- The particle size distribution and the colloidal stability of the latex product.

In the Maxwell-Morrison² approach for radical entry in emulsion polymerization, a radical generated in the aqueous phase by the decomposition of a water-soluble initiator propagates with monomer until it becomes sufficiently surface active and enters a polymer particle. The propagating radicals in the aqueous phase can also undergo a chain stoppage event, i.e. termination or chain transfer. Depending on the aqueous phase solubility of the CCTA, aqueous phase chain transfer can occur. This lowers the rate of entry of initiator-derived radicals. Monomeric radicals, originating from CCTA either in the aqueous phase or from exit from a polymer particle, can propagate until they become sufficiently surface active or terminate through termination or chain transfer. Entry radicals can be severely reduced depending on the amount of CCTA present in the aqueous phase. This reduced rate of entry also severely affects the nucleation period at the early stages of the emulsion polymerization, potentially altering the average particle size and the broadness of the particle size distribution. The increased complexity of oligomeric species giving entry into the polymer particles also affects the colloidal stability of the polymer particles as the chemical nature of the radicals giving entry is changed. Fewer polymer chains carry a hydrophilic initiator residue, which add to the colloidal stability, and consequently more fouling is observed in the presence of a CCTA.

Inside the polymer particles, desorption of primary radicals is enhanced due to an increase in the concentration of monomeric radicals originating from the CCT process. The increased rate of exit contributes to a significantly lower average number of radicals per particle and, as a consequence, CCT mediated emulsion polymerizations classify as

Smith-Ewart Case I polymerizations. The fundamental understanding of CCT in emulsion polymerization has proven to be a prerequisite for successful application on a technical scale.

In the following sections some chemical engineering aspects concerning the application of catalytic chain transfer in batch and continuous emulsion polymerization are discussed. A particular focus is the impact of the polymerization process on the product properties (i.e. the control of the molecular weight and particle size distribution).

PARTITIONING

In Chapter 2 an expression was derived and found applicable to predict the number-average degree of polymerization (DP_n) in the COBF mediated miniemulsion polymerization of MMA, see Equation 1. From this equation, it was concluded that the DP_n depends on (i) a constant ($C_{M,p}$), (ii) the choice of CCTA (C_T , m_{Co}) and (iii) the polymerization recipe ($N_{Co,0}$, β , V_M). The effect of the choice of monomer and CCTA on the partitioning behavior and DP_n are elucidated further.

$$DP_n = \frac{V_M C_{M,p}}{C_T} \frac{1}{N_{Co,0}} \left(\frac{m_{Co} \beta + 1}{m_{Co} (\beta + 1)} \right) \left(1 + \frac{1}{\beta} \right) \quad (1)$$

In emulsion polymerization, the active concentration of CCTA at the locus of polymerization depends strongly on the partitioning of the CCTA over the respective phases. The partition coefficient and the phase ratio govern the actual concentration of CCTA at the locus of polymerization and consequently the DP_n . The partition coefficient equals the ratio of the equilibrium concentrations of CCTA in the monomer and aqueous phase and is independent of the phase ratio. The phase ratio, however, does control the absolute amounts of CCTA present in either phase, see Equation 2.

$$f_{\text{COBF,M}} = \frac{N_{\text{Co,M}}}{N_{\text{Co,0}}} = \frac{m_{\text{Co}}(\beta+1)}{m_{\text{Co}}\beta+1} \left(\frac{\beta}{\beta+1} \right) \quad (2)$$

COBF is a fairly water-soluble catalytic chain transfer agent and has a preference for more polar solvents. The partition coefficient for methyl methacrylate, a fairly polar monomer, and water was determined to be $0.72 \text{ dm}_W^3 \cdot \text{dm}_M^{-3}$. Whereas in a more apolar monomer, such as styrene, a lower partition coefficient is observed and determined to be $0.052 \text{ dm}_W^3 \cdot \text{dm}_M^{-3}$. The choice of monomer has a significant influence on the partitioning behavior of the catalytic chain transfer agent and consequently on DP_n of the polymer produced, see Figure 2.

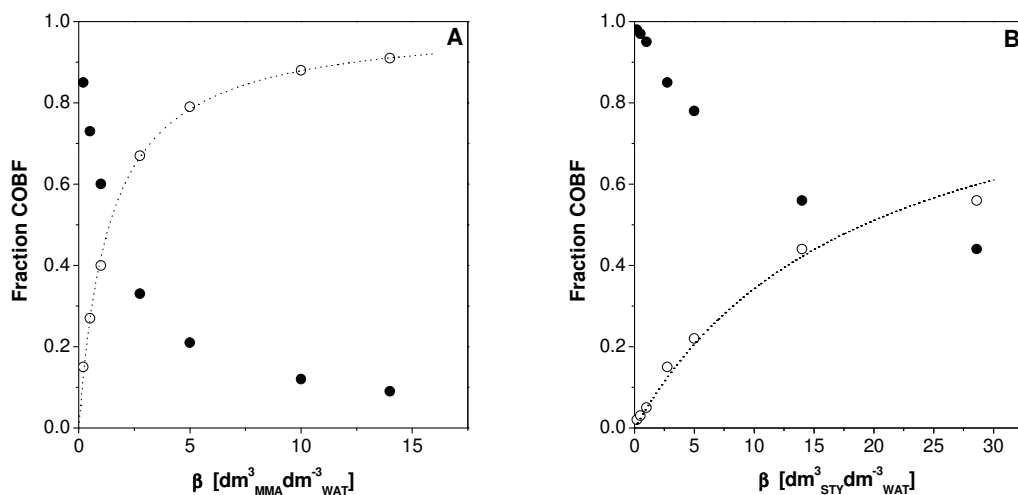


Figure 2. The partitioning of COBF in two water-monomer systems. A. water (○) – styrene (●) and B. water (○) – methyl methacrylate (●). (····) best fit obtained with Equation 2, $m_{\text{Co}} = 0.72 \text{ dm}_W^3 \cdot \text{dm}_M^{-3}$ for MMA / WAT and $0.052 \text{ dm}_W^3 \cdot \text{dm}_M^{-3}$ for STY / WAT.

Figure 3 presents DP_n as a function of the partition coefficient (m_{Co}), the overall amount of CCTA in the recipe ($N_{\text{Co,0}}$) and the phase ratio. An increase of the overall amount of CCTA in the system results, as predicted by the Mayo equation, in a lower DP_n , see Figure 3A. The effect of partitioning decreases for higher amounts of CCTA and the

value of the degree of polymerization converges to the bulk value (i.e. the degree of polymerization at infinite β).

The effect of the partition coefficient, i.e. different CCTA's, on the degree of polymerization is presented in Figure 3B. At very low values of the partition coefficient (i.e. $m_{Co} \rightarrow 0$) the CCTA partitions exclusively towards the aqueous phase and consequently polymer with high DP_n is produced. The opposite situation occurs for high values of the partition coefficient (i.e. $m_{Co} \rightarrow \infty$): the catalyst partitions exclusively towards the organic phase, resulting in a situation comparable to bulk polymerization. For both limiting cases, the effect of the phase ratio is negligible.

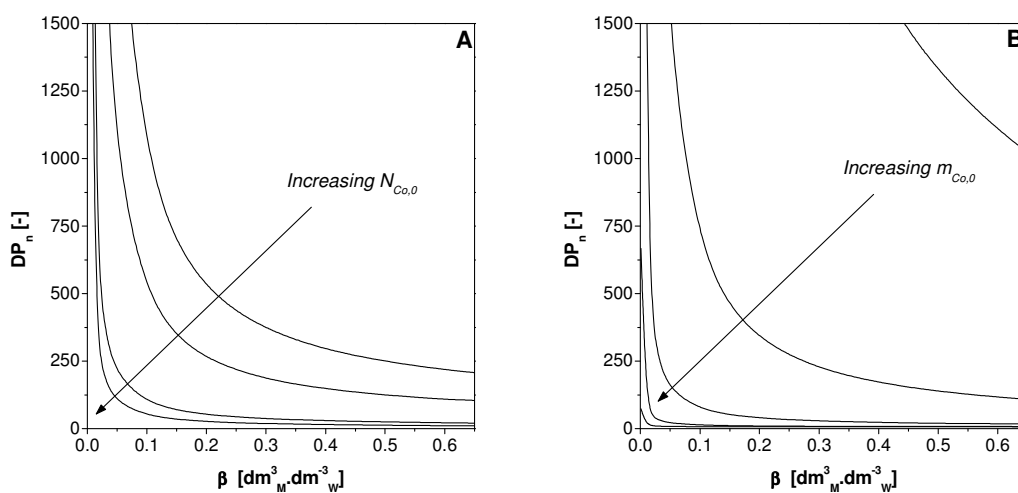


Figure 3. Calculated values of the instantaneous number-average degree of polymerization as a function of the phase ratio. A. The effect of the overall amount of CCTA in the system (0.5, 1.0, 5.0 and 10.0 ppm respectively), $C_T = 30 \cdot 10^3$, $m_{Co} = 0.72 \text{ dm}_W^3 \cdot \text{dm}_M^{-3}$ and B. The effect of the partition coefficient (0.01, 0.10, 1.0, 10 and 100 $\text{dm}_W^3 \cdot \text{dm}_M^{-3}$ respectively), $C_T = 30 \cdot 10^3$, $N_{Co,0} = 5$ ppm (mol CCTA per mol monomer).

Figures 2 and 3 clearly illustrate how the recipe ($N_{Co,0}$) as well as the choice of CCTA and monomer (m_{Co}) influence partitioning of the CCTA and consequently DP_n .

CATALYST DEACTIVATION

For proper control of the molecular weight distribution in catalytic chain transfer (CCT) mediated emulsion polymerization, CCTA partitioning, deactivation and mass transport should be taken into account. The effects of partitioning and mass transport have been addressed in Chapters 2 and 3. Deactivation of the active cobalt complex in the aqueous phase can have severe consequences for the application of CCT on an industrial scale.

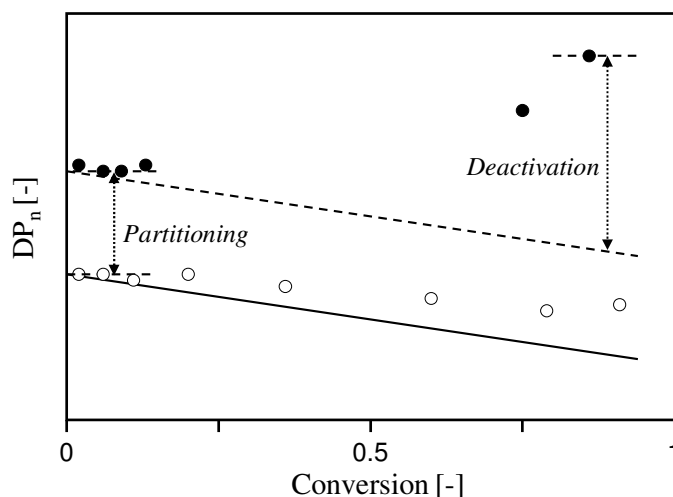


Figure 4. The instantaneous number average degree of polymerization as a function of conversion. (—) as predicted by the Mayo equation (Chapter 2, Equation 4) for solution polymerization and (- - -) predicted by the modified Mayo equation for miniemulsion polymerization (Equation 1).

Figure 4 clearly illustrates the effect of the heterogeneity of the (mini)emulsion polymerization system. The Mayo equation predicts a linear relation between DP_n and the CCTA concentration in the medium. Since the ratio of $C_{Co,0}$ to C_M should continuously increase as the conversion increases, a decrease in DP_n is expected, in general this decrease is not observed experimentally.³⁻⁵ The obtained molecular weights remain virtually unchanged throughout the course of polymerization. Only one study by Davis and co-workers, actually reported a decrease in DP_n at higher monomer conversion.⁶ In (mini)emulsion polymerization, however, two deviations from DP_n , as predicted by the Mayo equation (using overall concentrations), can be observed. First,

there appears to be an offset between the predicted and experimentally obtained instantaneous number-average degree of polymerization and secondly the number-average degree of polymerization appears to increase with conversion. The first can be accounted to CCTA partitioning in emulsion polymerization, whereas the latter can be accounted to deactivation of the active complex in the aqueous phase.

Determination of the rate coefficient of deactivation

The complexes used for CCT are derivatives of cobaloximes, which are highly susceptible towards hydrolysis and oxidation. COBF has improved stability due to the introduction of BF₂ bridges, but despite the improved stability the complex is still readily oxidized by oxygen^{7,8} or (peroxide) radicals^{7,9,10}, or hydrolyzed in acidic media.⁷ The cobalt complex can be oxidized by radicals in the monomer phase, forming stable Co(III)-R complexes. Preliminary results of Heuts and co-workers indicate, however, that the active Co(II) species is regenerated *in-situ* during bulk polymerization.¹¹ Although catalyst deactivation in the monomer phase can not be neglected,⁴⁻⁶ our investigation will focus on the deactivation in the aqueous phase. In conclusion, since oxygen is excluded from polymerization due to the high radical scavenging activity, three variables are found to affect the Co(II) deactivation:

- Initiator concentration in the aqueous phase ($C_{I,w}$).
- Reaction temperature (T).
- pH of the aqueous phase.

An empirical approach was chosen to estimate the rate of deactivation in order to predict the increase in DP_n during (mini)emulsion polymerization. Based on exploratory results we choose a 2³ full factorial experimental design to determine the pseudo-first order rate coefficient of decomposition (k_{dea}) of the COBF catalyst; the parameter settings of the three critical parameters are shown, see Table 1.

Table 1. The settings of the parameters used for the experimental design.

X_i	Variable	(-)	(+)
X_1	pH (-)	2	7
X_2	T^{-1} ($10^{-3} K^{-1}$)	2.78	3.36
X_3	$-\log(C_{1,W})$	2.78	4.78

The statistical evaluation showed that only the main effects were significant ($\alpha = 0.05$), hence the empirical model does not contain any interaction terms. The statistical evaluation of the experimental design results in a model equation that can be used to predict the rate constant of deactivation of the CCTA in the aqueous phase, see Equation 3.

$$\ln k_{\text{dea}} = -4.87 - 0.666X_1 - 1.53X_2 - 0.551X_3 \quad (3)$$

The deactivation of the CCTA in the aqueous phase is assumed to be first order in the CCTA concentration in the aqueous phase, see Equation 4, in which $C_{\text{Co,W}}^t$, $C_{\text{Co,W}}^0$ and k_{dea} are the concentration of CCTA in the aqueous phase at any time t ($\text{mol} \cdot \text{dm}_W^{-3}$), the concentration of CCTA in the aqueous phase at $t = 0$ ($\text{mol} \cdot \text{dm}_W^{-3}$) and the first order rate coefficient of deactivation (s^{-1})

$$C_{\text{Co,W}}^t = C_{\text{Co,W}}^0 e^{-k_{\text{dea}}t} \quad (4)$$

Substitution of Equation 4 in Equation 1 gives a time dependent expression for the instantaneous number-average degree of polymerization, incorporating CCTA deactivation, see Equation 5.

$$DP_n = \left\{ \frac{V_M C_{M,p}}{C_T} \frac{1}{N_{\text{Co},0}^0} \left(\frac{m_{\text{Co}}\beta + 1}{m_{\text{Co}}(\beta + 1)} \right) \left(1 + \frac{1}{\beta} \right) \right\} \exp(k_{\text{dea}}t) \quad (5)$$

Equation 5 shows that although DP_n strongly depends on the phase ratio, the increase in DP_n due to deactivation is independent of the phase ratio.

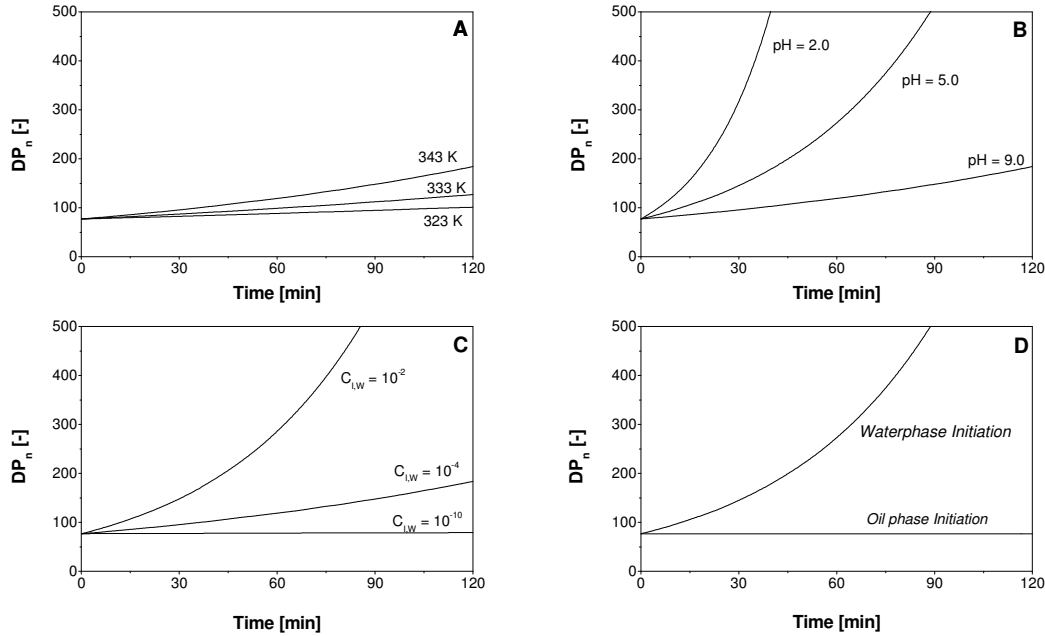


Figure 5. The effect of the process variables on the normalized number-average degree of polymerization (Equation 5). Model settings: $C_{Co,0} = 6 \cdot 10^{-6}$ mol·dm $^{-3}$, $C_T = 15 \cdot 10^3$ [-], $m_{Co} = 0.72$ [-], $\beta = 0.20$ dm 3 ·dm $^{-3}$. Variable settings: $pH = 9$, $T = 343$ K, $C_{I,W} = 10^{-4}$ mol·dm $^{-3}$ (AIBN) unless mentioned otherwise.

A. Effect of the temperature, $T = 323, 333$ and 343 K

B. Effect of the pH of the aqueous phase, $pH = 2.0; 5.0$ and 9.0

C. Effect of the initiator concentration, $C_{I,W} = 10^{-10}; 10^{-4}$ and 10^{-2} mol·dm $^{-3}$

D. Model calculations: (---) $pH = 9.0$, $T = 343$ K and $C_{I,W} = 1.5 \cdot 10^{-3}$ mol·dm $^{-3}$ and (—) $pH = 9.0$, $T = 343$ K and $C_{I,W} = 10^{-10}$ mol·dm $^{-3}$

The effect of the various process variables on DP_n was evaluated, and the results shown in Figure 5. The reaction temperature has the strongest effect on the rate coefficient of deactivation, as determined by the experimental design. When an acceptable temperature

range for (mini)emulsion polymerization (i.e. 323 – 348 K) is considered, model calculations predict that an approximately 3-fold reduction of the amount of COBF in the system after 2 h of reaction, even when a low radical concentration and a high pH of the aqueous phase are used, see Figure 5A. However, when lower pH values are considered, the decrease in the activity is more severe. Figure 5B shows that acidic conditions at 348 K result in complete deactivation of the catalyst and consequently a DP_n that approaches the situation where no catalytic chain transfer agent is present in the system.

Besides the strong effect of the pH of the aqueous phase on catalyst deactivation, there also appears to be a strong effect of the initiator concentration in the aqueous phase, see Figure 5C. When generally accepted initiator concentrations are used, the deactivation results in DP_n values that increase excessively. Proper control of DP_n can be obtained, when suitable process conditions are chosen. In Figures 5A-C, it is evident that at high pH and a low radical concentration in the aqueous phase hardly any catalyst deactivation occurs, even at relatively high temperatures.

Discussion

For CCT mediated (mini)emulsion polymerizations the use persulfate initiators should be avoided due to reduced activity of the Co(II) complex,¹² therefore the use of (water soluble) azo-initiators is preferred. Especially in miniemulsion polymerization, AIBN is often a well suitable initiator. An important factor in the experimental design is the presence of C-centered radicals in the aqueous phase. Although AIBN is a oil-soluble initiator, with a solubility in the aqueous phase of 0.04 w%,¹³ it is known that the AIBN-derived radicals significantly partition towards the aqueous phase.^{14,15} When it is assumed that virtually no radicals are present in the aqueous phase, a marginal increase in DP_n would be predicted. On the other hand, if radical partitioning is considered, DP_n should show a strong increase, see Figure 5D. From a mechanistic point of view, it is important to elucidate the fate of alkyl radicals in the aqueous phase.

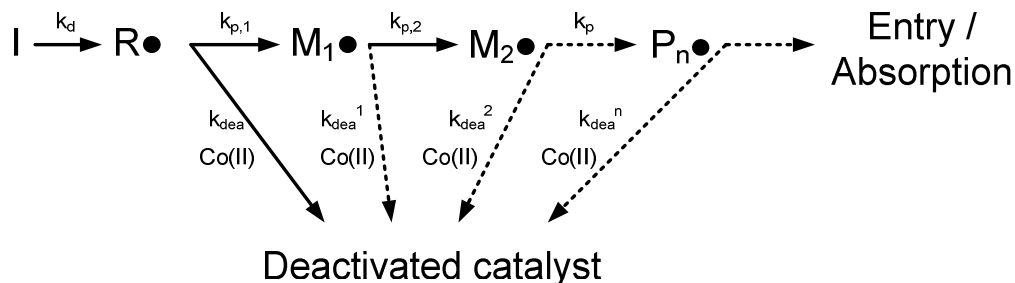


Figure 6. Kinetic representation of COBF deactivation and aqueous phase propagation.

When a C-centered radical is formed in the aqueous phase, it has two possibilities for reaction: (i) it can react with COBF present in the aqueous phase or (ii) it can propagate with dissolved monomer, initiating a growing chain, see Figure 6. C-centered radicals are known to reversibly form strong cobalt-carbon bonds, rendering a substantial amount of Co(II) unavailable for the chain transfer reaction.^{10,16} Once an alkyl radical has propagated with a monomeric unit, it is very likely that conventional catalytic chain transfer will occur, a Co(III)-H complex is formed which is a part of the catalytic cycle, and the active Co(II) complex is regenerated, see Chapter 1 Scheme 1. From the exploratory results it has been concluded that in the presence of alkyl radicals (derived from 4,4'-Azobis(4-cyanovaleric acid)) irreversible deactivation of the Co(II) complex occurs with a rate constant of deactivation k_{dea} . Although irreversible deactivation of the Co(II) species due to MMA derived radicals cannot be excluded ($k_{\text{dea}}^1, k_{\text{dea}}^2 \dots k_{\text{dea}}^n$), it is known that the formed cobalt-carbon bonds are weaker. If aqueous phase propagation is sufficiently fast, the concentration of C-centered radicals will be substantially lower than the bulk value concentration considered in the presented deactivation model, thereby reducing the effect of deactivation. An estimation of the time constants of aqueous phase propagation ($t_{\text{c,p}}$) compared to aqueous phase deactivation ($t_{\text{c,d}}$) will allow for a determination of the fate of alkyl radicals present in the aqueous phase, see Table 2.

$$t_{\text{c,i}} = \frac{1}{k_i C_{\text{W,i}}} \quad (6)$$

Table 2. Estimated time constants for the reaction of a radical with MMA and COBF at 70⁰C

	k_i [$dm_w^3 \cdot mol^{-1} \cdot s^{-1}$]	$C_{w,i}$ [$mol \cdot dm_w^{-3}$]	Time constant ^b [s]
MMA	$k_{p,1} = 16,8 \cdot k_p = 17,6 \cdot 10^3$ ^{17,18}	$1,5 \cdot 10^{-19}$	$0,4 \cdot 10^{-3}$
COBF	$k_{dea} = 0,4 \cdot 10^3$ ^a	$6 \cdot 10^{-6}$	$0,4 \cdot 10^3$

- a) Calculated based on the results of this work.
b) Calculated with Equation 6.

In order to calculate $k_{p,1}$, it is important to realize that the rate constant of propagation is strongly chain length dependent and can be calculated according to a model developed by Heuts et al.¹⁸ The value of $k_{p,1}$ can be calculated by multiplying the long-chain value for MMA ($1050 \text{ } dm_w^3 \cdot mol^{-1} \cdot s^{-1}$ at 343 K¹⁵) with a C_1 coefficient of 16,8.¹⁶ For k_{dea} a calculated value based on the results of this work is used. The ratio of the time constant for reaction of the initiator derived alkyl radical with MMA and the time constant for reaction with COBF is 10^6 , pointing to a considerably higher probability of the alkyl radical to propagate with MMA than reacting with COBF. This result implies that the experimental design, used to predict the value of k_{dea} , probably over-estimates the effect of alkyl radicals on deactivation of COBF present in the aqueous phase. New deactivation experiments have to be performed in the presence of monomer to disclose the effect of alkyl radicals on CCTA deactivation in the aqueous phase. Further insight will allow for a better understanding of the mechanism of deactivation and an improved interpretation of the experimental design.

Conclusions

The results obtained in this work demonstrate that, for typical (mini)emulsion conditions, CCTA deactivation can occur. However, by choosing appropriate reaction conditions (i.e. pH > 7, exclusion of oxygen, avoiding peroxide initiators) deactivation of the active

complex can be minimized and control of the molecular weight distribution remains possible during the course of the polymerization.

APPLICATION IN BATCH EMULSION POLYMERIZATION

Catalyst preparation

The active complex is typically synthesized in a two step process involving a cobalt salt, the glyoxime ligand and a large excess of boron trifluoride to introduce the boron difluoride bridges on the ligand system of the complex.²⁰⁻²² Main limitations for scale-up of the catalyst synthesis would be the large excess of toxic boron trifluoride that has to be used and the formation of hydrofluoric gas during the synthesis. However, multi-gram synthesis of the particular compounds should be attainable and should be sufficient to allow for the production of a number of batches of polymer. A typical 15 m³ emulsion polymerization reactor, containing a 40% solids emulsion recipe requires merely 0.25 g of COBF (= 10 ppm) to obtain low molecular weight polymer ($\sim 15 \cdot 10^3 \text{ g.mol}^{-1}$).

Another issue linked to limited scalability of the CCTA synthesis is the possibility of slight batch to batch differences. The activity, expressed as the chain transfer constant (C_T) of a batch of CCTA can be tested experimentally in bulk polymerization. The obtained C_T value can be used as a measure for the purity of the obtained complex. Once the intrinsic activity of a single batch has been determined, the performance in emulsion polymerization, with respect to the conversion-time profile, MWD and PSD, can be evaluated. The latex properties can be compared to a master-set and the polymerization recipe adjusted accordingly.

Recipe considerations

Deactivation of the active complex can be minimized by choosing appropriate polymerization conditions; a pH of the aqueous phase slightly higher than 7 and avoiding peroxide based initiators. Exclusion of oxygen is a prerequisite as the combination of

oxygen and alkyl radicals can result in the formation of peroxide radicals. As the catalytic chain transfer agent is added in very low amounts, traces of oxygen can be fatal for the control of the molecular weight distribution.

The effects a CCT agent has on the course of the emulsion polymerization process and the mechanism can be minimized by choosing a CCTA with limited aqueous phase solubility, i.e. a high partition coefficient. A high partition coefficient will reduce the effects in the aqueous phase and also contribute to the colloidal stability of the latex product. The enhanced rate of exit of primary radicals is tied to the CCT process and as a consequence CCT mediated emulsion polymerization will proceed in a regime where $\bar{n} < 0.5$ (i.e. Smith Ewart case I kinetics). For monomers with a relatively high aqueous phase solubility, such as methyl methacrylate, high amounts of surfactant and initiator are required to obtain acceptable reaction times for complete conversion. First, the higher the number of propagation steps required in the aqueous phase before sufficient surface activity is obtained, the longer a propagating radical resides in the aqueous phase. A high residence time in the aqueous phase increases the probability of chain transfer in and a higher radical concentration is required to achieve acceptable entry rates. Secondly, a low partition coefficient of monomeric radicals between the polymer particles and the aqueous phase enhances primary radical desorption and lowers \bar{n} . More hydrophobic monomers, such as butyl methacrylate, display higher rates of polymerization and a reduced impact on the particle size distribution.

Process operation strategies

Ab-initio CCT emulsion polymerization has detrimental effects on nucleation, see Chapters 4 and 6. This affects the particle size distribution and colloidal stability, limiting the applicability of *ab-initio* CCT emulsion polymerization. Semi-batch and seeded emulsion polymerization allow for the formation of particles prior to the CCTA feed. The nucleation stage is not affected by the presence of the CCTA and consequently the particle size distribution can be controlled and the colloidal stability of the latex dispersion maintained. Limitations in mass transport and / or compartmentalization

behavior can be avoided by maintaining a low viscosity inside the polymer particles, by working under monomer flooded conditions.

Catalytic chain transfer in emulsion polymerization can be used to obtain polymer particles with more challenging MWDs. Monomodal MWDs are only accessible via *ab-initio* emulsion polymerization. More complicated MWDs can be obtained from semi-batch and seeded emulsion polymerization. Depending on the desired properties of the final dispersion, high molecular weight seed latex can be further grown with low molecular weight polymer or *visa versa*. Multimodal MWDs are difficult to obtain from any one-stage emulsion polymerization process as a significant reduction in DP_n requires the addition of relatively large amounts of CCTA (factor 2 in the CCTA concentration reduces DP_n with a factor 2, which is hardly visible on the log M scale of a MWD, see Equation 1). Note that relatively large amounts of CCTA have a deleterious effect on the course of the polymerization. A multi-stage process where a seed latex is grown stepwise in the presence of different CCTA concentrations will allow effective and reproducible production of dispersions with multimodal MWDs.

APPLICATION IN CONTINUOUS EMULSION POLYMERIZATION

Continuously operated stirred tank reactor (CSTR)

Catalytic chain transfer mediated continuous emulsion polymerization in a continuous stirred tank reactor (CSTR) may result in sustained oscillations in conversion and particle number.^{23,24} Surfactant is used for the formation of micelles from which the polymer particles are formed. Surfactant is also necessary for the stabilization of the growing polymer particles. Sustained oscillations are caused by the competition between the formation of particles and adsorption on already particles to maintain colloidal stability. Initially there are no polymer particles present and all the surfactant in the feed will be quickly consumed due to the rapid formation and growing of the polymer particles. The rate of surfactant consumption for surface coverage exceeds the feed rate of surfactant to the reactor. Consequently the rate of particle formation will become negligible for a

certain period. The duration of this period depends on the surfactant feed rate, wash-out rate of polymer particles and the growth rate of the total surface area.²⁵ Eventually the total surface area will be saturated with surfactant and micelles and consequently new polymer particles will be formed again. This mechanism results in fluctuations in the particle number, rate of polymerization and conversion. Sustained oscillations only occur when particle nucleation and particle growth are not spatially separated.

This phenomenon predominantly occurs for the continuous emulsion polymerization of systems that display a high rate of radical desorption from the particles,²⁶ i.e. systems leading to Smith Ewart case I kinetics. These high rates of radical exit result in low growth rates of the small polymer particles due to the low average number of radicals per particles. For Smith Ewart case I the growth rate increases with the particle size and this causes the instability.

Emulsion polymerizations of methyl methacrylate classify as Smith-Ewart case I polymerization. As was demonstrated in Chapter 5, catalytic chain transfer mediated emulsion polymerizations of methyl methacrylate display a stronger case I behavior, the value for m (the ratio of the time constants of radical desorption and radical termination) is higher. This is due to the increased rate of radical exit as a consequence of the formation of primary radicals from the catalytic chain transfer mechanism. Sustained oscillations are therefore likely to occur in catalytic chain transfer mediated emulsion polymerizations.

Plug flow reactors (PFR)

In a plug flow reactor (PFR) particle nucleation and particle growth are spatially separated. If the reaction time in an ideally mixed isothermal batch reactor is equal to the residence time in a plug flow reactor, the product properties in terms of the conversion, particle number, particle size distribution and molecular weight distribution are the same for both reactor types. A disadvantage, however, is that plug flow in a tubular reactor demands for turbulent flow and as a consequence for high liquid velocities. For high

monomer conversions impractical reactor dimensions are required. Turbulence is also necessary for proper emulsification and for a low resistance against transfer of the heat of polymerization to the reactor wall. A combination of low net flow rates, limited backmixing, high local flow rates and intensive radial mixing is achieved with the pulsed sieve plate column (PSPC, see Chapter 6).

For respectively equal residence times and reaction times, the performance of a constant density PFR is equal to the performance of a constant density batch reactor. A comparison between the PFR and batch reactor can be made based on the modified Mayo equation. The instantaneous degree of polymerization in a PFR follows from Equations 1 and 5 by replacing V_M , V_W , $N_{Co,0}$ and t by $\phi_{V,M}$, $\phi_{V,W}$, $\phi_{mol,Co,0}$ and $\tau = V_r / \phi_{V,0}$, respectively, see Equations 7 and 8. $\phi_{V,M}$, $\phi_{V,W}$, $\phi_{mol,Co,0}$ and $\phi_{V,0}$ stand for the volumetric flow rate of the organic phase, the volumetric flow rate of water, the molar flow rate of COBF and the total volumetric flow rate, respectively.

$$DP_n = \frac{\phi_{V,M} C_{M,p}}{C_T} \frac{1}{\phi_{mol,Co,0}} \left(\frac{m_{Co} \beta + 1}{m_{Co} (\beta + 1)} \right) \left(1 + \frac{1}{\beta} \right) \quad \text{with } \beta = \frac{\phi_{V,M}}{\phi_{V,W}} \quad (7)$$

$$DP_n = \left\{ \frac{\phi_{V,M} C_{M,p}}{C_T} \frac{1}{\phi_{mol,Co,0}^0} \left(\frac{m_{Co} \beta + 1}{m_{Co} (\beta + 1)} \right) \left(1 + \frac{1}{\beta} \right) \right\} \exp(k_{dea} \tau) \quad (8)$$

The pulse wise addition of COBF in a (semi-) batch process corresponds with a COBF side feed in a plug flow reactor.²⁷ Therefore, a side feed of COBF to a tubular reactor with plug flow leads to the same result as shown in Figure 7A. However, pulsation in the PSPC results in some backmixing. For a COBF feed stream at axial position z_i , a stationary axial COBF concentration profile establishes upstream of the feeding point, see Equation 9.²⁸ Downstream the feeding point the COBF concentration is independent of the axial position, see Equation 10.

$$C_{Co,z} = C_{Co,z_i} \exp\left(\frac{u(z - z_i)}{E}\right) \quad \text{for } z < z_i \quad (9)$$

$$C_{Co,z} = C_{Co,z_i} \quad \text{for } z \geq z_i \quad (10)$$

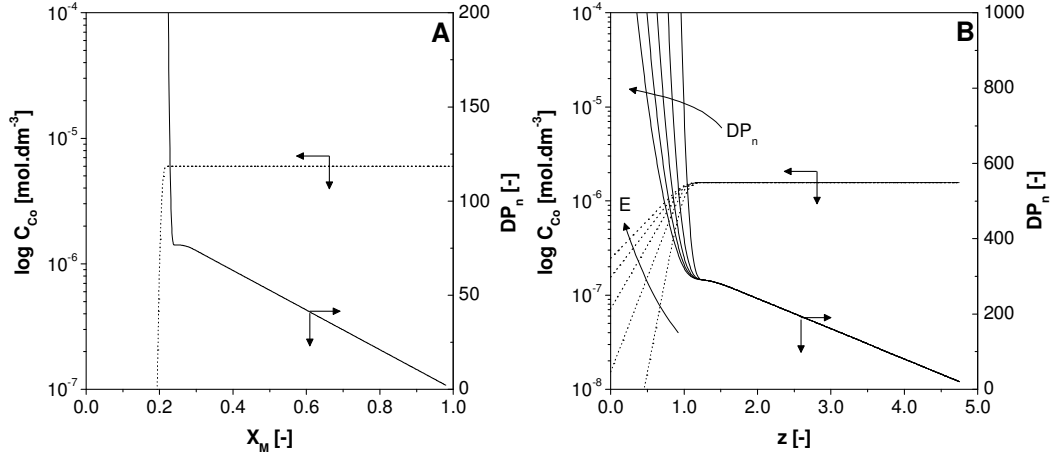


Figure 7. Simulation of the overall COBF concentration and the instantaneous degree of polymerization as a function of the monomer conversion for (A) batch emulsion polymerization and (B) continuous emulsion polymerization in the PSPC. (····) $C_{Co,0}$ and (—) DP_n . In all calculations $m_{Co} = 0.72 \text{ dm}_W^3 \cdot \text{dm}_M^{-3}$; $\beta = 0.20 \text{ dm}_M^3 \cdot \text{dm}_W^{-3}$; $C_T = 15 \cdot 10^3$ and $C_{M,p}^{sat} = 6.9 \text{ mol} \cdot \text{dm}_M^{-3}$

A. DP_n calculated using Equation 1 and $V_M = 0.20 \text{ dm}^3$ and $N_{Co} = 9.52 \cdot 10^{-6} \text{ mol}$.

B. DP_n calculated using Equations 7 and 9 and $\phi_{V,M} = 2.7 \cdot 10^{-4} \text{ dm}^3 \cdot \text{s}^{-1}$ and $\phi_{mol,Co} = 2.53 \cdot 10^{-9} \text{ mol} \cdot \text{s}^{-1}$. Operational conditions: $u = 9.3 \cdot 10^{-4} \text{ m} \cdot \text{s}^{-1}$; $E = 1.0\text{-}5.0 \cdot 10^{-4} \text{ m}^2 \cdot \text{s}^{-1}$. The feed position is simulated at $h = 0.2$ ($z = 1 \text{ m}$).

As result of backmixing a decrease of DP_n already starts upstream of the axial feeding position, see Figure 7B. Downstream the feeding point DP_n gradually decreases with z as a result of the continuously decreasing monomer concentration in the particles when the monomer droplets are completely consumed ($X_M > 0.27$), see Equation 7. However, due to catalyst deactivation a constant or slightly increasing instantaneous degree of polymerization is often observed, see Equation 8.²⁹⁻³⁵ Note that the final cumulative MWD of the latex product of the PSPC will be broad. The MWD and is most likely

strongly tailing towards the high molecular weight end of the distribution. Our experimental results³⁶ are qualitatively in line with these considerations about backmixing and catalyst deactivation downstream the feeding position.

Ab-initio emulsion polymerization in the PSPC is not favorable as the presence of the CCTA affects the nucleation of polymer particles. Seeded emulsion polymerization with or without a CCTA side feeds, despite some broadening of the MWD due to unavoidable backmixing, provides a good alternative for obtaining tailored MWD in continuous emulsion polymerization.

CONCLUDING REMARKS

The results of this work have demonstrated the potential of CCT in (continuous) emulsion polymerization. Despite CCTA deactivation and possible resistance to mass transport, low molecular weight polymer can be produced with only ppm amounts of active catalyst. In this work, a moderately water-soluble CCTA (COBF) was used to clearly illustrate the effects a CCTA can have on the course of the emulsion polymerization and the product properties in terms of the MWD and PSD. The effects of CCTA partitioning on the colloidal stability, entry and nucleation can be reduced to a minimum by opting for a CCTA which is not or very sparingly soluble in the aqueous phase. However, process parameters such as the rate of polymerization and the MWD are to a large extent governed by the choice of (co)monomer(s)

Many observations for CCT in emulsion polymerization hold for other mediating techniques. Partitioning of mediating agents is crucial in nitroxide mediated polymerization (NMP) as well as atom transfer radical polymerization (ATRP). Partitioning of the Cu(I) and Cu(II) species to the aqueous phase have deleterious effects on the polymerization, i.e. loss of control/livingness, broader MWDs, more termination and higher polymerization rates. Catalyst deactivation affects the concentration of the active catalyst can consequently affect the control/livingness of the polymerization.

Colloidal stability is a key issue, not only for catalytic chain transfer mediated emulsion polymerizations, but also for ATRP, NMP and reversible addition fragmentation transfer (RAFT) polymerization.

The results of this work have contributed to the fundamental understanding of catalytic chain transfer in (continuous) emulsion polymerization. Robust molecular weight control can be achieved, depending on the choice of catalytic chain transfer agent, monomer and process strategy.

REFERENCES

1. Nabuurs, T.; van der Slot, S.; Overbeek A. *Prog. Org. Coatings* 2007, 58, 80.
2. Maxwell, I.A.; Morrison, B.R.; Napper, D.H.; Gilbert, R.G. *Macromolecules* 1991, 24, 1629.
3. Heuts, J.P.A.; Muratore, L.M.; Davis, T.P. *Macromol. Chem. Phys.* 2000, 201, 2780
4. Kukulj, D.; Davis, T.P. *Macromol. Chem. Phys.* 1998, 199, 1697
5. Heuts, J.P.A.; Forster, D.J.; Davis, T.P. in *Transition Metal Catalysis in Macromolecular Design* (Ed. Boffa, L.S.; Novak, B.M.) ACS Symposium Series, 2000, Vol. 760, p.254 (American Chemical Society: Washington, DC).
6. Kowollik, C.; Davis, T.P. *J. Polym. Sci. . Part A. Polym. Chem* 2000, 38, 3303
7. Gridnev, A.A.; Ittel, S.D. *Chemical Reviews* 2001, 101, 3611.
8. Grindev, A.A. *Polym. Sci. USSR* 1989, 31, 2369
9. Gridnev, A.A. *Polym. J.* 1992, 7, 613
10. Morrison, D.A.; Davis, T.P.; Heuts, J.P.A.; Messerle, B.; Gridnev, A.A. *J. Polym. Sci. Part A. Polym. Chem.* 2006, 44, 6171
11. Biasutti, J.D.; Lucien, F.P.; Heuts, J.P.A. manuscript in preparation
12. Kukulj, D.; Davis, T.P.; Gilbert, R.G. *Macromolecules* 1997, 30, 7661.
13. Alduncin, J.A.; Forcada, J.; Asua, J.M. *Macromolecules* 1994, 27, 2256.
14. Asua, J.M.; Rodriguez, V.S.; Sudol, E.D.; El-Aasser, M.S. *J. Polym. Sci. Part A. Polym. Chem.* 1989, 27, 3569.
15. Luo, Y.; Schork, J. *J. Polym. Sci. Part A. Polym. Chem.* 2002, 40, 3200.
16. Heuts, J.P.A.; Forster, D.J.; Davis, T.P.; Yamada, B.; Yamazoe, H.; Azuzikawa, M. *Macromolecules* 1999, 32, 2511.
17. van Herk, A.M. *Macromol. Theory Simul.* 2000, 9, 433.

18. Heuts, J.P.A.; Russell, G.T.; Smith, G.B.; van Herk, A.M. *Macromol. Symp.* 2007, 248, 12.
19. Ballard, J.; Napper, D.H.; Gilbert, R.G. *J. Polym. Sci: Polym. Chem. Ed.* 2003, 22, 3225
20. Bakac, A.; Espenson, J.H. *J. Am. Chem. Soc.* 1984, 106, 5197
21. Bakac, A.; Brynildson, M.E.; Espenson, J.H. *Inorg. Chem.* 1986, 25, 4108
22. Sanayei, R.A.; O'Driscoll, K.F. *J. Macromol. Sci. Chem.* 1989, A26, 1137
23. Kiparissides, C.; MacGregor, J.F.; Hamielec, A.E. *Can. J. Chem. Eng.* 1980, 58, 48.
24. Kiparissides, C.; MacGregor, J.F.; Hamielec, A.E. *J. Appl. Polym. Sci.* 1979, 23, 401.
25. Meuldijk J.; van Strien, C.J.G.; van Doormalen F.H.A.C.; Thoenes, D. *Chem. Eng. Sci.* 1992, 47, 2603.
26. Penlides, A.; MacGregor, J.F.; Hamielec, A.M.; *Chem. Eng. Sci.* 1989, 44, 273.
27. Boomen, F.H.A.M.; Meuldijk, J.; Thoenes, D.; *Chem. Eng. Sci.* 1999, 54, 3283
28. Scholtens, C.A.; Meuldijk, J.; Drinkenburg, A.A.H., *Chem. Eng. Sci.* 2001, 56, 955.
29. Suddaby, K.G.; Haddleton, D.M.; Hastings, J.J.; Richards, S.N.; O'Donnell, J.P. *Macromolecules* 1996, 29, 8083.
30. Kukulj, D.; Davis, T. P.; Gilbert, R. G. *Macromolecules* 1997, 30, 7661.
31. Bon, S. A. F.; Morsley, D. R.; Waterson, J.; Haddleton, D. M.; Lees, M. R.; Horne, T. *Macromol. Symp.* 2001, 165, 29.
32. Kukulj, D.; Davis, T.P.; Suddaby, K.G.; Haddleton, D.M.; Gilbert, R.G. *J Polym. Sci. Part A: Polym. Chem.* 1997, 35, 859
33. Pierik, S.C.J.; Smeets, B.; van Herk, A.M. *Macromolecules* 2003, 36, 9271
34. Haddleton, D.M.; Morsley, D.R.; O'Donnell, J.P.; Richards, S.N. *J Polym. Sci. Part A: Polym. Chem.* 2001, 37, 3549.
35. Smeets, N.M.B.; Heuts, J.P.A.; Meuldijk, J.; van Herk, A.M. *J. Polym. Sci. Part A: Polym. Chem.* 2008, 46, 5839.
36. Smeets, N.M.B.; Dautzenberg, B.A.J.; Heuts, J.P.A.; Meuldijk, J.; van Herk, A.M. *Macromol. Symp.* 2009, 275, 149.

ACKNOWLEDGEMENT

Tijdens mijn afstuderen werd het vlammetje voor wetenschappelijk onderzoek aangewakkerd en ben ik aansluitend begonnen met een promotie-onderzoek. Mijn samenwerking met dr. Jan Meuldijk begon tijdens mijn interne researchstage, vond een vervolg in mijn afstudeerproject en mondde uiteindelijk uit in dit promotie onderzoek. Jan, jouw enthousiasme werkt aanstekelijk en ik kijk met veel plezier en tevredenheid terug op onze samenwerking. Hans Heuts wil ik hartelijk bedanken voor al zijn hulp bij de totstandkoming van dit werk en de prettige samenwerking. Hans, ik heb onze discussiesessies en jouw input enorm gewaardeerd. Naast al het mooie CCT werk hebben we beide ook veel plezier gehad aan ons uit de hand gelopen vrijdagmiddagexperimentje. En nu dat 't promotie onderzoek is afgerond, kan ik eindelijk beginnen met plat kalle! Ik wil mijn promotor prof. dr. Alex van Herk bedanken voor de mogelijkheid om binnen zijn vakgroep een promotie onderzoek te kunnen doen, 1 jaar van mijn onderzoek buiten Eindhoven uit te voeren en de organisatie van de Gordon Research Seminar deels op mij te nemen.

I would like to thank prof. Michael Cunningham for having me as a part of his research group at Queen's University. We had a fruitful cooperation, the coldest winter in years and a lot of fun during dodge ball.

Prof. T. Davis, prof. Michael Cunningham, prof J.C. Schouten and prof. D. Haddleton, I would like to thank for their constructive remarks and good suggestions, which contributed to this thesis, and for being a part of my defense committee. Mijn paranimfen, Paul van der Weide en Eric Boonen, wil ik graag bedanken voor hun aanwezigheid en vriendschap tijdens mijn studie/promotie, voor de geweldige afstudeertijd en een spannende Tour de France sinds 2004.

During my PhD I had the pleasure of supervising a great bunch of students. Without the help of Susana, Maria, Rene, Ujwal, Mohammed, Roger, Bart and Tom I could not have obtained these great results. Susana, obrigada pelo seu trabalho árduo e atitude entusiasta. Votos de muito boa sorte para o futuro. Maria, tu has sido mi ultima estudante. Espero

que lo hayas pasado bien trabajando en nuestro laboratorio y te hayas divertido en tu estando en Eindhoven. Gracias por trabajar tan duro y te deseo lo mejor en tu futuro!



Back row: Susana Gomes Santana, Maria Moreno Guerrero, Roger van Hal

Middle row: Tom Jansen, Bart Dautzenberg, Niels Smeets, Ujwal Shreenag Meda

Front row: Mohammed E-Rramdani, Patrick Kivit.

ಪ್ರೀತಿಯ ಉಜ್ವಲ್,

ನೀನು ನಿನ್ನ "ಗ್ರಾಜುಯೇಶನ್" ನಲ್ಲಿ ಉತ್ತೀರ್ಣನಾದುದಕ್ಕೆ ನನ್ನ ಹಾರ್ಡಿಕ ಶುಭಾಶಯಗಳು. ಇದು ನಿನ್ನ ಶ್ರದ್ಧೆ, ಆತ್ಮವಿಶ್ವಾಸದಿಂದ ಕೂಡಿದ ದುಡಿಮೆಯ ಫಲ.

ನೀನು ನನ್ನ ಒಬ್ಬ ಆತ್ಮೀಯ ಸ್ನೇಹಿತ ಮತ್ತು ನಿನ್ನನ್ನು ವಿದ್ಯಾರ್ಥಿಯನ್ನಾಗಿ ಪಡೆದುದಕ್ಕೆ ನಾನು ತುಂಬಾ ಹೆಮ್ಮೆಪಡುತ್ತೇನೆ. ನಿನ್ನ ಜೀವನದ ಬರುವ ಮುಂದಿನ ದಿನಗಳು ಸುಖೀಕರವಾಗಲಿ ಎಂದು ನಾನು ನಿನಗೆ ಶುಭಹಾರೈಸುತ್ತೇನೆ.

محمد ، أريد أن أشكرك على تفانيك ، حماسك والعمل الجيد الذي أنجزت.
كما أعرب لك عن تقديري الخاص فإنه يحق لك أن تفخر كثيراً ببحث تخرجك!
حطاً سعيداً في وظيفتك الحالية ، وأتمنى لك كل التوفيق في زواجك المقبل .

Roger, bedank veur dien inzat tijdens dien stage en aafsjtudeeropdrach. Dich kens trots zin op 't werk datse hubs gedoan. Ich wens dich vööl succes mit dien zäöktoch noa 'n baan. Bart, 't opsjtarte van de PSPC woar zonger dich 't sjtuk lestiger gewaes. Dien

ingenieursinstinct en 't gevööl vöör de opsjtelling hub ich enorm gewaardeerd. Ich wens dich en Marlou vööl geluk vöör de toekomst in Mesjtreech. Tom, ook jij mag trots zijn op de mooie resultaten die je hebt behaald op een moeilijk onderwerp. Ik wens je veel succes met de afronding van je studie en veel succes in de toekomst.

Tiedens mien promotie haet 't voetballe bie Nirbik een belangrieke rol gesjpeeld. Een speciaal bedankje vöör mien vrunj toes: in het biezonger Saskia, Ron, Linda, Henk, Monique, Chris, Barbara, Maurice, Monica, Luc, Sander, Rick en natuurlik auch al die angere. Geer zörg d'r vöör dat ich eedere kjèr weer mit gooje zin in de auto noa Nirbik rie. Ron, dich wil ich in 't biezonger nog bedanke vöör mien adjudante rol tiedens dien regeerperiode.

During my stay in Kingston I have made some great friends. Tara and Adam, thanks for showing me so much of Canada. I was very lucky to have the two of you around! Nicky, Mary, Jordan, Ula, Jerry, D, Dara and Mikey, thanks for a great atmosphere both inside and outside the lab. Nicky, thanks for giving me a place to stay when I arrived (and came back) and I hope that your experiences in the Netherlands will be as great as mine in Canada. Jen and Nick thanks for having me over all those nights watching hockey, one can only wish to have friends like you living around the corner. George and Krista, thanks for squash, Boston and the townie bars, wouldn't have wanted to miss that. Best of luck for the two of you in London. Nathan, thanks for always being around when I needed a beer and a game of pool. I wish you and Hanan all the best for the future.

Je collega's bepalen grotendeels of je met plezier naar je werk komt. Ik had met de "mannen van de korte vleugel" geen betere collega's kunnen wensen. Jo, Ard, Tom en Sjoerd, ons kantoor was niet altijd een optimale werkplek maar ik kijk met veel plezier terug op de afgelopen 4 jaar. Ik wens Jo en Sjoerd veel succes met de afronding van hun promotie en Ard en Tom veel succes met de volgende stap in hun carrière. Verder wil ik prof. Jos Keurentjes en al mijn (oud) collega's van SPD bedanken voor de prettige werksfeer en de geweldige studiereis naar Zuid-Afrika. In het bijzonder Chris Scholtens, Wil Heugen en Chris Luyk voor hun hulp met de PSPC.

Also I was lucky enough to be able to do my PhD in both SPD and SPC. Een groot deel van het labwerk is uitgevoerd in de labs van SPC. Ik wil prof Alex van Herk en prof. Cor Koning graag bedanken voor de mogelijkheid die ik heb gehad om ook aan alle SPC activiteiten deel te nemen. Special thanks to Nadia and Joost for showing me around in the labs and helping me with my first emulsion experiments. I have experienced SPC as an open, lively and enthusiastic research group. I would like to thank all my colleagues and former colleagues for creating that great atmosphere. Special thanks to Marie-Claire for the great trips that we have made.

During my PhD I have spend quite sometime on the squash courts and the indoor soccer hall. Christina, Marie-Claire, Hector, Olavio, Carlos and Ivo thanks for many Friday nights of squash. My fellow players on de Vlackers, Willem-Jan, Gaëtan, Olavio, Hector, Joost, Michiel, Sjoerd, Baris, Ard, Marcos, Vladimir, Serdar and on Spartak SPC, Mark, Evgeny, Donglin, Maurice, Hector and Joris thanks for so many hours of soccer. I loved it!

Ich höb 't gelök gehad öm op te greuie mit twè geweldige breurkes and een leef zusje. Allan, Juri en Alicja bedank vääor uche bezäökskes in Eindhoven. 't Woar zeker in 't begin (en soms nog ömmer es ich allein op de bank zit) vraem zonger uch! Pap en mam, geer zeet de beste ouwesj die ich mich houw kenne wèense. Zonger uch woar ich nwoats zwoa wiet gekomme. Bedank veur uche sjteun, hulp, interesse en vertroewe in mien beslissinge.

Lauren, you were always there for me during this last year of my PhD. You were often the first one to read many parts of my thesis, and you were never short of questions, remarks and comma's to add. Thanks for being your curious-self and I look forward to our future together. I will savory you always.

Niels

CURRICULUM VITAE

Niels Mathieu Barbara Smeets was born May 26th 1981 in Ermelo, the Netherlands. He completed his secondary education at “Scholengemeenschap Sint Michiel” in Geleen. Shortly after he started a masters program in chemical engineering and chemistry at Eindhoven University of Technology. In January 2005 he graduated in the field of applied organic chemistry on the scale-up of L-leucine-*N*-carboxyanhydride synthesis. In May of the same year he started a Ph.D project on the application of catalytic chain transfer in emulsion polymerization under the supervision of prof. Jan Meuldijk, dr. Hans Heuts and prof. Alex van Herk. One year of his Ph.D was spend at Queen’s University, Kingston Canada, working with prof. Michael Cunningham. The results of his Ph.D research are summarized in this thesis.

Niels Mathieu Barbara Smeets werd op 26 mei 1981 geboren te Ermelo. Hij volgde het atheneum op de Scholengemeenschap St. Michiel te Geleen. Vervolgens startte hij de opleiding scheikundige technologie aan de technische universiteit Eindhoven. Januari 2005 studeerde hij af in de richting toegepaste organische chemie op de opschaling van de een synthese voor L-leucine-*N*-carboxyanhydride. In mei 2005 startte hij een promotie onderzoek over katalytische ketenoverdracht in emulsie polymerisatie onder begeleiding van prof. Jan Meuldijk, dr. Hans Heuts en prof. Alex van Herk. Tijdens zijn promotie heeft hij een jaar doorgebracht aan Queen’s University, Kingston Canada in samenwerking met prof. Michael Cunningham. The resultaten van het promotie onderzoek staan beschreven in deze dissertatie.

LIST OF PUBLICATIONS

Smeets, N.M.B.; Meuldijk, J.; van Herk, A.M.; Heuts, J.P.A. A Simple One-Step Sonochemical Route to Functional Hairy Polymer Nanoparticles; *Chem. Comm.*; submitted for publication

Smeets, N.M.B.; Heuts, J.P.A.; Meuldijk, J.; Cunningham, M.F.; van Herk, A.M. Evidence of Compartmentalization in Catalytic Chain Transfer Mediated Emulsion Polymerization of Methyl Methacrylate; *Macromolecules*; submitted for publication (ma-2009-007829)

Smeets, N.M.B.; Heuts, J.P.A.; Meuldijk, J.; Cunningham, M.F.; van Herk, A.M. The Effect of Co(II) Mediated Catalytic Chain Transfer on the Emulsion Polymerization Kinetics of Methyl Methacrylate; *J. Polym. Sci. Part A: Polym. Chem.*; submitted for publication (JPOL-A-09-0331)

Smeets, N.M.B.; Heuts, J.P.A.; Meuldijk, J.; Cunningham, M.F.; van Herk, A.M. Mass Transport Limitations and their Effect on the Control of the Molecular Weight Distribution in Catalytic Chain Transfer Mediated Emulsion Polymerization; *Macromolecules*; submitted for publication (ma-2009-007225)

Smeets, N.M.B.; Dautzenberg, B.A.J.; Heuts, J.P.A.; Meuldijk, J.; van Herk, A.M. Control of the Molecular Weight Distribution in Continuous Emulsion Polymerization a Pulsed Sieve Plate Column; *Macromol. Symp.* **2009**, 275, 149.

Hermant, M.C.; Smeets, N.M.B.; van Hal, R.C.F.; Meuldijk, J.; Heuts, J.P.A.; Klumperman, B.; van Herk, A.M.; Koning, C.E. Influence of the Molecular Weight Distribution on the Percolation Threshold of Carbon Nanotube – Polystyrene Composites; *E-polymer* **2009**, 22.

Smeets, N.M.B.; Heuts, J.P.A.; Meuldijk, J.; van Herk, A.M. Effect of Catalyst Partitioning in Co(II) Mediated Catalytic Chain Transfer Miniemulsion Polymerization of Methyl Methacrylate; *J. Polym. Sci. Part A: Polym. Chem.* **2008**, 46, 5839.

Smeets, N.M.B.; Meda, U.S.; Heuts, J.P.A.; Keurentjes, J.T.F.; van Herk, A.M.; Meuldijk, J. Molecular Weight Control in Emulsion Polymerization by Catalytic Chain Transfer: A Reaction Engineering Approach; *Macromol. Symp.* **2007**, 1, 406.

Smeets, N.M.B; van der Weide, P.L.J.; Meuldijk, J.; Vekemans, J.A.J.M.; Hulshof, L.A. A Scalable Synthesis of L-Leucine-*N*-Carboxyanhydride; *Org. Proc. Res. Dev.* **2005**, *6*, 757.